Universidad de Concepción
Dirección de Postgrado
Facultad de Ciencias Naturales y Oceanográficas
Doctorado en Ciencias Biológicas área Botánica

Aplicación de la hipótesis de la centralidad del nicho ecológico para evaluar los cambios del metabloma y la actividad biológica en poblaciones de *Eucryphia cordifolia* Cav. (Cunoniaceae).

Tesis para optar al grado de Doctor en Ciencias Biológicas área Botánica

por

Camila Andrea Fuica Carrasco

Profesor Guía: Dr. Víctor Javier Hernández Santander
Profesor Co-Guía: Dr. Oscar Fernando Toro Núñez

SEPTIEMBRE 2023
Concepción, Chile

© Se autoriza la reproducción total o parcial, con fines académicos, por cualquier medio o procedimiento, incluida la cita bibliográfica del documento.

Esta tesis fue desarrollada en el Laboratorio de Química de Productos Naturales, Departamento de Botánica, Facultad de Ciencias Naturales y Oceanográficas; Laboratorio de Metabolómica de Plantas, Departamento de Análisis Instrumental, Facultad de Farmacia y el Laboratorio de Patogenicidad Bacteriana, Departamento de Microbiología, Facultad de Ciencias Biológicas.

COMISION EVALUADORA

Dr. Víctor Hernández Santander
Profesor guía _____

Dr. Oscar Toro Núñez
Profesor Co-Guía _____

Dr. Eduardo Ruiz Ponce
Evaluador Interno _____

Dr. Andy Pérez de Armas
Evaluador Externo _____

Dr. Andrés Lira Noriega
Evaluador Externo _____

Dr. Pablo Guerrero Martín
Director de Programa _____

AGRADECIMIENTOS

Al Laboratorio de Química de Productos Naturales, Departamento de Botánica, Facultad de Ciencias Naturales y Oceanográficas, Universidad de Concepción.

Al Laboratorio de Metabolómica de Plantas, Departamento de Análisis Instrumental, Facultad de Farmacia, Universidad de Concepción.

Al Laboratorio de Patogenicidad Bacteriana, Departamento de Microbiología, Facultad de Ciencias Biológicas, Universidad de Concepción.

Al Sr. Moisés Grimberg (CONAF) por permitir y coordinar el acceso restringido a las dependencias de los parques y monumentos nacionales en pandemia COVID19.

A Forestal Mininco S.A. (CMPC) por permitir el acceso al Área protegida Alto Escuadrón en pandemia COVID19.

A la fuente de financiamiento Agencia Nacional de Investigación y Desarrollo (ANID), Beca Doctoral Nº21170525.

TABLA DE CONTENIDO

INDICE DE FIGURAS

INDICE DE TABLAS

RESUMEN

La hipótesis de la centralidad del nicho ecológico establece que la abundancia de la población está determinada por la posición en el nicho ecológico, esperándose mayores abundancias hacia el centro del nicho y menores en la periferia. Sin embargo, las variaciones en las condiciones que favorecen la persistencia de las poblaciones entre el centro y la periferia del nicho pueden ser un sustituto de factores de estrés que se reflejan en la producción de metabolitos en las plantas. Esta investigación se basó en un enfoque multidisciplinario entre la hipótesis de la centralidad del nicho ecológico y la metabolómica como una herramienta que permite predecir la presencia de compuestos con interés biotecnológico, dirigiendo el muestreo y con ello evitando sobreexplotación de los recursos nativos.

En esta tesis se evaluaron las siguientes hipótesis (1) Las poblaciones de *E. cordifolia* que se encuentran en la periferia del nicho ecológico presentan una mayor abundancia y/o diversidad de metabolitos secundarios que poblaciones que se distribuyen en el centro del nicho ecológico (2) Los metabolitos secundarios sintetizados por poblaciones de *E. cordifolia* que se distribuyen en la periferia del nicho ecológico, presentan una mayor actividad biológica (e.g., antioxidante y antimicrobiana) comparados con poblaciones distribuidas en el centro del nicho ecológico.

Se emplearon tres enfoques metodológicos: primero, modelamos el nicho ecológico para determinar la idoneidad ambiental de *E. cordifolia* y seleccionar poblaciones centrales y periféricas para el muestreo en campo (objetivo 1). Segundo, aplicamos análisis de ordenamiento (PCA y NMDS) y el índice de diversidad de Shannon

Wiener para evaluar la diversidad metabólica entre las poblaciones y en diferentes estaciones (objetivo 2). Luego, mediante OPLS-DA, identificamos metabolitos diferenciadores entre la población central y periférica. En tercer término, se evaluó la actividad antioxidante y antimicrobiana contra cinco microorganismos de interés en salud pública, hipotetizando un efecto significativo en la población periférica (objetivo 3).

Los resultados del capítulo 2 indicaron que: las localidades centrales y periféricas de *E. cordifolia* en Chile no siguen un gradiente ambiental latitudinal evidente. La similitud metabólica entre poblaciones se explica más por la estacionalidad que por la posición en el nicho. La tendencia en la diversidad metabolómica aumenta a medida que nos alejamos del centro del nicho ecológico. Los análisis multivariados permitieron una diferenciación metabólica entre las poblaciones. En la población periférica (Puerto Montt) se identificaron derivados de quercetina, kaempferol-3-O-ramnósido, luteolina y procianidina B a lo largo de las estaciones, estando ausentes en la población central (Coronel). En cuanto a los análisis antioxidantes, estos variaron a lo largo de las estaciones, donde las poblaciones más cercanas a la periferia alcanzaron una alta capacidad antioxidante. Respecto a los ensayos microbianos, los extractos mostraron una fuerte inhibición en las etapas iniciales de crecimiento microbiano, pero no fueron eficientes en la inhibición de la formación de biopelículas en cuatro de los microorganismos estudiados.

En última instancia, nuestros resultados respaldan la utilidad de este enfoque multidisciplinario para prever variaciones en el metaboloma con posibles aplicaciones biotecnológicas y nos orienta a realizar muestreos eficientes.

ABSTRACT

The ecological niche centrality hypothesis states that species abundance is determined by position in the ecological niche, with higher abundances expected towards the centre of the niche and lower abundances at the periphery. However, variations in conditions that favour the persistence of populations between the centre and periphery of the niche may be a proxy for stress factors that are reflected in plant metabolite production. This research was based on a multidisciplinary approach between the hypothesis of ecological niche centrality and metabolomics as a predictive tool to predict the presence of compounds with biotechnological interest, directing sampling and thus avoiding overexploitation of native resources.

In this thesis the following hypotheses were evaluated (1) *E. cordifolia* populations found in the periphery of the ecological niche have a higher abundance and/or diversity of secondary metabolites than populations distributed in the centre of the ecological niche (2) Secondary metabolites synthesized by *E. cordifolia* populations distributed in the periphery of the ecological niche have a higher biological activity (e.g., antioxidant and antimicrobial) compared to populations distributed in the centre of the ecological niche.

Three methodological approaches were employed: first, we modelled the ecological niche to determine the environmental suitability of *E. cordifolia* and selected core and peripheral populations for field sampling (objective 1). Second, we applied ordination analyses (PCA and NMDS) and the Shannon Wiener diversity index to assess metabolic diversity among populations and in different seasons (objective 2). Then, using OPLS-DA, we identified differentiating metabolites between the central and peripheral

populations. Thirdly, antioxidant and antimicrobial activity was evaluated against five microorganisms of public health interest, hypothesising a significant effect in the peripheral population (objective 3).

The results of chapter 2 indicated that: central and peripheral localities of *E. cordifolia* in Chile do not follow an obvious latitudinal environmental gradient. Metabolic similarity between populations is explained more by seasonality than by niche position. The trend in metabolomic diversity increases as we move away from the centre of the ecological niche. Multivariate analyses allowed metabolic differentiation between populations. In the peripheral population (Puerto Montt), quercetin, kaempferol-3-O-rhamnoside, luteolin and procyanidin B derivatives were identified throughout the seasons, while they were absent in the central population (Coronel). Antioxidant assays varied across the seasons, with populations closer to the periphery achieving high antioxidant capacity. Regarding microbial assays, the extracts showed strong inhibition in the initial stages of microbial growth but were not efficient in inhibiting biofilm formation in four of the microorganisms studied.

Ultimately, our results support the usefulness of this multidisciplinary approach for predicting variations in the metabolome with potential biotechnological applications and guide us to efficient sampling.

CAPITULO 1: INTRODUCCION

1.1. *Eucryphia cordifolia* como especie modelo

Eucryphia Cav. es un género que comprende siete especies leñosas que habitan los bosques templados de América del Sur y Oceanía (Bull-Hereñu et al. 2018). Actualmente incluidas en la familia *Cunoniaceae*. En Chile, dos especies son parte de este género, *E. glutinosa* (Poepp. & Endl.) Baill y *E. cordifolia* Cav. (Rodríguez & Ruiz 1999). Esta última, es una especie arbórea endémica de los bosques del sur de Chile, el que se distribuye entre la Región del Bio-Bio y la Región de Aysén (36.8° S y 43.3° S), estando presente tanto en la cordillera de la costa como en la cordillera de los Andes; principalmente en zonas de baja elevación, inferiores a los 700 m.s.n.m (Segovia et al. 2012; Rodríguez et al. 2018). En su amplia distribución, *E. cordifolia*, comúnmente llamada Ulmo, abarca áreas con un rango climático diverso, desde el tipo mediterráneo, con inviernos suaves y veranos muy secos y cálidos, hasta el tipo templado, con inviernos más fríos y condiciones más moderadas durante el verano (Figueroa et al. 2010). *E. cordifolia* es capaz de colonizar hábitats alterados y corresponde a una especie semitolerante a la sombra, que alcanza

hasta 35 metros de altura y ocupa una posición emergente en el dosel del bosque (Díaz et al. 2010).

Por otro lado, es considerada una especie con gran potencial económico, particularmente por su madera de buena calidad, comúnmente usada para la construcción y como fuente de combustión (Uteau y Donoso 2009). La pudrición de la madera (pudrición blanca, por degradación) es apreciada comercialmente, ya que es usada como alimento para el ganado cuando se encuentra con un alto estado de degradación (Escobar et al. 2006). Desafortunadamente, estas propiedades son las razones de la alta presión antropogénica que ha llevado al estado de conservación vulnerable actual de la mayoría de sus poblaciones (Morales et al. 2014).

A nivel ecológico, la presencia de *E. cordifolia* resulta crucial para mantener grandes comunidades de polinizadores, debido al gran tamaño de sus flores (Smith- Ramírez 2014). *E. cordifolia* ha sido históricamente aprovechada en la industria apícola, debido a la gran producción de néctar floral (Morales 2013). Acevedo et al. (2017) aislaron compuestos volátiles, no volátiles y semivolátiles por medio de microextracción en fase sólida (SPME) en miel de Ulmo. Sus resultados demostraron la presencia de 50 compuestos volátiles los cuales contribuyen al sabor y aroma de la miel, son

sintetizados por la especie vegetal permitiendo la interacción entre las plantas y polinizadores.

Esta es una de las cuatro especies nativas en Chile, de la cual se puede obtener miel monofloral (Díaz-Forestier et al. 2016), y se ha observado que la misma presenta un buen efecto biológico en humanos (e.g. contra bacterias y hongos) además de ser un potente antioxidante (Schencke et al. 2016). La capacidad que tienen las mieles de disminuir el estrés oxidativo se debe a la presencia de compuestos fenólicos, como los ácidos aromáticos y los flavonoides, los cuales son proporcionados y sintetizados por las especies vegetales visitadas por las abejas (Bridi y Montenegro 2017; Montenegro et al. 2013).

Históricamente se ha demostrado que las condiciones ambientales y la posición geográfica de las especies, influyen en la composición de metabolitos secundarios sintetizados por las plantas (Sampaio et al. 2018). Este supuesto ha sido demostrado, en principio, con flavonoides en especies del género *Eucryphia*, donde Bate-Smith (1967) evidenció una correlación entre la síntesis de flavonoides a partir de extractos de hojas y la distribución geográfica en las especies del género. En su estudio, se aislaron 14 flavonoides, lo que permitió clasificar taxonómicamente a *Eucryphia* e

incluirla dentro de la familia *Cunoniaceae*. Además, se demostró una clara división entre las especies sudamericanas y australianas, carecían de flavonoides tales como azaleatina y cariatina. Wollenweber et al. (2000) evaluó el contenido de flavonoides de siete especies de *Eucryphia*, aislando un total de 28 flavonoides, donde solo las especies sudamericanas presentaron glucósidos de azaleatina. Por medio de los análisis cladísticos y composición fitoquímica, en este mismo estudio se demostró que las especies de Tasmania correspondían a taxones hermanos de las demás especies en estudio. Finalmente, por medio de análisis y ordenación de conglomerados se determinó la división de los taxones en tres grupos, donde *E. wilkei* se ubicó más distante del resto de las especies.

Mas allá de la mencionada evidencia, *Eucryphia* carece de estudios que evalúen una asociación entre ubicación geográfica, condición ambiental y la síntesis de metabolitos secundarios.

1.2. Nicho ecológico e hipótesis de la centralidad del nicho ecológico

Los procesos ecológicos que determinan el *fitness* de las especies están directamente influidos por las condiciones ambientales de su hábitat dentro de sus áreas de distribución y pueden evaluarse a partir de su nicho ecológico

(Hutchinson 1957; Maguirre 1973; Soberón 2007). La teoría del nicho representa la forma en que los individuos se relacionan con el entorno (Leibold & Geddes 2005). Hutchinson (1957) definió el nicho de una especie como un hipervolumen en el espacio ambiental, representado por *n*-ejes en los que cada uno corresponde a una variable específica, que en su conjunto permiten alcanzar tasas óptimas de crecimiento y supervivencia de forma indefinida. Según Hutchinson (1957) hay dos tipos de variables que constituyen este hipervolumen. Por un lado, están las variables abióticas no dinámicas, también llamadas variables escenopoéticas, que son determinantes en el *fitness* de un individuo y que permanecen fijas independientemente de los cambios en el número de individuos de una población, y operan a escalas gruesas. Por otro lado, están las variables dinámicas o bionómicas que corresponden a aquellas variables que son afectadas por la especie (es decir, de naturaleza biótica), como la competencia y el consumo de recursos que operan a resoluciones finas (Soberón 2007; Soberón & Nakamura 2009; Peterson 2011). Teniendo en cuenta este amplio espectro de variables, Soberón (2007) sugirió dos tipos de nichos ecológicos en función del tipo de variables que se utilizan para evaluar las condiciones ambientales de las que depende una especie: un nicho grinnelliano cuando se

utilizan variables abióticas no acopladas y un nicho eltoniano cuando se utilizan variables bióticas acopladas. En general, y según esta teoría, la distribución geográfica de una especie y la abundancia de sus poblaciones están determinadas por estos dos tipos de variables y por la capacidad de dispersión a un área accesible (Soberón & Peterson 2005; Barve et al. 2011; Soberón 2017). La conjunción de estos tres factores determina el área que puede ser realmente ocupada por las especies.

El modelamiento del nicho ecológico es una herramienta que permite modelar los datos de presencia georreferenciadas de especies y su relación con las variables ambientales. Esta herramienta ofrece un medio único para inferir patrones de abundancia geográfica que, de otro modo, serían difíciles de caracterizar (Osorio-Olvera et al. 2020). De manera teórica el modelamiento del nicho ecológico (ENM), es una herramienta que permite estimar las condiciones climáticas (únicamente variables escenopoéticas) donde una especie podría establecerse, sin considerar las interacciones bióticas (Soberón y Nakamura 2009). De esta manera se considera que se está modelando el nicho ambiental de una especie. El ENM opera en la dualidad de Hutchinson, la que establece una correspondencia entre un espacio geográfico (G) y su correspondiente espacio ambiental (E) (Soberón y

Peterson 2011). El espacio "E" suele construirse mediante una combinación de variables ambientales, expresando una representación multivariada de un espacio hipervolumétrico de condiciones escenopoéticas.

Igualmente, el espacio "G" es la correspondencia en la geografía de cada punto de "E" (o píxel). Cuando se trata de los nichos ecológicos esta dualidad se refiere entonces al rango potencial de distribución de la especie (Peterson et al. 2011). Bajo esta distinción, es que el modelamiento del nicho ecológico ha sido convenientemente explicado bajo el diagrama BAM (biótico, abiótico y movimiento) (Soberón & Peterson 2005). Mediante éste, se demuestra las probabilidades que tiene una población de ser observada en aquellas regiones donde i) existan condiciones abióticas necesarias, denotada por (A); ii) existan condiciones bióticas favorables (B) y iii) regiones accesibles para la dispersión (M). Por tanto, el propósito del modelamiento radica en la identificación de lugares adecuados para la supervivencia de las poblaciones, usando sólo la identificación de sus requerimientos ambientales para estimar su nicho ecológico (Soberón y Nakamura 2009). Dado que el componente biótico presenta una compleja medición, a menudo no son consideradas para realizar el ENM (Peterson et al. 2011; Soberón 2017). En este trabajo, seguimos los fundamentos de la teoría del nicho grinnelliano que

como ya se mencionó, se basa en un espacio multidimensional de variables ambientales no interactivas (e.i., el clima), y en la relación entre el espacio del nicho y el espacio geográfico donde el objeto principal es modelar el nicho fundamental (Osorio-Olvera et al. 2019).

Desde una perspectiva biogeográfica, se ha propuesto que la abundancia de las poblaciones tiende a ser mayor en el centro de su área de distribución geográfica en comparación con la periferia, lo que se conoce como la hipótesis del centro abundante (Sagarin et al. 2006). Esta idea ha sido debatida en numerosas investigaciones, ya que se ha demostrado que los patrones de abundancia de las poblaciones están determinados por las condiciones ecológicas de los lugares de ocupación de estas (hábitat) (Yañez-Arenas et al. 2012). Maguire (1973) propuso que la estructura interna del nicho determina la respuesta de las poblaciones a las condiciones ambientales locales (hábitat) a lo largo de la distribución geográfica de la especie.

Dentro del nicho existen diferentes regiones en las que el establecimiento de las poblaciones con las máximas tasas de supervivencia se encuentra en el centroide (es decir, centro del espacio volumétrico), y en otras se irá reduciendo paulatinamente a medida que las poblaciones se alejen hacia regiones subóptimas, donde la probabilidad de supervivencia es menor,

es decir, donde la tasa de mortalidad es mayor o igual a la tasa de natalidad hasta que las poblaciones no puedan sostenerse sin inmigración (i.e., periferia o margen del nicho ecológico). Todo esto independientemente de donde se encuentren geográficamente estos ambientes. Esta analogía es lo que actualmente se conoce como la "hipótesis de la centralidad del nicho ecológico" (Yañez-arenas et al. 2020; Osorio-Olvera et al. 2019).

Dado que los ambientes son heterogéneos y se encuentran en constante cambio, para testear la hipótesis de la centralidad del nicho ecológico se requiere caracterizar el nicho fundamental de las especies (espacio ambiental que consiste en las combinaciones de variables que permiten la supervivencia y la reproducción de individuos), con el fin de poder determinar poblaciones centrales (óptimo ambiental) y/o periféricas (subóptimas).

1.3. Investigaciones que respaldan la "hipótesis de la centralidad del nicho ecológico"

Artículos recientes que prueban la hipótesis basada en el nicho han encontrado que la distancia al centroide del nicho está negativamente relacionada con la abundancia de la población y la variación genética (medida principalmente como la heterocigosidad esperada, la diversidad de

nucleótidos y riqueza alélica) (Ochoa-Zavala et al. 2022). Algunos ejemplos de estas investigaciones han sido desarrollados por Lira-Noriega y Manthey (2014), quienes propusieron determinar si la diversidad genética era mayor en el centro o en la periferia del nicho ambiental versus la distribución geográfica en 40 especies de diferentes taxa. Sus resultados demostraron una relación negativa entre la diversidad genética y la distancia al centroide del nicho ecológico y la distancia al centro del rango geográfico. Por su parte, Martínez-Meyer et al. (2013) probaron una hipótesis alternativa en 4 aves, la cual establece que la abundancia de las especies disminuye a medida que aumenta la distancia al centro del nicho ecológico. Los resultados demostraron una tendencia positiva para *Toxostoma redivivum* donde la mayor abundancia poblacional se encontraba en el centro del nicho ecológico, mientras que en la periferia se evidenció poblaciones más pequeñas en número (Martínez-Meyer et al. 2013).

De Medeiros et al. (2018) estudiaron los requerimientos ambientales para cuatro poblaciones de plantas europeas mediante el uso del ENM, con el fin de determinar si las poblaciones se ubican en el centro o periferia del nicho ecológico y si estas últimas se encontraban fuera de sus requerimientos ambientales óptimos. Sus resultados demostraron que tres de las poblaciones

en estudio se encontraban en los márgenes de sus rangos de distribución bajo condiciones ambientales estresantes para la supervivencia. Sin embargo, la población restante se encontraba bajo condiciones ambientales óptimas. Martínez-Gutiérrez et al. (2018) evaluaron patrones a gran escala en la abundancia poblacional del pecarí de collar (*Pecari tajacu*) en relación con la hipótesis de centralidad de nicho ecológico asociado a diferentes niveles de perturbación humana. Sus resultados demostraron que la abundancia poblacional disminuye en función de la distancia al centroide del nicho ecológico. Esta disminución está directamente relacionada con el índice de influencia humana, que está construido con algunas variables como la densidad poblacional, presencia de infraestructura y presencia de caminos. Los resultados apoyan las hipótesis de que los patrones espaciales en la abundancia local están asociados con la estructura ambiental del nicho grinnelliano, como también de variables antropogénicas.

1.4. Metabolómica en plantas

Por medio de un enfoque metabolómico es posible tener una visión completa de todos los metabolitos celulares como compuestos orgánicos de bajo peso molecular, que participan en diferentes procesos celulares, representando así el estado fisiológico absoluto de una célula en un momento

dado (Arbona et al. 2013). La totalidad de metabolitos de bajo peso molecular (< 1500 Da) y su interacción dentro de un sistema biológico es lo que se conoce como metaboloma (Fiehn 2002). El resultado de un análisis metabolómico es la caracterización molecular del metaboloma extraído, obteniendo un perfil metabólico del estado actual del organismo, contando con que el metaboloma es el producto final de la expresión génica y la actividad proteica en las plantas (Anzano et al. 2021).

Existen dos estrategias principales para la cuantificación e identificación del metaboloma, que dependen principalmente de la pregunta experimental a la que se quiere dar respuesta (Gorrochategui et al. 2016). La metabolómica dirigida (*target metabolomics*) es el método de elección en un experimento impulsado por una hipótesis, es decir, si la investigación se centra en una o más vías metabólicas. Con esta estrategia, sólo se identifica un determinado grupo de metabolitos, lo que permite obtener una instantánea del contexto fisiológico deseado (Dunn 2008; Krastanov 2010). Por el contrario, la metabolómica no dirigida (*untarget metabolomics*) tiene como objetivo medir idealmente todos los metabolitos contenidos en una muestra biológica proporcionando una imagen global e imparcial del metabolismo (Allwood et al. 2011; Canuto et al. 2018).

Las herramientas metabolómicas que combinan una técnica de separación como la cromatografía y la espectroscopía de masas son las más comunes (Walker et al. 2022). Entre ellas se destaca la cromatografía de gases-espectrometría de masas (GC-MS), la cromatografía líquida (LC-MS), la electroforesis capilar (EC)-MS y la espectroscopía de resonancia magnética nuclear (RMN) (Yang et al. 2018). A grandes rasgos, estas herramientas se diferencian entre sí por presentar una afinidad preferente por distintos tipos de metabolitos en función de sus características fisicoquímicas y pueden utilizarse con fines de separación, cuantificación o incluso identificación (Kim & Verporte 2010; Obata & Fernie 2012).

Actualmente, la cromatografía LC-MS ha ganado popularidad en el campo de la metabolómica por sobre las otras herramientas mencionadas. Esto principalmente porque permite el análisis de una gama más amplia de metabolitos (polares y de mediana polaridad) sin necesidad de derivatización, como en el caso de GC-MS (Theodoridis et al. 2011). Las técnicas basadas en espectrometría de masas generan datos muy complejos, debido a la gran cantidad de mediciones (e.i., espectro de MS en cada tiempo de retención) relacionadas con la cantidad de observaciones (e.i., muestras). Para LC-MS los datos generados a partir de cada cromatograma se organizan en conjuntos

de datos que contienen información de masa a carga (m/z), tiempo de retención e intensidad de los iones (Gorrochategui et al. 2016).

Los datos obtenidos mediante las herramientas analíticas son procesados por diversas plataformas computacionales como Metaboscape (versión 3.0, bruker), XCMS (Mahieu et al. 2016), MS-DIAL (Tsugawa et al. 2015) entre otras, para realizar una extracción no sesgada de los picos de masa y generar la alineación de los datos (De Vos et al, 2007). Posteriormente a esto, se genera una tabla de cubos ("*bucket table*") la cual es una representación tridimensional de los datos. Se caracteriza por ser una tabla de intensidades que relaciona las muestras que se encuentran en columnas y los *features* (m/z, t_R) (metabolitos) ubicados en las filas y se carga en softwares o sitios web de bioinformática. Estas herramientas proveen una serie de análisis para estudios metabolómicos, principalmente de tipo estadístico, orientados a análisis univariados (prueba t de Student; ANOVA; prueba U de Mann-Whitney) y multivariados (PCA, PLS-DA, OPLS-DA) (Ren et al. 2015; Raza 2020) para realizar las comparaciones pertinentes de acuerdo con la estrategia implementada.

Para llevar a cabo un estudio metabolómico en primera instancia se realiza un análisis de componentes principales (PCA) éste es un método de

ordenación (Jansen et al. 2009). Se basa en una transformación lineal ortogonal de variables posiblemente correlacionadas en un número menor de variables no correlacionadas llamadas componentes principales (PC), donde la mayor varianza dentro de los datos según cualquier proyección se explica en la primera coordenada (PC1) y la menor varianza es explicada/proyectada por PC posteriores (Madala et al. 2014). Por lo tanto, el PCA y otros modelos de reducción convierten los datos en gráficos de puntuación, representaciones visuales donde los datos de diferentes orígenes biológicos se separan en distintos grupos (Xia & Wishart 2011). Además, permite detectar aquellos datos que generar outliers (Alonso et al. 2015). En segundo lugar, se realiza un análisis de cuadrados mínimos parciales ortogonales (OPLS-DA) que corresponde a un método de agrupamiento o de clasificación supervisado. Se utiliza para la identificación de variables o *features* que impulsan la separación o la diferenciación entre grupos (Worley & Powers 2016; Souza da Silva et al. 2017).

De manera posterior, la anotación de los *features* se realiza comparando una medición de masa (*m/z*) y sus patrones de fragmentación con compuestos ya identificados (De Vos et al. 2007), los cuales son almacenados y comparados con bases de datos globales como PubChem

(Kim et al. 2019), KEGG (Kanehisa 2016), Metlin (Smith et al. 2005) entre otras. Dado que los datos de intensidad son muy variables entre lotes experimentales, instrumentos y métodos o parámetros de preprocesamiento, ninguna herramienta estadística es capaz de abordar todo el metaboloma de una muestra biológica (Traquete et al. 2021). Por último, para lograr una interpretación biológica precisa de los datos metabolómicos, resulta crucial establecer conexiones entre los metabolitos identificados y las complejas redes y rutas metabólicas. Este enfoque permite trazar un contexto bioquímico completo, revelando así la respuesta de la planta al estímulo externo al que ha sido sometida (Schrimpe-Rutledge et al., 2016).

Finalmente, el flujo de trabajo en un estudio metabolómico en plantas se basa en al menos seis etapas principales (Figura 1.1): (1) diseño experimental, (2) preparación de las muestras, (3) adquisición de datos mediante el uso de UHPLC-MS/MS, (4) procesamiento de la data para la obtención del bucket table, (5) análisis de datos por métodos univariados o multivariados e identificación de los metabolitos y por último (6) interpretación biológica.

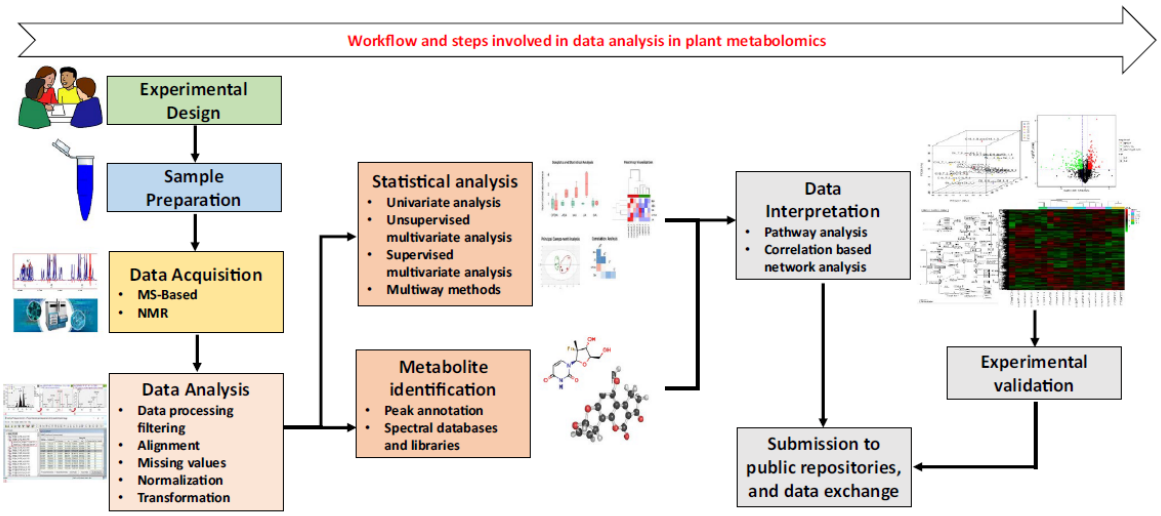

Figura 1.1. Flujo de trabajo y pasos involucrados en el análisis de datos de alto rendimiento en la metabolómica de plantas (adaptado de Raza et al. 2020).

1.5. Prospección de metabolitos secundarios de *E. cordifolia*.

Es conocido que, desde tiempos prehistóricos, las plantas han sido usadas como fuente medicinal para tratar diversas afecciones o como alimentos producidos de manera sostenible con efectos beneficiosos para la salud humana (Kumar & Goel 2019; Zanatta et al. 2021). Muchas de las frutas y plantas endémicas de América del Sur han mostrado un valioso potencial para el consumo humano como fuente de antioxidantes (Millan et al. 2023). Alrededor de 40% de las plantas vasculares en Chile son endémicas, y una proporción similar es nativa, atributo generalmente compartido con Perú, Bolivia y/o Argentina (Rodríguez et al. 2018).

Las plantas vasculares nativas y endémicas suman más de 80 % de la diversidad total de plantas vasculares, lo que convierte a Chile en uno de los 25 *hotspot* de biodiversidad de nivel mundial y además aporta con una fuente de recursos biológicos únicos; por ende, se vuelve importante su conservación (Arroyo et al. 2008; Rodríguez et al. 2018; Otero et al. 2022).

Investigaciones recientes han demostrado que plantas tanto endémicas como nativas de Chile presentan un potencial uso con fines terapéuticos (Salehi et al. 2021). Diaz-Foriester et al. (2019) realizaron un estudio sobre las plantas útiles de Chile y demostraron que las siguientes *familias Lamiaceae, Linaceae, Proteaceae, Cunoniaceae, Rhamnaceae, Rosaceae* y *Myrtaceae* están sobrerrepresentadas entre las especies con propiedades medicinales, destacando que las familias *Cunoniaceae y Rosaceae*, son ricas en taninos, y pueden tener una amplia gama de efectos farmacológicos como antibacterianos, antivirales, inmunomoduladores y antiinflamatorios. Por otro lado, Otero et al. (2022) realizaron una revisión exhaustiva de las propiedades antimicrobianas de plantas nativas y endémicas de Chile y demostraron que muchas de estas especies presentan una buena actividad antimicrobiana, las que podrían ser usadas para generar estrategias frente al control de patógenos alimentarios. Sin embargo, existe un vacío importante

de conocimiento de cuáles son los compuestos bioactivos que contribuyen a otorgar una cualidad bioactiva a estas especies, lo cual podría ayudar a comprender si el efecto biológico se debe a efectos únicos, aditivos o sinérgicos de los metabolitos antimicrobianos en plantas nativas y endémicas.

Los compuestos fenólicos, incluidos los flavonoides y los ácidos fenólicos, son reconocidos como importantes antioxidantes naturales y también desempeñan un papel clave en una amplia variedad de propiedades biológicas y/o farmacológicas (de Oliveira et al. 2012), como antiinflamatorias, anticancerígenas, antibacterianas, antialérgicas, antivirales, antitrombóticas, hepatoprotectoras y como moléculas de señalización (Jimenéz-Gonzalez et al. 2018; Kumar & Goel 2019). La ingesta de plantas con presencia de compuestos fenólicos se ha relacionado con la reducción del desarrollo de enfermedades crónicas y cardiovasculares (Jimenéz-Gonzalez et al. 2018; Olivares-Caro et al. 2020; Virdi et al. 2022). Esto se debe a que los compuestos bioactivos juegan un papel importante en la adsorción y neutralización de los radicales libres, o en la descomposición de los peróxidos, moléculas que contribuyen a la aparición de las enfermedades neurodegenerativas ya mencionadas (Pacífico et al. 2015).

Dentro de las principales desventajas al trabajar con especies vegetales con potenciales beneficios, es que la concentración de los compuestos bioactivos varía y no se mantiene constante en el tiempo (Pacífico et al. 2015; Jha & Sit 2022). Se estima que los factores genéticos y ecológicos son los aspectos más relevantes que afectan la concentración de los compuestos bioactivos (Pacífico et al. 2015; Zanatta et al. 2021). Tal como se mencionó, las variables ambientales (principalmente temperatura, precipitación y disponibilidad lumínica), la fenología, y las variaciones en el crecimiento dentro del hábitat son solo algunas de las respuestas a los cambios ambientales que impulsan a las plantas a desarrollar estrategias de adaptación y supervivencia y donde la síntesis de metabolitos secundarios es clave para sobrellevar tal presión ambiental (Pacífico et al. 2015; Yang et al. 2018). Dado que los factores fenológicos y fisiológicos influyen en la biosíntesis de los metabolitos secundarios de las plantas, la estacionalidad y el tiempo de cosecha son factores críticos que determinan la composición química (Vilkickyte & Raudone 2021).

La estacionalidad también es una variable que afecta la síntesis de metabolitos secundarios y se puede definir como los cambios regulares y periódicos de una condición en una escala de tiempo anual. La estacionalidad

es una característica ambiental predominante en diversos sistemas ecológicos impulsados por condiciones climáticas periódica (Williams et al. 2017; White & Hastings 2020) y que permite la persistencia y la coexistencia de las poblaciones. La mayoría de los factores de estrés tienen un patrón estacional claro, lo que implica que el contenido total y las proporciones relativas de metabolitos secundarios en las plantas oscilan dependiendo de los cambios estacionales, es decir, ambientales. En consecuencia, estos cambios también influyen en la eficacia terapéutica de la planta en particular (Lunic et al. 2022). Es ampliamente reconocido que la cantidad de luz solar disponible experimenta variaciones a lo largo del año. En respuesta a esta fluctuación, las plantas realizan ajustes tanto en el proceso de fotosíntesis como en la priorización de la síntesis de metabolitos secundarios con propiedades antioxidantes. Estos ajustes son esenciales para contrarrestar el estrés oxidativo que se origina debido a la exposición a la radiación ultravioleta. (Lee & Ding et al. 2016). Se ha informado que la biosíntesis de compuestos fenólico en *Baccharis dendata* se encuentra inducida por las condiciones ambientales a las que se encuentran expuestas, demostrando que la estacionalidad es un factor importante en su producción y acumulación (Sartor et al. 2013). Bajo este contexto, la consideración de los factores

ambientales es crucial cuando se desea investigar la producción de los compuestos bioactivos con fines aplicados (Li et al. 2020).

Actualmente, pocas investigaciones han realizado una aproximación química y biológica de la especie nativa *E. cordifolia.* Sin embargo, Viteri et al. (2022) recientemente consiguieron demostrar la presencia de triterpenos pentacíclicos, fitoesteroles y flavonoides; demostrando que estos metabolitos presentan indicadores sobre su efecto antioxidante y antibacteriano proporcionado principalmente por los compuestos fenólicos.

El 60% de la flora en Chile aún no ha sido objeto de bioprospección, y se carece de estudios que analicen el metaboloma de las plantas nativas para comprender los mecanismos asociados a la producción de compuestos bioactivos. Por lo tanto, resulta de suma importancia llevar a cabo investigaciones que permitan evaluar los metabolitos producidos por estas plantas, así como sus posibles aplicaciones, con singular preponderancia en el ámbito biomédico, tanto humano como animal, entre otras.

El propósito central de esta investigación doctoral fue desarrollar un modelo que facilitara la orientación del muestreo en campo, con el objetivo de evitar la sobreexplotación de los recursos naturales en Chile. Asimismo, se persiguió que este modelo fuera capaz de anticipar las variaciones en el metaboloma de la especie *E. cordifolia* frente a las condiciones ambientales de sus hábitats naturales. En este sentido, creemos que un enfoque multidisciplinario que incorpore tanto la hipótesis de la centralidad del nicho ecológico como la metabolómica resulta fundamental para enriquecer la comprensión de la variabilidad metabólica en las plantas y sus posibles usos aplicados con fines biotecnológicos.

El primer capitulo de esta tesis doctoral se basó en modelar el nicho ecológico de *E. cordifolia* y determinar poblaciones centrales y periféricas en su rango geográfico en Chile. Esta primera etapa fue esencial para poder dirigir el muestreo (hojas) en campo de las poblaciones. Todas las muestras vegetales colectadas fueron procesadas y sometidas al protocolo de extracción del metaboloma en condiciones de laboratorio. De manera posterior y teniendo en cuenta su papel adaptativo en la regulación de las actividades fisiológicas y celulares, es posible que la diversidad de metabolitos secundarios sintetizados en poblaciones de *E. cordifolia* pueda

seguir un patrón asociado a su posición dentro del nicho ecológico. Esta relación se deriva de la evidencia de que las especies vegetales tienden a cambiar su metaboloma (e.i., diversidad metabólica), dependiendo de las condiciones ambientales experimentadas localmente. Así, las poblaciones periféricas sometidas a condiciones ambientales subóptimas (estresantes) deberían presentar un patrón diferenciado en la síntesis de metabolitos secundarios (e.i., mayor abundancia, diversidad y singularidad de compuestos), en comparación con las poblaciones más cercanas al centro de su nicho ecológico. Por lo cual, utilizando modelos de ordenación como el análisis de componentes principales (PCA), escalamiento multidimensional no métrico (NMDS) y índice de Shannon-Wiener se evaluaron sólo las tendencias generalizadas del comportamiento metabolómicos a nivel estacional en cuatro poblaciones de *E. corifolia* respecto de su posición en su nicho ecológico.

En el segundo capítulo de esta tesis doctoral se basó en evaluar los cambios del metaboloma mediante la identificación de aquellos metabolitos que generan una clara diferenciación sólo entre la población centroide y periférica de *E. cordifoila*. Para esto los extractos fueron analizados mediante cromatografía líquida acoplada a espectrometría de masas, UHPLC-QTOF-

MS/MS. Posteriormente los datos fueron analizados mediante un modelo estadístico exploratorio PCA el cual es utilizado para la reducción de la data y el reconocimiento de patrones de agrupación (centro-periferia). A continuación, se aplicó al conjunto de datos un análisis discriminante por mínimos cuadrados parciales ortogonales (OPLS-DA) para la identificación de las variables o *features* significativos que aportan a la diferenciación entre los dos grupos (población centroide y periférica). La identificación se realizó mediante la comparación del patrón de fragmentación MS/MS de los metabolitos con datos de fragmentación de libre acceso en forma de librerías espectrales.

El último capítulo se centró en evaluar la actividad biológica de los extractos de hojas de *E. cordifolia*, considerando su ubicación en el nicho ecológico. Esto es relevante para explorar posibles aplicaciones biotecnológicas, anticipando un efecto más notable en la población periférica. Se realizó una evaluación detallada del perfil químico a partir de extractos de hoja mediante UHPLC-QTOF-MS/MS. Se evaluó la capacidad antioxidante de los extractos mediante los métodos DPPH, ABTS, ORAC y la cuantificación de polifenoles totales con el ensayo Folin-Ciocalteu. Para concluir, se realizaron pruebas microbiológicas, como el método de difusión

en pozo de agar, la determinación de concentraciones mínimas inhibitorias y bactericidas, y el análisis de formación de biopelículas. Estas pruebas permitieron valorar la capacidad de los extractos para inhibir el crecimiento de microorganismos (*E. coli*, *S. aureus*, *P. aeruginosa*, *C. albicans* y *C. glabrata*) relevantes en salud pública.

HIPOTESIS Y OBJETIVOS

Hipótesis

- Las poblaciones de *E. cordifolia* que se encuentran en la periferia del nicho ecológico presentan una mayor abundancia y/o diversidad de metabolitos secundarios que poblaciones que se distribuyen en el centro del nicho ecológico.
- Los metabolitos secundarios sintetizados por poblaciones de *E. cordifolia* que se distribuyen en la periferia del nicho ecológico, presentan una mayor actividad biológica (e.g., antioxidante y antimicrobiana) comparados con poblaciones distribuidas en el centro del nicho ecológico.

Objetivo General

Evaluar la relación entre la posición que ocupan las poblaciones de *E. cordifolia* en su nicho ecológico y la estacionalidad sobre su influencia en la síntesis de metabolitos secundarios con actividad biológica.

Objetivos Específicos

- Determinar poblaciones centrales y periféricas de *E. cordifolia* dentro de su rango geográfico en Chile.
- Evaluar los cambios del metaboloma de poblaciones de *E. cordifolia* en función de su posición dentro de su nicho ecológico y la estacionalidad.
- Determinar si el perfil químico y la actividad biológica varía en función de la posición de poblaciones de *E. cordifolia* dentro del nicho ecológico y la estacionalidad.

CAPITULO 2: RESULTADOS

2.1. Metabolome expression in *Eucryphia cordifolia* Cav. populations: Role of seasonality and ecological niche centrality hypothesis.

Manuscrito publicado en la revista *Journal of Plant Research* el 24 de Julio 2023. 10.1007/s10265-023-01483-3

Metabolome expression in *Eucryphia cordifolia* Cav. populations: Role of seasonality and ecological niche centrality hypothesis.

Camila Fuica-Carrasco [a]* Óscar Toro-Núñez [b] Andrés Lira-Noriega [c] Andy J. Pérez [d] Víctor Hernández [a]

[a] Laboratorio de Química de Productos Naturales, Departamento de Botánica, Facultad de Ciencias Naturales y Oceanográficas, Universidad de Concepción, Casilla 160-C, CP 40300000, Concepción, Chile, camilafuica@gmail.com, vhernand@udec.cl

[b] Departamento de Botánica, Facultad de Ciencias Naturales y Oceanográficas, Universidad de Concepción, Casilla 160-C, CP 40300000, Concepción, Chile, oftoro@gmail.com

[c] CONAHCyT Research Fellow, Red de Estudios Moleculares Avanzados, Instituto de Ecología, A.C., México, aliranoriega@gmail.com

[d] Departamento de Análisis Instrumental, Facultad de Farmacia, Universidad de Concepción, Casilla 160-C, CP 40300000, Concepción, Chile, aperezd@udec.cl

*corresponding author: Camila Andrea Fuica-Carrasco, email: camilafuica@gmail.com

Abstract

The ecological niche centrality hypothesis states that population abundance is determined by the position in the ecological niche, expecting higher abundances towards the center of the niche and lower at the periphery. However, the variations in the conditions that favor the persistence of populations between the center and the periphery of the niche can be a surrogate of stress factors that are reflected in the production of metabolites in plants. In this study we tested if metabolomic similarity and diversity in populations of the tree species Eucryphia cordifolia Cav. vary according to their position with respect to the structure of the ecological niche. We hypothesize that populations growing near the centroid should exhibit lower metabolites diversity than plants growing at the periphery of the niche. The ecological niche of the species was modeled using correlative approaches and bioclimatic variables to define central and peripheral localities from which we chose four populations to obtain their metabolomic information using UHPLC-DAD-QTOF-MS. We observed that populations farther away from the centroid tend to have higher metabolome diversity, thus supporting our expectation of the niche centrality hypothesis. Nonetheless, the Shannon index showed a marked variation in metabolome diversity at the seasonal

level, with summer and autumn being the periods with higher metabolite diversity compared to winter and spring. We conclude that both the environmental variation throughout the year in combination with the structure of the ecological niche are relevant to understand the variation in expression of metabolites in plants.

Keywords: Ecological niche structure, environmental condition, season, secondary metabolites, south-central Chile.

2.1.1 Introduction

Given that plants are sessile organisms, numerous mechanisms have evolved to generate an adaptive response to the local environmental conditions (Sampaio et al. 2016). Such responses promote resilience and adaptation, usually without altering the fundamental physiological processes of the individual (Isah 2019). Transduction and activation of numerous genes are mechanisms that enable the reorganization of metabolic processes and the restoration of optimal cellular homeostasis (de Simón et al. 2017; Jorge et al. 2016; Padilla-González et al. 2019). As such, secondary metabolites, as direct products of metabolic reactions, play a key role in the adaptive response to physiological changes; helping to maximize *fitness* by prioritizing immediate

defense over growth or reproduction (Fiehn 2001; Sampaio et al. 2016; Walker et al. 2022).

Metabolomics provides a comprehensive view of all low molecular weight metabolites, which are involved in different cellular processes and represent the absolute physiological state of a cell at a given time (Fernie et al. 2011; Peters et al. 2018b). These metabolites, and their interactions within a biological system, is what is known as the metabolome (Fiehn 2001). This concept allows a multidimensional view of the molecular pathways triggered by the evolutionary and ecological processes, which are also involved in a diverse array of plant functions (Walker et al. 2022). Metabolome behavior is usually well understood thanks to extensive studies conducted with model-system plants, as their known genotypes allow for establishing predictable "causal and response" relationships under highly controlled conditions (Fernie et al. 2011). The same behavior is considerably less covered with non-model systems plants, as they require complex experimental designs to evaluate and control confounding effects from variable and unpredictable local environmental conditions(Fernie et al. 2011; Field and Lake 2011). Yet, this gap of knowledge has promoted the evaluation of metabolome response in local populations, under the assumption that variation associated to

temporal and spatial scales, as well as at intra- and interspecific levels, are properly covered (Allevato et al. 2019; Li et al. 2020). Metabolomics tools that combine a separation technique such as chromatography and mass spectroscopy are the most common in chemical ecology studies (Walker et al. 2022), as they allow the detection of many features and offer high selectivity and sensitivity analysis (Gorrochategui et al. 2016).

Given the inherent relationship between secondary metabolite synthesis and local adaptation, it is possible to speculate with a predictive relationship that metabolome diversity is conditioned by the environmental variables faced by plant populations in their natural habitats (Král'ová et al. 2012). This relationship can be approximated using the ecological niche theory, in which population abundance patterns are defined by the environmental conditions of a particular location and time (Maguire, 1973). This idea has now been presented as the "ecological niche centrality hypothesis", which is considered one of the most representative models for predicting the tolerance and adaptation ranges of species (Hutchinson 1957; Sagarin et al. 2006). This hypothesis states that the performance of individuals and populations (i.e., biological *fitness*) will depend on their location within the hypervolume of their ecological niche (Martínez-Meyer

et al. 2013). The center of the niche will represent sites with optimal environmental conditions for survival and reproduction, harboring populations under very low abiotic and biotic stress (Lira-Noriega and Manthey 2014; VanDerWal et al. 2009). In contrast, populations located in areas representative of the periphery of the ecological niche should exhibit suboptimal physiological activity, as unfavorable environmental conditions should lead to higher stress response compared to other localities close to the centroid or ecological optimum (Papuga et al. 2018).

Considering their adaptive role in the regulation of physiological and cellular activities it is expected that the metabolome expressed in populations may follow a pattern relative to their position within their ecological niche space. This relationship is derived from evidence that plant species tend to change their metabolome (or metabolic diversity), depending on the environmental conditions experienced locally (Sampaio et al. 2016). As such, peripheral populations subjected to environmentally suboptimal conditions should differ significantly in the synthesis of secondary metabolites (higher abundance, diversity, and uniqueness of compounds), compared to populations closer to the center of their ecological niche where favorable conditions occur. Among the processes that induce metabolome diversity are,

for example, seasonal differences related to phenology or environmental changes in their biotic and abiotic environment (Kotilainen et al. 2010; Sampaio et al. 2016). We believe that, given the advances in their conceptual formalization, the integration of both ecological niche attributes and the study of metabolomic adaptation in plants can effectively contribute to assessing metabolomic variation under spatial and temporal scales of environmental variation, a hypothesis not yet explored explicitly (Figure 2.1.1).

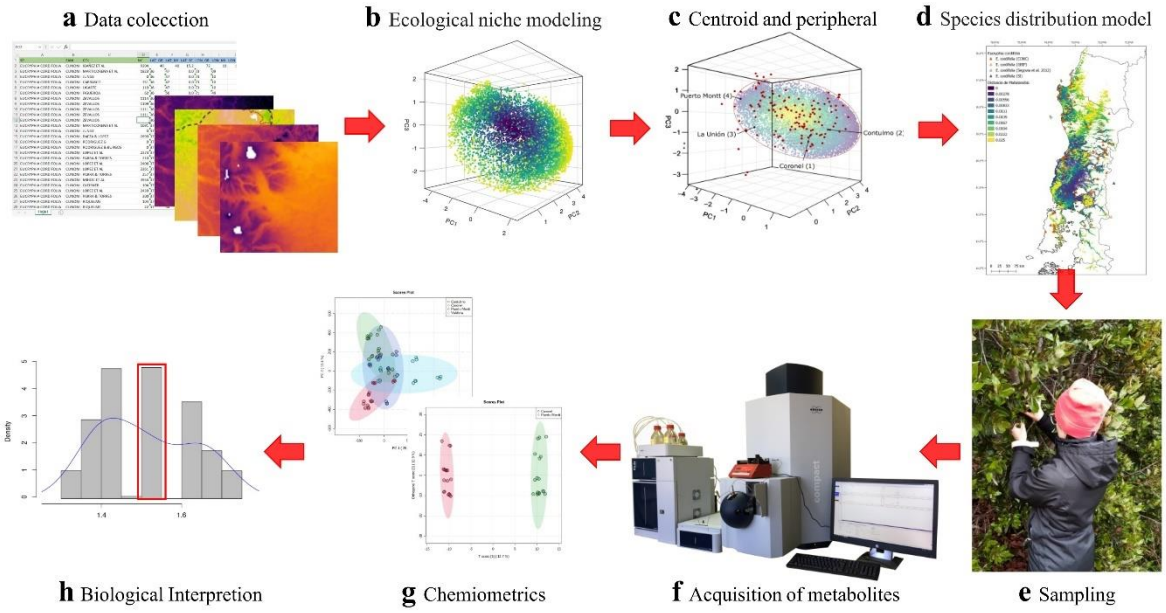

Figure 2.1.1. Workflow for establishing the relationship between the ecological niche centrality hypothesis and the metabolomic study in plants. (a) Information on species occurrence and environmental variables was compiled from various sources such as GIBIF, the Herbarium of the University of Concepción, Segovia et al. (2012), and the CHELSA database (b) An ecological niche model (ENM) was constructed to recreate the fundamental niche of *E. cordifolia* (c) Central

and peripheral populations were determined in relation to the ecological niche structure of *E. cordifolia* (d) Environmental suitability values were projected to determine the geographical location of *E. cordifolia* populations, which proved useful in guiding field sampling (see more details in the materials and methods section) (e) Field sampling was conducted in each population, collecting 6 individuals as biological replicates, and subsequently the samples were immediately submerged in liquid nitrogen and transported to the laboratory (f) Metabolic data were obtained using UHPLC-DAD-QTOF-MS. The analysis included three technical replicates for each biological replicate, in addition to preparing quality control (QC) samples (g) Data processing and modeling were performed using MetaboAnalyst and Rstudio (h) Biological interpretation of the results was carried out.

Given that sites at the periphery of the environmental niche should be subjected to higher abiotic stress, our expectation is that a higher metabolic diversity of populations should be evidenced compared to those in at the centroid. Hence, we performed a metabolomic study LC-MS in order based to evaluate how metabolome diversity (trends) varies according to the position of plant populations along the gradient between center and periphery of its ecological niche. For this purpose, we used *Eucryphia cordifolia* Cav. (Cunoniaceae) as the study species, which is an endemic tree from the Southern Chilean Forest distributed between the Bio-Bio Region and the Aysén Region (36.8° S and 43.3° S). This species may be found in both the Coastal and Andean Cordillera, mainly between 700 and 1000 m.a.s.l

(Rodriguez et al. 2018; Segovia et al. 2012). Its distribution covers areas with a diverse climatic range, from the Mediterranean type with mild winters and very dry and hot summers, to the temperate type with colder winters and moderate conditions during the summer (Figueroa et al. 2010). Do to this large environmental range in which *E. cordifolia* populations grow, this species becomes ideal to evaluate metabolomic response across the ecological niche space.

2.1.2 Materials and methods

2.1.2.1. Ecological niche modeling and estimation of distances to the niche centroide.

To reconstruct the position of populations of *E. cordifolia* in environmental space and obtain the distances from the ecological niche centroid, we first estimated the ecological niche using the correlative modeling approach based on the minimum volume ellipsoid following Osorio-Olvera et al. (2020a). This approach has been preferred over other more complex approaches (Phillips et al. 2006) given its simplicity and easier correspondence to the fundamental ecological niche (Osorio-Olvera et al. 2020b). Occurrences for the species were retrieved from various sources including the Global Biodiversity Information Facility database (GIBIF;

https://www.gbif.org/es/), the herbarium of the Universidad de Concepción (CONC), and additional work by Segovia et al. (2012). In total we compiled 197 occurrences, from which 149 corresponded to unique geographic coordinates. Before model calibration we spatially filtered these localities using a 10 km distance and discarded those with distances less than or equal to this threshold, resulting in a final count of 95 occurrences. This step is a common practice in ecological niche modelling (ENM) useful to eliminate spatial autocorrelation and model overfitting (Boria et al. 2014). For the environmental variables we used a combination of 19 bioclimatic variables from the CHELSA v. 1.2 database (https://chelsa-climate.org/bioclim/) corresponding to high-resolution (30 arc seconds) climate data for the Earth's land surface areas, based on temperature and precipitation parameters (Karger et al. 2017). Soil variables of the following parameters from the SOILGRID v1.0 database: predicted occurrence (0-100%), soil physical properties (clay and silt) and chemical properties (organic carbon content and soil pH) (https://soilgrids.org/) (Hengl et al. 2017). All variables were rescaled at a spatial resolution of 30 arcseconds (~1 km2) and were trimmed to an extent that contains the hypothesized area of dispersal and survival of the species ("M") (Barve et al. 2011). This area was estimated using a

rounding buffer of 25, 50, 130 km as limits together with the coastal line from the northernmost, southernmost, and easternmost collecting point, respectively (Fig. S1.1). The trimmed layers were then transformed via principal components analysis (PCA) using a Pearson correlation matrix with the rasterPCA function from the RStoolbox package (Yañez-Arenas et al. 2012).

Using the package ntbox v. 0.6.6.5 (Osorio-Olvera et al. 2020a), an ellipsoid was constructed using the first three principal components (87% total variance), from which the Mahalanobis distance from the centroid was obtained for each occurrence point. The obtained ENM and binary models were evaluated using the Partial Receiver Operating Characteristic Curve and the protected Area Under the Curve (pROC-AUC) after 500 replicates (Peterson et al. 2008), and a binomial test to determine non-random distribution in predicted occurrences (Anderson et al. 2003), respectively.

The final model was converted to a binary map using a 10% threshold of the suitability value, from which niche distances to the centroid were sampled. The resulting distances were then categorized into four environmental categories (center, two intermediate zones, and periphery; Figure 2.1.2 a, b), which were delimited using the k-means algorithm based

on the Calinski-Harabasz (Caliñski and Harabasz 1974) criterion implemented in the package fpc v2.2-9 (Hennig C 2020). All analyses were conducted in the statistical software R v.4.12 (R Development Core Team 2022).

2.1.2.2. Plant material and metabolome extraction

We selected a locality per each of the four categories of environmental distances (see previous section). These sites were chosen based on accessibility and procuring their distribution across the species' latitudinal range in Chile and presence within a national park to try to ensure that metabolite profiles reflect variation with the least degree of anthropogenic disturbance (Fig. 2.1.2. b). At each site, we chose six trees at random (mature, older than 10 years) 100 m apart, then marked them with the objective of always sampling the same individuals in each season (summer, autumn, winter and spring) (Table S1.1). The only exception to this sampling scheme was the Puerto Montt population (Alerce Andino National Park), which was not available for sampling due to COVID-19 pandemic restrictions during the winter of 2020. Fresh leaves (40 leaves per tree) were collected from the upper third of the crown of each tree, and care was taken to always collect them in the same position and that they were always of similar age (mature

leaves). In addition, we avoided taking samples with apparent morphological damage, however, it was difficult for the Contulmo population to fully comply with these requirements, since most of the trees in the park had leaves damaged by herbivory. All sampling was done in the morning (between 9:00 a.m 12.00 p.m) and immediately after collection, leaves were frozen in liquid nitrogen, transported to the laboratory and stored at -80 °C until needed.

For metabolite extraction, frozen fresh samples were freeze-dried and ground to fine powder in a ball mill MM-400 (GmbH, Haan, Germany) at 30 Hz for 1 min (Rivas-Ubach et al. 2013). Extraction was performed following the procedure suggested by Valledor et al. (2014). Briefly, 50 mg of each sample (in triplicate, technical replicates) were extracted with 1 mL of MeOH/Cl_2CH_2/H_2O (2.5:1:0.5), shaking at 30 hz for 1 min. After centrifuging at 1300 rpm for 10 min at 4 °C, 700 µL of the supernatant were transferred to new eppendorf tubes to perform a liquid-liquid extracted adding 400 µL H2O and 400 µL Cl_2CH_2. The tubes were shaken at 20 hz for 30 sec and subsequently centrifuged at 1300 rpm for 10 min at 4 °C. 600 µL of the aqueous upper phase were recovered, transferred to new tubes, and dried in speedvac for 5 hours at 30 °C. Dried extracts were stored at -20 °C until analysis. Immediately before analysis, the extracts were reconstituted in

MeOH 80% in water (v/v), shaken (30 hz for 1 min) and centrifuged (1300 rpm for 10 min at 4 °C). A pooled quality control sample (QC) was obtained by taking100 µL aliquot of each reconstituted extract (72 samples in total by season, except for the winter, which had only 54 samples).

2.1.2.3. LC-MS analysis

Metabolomics analysis was performed by LC-MS using an UHPLC-DAD system (Elute, Bruker Daltonics GmbH, Bremen, Germany) coupled to a quadrupole-time-of-flight mass spectrometer equipped with an atmospheric pressure electrospray ion source (Compact ESI-QTOF, Bruker Daltonik GmbH, Bremen, Germany). Chromatographic separation of the metabolome components was performed on a Kinetex C18 UHPLC column (100 × 3.0 mm,1.7 µm, Phenomenex) using a SecurityGuard Ultra Cartridge UHPLC C18 3.0 mm pre-column. The mobile phase consisted of solvent A (water with 0.1% formic acid) and solvent B (acetonitrile with 0.1% formic acid). Gradient elution was performed as follows: 5-50% of B from 0-15 min (concave increase), 50-95% of B (linear increases) from 15-15.5 min, 95% of B isocratic for 4 min, at a flow rate of 0.4 mL/min. The total chromatographic run time was 15 min. The oven temperature was set at 30 °C and the injection volume was 2 µL.

The mass spectrometer was operated in negative ion mode (-ESI) with the following parameters: mass range, 50-1500 m/z; scan cycle time, 0.2 s; dry temperature of 200 ºC; capillary voltage of 3500 V; endplate offset, 0.5 kV; desolvation gas flow of 9.0 l min-1 (N2); nebulizer pressure of 2.0 Bar. MS/MS spectra were acquired from each scan by subjecting ions (maximum 2) to collision-induced dissociation (CID) if their absolute intensities exceeded 1000 counts per 0.2 s cycle. The collision energy used ranged from 20 to 50 eV. After obtaining a spectrum, an active exclusion of the precursor ion was performed. If the fragmentation intensity was equal to than the previous measurement, its inclusion was reconsidered. Internal calibration was performed with sodium formate (10 mM in isopropanol/water, 1:1, v/v), which was pumped continuously at a rate of 1 µL/ min. through a six-port-valve so that 20 µL of it was delivered to the mass spectrometer just before each analysis. Extracts were injected in a complete random block, beginning with 1 reconstitution blank (solvente only), 3 technical blanks (considering extraction process), 6 initial QC and another QC every ten samples, maintained at 4 °C in an autosampler.

2.1.2.4. LC-MS data processing and statistical analysis

The raw LC-MS data was processed in MetaboScape 3.0 software (Bruker Daltonics, Bremen, Germany). Data were grouped according to their position regarding the ecological niche centroid (i.e., category of environmental distance) per season. The software applies T-ReX 3D algorithm (full extraction of time-aligned regions) for mass recalibration, retention time (Rt) alignment, feature extraction (m/z – Rt pairs), adducts and neutral losses handling, whole region feature extraction, and import of MS/MS spectra (Riquelme et al. 2022). The processing of the raw data signals generated a unique alignment matrix (cube table) composed of retention time, m/z and intensity, each of which indicates that, at a particular time, an ion with a particular m/z ratio was detected with a particular intensity (see Alonso et al. 2015; Garibay-Hernández et al. 2021; Smith et al. 2014). The parameters set for generation of bucket tables through T-ReX 3D algorithm were the following: intensity threshold, 400 counts; minimum spectral peak length, 4; minimum recursive peak length, 5; minimum number of recursive features to be extracted, if present in 1/3 of a group; features in a minimum number of analysis, present in 1/3 of a group; m/z range of 50-1500 and retention time ranges from 0.5 to 15 min.

The bucket tables were exported to MetaboAnalyst 5.0 for processing of the metabolomics data. Subsequently, the data was filtered using the robust interquartile range (IQR) estimation mode and escalated using the paretto algorithm, which allows eliminating deviations and adjusting the importance of high and low abundance ions to the same level. Finally, the data was used to perform a PCA as a first exploratory filter (Hervé et al. 2018; Pang et al. 2021).

Consequently, a binary matrix, a viable pretreatment that effectively simplifies metabolomics data analysis pipelines, was built by considering only the occurrence of spectral features, coding feature presence as 1 and absence as 0 (Iwanycki Ahlstrand et al. 2018; Peters et al. 2018a; Traquete et al. 2021). This matrix was constructed by reducing replicates by medians (to avoid experimental error) and subsequently used to determine the existence of clusters according to their degree of similarity and to assess the richness of metabolites synthesized in each population. For this purpose, a non-metric multidimensional scaling (NMDS) was conducted the R package vegan v.2.5-7 using the Jaccard dissimilarity index (Hervé et al. 2018; Padilla-González et al. 2017; Xu et al. 2007). For addressing richness or diversity of metabolites, the Shannon-Wiener diversity index was calculated (Peters et al.

2018a; Reverter et al. 2018)with the "diversity" function available in the BiodiversityR v2.13-1 (Kindt and Coe 2022) package in R. Finally, to demonstrate if populations or seasons can explain differences in secondary metabolite diversity, a non-parametric Kruskal-Wallis analysis was performed, using the kruskal.test function in R. Subsequently, a Dunn's test for multiple comparisons was performed using the FSA v0.9.3 package in R, using the bonferroni method to correct the cumulative p-value (Dunn 1964).

2.1.3. Results

2.1.3.1. Ecological niche modeling

The ecological niche model and corresponding binary suitability prediction were statistically significant (AUC = 0.901, pAUC = 0.659 and binomial random tests p-values < 0.05; Fig. S2) and representative of the distribution of the species (Figure 2.1.2a). The calculation of the Mahalanobis distance and the projection of the model in geographic space resulted in the identification of the following populations of *E. cordifolia* distributed at different distances from the niche centroid (Figure 2.1.2b): The population of Coronel was identified at the ecological niche centroid, specifically in the Alto Escuadrón (36°56’24.0’’S 73°04’48.0’’ W); Contulmo, corresponded as the intermediate position 1 in the Contulmo

National Monument (38°00’36.0’’ S 73°10’48.0’’ W); La Unión, was identified as the intermediate position 2 at the Alerce Costero National Park

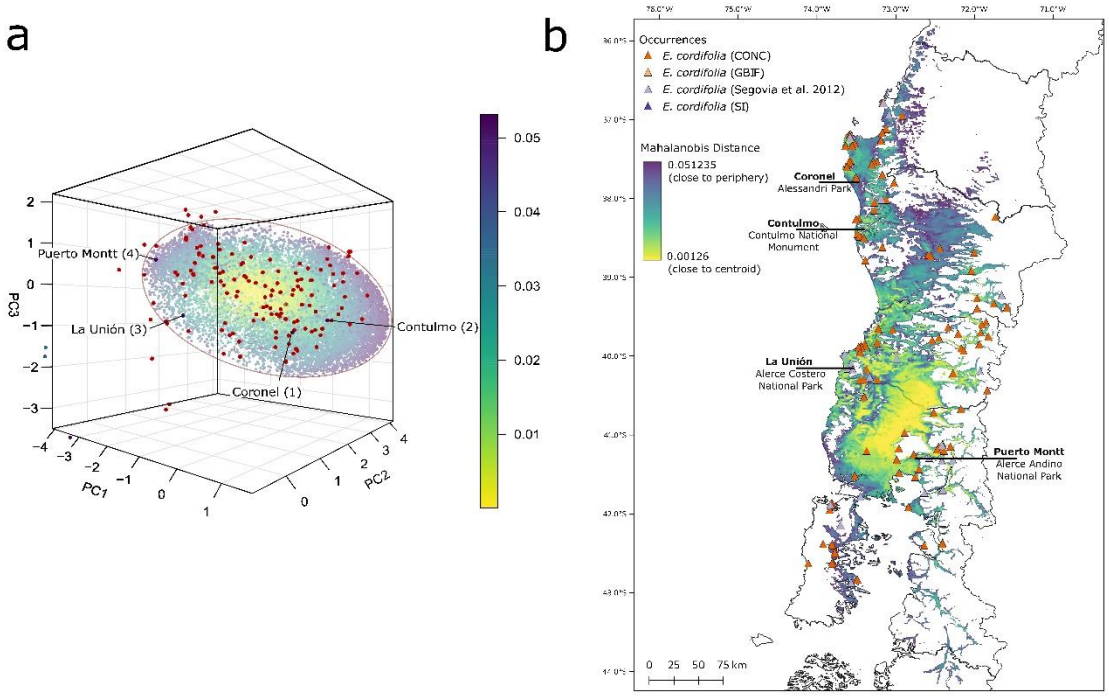

(40°12’00.0’’ S 73°24’00.0’’ W); and finally, the Puerto Montt population was labeled as peripheral in the Alerce Andino National Park (41°34’48.0’’ S 72°34’48.0’’ W).

Figure 2.1.2. Modeling of the ecological niche of *Eucryphia cordifolia*. (a) 3D characterization of *E. cordifolia* ecological niche of based on principal components from bioclimatic variables, and (b) its projection in geographic space. Yellow corresponds to environmental combinations closer to the ecological niche centroid, while blue-to-purple corresponds to combinations further aways from the centroid. Thus, Coronel corresponds to the

centroid population (mahalanobis value= 0.0766), Contulmo and La Unión are the intermediate populations (mahalanobis value= 0.00824 and 0.01248), and Puerto Montt is the peripheral population of *E. cordifolia* (mahalanobis value= 0.01904).

2.1.3.2. LC-MS data processing

Metabolomic analysis by UHPLC-DAD-QTOF-MS/MS of methanolic extracts from 270 *E. cordifolia* samples (four populations), detected a total of 10817, 10575, 6923, and 7531 negative ionization mode mass signals for summer, autumn, winter, and spring (Table S2-S5). However, after scaling, 2499 features were retained to make unsupervised methods by PCA. The first two principal components explained 40.6% of the total variation for summer (Figure 2.1.3 a, Fig. S1.3 a), 39.7% for autumn (Figure 2.1.3 b; Fig. S1.3 b), 42.7% for winter (Figure 2.1.3c; Fig. S1.3 c), and finally 34.6% for spring (Figure 2.1.3 d; Fig. S1.3 d). Observation of technical replicates revealed high concordance in their ordination of the PCA space, suggesting a limited influence in the use of mean values as summary of individual metabolic variation across similarity analyses (Figure 2.1.3 a-d).

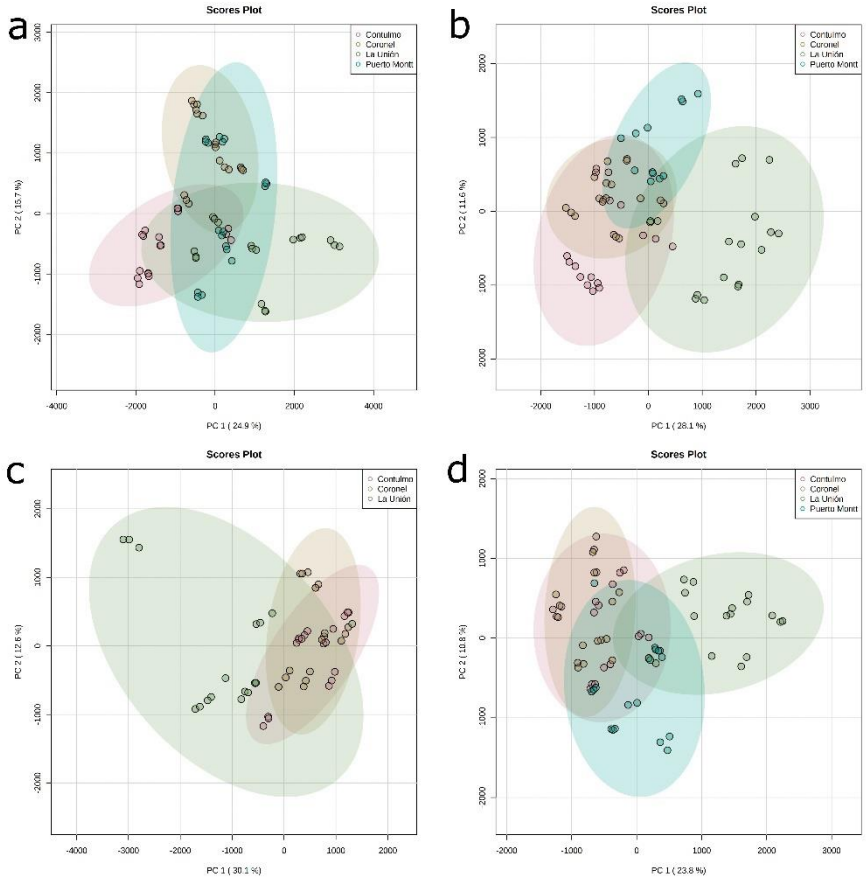

Figure 2.1.3. Principal component analysis (PCA) of metabolic data in negative ion mode for the different populations of *E. cordifolia* in each season: (a) Summer (b) Autumn (c) Winter and (d) Spring. In yellow Coronel (centroid population, n = 18), red and green Contulmo (n = 18) and La Unión (intermediate populations, n = 18) and in light blue Puerto Montt (peripheral population, n = 18). In winter, the Puerto Montt population is absent, as it could not be sampled due to COVID-19 pandemic restrictions. * n corresponds to the total number of samples per population (6 biological replicates x 3 technical replicates).

The ordination analysis (NMDS) for the four populations and seasons resulted in a two-dimensional solution with a moderately low minimum stress (stress = 0.04-0.10) (Figure 2.1.4.). As a general trend, all four populations were identified at different zones of the metabolite space. Yet, just like PCA, scatters exhibited different patterns of ordination depending upon the season under analysis. Specifically, a frequent overlap was detected among seasons between Contulmo and Coronel (except in Summer), while only sporadic associations with Puerto Montt were observed during Summer. La Union population remained as the less associated by similarity from all the analyzed populations. For summer, Puerto Montt showed greater similarity with Coronel and La Union, than Contulmo (Figure 2.1.4.a). In autumn, the separation between the central and peripheral populations was evident, showing two groups with greater metabolic similarity: Coronel with Contulmo and Puerto Montt with La Unión (Figure 2.1.4.b). In winter, while Puerto Montt was absent (see materials and methods), both Contulmo and Coronel showed more metabolic similarity than La Unión (Figure 2.1.4.c).

Finally, in spring, all populations showed less similarity among them, with the exception Coronel and Contulmo (Figure 2.1.4.d).

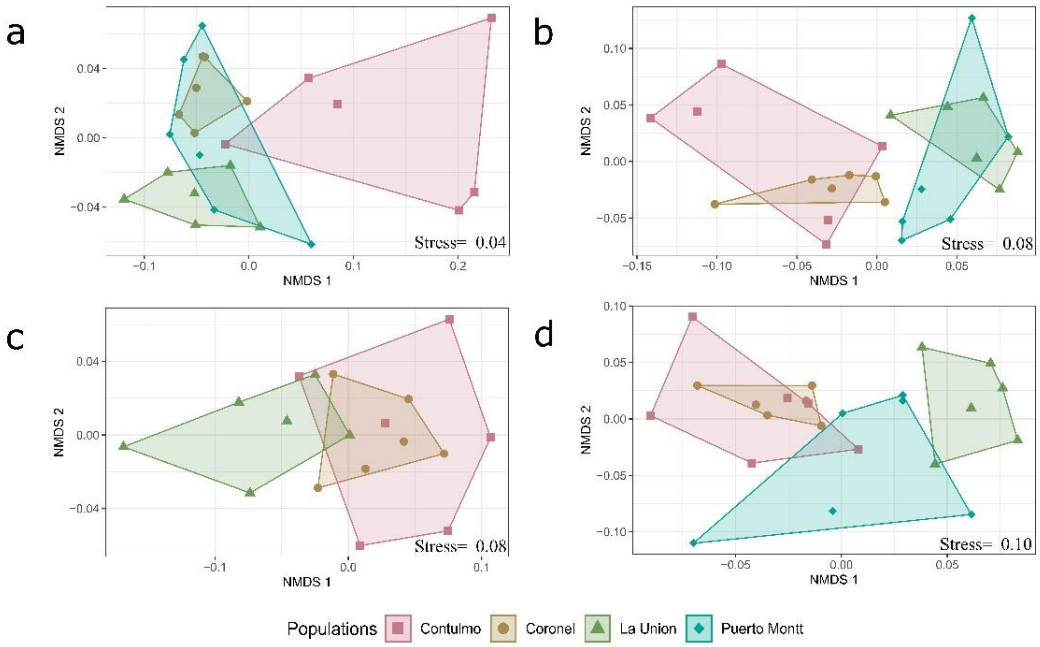

Figure 2.1.4. Non-metric multidimensional scaling (NMDS) showing the similarity between *E. cordifolia* populations in relation to their position in the ecological niche using the Jaccard dissimilarity index. (a) Summer (b) Autumn (c) Winter and (d) Spring. The centroid population in yellow (Coronel, n = 18), the intermediate populations in red and green (Contulmo, n = 18 and La Unión, n = 18) and the peripheral population in light blue (Puerto Montt, n = 18). Due to COVID-19 pandemic restrictions, Puerto Montt could not be sampled in winter. * n corresponds to the total number of samples per population (6 biological replicates x 3 technical replicates).

The comparisons conducted with the Shannon-Wiener diversity index showed significant differences in the diversity of secondary metabolites when the season of the year as a variable is considered ($\chi 2 = 71.07$; $p < 0.001$). Instead, when comparisons were conducted using populations as a factor, no significant differences were detected ($\chi 2 = 5.26$; $p = 0.1536$). Regarding seasonality, pairwise comparisons determined that both summer/autumn and spring/winter seasons were significantly different among them, with the later exhibiting the highest secondary metabolite diversity index levels (Figure 2.1.5). Regarding the distance to the centroid of the ecological niche, a tendency for the peripheral population (Puerto Montt) to have a greater diversity of metabolites in all seasons was observed (Figure 2.1.5), while the intermediate population of Contulmo presented lower diversity compared to the central population (Coronel) (Figure 2.1.5).

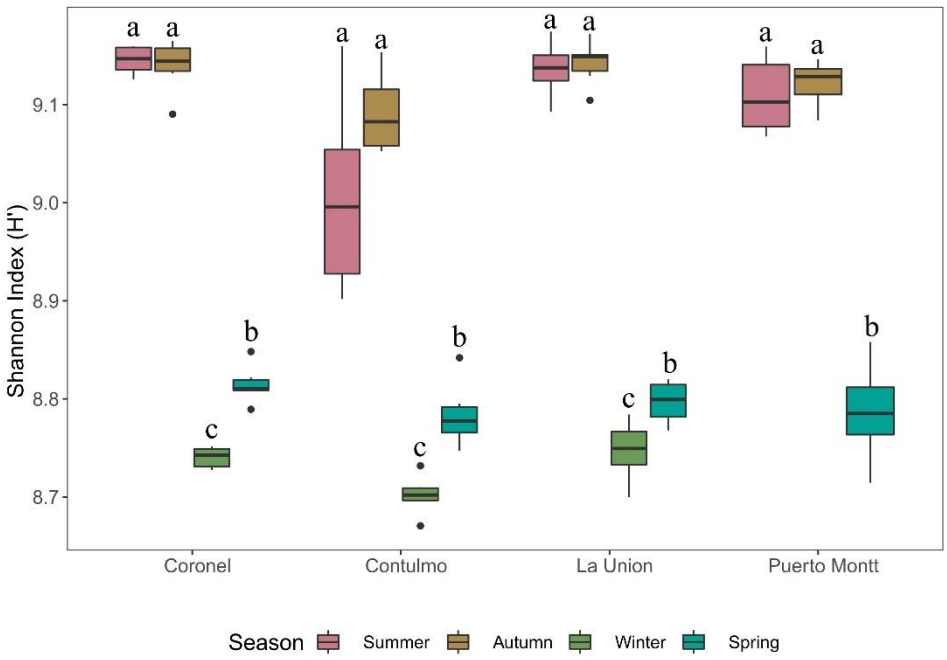

Figure 2.1.5. Seasonal variation of the metabolic diversity (Shannon diversity index) of *E. cordifolia* populations with respect to position within their ecological niche. The X axis corresponds to the populations ordered from the center to the periphery of the ecological niche of *E. cordifolia*. Coronel corresponds to the centroid (n = 18), Contulmo (n = 18) and La Unión (n = 18) to intermediate populations and Puerto Montt (n = 18) to the peripheral population. In winter, the peripheral population (Puerto Montt) was not included as it could not be sampled due to COVID-19 pandemic restrictions. * n corresponds to the total number of samples per population (6 biological replicates x 3 technical replicates).

2.1.4. Discussion

Investigating how the metabolome varies is crucial to understand its role in adaptation and *fitness* of natural populations. As such, we consider

that the ecological niche centrality hypothesis provides a starting point to analyze how metabolic variability behaves under local conditions and across environmental gradients in non-model organisms. In this sense, our study allowed us to determine some key elements which suggest the existence of patterns of metabolome variation associated with the position in the structure of the ecological niche and the temporal fluctuation of environmental conditions. The results suggested that: (1) central and peripheral localities don`t necessarily follow an obvious latitudinal environmental gradient for *E. cordifolia* in Chile, (2) the metabolic similarity between populations is better explained by seasonality than niche position and, (3) metabolomic diversity is greater as we move away from the center of the ecological niche.

2.1.4.1. Niche positioning and environmental gradient of *E. cordifolia* in Chile

Ecological niche models have proven to be efficient in predicting species habitat suitability (Peterson et al. 2011). Numerous studies have employed this approach to evaluate a series of predictions associated with key biological processes associated to trends of variation in species, such as how abundance and genetic diversity vary with respect to the distance to the ecological niche centroid (Lira-Noriega and Manthey 2014; Manthey et al.

2015; Martínez-Meyer et al. 2013; Ochoa-Zavala et al. 2022; Osorio-Olvera et al. 2020b).

From the ecological niche model, we were able to identify a suitability gradient for *E. cordifolia*, following a north-south latitudinal distributional trend. This pattern is consistent with the climatic preferences for the species, where environmentally peripheral populations are found close to the cold-temperate climates of southern Chile and those closer to the centroid are located in the Mediterranean-temperate transition zone at the north of Chile (Figueroa et al. 2010). These areas are characterized by different regimes of precipitation and temperatures, which also have been characterized to determine distinctive distributional patterns in the lineages of the Chilean Flora (Fig. S5) (Luebert and Pliscoff 2006). As posed by Hutchinson's duality (i.e., the correspondence between environmental and geographic spaces) (Colwell and Rangel 2009), the areas corresponding to the centroid or the periphery of the niche are not homogeneously distributed in the geography, a likely result of the abrupt and diverse topography present in the study area (Luebert and Pliscoff 2006); the position of the sampled populations did not follow the expected trend from north to south with respect to their position in the ecological niche, with the centroid locality (Coronel)

located in areas identified as peripheral (northern zones) and the peripheral locality (Puerto Montt) located in localities to the south of the distribution of *E. cordifolia* (Figure 2.1.2 b).

2.1.4.2. Metabolic similarity is better explained by seasonality than niche positioning

The results from the non-metric multidimensional scaling (NMDS) to assess similarity of metabolomic profiles suggests that these are better explained by seasonality rather than by their position with respect to the niche centroid. Nonetheless, under the context of seasonality, patterns of similarity were more consistently associating localities close to the centroid throughout seasons than those at the periphery. This pattern could be explained by the influence of local environmental conditions arranged along the suitability gradient and how stable conditions are throughout the year, forcing the production of metabolites that may result in a higher diversity of arrays at the periphery of the niche. Conversely, populations located in areas with optimal local environmental conditions closer to the niche centroid should present more stable metabolomic profiles. This response could be the result of the necessary phenotypic plasticity that peripheral populations show in harsher habitats (Brunetti et al. 2013; Wink 2003). This suggests there is a higher

probability for continuous changes in the synthesis of secondary metabolites that prevails in peripheral populations, thus altering their abundance, diversity, and specificity, and that result in the species' adaptation to different environments (Marr et al. 2021).

Contrary the described patterns, the intermediate population of Contulmo presented a greater metabolic dissimilarity to the centroid population during summer and depicting the highest dispersion of observations in the ordination plot (Figure 2.1.4). This pattern could be explained by elements not depicted in the environmental niche model as we implemented here with only coarse resolution interpolated variables. Instead, more refinement in variability could be achieved when microclimatic variation or biotic interactions are incorporated (Barve et al. 2011; Peterson et al. 2011; Soberón and Peterson 2020). Nevertheless, despite the apparent deficiency of this correlative modeling approach for estimating the ecological niche, it has been shown that it provides robust support for large scale analysis as we conducted here (Osorio-Olvera et al. 2020b; Peterson et al. 2008, 2011; Soberón et al. 2017). In this case, signals of herbivory were detected in the leaves of sampled trees in Contulmo (Fig. S6), which could explain the existence of metabolites not necessarily associated to

environmental adaptation. Reports of plant populations subject to insect or other pathogen attacks can induce the production of specific secondary metabolites that allow leaf damage to be arrested (Kfoury et al. 2019; Zhou et al. 2019). Under these cases, a significant increase in the production of glucose, ferulic acid, and gluconapine have been reported, which support the existence of a coordinated metabolic response to strengthen leaf resistance (Hartmann 2007; Lieurance et al. 2015).

2.1.4.3 Metabolomic diversity trends from centroid to periphery of the ecological niche

Until now, there are few works that relate studies of metabolomic in populations growing under natural conditions with seasonal variation. Such studies have been mainly oriented to evaluate the influence of seasonality on the yield and quality of plants for commercial purposes (tea leaves, essential oils, berries, among others) (Paolini et al. 2010; Zhou et al. 2019) or are limited to a few organisms such as marine sponges and bryophytes (Peters et al. 2018a; Reverter et al. 2018).

We found that the metabolomic diversity at the seasonal level in *E. cordifolia* varies throughout the seasons, being generally higher towards environmentally peripheral rather than central populations. The exception to

this trend was the intermediate population of Contulmo, for which dissimilar trends of variation could be explained by potential biotic interactions due to pathogen attacks – as aforementioned. For the rest of populations, the trend is consistent with other reports that indicate that primary metabolism generally has its highest activity in seasons favorable for plant productivity and growth, likely influencing higher or lower levels of metabolic synthesis (Gargallo-Garriga et al. 2020). Such response suggests that seasonality could inflict a direct effect on resource allocation patterns, reflecting different physiological demands associated with growth, defense, and reproduction (Gomes et al. 2019), or even inducing the development of specific adaptation strategies to changing environmental conditions (Gouvea et al. 2012; Ma et al. 2011; Zhou et al. 2019). For example, these trends can be exemplified in observations made in the metabolome of French Guiana trees, which presents specific metabolomic niches that may have resulted from their ability to adapt to dry and wet forest conditions (Gargallo-Garriga et al. 2020). Also, a direct relationship between secondary metabolite synthesis and seasonality has been demonstrated in Eremanthus mattogrossensis, which suggest rates of change over 93.48% of metabolic variation explained only by seasonal variation (Gouvea et al. 2012).

We observed that the use of the population as factor and proxy of environmental conditions did not show explanatory power of metabolomic diversity in *E. cordifolia*. This contradicts other studies that have found relevant the use of geographic position as a surrogate of the environmental conditions (e.g., climate), and of the expression rates of secondary metabolites in plants (Iwanycki Ahlstrand et al. 2018; Sampaio et al. 2016). In this sense, we suggest a couple of explanations for these findings. First, the estimate of the ecological niche and its centroid are possibly not completely captured by the ecological niche approach used in this work, as this is based on PCA-transformed bioclimatic variables (macroclimatic), which might not necessarily explain the complete amount of seasonal variation observed in metabolomic expression of the analyzed populations and the species. Second, and as mentioned in the previous section the observed differences could be the result of different stressors acting in levels that could not be possibly captured in the bioclimatic dataset proposed in this study (such as biotic interaction, microclimatic variables, anthropogenic activity, competitive interactions among others). These factors not only affect the modeling of the ecological niche, but have also been shown, together with soil pH, habitat type, leaf area or light intensity, to influence metabolomic

diversity in plants (Iwanycki Ahlstrand et al. 2018). For example, the population of Coronel is located within a highly fragmented matrix with high influence of introduced forest plantations of Eucalyptus nitens, E. globulus and Pinus radiata (Braun et al. 2017; Echeverria et al. 2006), which could influence on a generalized competition pressure for resources with potential effects on the *fitness* of local populations due to deviations in the production of secondary metabolites (Lieurance et al. 2015; Ramawat and Goyal 2020). Such biotic interactions, unfortunately, are not straightforwardly incorporated in this type of correlative ecological niche modelling, mainly due to the current paucity of biological interaction data for the focal specie.

2.1.5. Conclusion

To our knowledge, no research has been conducted on the connection between metabolite diversity and its annual expression considering the hypothesis of ecological niche centrality. Here, we demonstrate that this connection between two emerging fields of research is a promising approach to better understand the phenological responses that plants have given the influence of the environment and more specifically considering their position with respect to the ecological niche structure.

The influence of seasonality and the position of populations in their ecological niche may be useful to develop efficient experimental designs to guide field sampling of tissues (or metabolome). In such a way, this strategy could help to avoid overexploitation of resources when they are scarce or in the case of rare, endemic or endangered species. In addition, the evaluation of the metabolic behavior of plants in relation to their position within the ecological niche could be useful to putatively identify secondary metabolites, enhancing their use in the biotechnology industry. For example, recent evidence supports the presence of pentacyclic triterpene compounds, phytosterols and flavonoids for *E. cordifolia*, all important metabolites known for their seasonal variation (Viteri et al. 2022) and making them potential candidates as marker compounds for this species. Therefore, as future challenges, we hope to identify the metabolites that allow us to differentiate between central and peripheral populations and their relationship with environmental variables that determine the ecological niche of the species under study. Finally, we consider that in order to strengthen the estimation of environmental variables that influence the synthesis of secondary metabolites in plants, it would be appropriate to consider microclimatic and anthropogenic variables when modeling the ecological

niche. Furthermore, investigating how the genetic structure of environmental populations varies could be an important component to support this type of research.

This work will help broaden the horizons of theoretical and empirical research by incorporating new factors of interest in metabolomics studies. Specifically, the implementation of ecological niche theory could be important to understand how plant metabolism varies with seasonality, evolutionary history and even how species might adapt to climate change.

Author contribution

Camila Fuica Carrasco contributed to the research design, fieldwork, laboratory work and drafting of the manuscript.

Óscar Toro-Núñez contributed to research design, elaboration of the ecological niche modeling, data processing in R, revision and editing manuscript.

Andrés Lira-Noriega contributed to research design, elaboration of the ecological niche modeling, revision and editing of the manuscript.

Andy J. Pérez contributed to interpretation of metabolomic data and revision of the manuscript.

Víctor Hernández contributed to the management of access to Chile protected and private areas, financing, and manuscript review.

Acknowledgments

C.F.C gratefully acknowledge financial support was provided by National Research and Development Agency (ANID), Doctoral Scholarship Nº 21170525. O.T.N. was funded by CONICYT PAI Subvención a la Instalación en la Academia Convocatoria 2019 N°77190055. A.J.P was supported by ANID/CONICYT FONDECYT Regular 1181915 and FONDEQUIP EQM170023. We thank a National Forestry Corporation (CONAF) and Forestal Mininco S.A. (CMPC) or allowing us access to obtain plant material at their facilities. To the Laboratory of Natural Products Chemistry and Plant Metabolomics Laboratory, Universidad de Concepción for providing us with the facilities for processing the samples.

Supplementary Information

References

Allevato DM, Kiyota E, Mazzafera P, Nixon KC (2019) Ecometabolomic analysis of wild populations of *Pilocarpus pennatifolius* (Rutaceae) using unimodal analyses. Front Plant Sci 10:258. https://doi.org/10.3389/FPLS.2019.00258/BIBTEX.

Alonso A, Marsal S, Julià A, James Carroll A (2015) Analytical methods in untargeted metabolomics: state of the art in 2015. Bioengineer Biotechnol 3:1–20. https://doi.org/10.3389/fbioe.2015.00023.

Anderson RP, Lew D, Peterson AT (2003) Evaluating predictive models of species' distributions: criteria for selecting optimal models. Ecol Modell 162:211–232. https://doi.org/10.1016/S0304-3800(02)00349-6.

Barve N, Barve V, Jiménez-Valverde A, et al (2011) The crucial role of the accessible area in ecological niche modeling and species distribution modeling. Ecol Modell 222:1810–1819. https://doi.org/10.1016/J.ECOLMODEL.2011.02.011.

Boria RA, Olson LE, Goodman SM, Anderson RP (2014) Spatial filtering to reduce sampling bias can improve the performance of ecological niche models. Ecol Modell 275:73–77. https://doi.org/10.1016/J.ECOLMODEL.2013.12.012.

Braun AC, Troeger D, Garcia R, et al (2017) Assessing the impact of plantation forestry on plant biodiversity: A comparison of sites in Central

Chile and Chilean Patagonia. Glob Ecol Conserv 10:159–172. https://doi.org/10.1016/J.GECCO.2017.03.006.

Brunetti C, George RM, Tattini M, et al (2013) Metabolomics in plant environmental physiology. J Exp Bot 64:4011–4020.

Caliñski T, Harabasz J (1974) A Dendrite Method Foe Cluster Analysis. Commun Statistics 3:1–27. https://doi.org/10.1080/03610927408827101.

Colwell RK, Rangel TF (2009) Hutchinson's duality: The once and future niche. Proc Natl Acad Sci U S A 106:19651–19658. https://doi.org/10.1073/PNAS.0901650106.

de Simón BF, Sanz M, Cervera MT, et al (2017) Leaf metabolic response to water deficit in Pinus pinaster Ait. relies upon ontogeny and genotype. Environ Exp Bot 140:41–55. https://doi.org/10.1016/J.ENVEXPBOT.2017.05.017.

Dunn OJ (1964) Multiple comparisons using rank sums Technometrics. Multiple comparisons using rank sums Technometrics 6:241–252.

Echeverria C, Coomes D, Salas J, et al (2006) Rapid deforestation and fragmentation of Chilean Temperate Forests. Biol Conserv 130:481–494. https://doi.org/10.1016/J.BIOCON.2006.01.017.

Fernie AR, Aharoni A, Willmitzer L, et al (2011) Recommendations for Reporting Metabolite Data. Plant Cell 23:2477–2482. https://doi.org/10.1105/TPC.111.086272.

Fiehn O (2001) Combining genomics, metabolome analysis, and biochemical modelling to understand metabolic networks. Comp Funct Genomics 2:155–168. https://doi.org/10.1002/CFG.82.

Field KJ, Lake JA (2011) Environmental metabolomics links genotype to phenotype and predicts genotype abundance in wild plant populations. Physiol Plant 142:352–360. https://doi.org/10.1111/j.1399-3054.2011.01480.x.

Figueroa JA, Cabrera HM, Queirolo C, Hinojosa LF (2010) Variability of water relations and photosynthesis in *Eucryphia cordifolia* Cav. (Cunoniaceae) over the range of its latitudinal and altitudinal distribution in Chile. Tree Physiol. https://doi.org/10.1093/treephys/tpq016.

Gargallo-Garriga A, Sardans J, Granda V, et al (2020) Different "metabolomic niches" of the highly diverse tree species of the French Guiana rainforests. Sci Rep 10:. https://doi.org/10.1038/s41598-020-63891-y.

Garibay-Hernández A, Kessler N, Józefowicz AM, et al (2021) Untargeted metabotyping to study phenylpropanoid diversity in crop plants. Physiol Plant 173:680–697. https://doi.org/10.1111/PPL.13458.

Gomes AF, Almeida MP, Leite MF, et al (2019) Seasonal variation in the chemical composition of two chemotypes of *Lippia alba*. Food Chem 273:186–193. https://doi.org/10.1016/J.FOODCHEM.2017.11.089.

Gorrochategui E, Jaumot J, Lacorte S, Tauler R (2016) Data analysis strategies for targeted and untargeted LC-MS metabolomic studies: Overview and workflow. Trends Analyt Chem 82:425–442. https://doi.org/10.1016/J.TRAC.2016.07.004.

Gouvea DR, Gobbo-Neto L, Sakamoto HT, et al (2012) Seasonal variation of the major secondary metabolites present in the extract of *Eremanthus mattogrossensis* Less (Asteraceae: Vernonieae) leaves. Quim Nova 35:2139–2145.

Hartmann T (2007) From waste products to ecochemicals: Fifty years research of plant secondary metabolism. Phytochemistry 68:2831–2846. https://doi.org/10.1016/J.PHYTOCHEM.2007.09.017.

Hengl T, De Jesus JM, Heuvelink GBM, et al (2017) SoilGrids250m: Global gridded soil information based on machine learning. PLoS One 12:1–40. https://doi.org/10.1371/JOURNAL.PONE.0169748.

Hennig C (2020) Package 'fpc': Flexible Procedures for Clustering. 2020

Hervé MR, Nicolè F, Lê Cao KA (2018) Multivariate analysis of multiple datasets: a practical guide for chemical ecology. J Chem Ecol 44:215–234. https://doi.org/10.1007/S10886-018-0932-6/FIGURES/3.

Hutchinson GE (1957) Concluding remarks. Cold Spring Harb Symp Quant Biol 22:415–427. https://doi.org/10.1101/SQB.1957.022.01.039.

Isah T (2019) Stress and defense responses in plant secondary metabolites production. Biol Res 52:39. https://doi.org/10.1186/S40659-019-0246-3.

Iwanycki Ahlstrand N, Havskov Reghev N, Markussen B, et al (2018) Untargeted metabolic profiling reveals geography as the strongest predictor of metabolic phenotypes of a cosmopolitan weed. Ecol Evol 8:6812–6826. https://doi.org/10.1002/ECE3.4195.

Jorge TF, Mata AT, António C (2016) Mass spectrometry as a quantitative tool in plant metabolomics. Philosoph Transact Royal Society A: Math Physical Engineer Sci 374:1–26. https://doi.org/10.1098/RSTA.2015.0370.

Karger DN, Conrad O, Böhner J, et al (2017) Climatologies at high resolution for the earth's land surface areas. Sci Data 4:1–20. https://doi.org/10.1038/sdata.2017.122.

Kfoury N, Scott ER, Orians CM, et al (2019) Plant-climate interaction effects: changes in the relative distribution and concentration of the volatile

tea leaf metabolome in 2014–2016. Front Plant Sci 10:. https://doi.org/10.3389/fpls.2019.01518.

Kindt R, Coe R (2022) Tree diversity analysis: A manual and software for common statistical methods for ecological and biodiversity studies.

Kotilainen T, Tegelberg R, Julkunen-Tiitto R, et al (2010) Seasonal fluctuations in leaf phenolic composition under UV manipulations reflect contrasting strategies of alder and birch trees. Physiol Plant 140:297–309. https://doi.org/10.1111/J.1399-3054.2010.01398.X.

Král'ová K, Jampílek J, Ostrovský I (2012) Metabolomics - Useful tool for study of plant responses to abiotic stresses. Ecol Chem Engineer S 19:133–161. https://doi.org/10.2478/v10216-011-0012-0.

Li Y, Kong D, Fu Y, et al (2020) The effect of developmental and environmental factors on secondary metabolites in medicinal plants. Plant Physiol Biochem 148:80–89. https://doi.org/10.1016/J.PLAPHY.2020.01.006.

Lieurance D, Chakraborty S, Whitehead SR, et al (2015) Comparative herbivory rates and secondary metabolite profiles in the leaves of native and non-native Lonicera species. J Chem Ecol 41:1069–1079. https://doi.org/10.1007/s10886-015-0648-9.

Lira-Noriega A, Manthey JD (2014) Relationship of genetic diversity and niche centrality: a survey and analysis. Evolution 68:1082–1093. https://doi.org/10.1111/EVO.12343.

Luebert, Pliscoff (2006) Sinopsis bioclimática y vegetacional de Chile. Universitaria, Santiago, Chile.

Ma S, Baldocchi DD, Mambelli S, Dawson TE (2011) Are temporal variations of leaf traits responsible for seasonal and inter-annual variability in ecosystem CO2 exchange? Funct Ecol 25:258–270. https://doi.org/10.1111/j.1365-2435.2010.01779.x.

Maguire, B (1973) Niche response structure and the analytical potentials of its relationship to the Habitat. Am Nat 107:213–246. https://doi.org/10.1086/282827.

Manthey JD, Campbell LP, Saupe EE, et al (2015) A test of niche centrality as a determinant of population trends and conservation status in threatened and endangered North American birds. Endanger Species Res 26:201–208. https://doi.org/10.3354/ESR00646.

Marr S, Hageman JA, Wehrens R, et al (2021) LC-MS based plant metabolic profiles of thirteen grassland species grown in diverse neighbourhoods. Sci Data 8:. https://doi.org/10.1038/s41597-021-00836-8.

Martínez-Meyer E, Díaz-Porras D, Peterson AT, Yáñez-Arenas C (2013) Ecological niche structure and rangewide abundance patterns of species. Biol Lett 9:1–5. https://doi.org/10.1098/RSBL.2012.0637.

Ochoa-Zavala M, Osorio-Olvera L, Cerón-Souza I, et al (2022) Reduction of genetic variation when far from the niche centroid: prediction for mangrove species. Front Conserv Sci 2:1–14. https://doi.org/10.3389/fcosc.2021.795365.

Osorio-Olvera L, Lira-Noriega A, Soberón J, et al (2020a) ntbox: An r package with graphical user interface for modelling and evaluating multidimensional ecological niches. Methods Ecol Evol 11:1199–1206. https://doi.org/10.1111/2041-210X.13452.

Osorio-Olvera L, Yañez-Arenas C, Martínez-Meyer E, Peterson AT (2020b) Relationships between population densities and niche-centroid distances in North American birds. Ecol Lett 23:555–564. https://doi.org/10.1111/ELE.13453.

Padilla-González GF, Diazgranados M, Da Costa FB (2017) Biogeography shaped the metabolome of the genus Espeletia: a phytochemical perspective on an Andean adaptive radiation. Sci Rep 7:1–11. https://doi.org/10.1038/s41598-017-09431-7.

Padilla-González GF, Frey M, Gómez-Zeledón J, et al (2019) Metabolomic and gene expression approaches reveal the developmental and environmental regulation of the secondary metabolism of yacón (Smallanthus sonchifolius, Asteraceae). Sci Rep 9:1–15. https://doi.org/10.1038/s41598-019-49246-2.
Pang Z, Chong J, Zhou G, et al (2021) MetaboAnalyst 5.0: narrowing the gap between raw spectra and functional insights. Nucleic Acids Res 49:W388–W396. https://doi.org/10.1093/NAR/GKAB382.

Paolini J, Barboni T, Desjobert JM, et al (2010) Chemical composition, intraspecies variation and seasonal variation in essential oils of Calendula arvensis L. Biochem Syst Ecol 38:865–874. https://doi.org/10.1016/j.bse.2010.07.009.

Papuga G, Gauthier P, Pons V, et al (2018) Ecological niche differentiation in peripheral populations: a comparative analysis of eleven Mediterranean plant species. Ecography 41:1650–1664. https://doi.org/10.1111/ECOG.03331.

Peters K, Gorzolka K, Bruelheide H, Neumann S (2018a) Computational workflow to study the seasonal variation of secondary metabolites in nine different bryophytes. Sci Data 5:1–11. https://doi.org/10.1038/sdata.2018.179.
Peters K, Worrich A, Weinhold A, et al (2018b) Current challenges in plant eco-metabolomics. Int J Mol Sci 19:1385. https://doi.org/10.3390/IJMS19051385.

Peterson A, Soberón J, Pearson RG, et al (2011) Ecological niches and geographic distributions (MPB-49). Princeton University Press, Princeton and Oxford.

Peterson AT, Papeş M, Soberón J (2008) Rethinking receiver operating characteristic analysis applications in ecological niche modeling. Ecol Modell 213:63–72. https://doi.org/10.1016/J.ECOLMODEL.2007.11.008.

Phillips SB, Aneja VP, Kang D, Arya SP (2006) Modelling and analysis of the atmospheric nitrogen deposition in North Carolina. Int J Glob Environ Issues 6:231–252. https://doi.org/10.1016/J.ECOLMODEL.2005.03.026.

R Development Core Team (2022) a language for statistical computing. R Foundation for Statistical Computing. Vienna, Austria.

Ramawat KG, Goyal S (2020) Co-evolution of secondary metabolites during biological competition for survival and advantage: an overview. Reference Series Phytochem 3–17. https://doi.org/10.1007/978-3-319-96397-6_45.

Reverter M, Tribalat MA, Pérez T, Thomas OP (2018) Metabolome variability for two Mediterranean sponge species of the genus *Haliclona*: specificity, time, and space. Metabolomics 14:1–12. https://doi.org/10.1007/S11306-018-1401-5.

Riquelme S, Campos J V., Pecio Ł, et al (2022) *Sirex noctilio* infestation led to inevitable pine death despite activating pathways involved in tolerance. Phytochemistry 203:. https://doi.org/10.1016/J.PHYTOCHEM.2022.113350.

Rivas-Ubach A, Pérez-Trujillo M, Sardans J, et al (2013) Ecometabolomics: optimized NMR-based method. Methods Ecol Evol 4:464–473. https://doi.org/10.1111/2041-210X.12028.

Rodriguez R, Marticorena C, Alarcón D, et al (2018) Catálogo de las plantas vasculares de Chile. Gayana Bot 75:1–430. https://doi.org/10.4067/S0717-66432018000100001.

Sagarin RD, Gaines SD, Gaylord B (2006) Moving beyond assumptions to understand abundance distributions across the ranges of species. Trends Ecol Evol 21:524–530. https://doi.org/10.1016/J.TREE.2006.06.008.

Sampaio BL, Edrada-Ebel R, Da Costa FB (2016) Effect of the environment on the secondary metabolic profile of *Tithonia diversifolia*: a model for environmental metabolomics of plants. Sci Rep 6:1–11. https://doi.org/10.1038/srep29265.

Segovia RA, Pérez MF, Hinojosa LF (2012) Genetic evidence for glacial refugia of the temperate tree *Eucryphia cordifolia* (Cunoniaceae) in southern South America. Am J Bot 99:121–129. https://doi.org/10.3732/AJB.1100013.

Smith R, Mathis AD, Ventura D, Prince JT (2014) Proteomics, lipidomics, metabolomics: A mass spectrometry tutorial from a computer scientist's point of view. BMC Bioinform 15:1–14. https://doi.org/10.1186/1471-2105-15-S7-S9/FIGURES/10.

Soberón J, Osorio-Olvera L, Peterson T, et al (2017) Diferencias conceptuales entre modelación de nichos y modelación de áreas de distribución. Rev Mex Biodivers 88:437–441. https://doi.org/10.1016/J.RMB.2017.03.011.

Soberón J, Peterson & AT (2020) What is the shape of the fundamental Grinnellian niche? Theor Ecol 13:105–115. https://doi.org/10.1007/s12080-019-0432-5.

Traquete F, Luz J, Cordeiro C, et al (2021) Binary simplification as an effective tool in metabolomics data analysis. Metabolites 11:788. https://doi.org/10.3390/METABO11110788.

Valledor L, Escandón M, Meijón M, et al (2014) A universal protocol for the combined isolation of metabolites, DNA, long RNAs, small RNAs, and proteins from plants and microorganisms. Plant J 79:173–180. https://doi.org/10.1111/TPJ.12546.

VanDerWal J, Shoo LP, Johnson CN, Williams SE (2009) Abundance and the environmental niche: Environmental suitability estimated from niche models predicts the upper limit of local abundance. Am Nat 174:282–291. https://doi.org/10.1086/600087.

Viteri R, Giordano A, Montenegro G, Zacconi FC (2022) Flavonoids and triterpenes isolated from *Eucryphia cordifolia* (Cunoniaceae). Biochem Syst Ecol 104:104476. https://doi.org/10.1016/j.bse.2022.104476.

Walker TWN, Alexander JM, Allard PM, et al (2022) Functional Traits 2.0: The power of the metabolome for ecology. J Ecol 110:4–20. https://doi.org/10.1111/1365-2745.13826.

Wink M (2003) Evolution of secondary metabolites from an ecological and molecular phylogenetic perspective. Phytochemistry 64:3–19.

Xu Y, Gong F, Dixon SJ, et al (2007) Application of dissimilarity indices, principal coordinates analysis, and rank tests to peak tables in metabolomics of the gas chromatography/mass spectrometry of human sweat. Anal Chem 79:5633–5641. https://doi.org/10.1021/AC070134W.

Yañez-Arenas C, Martínez-Meyer E, Mandujano S, Rojas-Soto O (2012) Modelling geographic patterns of population density of the white-tailed deer in central Mexico by implementing ecological niche theory. Oikos 121:2081–2089. https://doi.org/10.1111/J.1600-0706.2012.20350.X

Zhou P, Hu O, Fu H, et al (2019) UPLC–Q-TOF/MS-based untargeted metabolomics coupled with chemometrics approach for *Tieguanyin* tea with seasonal and year variations. Food Chem 283:73–82. https://doi.org/10.1016/j.foodchem.2019.01.050.

2.2. Enfoque metabolómico no dirigido para evaluar la variación intraespecífica de metabolitos secundarios en poblaciones de *Eucryphia cordifolia* Cav. (Cunoniaceae) en función de su nicho ecológico.

2.2.1. Introducción

El metaboloma vegetal abarca tanto metabolitos primarios (azúcares, aminoácidos y nucleótidos) como secundarios (terpenoides y fenoles), los cuales desempeñan un papel crucial en la regulación de diversas funciones biológicas (Hong et al., 2016; Patel et al., 2021). Estos metabolitos actúan como receptores finales de la información biológica, y su nivel puede influir en la estabilidad de las proteínas, la regulación metabólica y la expresión génica (Summer et al., 2003; Hill et al., 2015; Anzano et al. 2021). La composición química del metaboloma vegetal es responsable de una amplia variedad de funciones ecológicas y fisiológicas, como la integridad estructural celular, la transmisión de señales intercelulares e intracelulares, la respuesta a factores de estrés abiótico y biótico, y las funciones fundamentales de las células vegetales (Mohiuddin et al., 2019; Walker et al., 2022; Hong et al., 2016). Por lo tanto, la medición cualitativa y cuantitativa de estos metabolitos en condiciones definidas puede reflejar el estado celular y proporcionar información esencial sobre los procesos que controlan el fenotipo bioquímico tanto de la célula como de la planta en su conjunto (Sumner et al., 2003; Tugizimana et al., 2013), a esta medición se le conoce como metabolómica (Arabona et al. 2013).

Metabólomica es una herramienta holística orientada a proporcionar una visión general cualitativa y semi cuantitativa esencialmente imparcial y completa de los metabolitos presentes en un organismo (Fernie & Keurentjes, 2011). El resultado de un análisis metabolómico es altamente dependiente de las metodologías e instrumentos analíticos para identificar y cuantificar exhaustivamente cada metabolito (Hong et al. 2016). Estas metodologías difieren en su sensibilidad, el número y tipo de compuestos analizados y el nivel de información estructural proporcionada (Summer et al. 2003; Moco et al. 2006).

Una sola técnica analítica no es adecuada para detectar y cuantificar los metabolitos (Raza et al. 2020). Las herramientas analíticas que combinan una técnica de separación como la cromatografía y la espectroscopía de masas son las más comunes en estudios metabolómicos (Wong et al. 2020). LC-ESI-MS (cromatografía líquida acoplada a espectrometría de masas con ionización electrospray) es una plataforma ampliamente aceptada para el perfilado no dirigido de metabolitos en extractos de plantas (Farag et al. 2013). En comparación con la cromatografía líquida convencional (LC), la cromatografía líquida de ultra rendimiento (UHPLC) permite un análisis más rápido de metabolitos y una mejor separación de picos por su eficiencia. La

tecnología UHPLC-Q-TOF-MS ofrece una amplia variedad de metabolitos y una alta sensibilidad para detectar compuestos químicos. Cuando se acopla con espectrometría de masas (MS), se obtiene la relación masa-carga y tiempo de retención, parámetros cruciales para lograr una identificación más precisa de los compuestos (Sun et al. 2012; Geng et al. 2018). Esta tecnología se ha utilizado para estudiar perfiles de metabolitos en taxa estrechamente relacionados, diferentes cultivares de taxa individuales y plantas en distintas etapas de desarrollo y/o sitios geográficos (Farag et al., 2013; Mais et al. 2018).

Partimos de la suposición de que cada especie posee un perfil metabolómico único y específico a nivel de especie, el cual se correlaciona con su posición en un espacio ambiental del nicho ecológico (Gargallo-Garriaga et al. 2020). Este espacio corresponde la combinación de diversas variables ambientales que definen el nicho ecológico de una especie (Soberón et al. 2017). La teoría ecológica propone que la estructura interna del nicho de una especie determina su abundancia (Maguire 1973). Específicamente, se hipotetiza que la abundancia debería disminuir desde el centroide del nicho hasta la periferia, mostrando una relación negativa (Osorio-Olvera et al. 2020), independientemente de donde se encuentre geográficamente (Ferrer-

Sánchez et al. 2021). Tal tendencia varía en función de la combinación de las variables ambientales, siendo favorables en el centro del nicho ecológico y lo contrario ocurre en la periferia. Bajo este supuesto, es probable que el metaboloma en plantas debería exhibir cierto grado de flexibilidad (componente fenotípico) para adaptarse a la variabilidad espacial y temporal de las condiciones ambientales en función de la posición de las especies en su nicho ecológico.

Eucryphia cordifolia es un árbol siempreverde que se encuentra en los bosques del sur de Chile (Morales et al. 2014). Su distribución abarca una amplia franja latitudinal, que se extiende desde la zona Centro-Sur hasta el Sur de Chile, entre los 36.8° S y 43.3° S (Figueroa et al. 2010). Esta especie está presente tanto en la Cordillera de la Costa como en la Cordillera de los Andes, principalmente en áreas de baja elevación que oscilan entre los 700 y los 1000 m.s.n.m (Segovia et al., 2012; Rodríguez et al., 2018). Dentro de su rango latitudinal, *E. cordifolia* se adapta a una amplia variedad de climas, desde zonas de clima mediterráneo con inviernos suaves y veranos muy secos y cálidos, hasta zonas de clima templado con inviernos más fríos y condiciones más húmedas durante el verano (Figueroa et al. 2010). Esto sugiere que *E. cordifolia* tiene la capacidad de habitar en una amplia gama

de hábitats con diversas condiciones ambientales (Figueroa et al. 2010), lo cual la hacen una especie atractiva para evaluar el comportamiento de su metabolismo.

Bajo estos supuestos, el objetivo de este estudio fue examinar si la posición de las poblaciones de *E. cordifolia* ubicados en el centro o la preriferia de su nicho ecológico influye en su comportamiento metabólico y si se observan diferencias entre estas poblaciones. Para ello, se utilizó un enfoque multidisciplinario integrando la teoría del nicho ecológico y la metabolómica no dirigida basado en UHPLC-DAD-QTOF-MS/MS

2.2.2. Materiales y Métodos

2.2.2.1. Material vegetal

Las muestras de hojas de *E. cordifolia* se recolectaron de acuerdo con su posición en su nicho ecológico (centroide o periferia) previamente definidas por Fuica-Carrasco et al. (2023). La población central de Coronel (36°56'45"S 73°05'10"O), la población intermedia 1 de Contulmo (38°00'47"S 73°11'09"O), la población intermedia 2 de La Unión (40°11'59"S 73°25'43"O) y la población periférica de Puerto Montt (41°35'35"S 72°35'36"O). Se tomaron muestras aleatorias de 6 árboles sólo de la población ambientalmente periférica (Puerto Montt) y central (Coronel) durante las estaciones de verano, otoño y primavera. En este estudio, la temporada de invierno no se consideró debido a las restricciones impuestas por la pandemia de COVID-19, lo cual impidió la recolección de las muestras en Puerto Montt. Las hojas frescas colectadas del tercio superior de la copa de cada árbol se congelaron inmediatamente en nitrógeno líquido, se transportaron al laboratorio y se almacenaron a -80°C hasta su uso posterior.

2.2.2.2. Manipulación de muestras y extracción de metabolomas

Para la extracción de metabolitos, las muestras frescas congeladas se liofilizaron y se trituraron hasta obtener un polvo fino en un molino de bolas MM-400 (Retsch GmbH, Haan, Alemania) a 30 Hz durante 1 minuto (Rivas-Ubach et al., 2013). Todas las muestras fueron procesadas en triplicado utilizando un diseño de bloque completo al azar para la extracción y análisis del metaboloma. La extracción se realizó siguiendo el procedimiento sugerido por Valledor et al., (2014). En resumen, se llevó a cabo en primera instancia una extracción sólido-líquido donde se extrajo 50 mg de cada muestra (en triplicado, réplicas técnicas) con 1 ml de MeOH/Cl_2CH_2/H_2O (2,5:1:0,5), agitando a 30 Hz durante 1 minuto. Después de centrifugar a 1300 rpm durante 10 minutos a 4°C, se transfirieron 700 µL del sobrenadante a nuevos tubos de Eppendorf para realizar una extracción líquido-líquido, añadiendo 400 µL de H_2O y 400 µL de Cl_2CH_2. Los tubos se agitaron a 20 Hz durante 30 segundos y posteriormente se centrifugaron a 1300 rpm durante 10 minutos a 4°C. Se recuperaron 600 µL de la fase acuosa superior, se transfirieron a nuevos tubos y se secaron en un speedvac durante 5 horas a 30°C. Los extractos secos se almacenaron a -20°C hasta su análisis.

2.2.2.3. Análisis LC-MS

Justo antes del análisis, los extractos se reconstituyeron en MeOH al 80% en agua (v/v), se agitaron (30 Hz durante 1 minuto) y se centrifugaron (1300 rpm durante 10 minutos a 4°C). Se obtuvo una muestra de control de calidad (QC) combinada, tomando una alícuota de 100 µL de cada extracto reconstituido. A continuación, las muestras en blanco, el control de calidad y los extractos de las plantas se transfirieron a insertos de 200 µL ubicados en viales ámbar de 1,5 ml. Estos viales se colocaron en un muestreador automático de cromatografía líquida, que se mantuvo a 4 °C y operó como una secuencia aleatoria predeterminada. El proceso comenzó con un blanco de reconstitución (solo disolvente), seguido de tres blancos técnicos (considerando el proceso de extracción), seis controles de calidad iniciales y luego un control de calidad cada diez muestras.

El análisis metabolómico se realizó mediante LC-MS utilizando un sistema UHPLC-DAD (Elute, Bruker Daltonics GmbH, Bremen, Alemania) acoplado a un espectrómetro de masas cuadrupolo-tiempo de vuelo equipado con una fuente de ionización por electrospray a presión atmosférica (Compact ESI-QTOF, Bruker Daltonik GmbH, Bremen, Alemania). La separación cromatográfica de los componentes del metaboloma se llevó a cabo en una columna UHPLC Kinetex C18 (100 × 3.0 mm, 1.7 µm,

Phenomenex) utilizando una pre-columna SecurityGuard Ultra Cartridge UHPLC C18 de 3.0 mm. La fase móvil consistió en el solvente A (agua 0.1% de ácido fórmico) y el solvente B (acetonitrilo 0.1% de ácido fórmico). La elución gradiente se realizó de la siguiente manera: 5-50% de B de 0-15 min (aumento cóncavo), 50-95% de B (aumentos lineales) de 15-15.5 min, 95% de B isocrático durante 4 min, a un caudal de 0.4 mL/min. El tiempo total de ejecución cromatográfica fue de 15 min. La temperatura del horno se fijó a 30°C y el volumen de inyección fue de 2 µL.

El espectrómetro de masas se operó en los modos de adquisición ESI negativo y positivo. En un rango de masas de 50 a 1500 m/z, el tiempo de ciclo de exploración fue de 2.0 s (-ESI) y 1.0 s (+ESI); la temperatura de secado fue de 200°C; el voltaje de la capilar fue de 3.4 kV (-ESI) y 4.0 kV (+ESI); el desplazamiento de la placa final fue de 0.5 kV; el flujo del gas de desolvatación fue de 9.0 l/min (N_2); el nebulizador fue de 2.0 bar. Los espectros MS/MS se adquirieron en cada exploración sometiendo a los iones (máximo 2) a una disociación inducida por colisión (CID) si sus intensidades absolutas superaban las 1000 cuentas por ciclo de 0.1 s, con una energía de colisión variable en el rango de 20 a 50 eV (-ES) y 5-10 eV (+ES). Se aplicó la exclusión activa del ion precursor después de un espectro, y la

fragmentación se volvió a considerar si su intensidad era al menos igual a la medida previamente. La calibración interna se realizó con formiato de sodio (10 mM en iso-PrOH/H_2O, 1:1, v/v), que se bombeó continuamente a una velocidad de 1 µL/min a través de una válvula de seis puertos, de modo que 20 µl de él se entregaron al espectrómetro de masas justo antes de cada análisis.

2.2.2.4. Procesamiento de datos y estadísticas

Los datos brutos de LC-MS fueron procesados con el software MetaboScape 3.0 (Bruker Daltonics, Bremen, Alemania). Los datos se agruparon según su posición con respecto al centroide del nicho ecológico (es decir, la categoría de distancia ambiental) por temporada. El software aplica el algoritmo T-ReX 3D (extracción completa de regiones alineadas en el tiempo) para la recalibración de masas, alineación del tiempo de retención (Rt), extracción de características (pares m/z - Rt), manejo de aductos y pérdidas neutras, extracción de características de la región completa, importación de espectros MS/MS (Riquelme et al., 2022). El procesamiento de las señales de los datos brutos generó una matriz de alineación única (tabla de cubos) compuesta por tiempo de retención, m/z e intensidad, cada uno de los cuales indica que, en un momento particular, se detectó un ion con una

relación m/z particular con una intensidad particular (ver Smith et al., 2014; Alonso et al., 2015; Garibay-Hernández et al., 2021). Los parámetros establecidos para la generación de tablas de cubos mediante el algoritmo T-ReX 3D fueron los siguientes: umbral de intensidad, 400 cuentas; longitud mínima del pico espectral, 4; longitud mínima del pico recursivo, 5; número mínimo de características recursivas a extraer, si están presentes en 1/3 de un grupo; características en un número mínimo de análisis, presentes en 1/3 de un grupo; rango de m/z de 50-1500 y rangos de tiempo de retención de 0.5 a 15 min.

Las tablas de cubos se exportaron a MetaboAnalyst 5.0 para el procesamiento de los datos de metabolómica. Posteriormente, los datos se filtraron utilizando el modo de estimación robusta del rango intercuartílico (IQR) y se escalonaron utilizando el algoritmo de Pareto, que permite eliminar desviaciones y ajustar la importancia de los iones de alta y baja abundancia al mismo nivel. Posteriormente, los datos se utilizaron para realizar un PCA como primer filtro exploratorio (Hervé et al., 2018; Pang et al., 2021). A continuación, se realizó un análisis de discriminación por mínimos cuadrados parciales ortogonales supervisado (OPLS-DA), que permitió descubrir *features* que mejor discriminaban entre las muestras de *E.*

cordifolia en su nicho ecológico. Los *features* que desempeñan un papel importante en la distinción entre las muestras de *E. cordifolia* en diferentes comparaciones de nicho ecológico se seleccionaron mediante *S*-plot. El modelo OPLS-DA impone agresivamente la separación de estas dos clases, lo que provoca un riesgo de ajuste excesivo del modelo a los datos. Por lo tanto, el modelo fue validado en base a pruebas de permutación (n=1000) con validación cruzada con los parámetros de validación, R^2Y para evaluar el ajuste del modelo a los datos y Q^2 para evaluar la capacidad de predicción del modelo. (Chen et al. 2021).

2.2.2.5. Anotación de metabolitos

La anotación de los metabolitos detectados en el enfoque metabolómico se basó en múltiples criterios, como m/z precisos, tiempo de retención, patrón isotópico y patrón de fragmentación. Para lograr esto, se utilizó MetaboScape 3.0, que ofrece diversas funciones. En primer lugar, SmartFormula determinó las fórmulas moleculares con alta precisión utilizando información detallada de patrones isotópicos y de masa, con una tolerancia de 5 ppm. Luego, Compound Crawler exploró bases de datos de libre acceso como ChEBI, ChemSpider y PubChem para encontrar

estructuras compatibles con las fórmulas clasificadas. Finalmente, Metfrag analizó los posibles candidatos proporcionados por Compound Crawler, buscando iones que coincidieran con los patrones de fragmentación esperados y clasificándolos en función de los picos de fragmentos explicados y la intensidad. Se utilizaron bibliotecas MS/MS en MetaboScape 3.0 para comparar los espectros MS/MS de una función con los espectros de compuestos conocidos en bibliotecas espectrales previamente importadas, como Bruker MetaboBASE y Vaniya/Fiehn del MassBank of North America (MoNA). Además, se aprovechó la utilidad de SIRIUS 4.0, un servicio web gratuito que combina el análisis de patrones isotópicos de alta resolución y los árboles de fragmentación para mejorar la anotación de los metabolitos.

2.2.3. Resultados

2.2.3.1. Análisis no dirigido de datos LC-QTOF/MS utilizando estadística multivariante.

Para evaluar las tendencias en la diferenciación química de las poblaciones de *E. cordifolia* en función de su nicho ecológico se realizó un Análisis de Componentes Principales (PCA) por estación del año investigada. En la Figura 2.2.1*a* se observa el gráfico de *score* de la población centroide (Coronel) frente a la población periférica (Puerto Montt) en verano en los

modos de adquisición negativo (-ESI), evidenciando una agrupación parcial de las poblaciones a lo largo del PC1 y PC2 con una varianza explicada total de 40.7% (-ESI) (Figura 2.2.1*a*) y 36.4 (+ESI) (ver material suplementario Fig. S2.1*e*). Para encontrar claramente los metabolitos significativamente correlacionados con la posición de las poblaciones en su nicho ecológico se construyó un modelo predictivo de discriminación utilizando el modelo OPLS-DA. Los gráficos de puntuación de los modelos de regresión OPLS-DA lograron una separación perfecta entre ambos grupos, mostrando una correlación del 13.5 % (-ESI) (Figura 2.2.1*b*) y 12.7% (+ESI) (Fig S2.1*f*) en relación con la varianza de los datos Los *features* (metabolitos) potenciales para la separación por efecto de la posición de las poblaciones en su nicho ecológico se identificaron posteriormente mediante *S*-plots, que se representan con covarianza (p) frente a la correlación (pcorr) y donde cada punto indica un par ion rt-m/z. En este gráfico, cuanto más lejos esté un punto de datos específico de cero en el eje X o Y, mayor será su contribución o nivel de confianza para la separación de las poblaciones, respectivamente. Los puntos en ambos extremos de la curva en forma de "S", representan posibles marcadores químicos con la mayor confianza. En base a nuestros resultados, los *features* ubicados en el extremo superior derecho

se correlacionan con la población ambientalmente periférica (Puerto Montt), mientras que los *features* ubicados en el extremo izquierdo están correlacionados con la población centroide (Coronel) (Figura 2.2.1*c*).

Se identificó un total de 6 metabolitos significativamente regulados al alza en los extractos de hojas de *E. cordifolia* correspondiente a la población periférica (Puerto Montt) durante la estación de verano, como se muestra en la Figura 2.2.1*c*. Entre estos metabolitos se destacan compuestos como glucósidos de flavonol, como quercetin-3-O-hexoside (**1**) y quercetin -3-O-deoxyhexoside (**3**); glucósido de flavanonol, como taxifolin-deoxyhexose (**4**); compuestos sulfatados, como Ethyl-5-octyl-2.2-dioxo-1.3.2-dioxathiolane-4-carboxylate (**2**) y dimethoxy apigenin sulfonic acid (**6**). Por último, se encontró un glucósido de sesquiterpeno cicloxano identificado como 7-Megaestigmene-3,6,9-triol hexoside (5).

Por otro lado, los *features* ubicados en el extremo izquierdo de la gráfica *S*-plot muestran una correlación con la población centroide de E. cordifolia en Coronel, lo que indica una regulación a la baja en la población periférica de Puerto Montt. Se identificaron un total de 12 metabolitos, entre los cuales destacan la presencia de glucósidos de flavanona, como taxifolin pentoside (**1′** y **2′**); flavonoles, como dimetil quercetina (**3′**) y syringetin (**7′**);

glucósido de flavanonol, como taxifolin-deoxyhexose (**12′**); glucósido de sesquiterpeno cicloxano, como ácido quínico (**10′**) y compuestos sulfatados (**2′ 4′ 5′ 6′ y 8′**).

En el modo de ionización positiva (+ESI), se identificaron un total de 7 compuestos que mostraron una regulación al alza en Puerto Montt durante la estación de verano (Fig S2.1*g*, Tabla S2.1). En esta ocasión, solo se incluyeron aquellos iones que no se reportaron en el modo de ionización -ESI. Se identificaron flavonol, como quercetina (**1** y **2**); flavanonas, como taxifolin (**5**); flavanoles, como procyanidin B1 (**6**) y flavonas, como luteolin (**7**). Por otro lado, los metabolitos que mostraron una regulación significativa a la baja fueron los siguientes: flavonas, como cirsiliol (**1′**) y tricin hexoside (**6′**); flavanoles, como syrgetin hexoside (**3′**), isorhamnetin-hexoside (**5′**) y laricitrin-hexoside (**7′**).

Finalmente, se llevó a cabo una validación cruzada y una prueba de permutación aleatoria (1000 veces) para validar el modelo OPLS-DA correspondiente. En los gráficos de la prueba de permutación, se obtuvieron valores de $Q^2 = 0.965$ y $R^2Y = 0.991$ para -ESI (Figura 2.2.1*d*), y $Q^2 = 0.963$ y $R^2Y = 0.996$ para +ESI (Fig S2.1*h*), lo que indica una alta predictibilidad y

un buen ajuste del modelo. Estos resultados demuestran la estabilidad y reproducibilidad del modelo OPLS-DA.

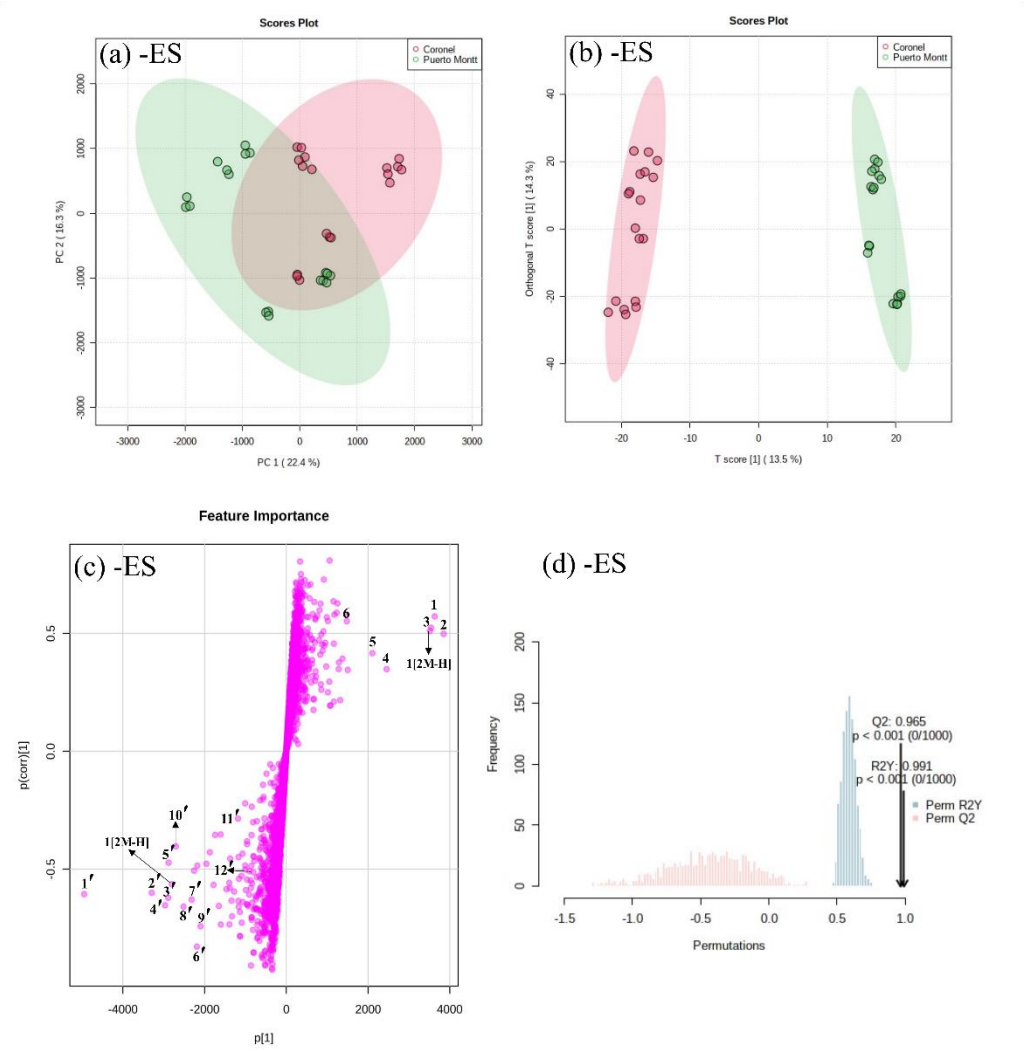

Figura 2.2.1. (a) Análisis de Componentes Principales (PCA) basado en el conjunto de datos LC-MS adquiridos en modo de ionización negativo (-ESI) para las poblaciones centroide y periférica de *E. cordifolia* en la estación de Verano (b) gráfico de *score* del modelo supervisado OPLS-DA (c) diagrama *S*-plot, que ilustra la covarianza p[1] frente a la correlación p(cor)[1] de

las variables del componente discriminante del modelo OPLS-DA (d) validación cruzada y prueba de permutación para el modelo OPLS-DA.

Los gráficos de modelos de PCA para otoño se presentan en la Figura 2.2.2*a* y Fig. S2.2*e* en los modos de ionización -ESI y +ESI. En ambos modos, se puede observar claramente que la población centroide se separa completamente de la población periférica en términos metabólicos a través del primer y segundo componente principal. En ambos casos, la varianza total explicada es superior a 43%.

Posteriormente, se realizó un análisis multivariado OPLS-DA para identificar los *features* expresados de manera diferencial en los extractos de hojas de *E. cordifolia*, en respuesta a la posición que ocupan las poblaciones en su nicho ecológico ambiental. En el modo -ESI, la varianza explicada fue de 16.6% (Figura 2.2.2*b*), mientras que en el modo +ESI fue de 16% (Fig. S2.2*e*). Al igual que en la estación de verano, se utilizó el gráfico *S-plot* para seleccionar aquellos *features* que contribuyen principalmente a la distinción entre las poblaciones de *E. cordifolia*. En la Figura 2.2.2*c*, los *features* ubicados en el extremo superior derecho corresponden a aquellas que están estrechamente correlacionadas con la población ambientalmente periférica,

Puerto Montt, mientras que los *features* ubicados en el extremo inferior izquierdo están correlacionadas con la población centroide, Coronel.

En modo de ionización -ESI, se identificaron un total de 10 metabolitos que mostraron una regulación significativa al alza en Puerto Montt durante la estación de otoño. Entre ellos, se destaca la presencia de glucósidos de flavonoles, tales como quercetin-3-O-hexoside (**7**), quercetin-3-O-deoxyhexose (**8**), quercetin pentoside (**9**) y kaempferol-3-O-rhamnoside (**16**); trisacárido, como rafinosa (**10**); flavanoles, como procyanidina B1 (**13**) y catequina (**15**); compuesto sulfatado (**12**), glucósido de sesquiterpeno cicloxano identificado como 7-Megaestigmene-3,6,9-triol hexoside (**11**) y un glucósido de flavanonol, como taxifolin-deoxyhexose (**14**). Los metabolitos que mostraron una regulación significativa al alza en la población centroide fueron 5 (Figura 2.2.2*c*, Tabla S1). Se evidenció la presencia de taxifolin pentoside (**13′**) (glucósido de flavanona), ácido quínico (**14′**) y dihexósido de ácido quínico (**17′**) (*ácido* ciclohexano carboxílico), se detectó la presencia de un compuesto sulfatado (**15′**) y finalmente se identificó taxifolin-deoxyhexose (**16′**) (glucósido flavanonol).

En modo de ionización +ESI, se identificaron un total de 4 metabolitos que mostraron una regulación significativa al alza en la población periférica

(Fig S2.2*g*, Tabla S2.1). Se encontró un compuesto del tipo flavonol, como quercetin (**8**); flavanols, como procyanidina (**10**); y flavanone como taxifolin (**11**). Por otro lado, un total de 6 metabolitos mostraron una regulación al alza en la población centroide, donde se destaca la presencia de taxifolin (**8′**) syringetin hexoside (**11′**), cirsiliol (**9′**), tricin hexoisede (**13′**) y otros.

La validación arrojó valores de Q2 = 0.967 y R2Y = 0.989 para -ESI, y Q2 = 0.981 y R^2Y = 0.998 para +ESI (Figura 2.2.2*d*, Fig. S2.2*h*).

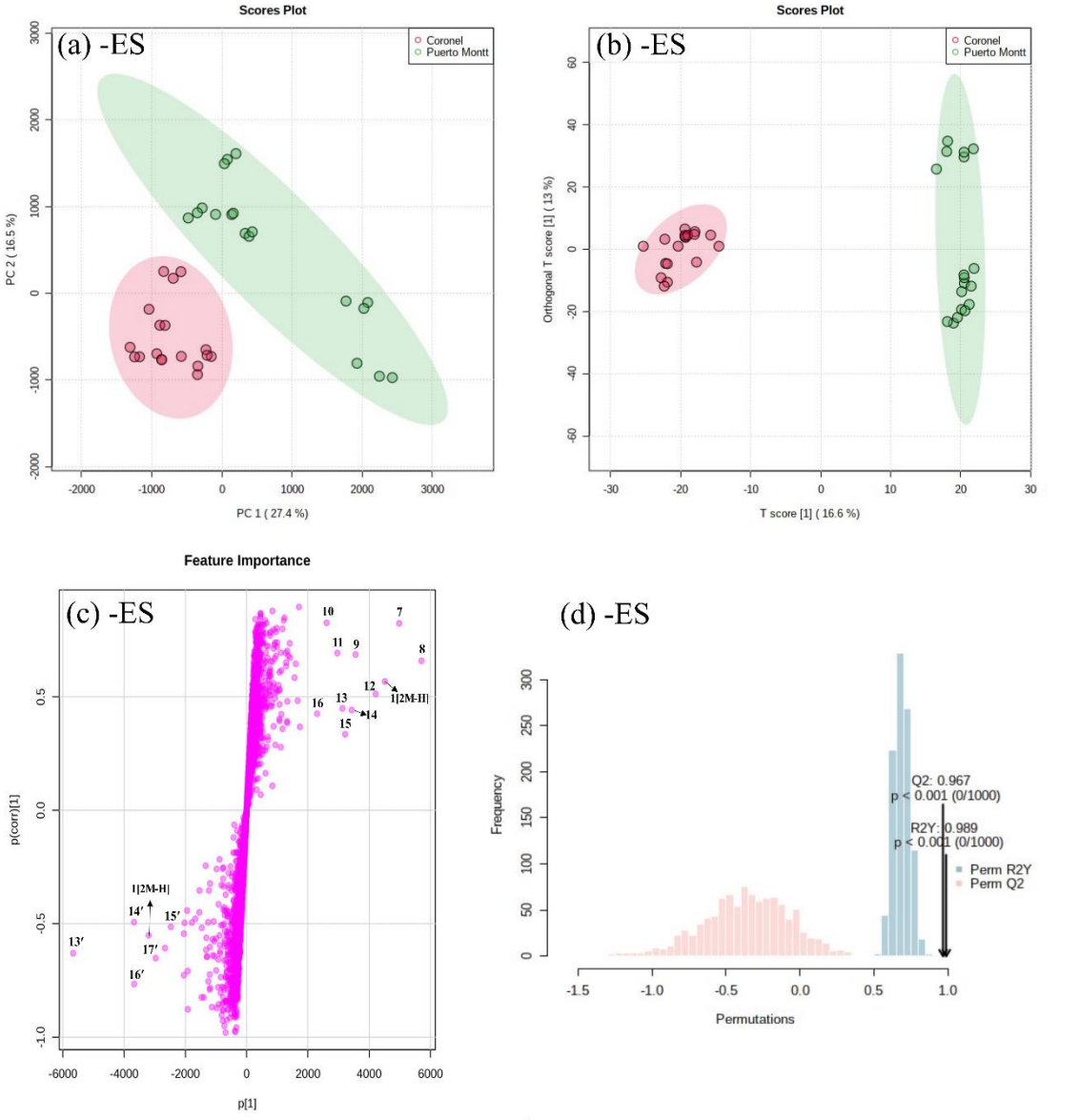

Figura 2.2.2. (a) Análisis de Componentes Principales (PCA) basado en el conjunto de datos LC-MS adquiridos en modo de ionización negativo (-ESI) para las poblaciones centroide y periférica de *E. cordifolia* en la estación de Otoño (b) gráfico de *score* del modelo supervisado OPLS-DA (c) diagrama *S*-plot, que ilustra la covarianza p[1] frente a la correlación p(cor)[1] de las variables del componente discriminante del modelo OPLS-DA (d) validación cruzada y prueba de permutación para el modelo OPLS-DA.

Finalmente, en primavera, se observan los modelos de PCA en la Figura 2.2.3*a*. Es posible apreciar una separación parcial entre las poblaciones de *E. cordifolia* investigadas. La varianza total explicada por el PC1 y PC2 fue del 39.2% para -ESI (Figura 2.2.3*a*), mientras que se obtuvo un 36.7% para +ESI (Fig. S2.3*e*). Con el fin de identificar los *features* que contribuyen a la separación de las poblaciones de *E. cordifolia*, se llevó a cabo un análisis OPLS-DA y posteriormente se generaron los gráficos S-plot. Los gráficos de *score* (Figura 2.2.3*b*) muestran una separación drástica entre las muestras, donde las muestras de la población ambientalmente periférica (Puerto Montt) se representan en color verde, mientras que las de la población centroide (Coronel) se visualizan en rojo a lo largo del componente predictivo (T *score*[1]) en ambos modos de ionización. La varianza explicada fue de 16.4% para -ESI (Figura 2.2.3*b*) y de 13.7% para +ESI (Fig S2.3*f*).

En los gráficos *S*-plots cada punto representa un *feature* o metabolito específico. Al igual que en los casos anteriores los *features* ubicados en el extremo superior derecho corresponden a aquellas que están estrechamente correlacionadas con la población ambientalmente periférica, Puerto Montt, mientras que los *features* ubicados en el extremo inferior izquierdo están correlacionadas con la población centroide, Coronel (Figura 2.2.3*c*).

Durante la estación de primavera, se identificaron un total de 7 compuestos que mostraron una regulación significativamente al alza en la población periférica en el modo de ionización negativa (-ESI). Entre ellos se encontraron varios tipos de compuestos, como glucósidos de flavanol, como quercetin-3-O-hexoside (**17**), quercetin-3-O-deoxyhexoside (**19**), kaempferol-3-O-rhamnoside (**20**) y quercetin pentoside (**21**). Además, se detectaron dos compuestos sulfatados (**18** y **23**), y se identificó un glucósido de flavanonol como taxifolin deoxyhexose (**22**). Por otra parte, en la población centroide se registraron 6 metabolitos regulados al alza. Entre ellos destacan la presencia de glucósidos de flavanona, como taxifolin pentoside (**18′**); un compuesto sulfatado (**21′**), flavonol, como catequina (**19′**), así como dos *ácidos* ciclohexanocarboxílicos, como ácido quínico (**20′**) y dihexósido de ácido quínico (**22′**).

En modo de ionización positivo (+ESI) se identificaron 4 metabolitos que mostraron una regulación al alza en la población periférica (Fig. S2.3*g*, Tabla S2.1). Se destacó la presencia de compuestos del tipo flavonoles como quercetin (**12**), quercetin-3-O-hexoside (**13**) y quercetin-rhamnoside (**15**). Además, se encontró una flavona, como luteolin (**14**). En la población centroide, se identificaron solo 3 metabolitos que mostraron una regulación

al alza. Se destacó la presencia de dos flavonoles tales, como taxifolin (**14′**) y syringetin (**15′**) y una flavona, como cirsiliol (**16′**).

La validación arrojó valores de Q2 = 0.970 y R2Y = 0.991 para -ESI (Figura 2.2.3*d*), y Q2 = 0.942 y R2Y = 0.988 para +ESI (Fig. S2.3*h*).

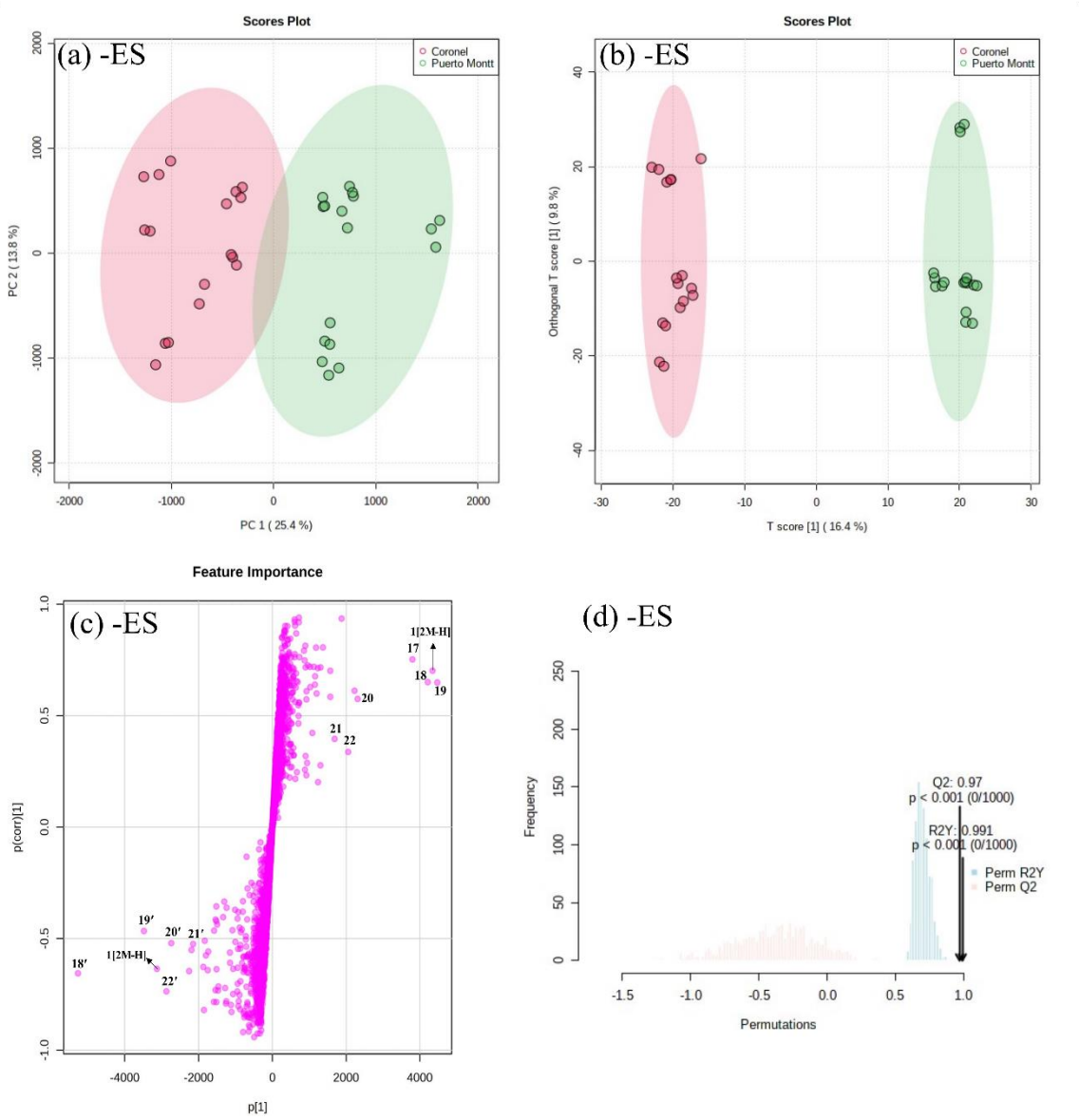

Figura 2.2.3. (a) Análisis de Componentes Principales (PCA) basado en el conjunto de datos LC-MS adquiridos en modo de ionización negativo (-ESI) para las poblaciones centroide y periférica de *E. cordifolia* en la estación de Verano (b) gráfico de *score* del modelo supervisado OPLS-DA (c) diagrama *S*-plot, que ilustra la covarianza p[1] frente a la correlación p(cor)[1] de las variables del componente discriminante del modelo OPLS-DA (d) validación cruzada y prueba de permutación para el modelo OPLS-DA.

Tabla 2.2.1. Datos químicos de metabolitos relevantes para distinguir entre la población centroide y periférica de *E. cordifolia*, clasificados por estación y analizados en modo de ionización negativo (-ES) UHPLC-DAD-QTOF-MS/MS.

No	Rt (min)	Metabolite name	Metabolite class	Mol. formula	ESI (-) Theor m/z	ESI (-) Meas m/z	ESI (+) Theor m/z	ESI (+) Meas m/z	m/z error (ppm)[a]	MS/MS ESI (-) fragments (int. %)	MS/MS ESI (+) fragments (int. %)	UV/Vis (nm)	InChI-Key	Ident. level (A-D)
VERANO														
Metabolitos regulados al alza en hojas de *E. cordifolia* localizadas en Puerto Montt al compararlas con las de Coronel														
1	9.76	Quercetin-3-O-hexoside	Flavonol glycoside	$C_{21}H_{20}O_{12}$	463.0882	463,0879 $[M-H]^-$	465.1028	465.1037 $[M+H]^+$	0.66, 2.10	463.0 (100), 300.0 (68), 271.0 (58), 255.0 (25), 243.0 (13), 227.0 (3), 151.0 (5.6)	303.0 (100), 257.0 (2), 229.0 (2)	255, 355	OVSQVDMCBVZWGM-QSOFNFLRSA-N	B
2	6.47	Ethyl-5-octyl-2.2-dioxo-1.3.2-dioxathiolane-4-carboxylate	Sulfonate	$C_{13}H_{24}O_6S$	307.1221	307.1217 $[M-H]^-$	n.d.	n.d.	1.41, n.d.	307.1 (100), 96.9 (8)	n.d.	250	HWYWSWKEJSIOBK-UHFFFAOYSA-N	B
3	10.79	Quercetin-3-O-deoxyhexoside	Flavonol glycoside	$C_{21}H_{20}O_{11}$	447.0933	447.0921 $[M-H]^-$	449.1078	449.1091 $[M+H]^+$	2.55, 2.89	447.0 (100), 300.0 (58), 271.0 (50), 255.0 (24), 243.0 (13), 151.0 (6)	303.0 (100), 129.0 (5)	255, 348	OXGUCUVFOIWWQJ-HQBVPOQASA-N	B
4	9.97	Taxifolin-deoxyhexose	Flavanonol glycoside	$C_{21}H_{22}O_{11}$	449.1089	449.1087 $[M-H]^-$	451.1235	451.1240 $[M+H]^+$	0.63, 1.13	449.1 (34), 303.0 (9.2), 285.0 (61), 151.0 (100), 125.0 (6)	305.0 (100), 287.0 (21), 259.0 (44), 153.0 (17), 123.0 (15)	287	ZROGCCBNZBKLEL-MPRHSVQHSA-N	B
5	7.3	7-Megaestigmene-3,6,9-triol hexoside	Cyclohexan sesquiterpene glycoside	$C_{19}H_{34}O_8$	435.2236	435.2236 $[M+HCOOH-H]^-$	n.d.	n.d.	0.10, n.d.	435.0 (100), 389.2 (58), 227.1 (15), 161.0 (31), 113.0 (4)	n.d.	278	MRPDHXXPDCVBPQ-AATRIKPKSA-N	B

6	10.01	Dimethoxy apigenin sulfonic acid	Flavone Sulfonate	$C_{17}H_{14}O_{10}S$	409.0235	409.0233 [M-H]-	411.038	411.0381 $[M+H]^+$	0.44, 0.10	409.0 (20), 329.0 (100), 271.0 (42), 257.0 (11), 243.0 (11)	331.0 (100), 316.0 (40), 301.0 (24), 284.0 (30)	284, 3.40	WHUWTHLRYAPDIX-UHFFFAOYSA-N	B
Metabolitos regulados a la baja en hojas de *E. cordifolia* localizadas en Puerto Montt al compararlas con las de Coronel														
1′	8.89	Taxifolin pentoside I	Flavanone glycoside	$C_{20}H_{20}O_{11}$	435.0933	435.0927 $[M-H]^-$	n.d.	n.d.	1.28, n.d.	435.1 (34), 303.1 (27), 285.0 (70), 151.0 (100), 125.0 (10).	n.d.	290	UKSPRKDZNYSFRL-ARLBNVOWSA-N	B
2′	7.39	Dehydroderivative of **2**	Sulfonate	$C_{13}H_{22}O_6S$	305.1064	305.1064 $[M-H]^-$	n.d.	n.d.	0.19, n.d.	305.1 (100), 96.9 (21).	n.d.	250	OZZZAPCMMGMTGD-NEPJUHHUSA-N	B
3′	10.8	Dimethyl quercetin	Flavonol methoxyl	$C_{17}H_{14}O_7$	329.0665	329.0665 $[M-H]^-$	331.0812	331.0820 $[M+H]^+$	0.66, 2.22	314.0 (100), 299.0 (5), 286.0 (8), 271.0 (59), 257.0 (1), 242.0 (8)	331.0 (100), 315.0 (14), 298.0 (10), 285.0 (7), 270.0 (17), 253.0 (3)	349	FMEHGPQTMOPUGM-UHFFFAOYSA-N	B
4′	11.1	Deoxyderivative of **2′**	Sulfonate	$C_{13}H_{22}O_5S$	289.1115	289.1114 $[M-H]^-$	n.d.	n.d.	0.51, n.d.	289.1 (100), 96.9 (20)	n.d.	250	HWYWSWKEJSIOBK-UHFFFAOYSA-N	B
5′	10.83	Deoxyderivative of **2**	Cycle Sulfonate	$C_{13}H_{24}O_5S$	291.1272	291.1269 $[M-H]^-$	n.d.	n.d.	0.86, n.d.	291.1 (100), 96.9 (11)	n.d.	255-349	HWYWSWKEJSIOBK-UHFFFAOYSA-N	B
6′	9.41	Dehydroderivative of 2′	Cycle Sulfonate	$C_{13}H_{20}O_6S$	303.0908	303.0909 $[M-H]^-$	n.d.	n.d.	0.30, n.d.	303.0(100), 96.9(41)	n.d.	250	HWYWSWKEJSIOBK-UHFFFAOYSA-N	B
7′	9.08	Syringetin	Flavonol	$C_{17}H_{14}O_8$	345.0615	345.0616 $[M-H]^-$	347.0761	347.0767 [M+H]+	0.84, 1.68	330.0 (100), 315.0 (10), 287.0 (84), 271.0 (21), 259.0 (7.1), 242.0 (10)	347.0 (100), 332.0 (13), 314.0 (9), 286.0 (13), 269.0 (2), 257.0 (3)	287	KIGVXRGRNLQNNI-UHFFFAOYSA-N	B

8′	11.35	Persicarin	Sulfonate	$C_{16}H_{12}O_{10}S$	395.0078	395.0078 $[M-H]^-$	397.0223	397.0225 $[M+H]^+$	0.16, 0.15	395.0(7), 315.0 (100), 300.0(12), 271.0(32), 243.0 (13)	347.1 (21), 317.0 (100), 302.0 (18), 273.0 (17), 217.0 (24), 203.0 (19)	250	CZFNXFXZXWDYMZ-UHFFFAOYSA-N	B
9′	10.02	Taxifolin pentoside II	Flavanone glycoside	$C_{20}H_{20}O_{11}$	435.0933	435.0931 $[M-H]^-$	n.d.	n.d.	0.35, n.d.	435.0 (34), 417.0 (2), 285.0 (70), 259.0 (1), 241.0 (2), 178.9 (10), 151.0 (100)	n.d.	215	UKSPRKDZNYSFRL-ARLBNVOWSA-N	B
10′	1.33	Quinic acid	Cyclitol carboxylic acid	$C_7H_{12}O_6$	191.0561	191.0558 [M-H]-	n.d.	n.d.	1.41, n.d.	191.0 (100), 173.0 (3), 127.0 (6), 111.0 (1)	n.d.	203	AAWZDTNXLSGCEK-ZHQZDSKASA-N	B
11′	1.3	Disacarido clorado	Disacarido	$C_{12}H_{22}O_{11}$	377.0854	377.0857 $[M-H]^-$	n.d.	n.d.	0.88, n.d.	377.0 (46), 341.1 (100), 215.0 1950 (10), 179.0 1650 (25)	n.d.	205	LGIBBNHSMMNNOH-WFSGIGAVSA-N	B
12′	9.76	Taxifolin-Deoxyhexose	Flavanonol glycoside	$C_{21}H_{22}O_{11}$	449.1089	449.1088 [M-H]-	452.1162	451.1241 $[M+H]^+$	0.30, 1.13	449.1 (34), 303.0 (9), 285.0 (61), 199.0 (2), 178.9 (9), 151.0 (100)	345.2 (6), 325.0 (5), 305.0 (100), 287.0 (21), 259.0 (44), 231.0 (18)	207	ZROGCCBNZBKLEL-MPRHSVQHSA-N	B
OTOÑO														
Metabolitos regulados al alza en hojas de *E. cordifolia* localizadas en Puerto Montt al compararlas con las de Coronel														
7	9.69	Quercetin-3-O-hexoside	Flavonol glycoside	$C_{21}H_{20}O_{12}$	464.0954	463.0879 [M-H]-	465.0954	465.0879 [M+H]+	0.82, 7.44	463.0 (100), 271.0 (61), 255.0 (29), 227.0 (3), 178.9 (2), 151.0 (6)	303.0 (100), 257.0 (2), 229.0 (2)	217	OVSQVDMCBVZWGM-QSOFNFLRSA-N	B
8	10.72	Quercetin-3-O-deoxyhexoside	Flavonol glycoside	$C_{21}H_{20}O_{11}$	447.0933	447,0922 [M-H]-	449.1005	449,0922 $[M+H]^+$	2.54,	447.0 (100), 300.0 (62), 283.0 (1), 271.0 (52), 255.0 (23), 227.0 (3), 178.0 (2), 151.0 (7)	303.0 (100), 257.0 (2), 229.0 (2), 129.0 (3)	349	OXGUCUVFOIWWQJ-HQBVPOQASA-N	B

9	10,38	Quercetin pentoside	Flavonols glycoside	$C_{20}H_{18}O_{11}$	433.0849	433,0771 [M-H]-	4360849	433,0771 [M+H]+	1.76, 7.70	433.0 (100), 300.0 (99), 271.0 (72), 255.0 (30), 243.0 (19), 227.0 (4), 215.0 (1), 199.0 (16), 187.0 (0.5), 178.9 (1), 163.0 (1), 151.0 (3)	303.0 (100), 285.0 (1), 229.0 (2)	219	PZZRDJXEMZMZFD-BWYUNELBSA-N	B
10	1.2	Rafinosa	Trisacárido	$C_{18}H_{32}O_{16}$	549.169	549.1672 [M + HCOOH - H]-	n.d.	n.d.	0.06, n.d	503.1 (100), 341.1 (3), 221.0 (26), 179.0 (9), 161.0 (3), 113.0 (3)	n.d.	n.d	MUPFEKGTMRGPLJ-ZQSKZDJDSA-N	B
11	7.23	7-Megaestigmene-3,6,9-triol hexoside	Cyclohexan sesquiterpene glycoside	$C_{19}H_{34}O_8$	435.2236	435.2230 $[M+HCOOH-H]^-$	n.d.	n.d.	1.33, n.d	344.0 (100), 179.0 (96)	n.d.	n.d	MRPDHXXPDCVBPQ-AATRIKPKSA-N	B
12	6.41	Ethyl-5-octyl-2.2-dioxo-1.3.2-dioxathiolane-4-carboxylate	Sulfonate	$C_{13}H_{24}O_6S$	307.1222	307.1216 $[M-H]^-$	n.d.	n.d.	1.41, n.d.	307.1 (100), 96.9 (8)	n.d.	250	HWYWSWKEJSIOBK-UHFFFAOYSA-N	B
13	5.52	Procianidina B1	Flavanols	$C_{30}H_{26}O_{12}$	577.1424	577.1348 [M-H]-	579.1424	579.1348 [M+H]+	0.48, 3.97	557.1 (78), 559.1 (3), 425.0 (87), 407.0 (64), 381.0 (3), 339.0 (7), 289.0 (100)	579.1 (12), 439.0 (2), 409.0 (41), 289.0 (41), 247.0 (21), 201.0 (5), 163.0 (19), 127.0 (100)	206	XFZJEEAOWLFHDH-NFJBMHMQSA-N	A
14	9,89	Taxifolin-Deoxyhexose	Flavanonol glycoside	$C_{21}H_{22}O_{11}$	449.1162	449.10848 [M-H]-	451.1162	451,1084 [M+H]+	1.02, n.d.	449.1 (43), 285.0 (71), 257.0 (1), 241.0 (1), 199.0 (2), 178.9 (6), 151.0 (100)	n.d.	290	ZROGCCBNZBKLEL-MPRHSVQHSA-N	B
15	6.24	Catechin	Flavanols	$C_{15}H_{16}O_7$	289.0717	289.0723 $[M-H]^-$	n.d.	n.d.	1.99, n.d	245.0 (100), 289.0 (89), 271 (8), 221.0 (36), 151.0 (32)	n.d	204-279	OFUMQWOJBVNKLR-NQQJLSKUSA-N	A

16	11.65	Kaempferol-3-rhamnoside	Flavonols glycoside	$C_{21}H_{20}O_{10}$	431.1056	431.0982 [M-H]-	n.d.	n.d.	0.70, n.d.	431.0 (75), 285.0 (100), 255.0 (63), 227.0 (61), 211.0 (3), 185.0 (1)	n.d.	219	SOSLMHZOJATCCP-AEIZVZFYSA-N	B
Metabolitos regulados a la baja en hojas de *E. cordifolia* localizadas en Puerto Montt al compararlas con las de Coronel														
13′	8.81	Taxifolin pentoside III	Flavanone glycoside	$C_{20}H_{20}O_{11}$	435.1005	435.0981 [M-H]-	n.d.	n.d.	1.14, n.d.	435.0 (34), 417.0 (1), 285.0 (70), 257.0 (2), 217.0 (1), 199.0 (2), 151.0 (100)	n.d.	216	UKSPRKDZNYSFRL-ARLBNVOWSA-N	B
14′	1.2	Quinic acid	Cyclitol carboxylic acid	$C_7H_{12}O_6$	192.0633	191.0559 [M-H]-	n.d.	n.d.	0.96, n.d.	191.0 (100), 173.0 (3), 127.0 (6), 111.0 (2)	n.d	205	AAWZDTNXLSGCEK-WYWMIBKRSA-N	B
15′	7.33	Dehydroderivative of **2**	Sulfonate	$C_{13}H_{22}O_6S$	305.1064	305.1062 $[M-H]^-$	n.d.	n.d.	4.71, n.d.	305.1 (100), 96.9 (21).	n.d.	250	OZZZAPCMMGMTGD-NEPJUHHUSA-N	B
16′	10.67	Taxifolin-Deoxyhexose	Flavanonol glycoside	$C_{21}H_{22}O_{11}$	450.1162	449.1087 [M-H]-	452.1162	451.1267 $[M+H]+$	0.47	449.1 (43), 431.0 (1), 402.9 (5), 285.0 (78), 271.0 (8), 255.0 (6), 151.0 (100)	305 (100), 287.0 (31), 259.0 (23), 231.0 (20),195.0 (12), 153.0 (26)	218	UKSPRKDZNYSFRL-ARLBNVOWSA-N	B
17′	1.28	Quinic acid dihexoside	Cyclitol carboxylic acid	$C_{19}H_{34}O_{17}$	533.1723	533.1794 $[M-H]^-$	n.d.	n.d.	0.58, n.d	191.0 (100)	n.d.	200-230	n.d	B
PRIMAVERA														
Metabolitos regulados al alza en hojas de *E. cordifolia* localizadas en Puerto Montt al compararlas con las de Coronel														
17	9.94	Quercetin-3-O-hexoside	Flavonol glycoside	$C_{21}H_{20}O_{12}$	463.0882	463.0869 $[M-H]^-$	465.1028	465.1018 $[M+H]^+$	0.74, 2.07	463.0 (100), 271.0 (59), 255.0 (25), 227.0 (2), 178.9 (2), 151.0 (5)	300.0 (100), 285.0 (1), 257.0 (1), 229.0 (3)	250, 354	OVSQVDMCBVZWGM-QSOFNFLRSA-N	B

18	6.67	Ethyl-5-octyl-2.2-dioxo-1.3.2-dioxathiolane-4-carboxylate	Sulfonate	$C_{13}H_{24}O_6S$	307.1220	307.1281 $[M-H]^-$	n.d.	n.d.	0.94, n.d.	307.1 (100), 96.9 (5)	n.d.	250	HWYWSWKEJSIOBK-UHFFFAOYSA-N	B
19	10.97	Quercetin-3-O-deoxyhexoside	Flavonol glycoside	$C_{21}H_{20}O_{11}$	477.0933	447.0922 $[M-H]^-$	449.1078	449.1101 $[M+H]^+$	2.37, 5.03	447.0 (100), 300.0 (64), 283.0 (1), 271.0 (57), 255.0 (27), 227.0 (4)	300.0 (100), 257.0 (2), 229.0 (2), 129.0 (4)	255	OXGUCUVFOIWWQJ-HQBVPOQASA-N	B
20	11.91	Kaempferol 3-O-rhamnoside	Flavonols glycoside	$C_{21}H_{20}O_{10}$	431.0984	431.0981 $[M-H]^-$	n.d.	n.d.	0.57, n.d.	431.0 (76), 285.0 (100), 255.0 (64), 239.0 (1), 227.0 (57), 211.0 (2), 187.0 (29)	n.d.	250	SOSLMHZOJATCCP-UHFFFAOYSA-N	B
21	10.64	Quercetin pentoside	Flavonols glycoside	$C_{20}H_{18}O_{11}$	433.0776	433.0773 $[M-H]^-$	435.0922	435.0910 $[M+H]^+$	0.86, 2.07	433.0 (94), 300.0 (100), 271.0 (84), 255.0 (29), 227.0 (5), 151.0 (4)	303.0 (100), 285.0 (1), 229.0 (3), 153.0 (1)	252	PZZRDJXEMZMZFD-BWYUNELBSA-N	B
22	10.15	Taxifolin-deoxyhexose	Flavanonol glycoside	$C_{21}H_{22}O_{11}$	449.1089	449.1091 $[M-H]^-$	451.1235	451.1250 $[M+H]^+$	0.36, 3.41	449.1 (44), 285.0 (67), 241.0 (2), 199.0 (2), 178.9 (6), 151.0 (100)	305.0 (100), 287.0 (30), 259.0 (64), 231.0 (42), 153.0 (42), 123.0 (22)	253, 291	ZROGCCBNZBKLEL-MPRHSVQHSA-N	B
23	10.2	Dimethoxy apigenin sulfonic acid	Flavone Sulfonate	$C_{17}H_{14}O_{10}S$	409.0235	409.0232 $[M-H]^-$	n.d.	n.d.	0.64, n.d.	409.0 (19), 329.0 (100), 299.0 (7), 271.0 (45), 257.0 (12), 243.0 (13)	n.d.	255	WHUWTHLRYAPDIX-UHFFFAOYSA-N	B
Metabolitos regulados a la baja en hojas de *E. cordifolia* localizadas en Puerto Montt al compararlas con las de Coronel														
18′	9.08	Taxifolin pentoside IV	Flavanone glycoside	$C_{20}H_{20}O_{11}$	435.0933	435.0926 $[M-H]^-$	459.0988	459.0906 $[M+H]^+$	1.86, 1.83	435.0 (31), 285.0 (65), 257.0 (3), 178.9 (12), 151.0 (100), 125.0 (10)	459.0 (100)	258	UKSPRKDZNYSFRL-ARLBNVOWSA-N	B

19′	6.52	Catechin	Flavanols	$C_{15}H_{14}O_6$	289.0718	289.0714 $[M-H]^-$	291.0864	291.0868 $[M+H]^+$	1.30, 1.81	289.0 (100), 271.0 (5), 245.0 (90), 221.0 (31), 203.0 (51), 179.0 (24), 165.0 (15), 151.0 (15), 137.0 (29), 123.0 (39), 109.0 (42), 97.0 (1)	207.0 (6), 165.0 (3), 139.0 (100), 123.0 (73), 115.0 (6)	254-279	PFTAWBLQPZVEMU-HIFRSBDPSA-N	B
20′	1.4	Quinic acid	Cyclitol carboxylic acid	$C_7H_{12}O_6$	191.0561	191.0560 $[M-H]^-$	n.d.	n.d.	0.66, n.d.	191.0 (100), 173.0 (3), 127.0 (5), 111.0 (2)	n.d.	2.38	AAWZDTNXLSGCEK-ZHQZDSKASA-N	B
21′	8.46	Dehydroderivative of **2**	Sulfonate	$C_{13}H_{22}O_6S$	305.1064	305.1062 $[M-H]^-$	n.d.	n.d.	4.71, n.d.	305.1 (100), 96.9 (21).	n.d.	250	OZZZAPCMMGMTGD-NEPJUHHUSA-N	B
22′	1.38	Quinic acid dihexoside	Cyclitol carboxylic acid	$C_{19}H_{34}O_{17}$	533.1723	533.1794 $[M-H]^-$	n.d.	n.d.	0.49, n.d	191.0 (100)	n.d.	202-230	n.d	B
23′	1.3	Disacarido clorado	Disacarido	$C_{12}H_{22}O_{11}$	377.0854	377.0857 $[M-H]^-$	n.d.	n.d.	0.82, n.d.	377.0 (42), 341.1 (100), 215.0 (13), 179.0 (23), 165.0 (14)	n.d.	205	LGIBBNHSMMNNOH-WFSGIGAVSA-N	B

[a]: "Error medio de masa exacta para los modos de adquisición ESI negativo y positivo."; [b]: fragmentación en fuente; UV/Vis: Absorbancia máxima; InChI-Key: Identificador internacional de la IUPAC para sustancias químicas según PubChem; Nivel de identificación (A-D): A–*standard*, B–MS/MS, C–MS^E, D–MS; I, II: compuestos isobáricos con espectro MS/MS similar; n.d.: no detectado.

2.2.4. Discusión

En este estudio, hemos investigado la posible correlación entre la distancia de las poblaciones de *E. cordifolia* al centro del nicho y las variaciones en su metaboloma.

El nicho investigado en este estudio se basa en la descripción realizada por Hutchinson, la cual representa una visión más cuantitativa de los recursos bióticos y condiciones abióticas que influyen en el *fitness* de una especie (Hutchinson 1957 Martínez-Meyer et al. 2013). En otras palabras, el nicho se refiere al lugar donde las condiciones ambientales permiten el funcionamiento óptimo de la especie y su homeostasis celular. Se ha argumentado que la bioquímica juega un papel clave en el nicho de una especie, ya que la adquisición, almacenamiento e intercambio de energía y elementos son fundamentales para la vida, y la composición química de un organismo influye en su ecología (González et al. 2017; Sardans y Peñuelas 2014).

Los resultados de este capítulo presentan pruebas sólidas acerca de un enfoque novedoso para caracterizar el nicho ecológico utilizando el metaboloma de *E. cordifolia*. Esto facilita la distinción entre las regiones

fisiológicamente óptimas y subóptimas dentro del nicho, brindando una comprensión más precisa de cómo esta especie se adapta a su entorno.

Mediante el análisis metabolómico no dirigido a través de UHPLC-DAD-QTOF-MS/MS, se ha revelado un perfil amplio y químicamente diverso de compuestos flavonoides y sulfónicos en la especie *E. cordifolia*, muestreada respecto a su posición en su nicho ecológico y a nivel estacional.

2.2.4.1. Presencia de compuestos sulfónicos en poblaciones de *E. cordifolia* respecto al centro del nicho ecológico.

En primer lugar, los resultados presentados revelan un aumento significativo en la presencia de compuestos sulfatados tanto en la población central como en la población periférica durante las tres estaciones investigadas (verano, otoño y primavera). Es importante destacar que durante la estación de verano se observó la mayor expresión de compuestos sulfatados. En verano, en la población periférica, se identificaron dos compuestos regulados al alza: ethyl-5-octyl-2.2-dioxo-1.3.2-dioxathiolane-4-carboxylate (2) y dimethoxy apigenin sulfonic acid (6). Por otro lado, en la población centroide, se observó la presencia de cinco compuestos sulfatados regulados al alza, de los cuales cuatro derivan del compuesto 2 (2', 4', 5', 6').

Además, se identificó la presencia de un flavonoide sulfatado llamado persicarina (isorhamnetin 3-sulfate, 8'). En la estación de otoño, solo se identificó un compuesto sulfónico al alza tanto en la población periférica (12) como en la población centroide (15'). En primavera, se observó una tendencia similar, con solo dos compuestos sulfónicos regulados al alza en la población periférica (18) y solo uno en la población centroide (21'). Es importante destacar que los compuestos reportados en otoño y primavera corresponden a los mismos identificados en verano.

Hasta el momento, no se ha informado sobre la presencia de este tipo de compuestos ni en la especie en estudio ni en otras especies de la misma familia. En general, se reconoce que el azufre (S) es un macronutriente esencial para su crecimiento, desarrollo y capacidad de respuesta de las plantas ante los cambios ambientales (Gigolashvili et al., 2018); sin embargo, el papel funcional de los sulfatos de flavonoides en las células y tejidos vegetales aún no está claro (Teles et al. 2018). A pesar de esto, se ha demostrado una fuerte correlación entre las plantas que crecen cerca de áreas acuáticas y/o húmedas ricas en sales minerales y la biosíntesis de flavonoides sulfatados, considerándose una adaptación ecológica al medio (Correia da

Silva et al. 2013; Teles et al. 2015; 2018) lo que ha sido principalmente reportada en pastos marinos (Grignon-Dubois et al. Rezzonico).

Persicarina es uno de los compuestos diferenciadores entre las poblaciones de *E. cordifolia*, ya que sólo fue registrado en la población centroide durante la estación de verano. Este es uno de los flavonoides sulfatados más reportados en investigaciones sobre especies vegetales y fue uno de los primeros aislados de *Polygonum hydropiper* L. (Polygonaceae) (Harborner et al., 1975; Teles et al., 2018). Una de las investigaciones más recientes estima que este flavonoide podría ser considerado como un herbicida natural (fitoalexina) extraído de las hojas de *Conyza dioscoridis* para controlar malezas que afectan cultivos comerciales (Balah et al. 2016). Sin embargo, no se han realizado investigaciones sustanciales que respalden su aparición de este compuesto un mecanismo protector frente a las condiciones abióticas de crecimiento y tampoco sobre su síntesis a nivel estacional.

Las plantas muestran una gran sensibilidad ante la calidad del aire que las rodea. Diversos contaminantes presentes en la atmósfera suponen una seria amenaza para la producción vegetal y la estabilidad de los ecosistemas en general (Oksanen & Kontunen-Soppela 2021). Dada esta afirmación,

hemos formulado una hipótesis para explicar la probabilidad de presencia de este tipo de compuestos. Nos planteamos que dicha probabilidad podría estar asociada a aerosoles atmosféricos, principalmente generados por la contaminación industrial en la población de Coronel debido a la presencia de la industria Celulosa Arauco. Tal contaminación puede tener un impacto directo sobre las hojas de los árboles, afectando también el suelo y generando cambios fisiológicos antes de que los daños sean visibles en las hojas (Skrynetska et al. 2018).

Además, consideramos que la población en las áreas periféricas de Puerto Montt podría estar vinculada a la presencia de partículas procedentes de las erupciones volcánicas (Lopes et al. 2019). Aunque ha transcurrido un considerable tiempo desde la última erupción cercana al área de muestreo (Volcán Calbuco, 2015), se ha observado que estas partículas siguen suspendidas en el ambiente durante un período prolongado (Payne & Egan 2019). Esto podría afectar principalmente a las hojas de los árboles, en particular a los estomas que cubren su superficie (Bertin et al. 2021), lo que a su vez podría obstaculizar la fotosíntesis de las plantas, el intercambio de gases, procesos metabólicos, entre otros procesos vitales (Tognetti et al. 2012).

Cabe destacar que llegamos a esta hipótesis debido a la ausencia de registro de compuestos sulfutados similares en poblaciones intermedias, como Contulmo y La Unión (datos no mostrados) en nuestros modelos multivariados. Asimismo, es relevante mencionar que la obtención de muestras se llevó a cabo en el Parque Nacional Alerce Andino, un área altamente protegida por nuestro país con menor intervención antropogénica en comparación con Coronel.

2.2.4.2. Presencia de compuestos fenólicos en poblaciones de *E. cordifolia* respecto a su distancia al centro del nicho ecológico.

Durante el verano, otoño y primavera, se observó una tendencia generalizada en ambas poblaciones de *E. cordifolia* investigadas, donde predominó la presencia de compuestos fenólicos, al igual que con los compuestos sulfatados.

Durante el verano, se observaron aumentos en la presencia de ciertos compuestos en la población centroide. Estos incluyeron taxifolin pentoside y deoxyhexose (1', 9', 12'), dimetil quercetina (3'), syringetin (7') y ácido quínico (10'). En contraste, en la población periférica, los compuestos que mostraron un incremento fueron la quercetin hexoside y deoxihexoside (1 y 3), así como el taxifolin deoxyhexoside (4).

En otoño, se registraron incrementos principalmente en compuestos como el taxyfolin pentoside (13') y deoxyhexose (16'), ácido quínico (14') y dihexósido de ácido quínico (17') en la población centroide. Mientras tanto, en la población periférica, se observó un aumento en los compuestos quercetin-3-O-hexoside (7), deoxyhexoside (8), quercetin pentoside (9), kaempherol-3-O-rhamnoside (16), catequina (15) y procianidina B1 (13).

Finalmente, en primavera, los metabolitos registrados al alza en la población centroide fueron del tipo flavanoles, como catechin (19'); flavanone como el taxifolin pentoside (18') y la presencia de ácido quínico (20'). Por otro lado, los metabolitos que aumentaron en la población periférica fueron quercetin hexoside (17), deoxyhexoside (19), pentoside (21) y un flavanonol como el taxifolin deoxyhexose (22).

Los resultados obtenidos demuestran la presencia de al menos un metabolito regulado al alza, lo que permite diferenciar entre la población próxima al centroide y periférica en el nicho de *E. cordifolia*. Esta tendencia también se confirmó a lo largo de las diferentes estaciones del año. Es bien conocido que los compuestos fenólicos son sintetizados como respuesta a las condiciones ambientales, y la estacionalidad desempeña un papel crucial en su producción y acumulación (Sartor et al., 2013). Estos desempeñan un

papel fundamental en la protección contra la radiación ultravioleta, en la alelopatía (interacciones químicas entre plantas) y en la atracción de polinizadores (Kumar et al. 2020). Se observó que la población periférica presentó una mayor alza de quercetina y sus derivados, Kaemferol-3-O-ramnoside y Luteolin, a diferencia de la población centroide donde no se evidenciaron en ninguna estación del año. Su presencia puede estar relacionada a un mecanismo fotoprotector frente a la radiación UV-B, neutralizando la producción de radicales libres generados por la absorción excesiva de energía luminosa con respecto a los requisitos de asimilación de las plantas (Santini et al. 2012; Majer et al. 2014). Así también las bajas temperaturas generalmente aumentan el estrés fotooxidativo en relación con la intensidad de la luz al limitar la capacidad de las enzimas fotosintéticas (Stark et al. 2018; Singh et al. 2021). La mayoría de las veces, el kaempferol y la quercetina se encuentran glicosilados, lo que representa una estrategia para el *fitness* de las plantas frente a la radiación UV (Sartor et al. 2013). La luteolin al igual que los metabolitos anteriores su principal función fisiológica en plantas es la captación especifica de los rayos UV-B actúan como filtros efectivos de alta energía protegiendo así los tejidos fotosintéticos de las plantas del daño (Wu et al. 2023).

2.2.5. Conclusión

Nuestros resultados revelan una diferenciación a nivel metabolómico entre la población centroide y periférica de *E. cordifolia*, en la que un número limitado de metabolitos contribuyen a esta diferencia. Aunque esta investigación no midió las condiciones climáticas de cada población en campo, se observaron contrastes significativos entre las condiciones en Coronel y Puerto Montt. Las principales diferencias climáticas entre estas dos áreas radican en las temperaturas estacionales y la cantidad de precipitaciones recibidas. Puerto Montt tiende a tener un clima con bajas temperaturas durante todo el año y puede experimentar precipitaciones más abundantes en comparación con Coronel.

Además, nuestros hallazgos destacan la importancia de considerar el nicho ecológico de la especie como un sustituto de la escala geográfica y latitudinal para explicar el comportamiento del metaboloma en *E. cordifolia*. Esto sugiere que las condiciones ambientales y ecológicas locales pueden tener un papel crucial en la variabilidad metabólica observada entre las poblaciones estudiadas.

Para futuros estudios, recomendamos realizar un análisis de rutas metabólicas para comprender el comportamiento fisiológico y proporcionar

una explicación más detallada de cada uno de los metabolitos expresados bajo las condiciones naturales de crecimiento. Esto permitirá una comprensión más profunda de los mecanismos metabólicos implicados en la adaptación de *E. cordifolia* a diferentes ambientes.

Referencias

Alonso, A., Marsal, S., & Julià, A. (2015). Analytical methods in untargeted metabolomics: state of the art in 2015. Frontiers in bioengineering and biotechnology, 3, 23.

Anzano, A., Bonanomi, G., Mazzoleni, S., & Lanzotti, V. (2021). Plant metabolomics in biotic and abiotic stress: a critical overview. Phytochemistry Reviews, 1-22.

Arbona, V., Manzi, M., de Ollas, C., & Gómez-Cadenas, A. (2013). Metabolomics as a tool to investigate abiotic stress tolerance in plants. International journal of molecular sciences, 14(3), 4885-4911.

aziz Balah, M. A. (2016). Chemical and biological characterization of *Conyza dioscoridis* (L.) desf. family (Compositae) in some perennial weeds control. South African Journal of Botany,103, 268-274.

Bertin, L. J., Christie, D. A., Sheppard, P. R., Muñoz, A. A., Lara, A., & Alvarez, C. (2021). Chemical signals in tree rings from northern patagonia as indicators of calbuco volcano eruptions since the 16th century. Forests, 12(10), 1305.

Chen, L. D., Huang, Z. W., Huang, Y. Z., Huang, J. F., Zhang, Z. P., & Lin, X. J. (2021). Untargeted metabolomic profiling of liver in a chronic intermittent hypoxia mouse model. Frontiers in physiology, 12, 701035.

Correia-da-Silva, M., Sousa, E., & Pinto, M. M. (2014). Emerging sulfated flavonoids and other polyphenols as drugs: Nature as an inspiration.Medicinal research reviews, 34(2), 223-279.

Farag, M. A., El Sayed, A. M., El Banna, A., & Ruehmann, S. (2015). Metabolomics reveals distinct methylation reaction in MeJA elicited *Nigella sativa* callus via UPLC–MS and chemometrics. Plant Cell, Tissue and Organ Culture (PCTOC), 122, 453-463.

Fernie, A. R., & Keurentjes, J. J. (2011). Genetics, genomics and metabolomics. Annual Plant Reviews Volume 43: Biology of Plant Metabolomics, 43, 219-259.

Ferrer-Sánchez, Y., & Rodríguez-Estrella, R. (2021). Identifying best conservation areas for an endangered and endemic raptor in Cuba through abundance spatial modeling: A niche-centroid distances approach. Global Ecology and Conservation, 31, e01877.

Figueroa, J. A., Cabrera, H. M., Queirolo, C., & Hinojosa, L. F. (2010). Variability of water relations and photosynthesis in *Eucryphia cordifolia* Cav. (Cunoniaceae) over the range of its latitudinal and altitudinal distribution in Chile. Tree physiology, 30(5), 574-585.

Gargallo-Garriga, A., Sardans, J., Granda, V., Llusià, J., Peguero, G., Asensio, D., ... & Peñuelas, J. (2020). Different “metabolomic niches” of the highly diverse tree species of the French Guiana rainforests. Scientific Reports, 10(1), 6937.

Garibay-Hernández, A., Kessler, N., Józefowicz, A. M., Türksoy, G. M., Lohwasser, U., & Mock, H. P. (2021). Untargeted metabotyping to study phenylpropanoid diversity in crop plants. Physiologia Plantarum, 173(3), 680-697.

Gigolashvili, T., & Kopriva, S. (2014). Transporters in plant sulfur metabolism. Frontiers in Plant Science, 5, 442.

González, A. L., Dézerald, O., Marquet, P. A., Romero, G. Q., & Srivastava, D. S. (2017). The multidimensional stoichiometric niche. Frontiers in Ecology and Evolution, 5, 110.

Grignon-Dubois, M., & Rezzonico, B. (2023). Phenolic chemistry of the seagrass *Zostera marina* Linnaeus: First assessment of geographic variability among populations on a broad spatial scale. Phytochemistry, 113788.

Harborne, J. B. (1975). Flavonoid sulphates: a new class of sulphur compounds in higher plants. Phytochemistry, 14(5-6), 1147-1155.

Hervé, M. R., Nicolè, F., & Lê Cao, K. A. (2018). Multivariate analysis of multiple datasets: a practical guide for chemical ecology. Journal of Chemical Ecology, 44, 215-234.

Hill, C. B., Czauderna, T., Klapperstück, M., Roessner, U., & Schreiber, F. (2015). Metabolomics, standards, and metabolic modeling for synthetic biology in plants. Frontiers in bioengineering and biotechnology, 3, 167.

Hong, J., Yang, L., Zhang, D., & Shi, J. (2016). Plant metabolomics: an indispensable system biology tool for plant science. International journal of molecular sciences, 17(6), 767.

Kumar, S., Abedin, M. M., Singh, A. K., & Das, S. (2020). Role of phenolic compounds in plant-defensive mechanisms. Plant Phenolics in Sustainable Agriculture: Volume 1, 517-532.

JS Lopes, F., Silva, J. J., Antuna Marrero, J. C., Taha, G., & Landulfo, E. (2019). Synergetic aerosol layer observation after the 2015 calbuco volcanic eruption event. Remote Sensing, 11(2), 195.

Mais, E., Alolga, R. N., Wang, S. L., Linus, L. O., Yin, X., & Qi, L. W. (2018). A comparative UPLC-Q/TOF-MS-based metabolomics approach for distinguishing *Zingiber officinale* Roscoe of two geographical origins. Food chemistry, 240, 239-244.

Majer, P., Neugart, S., Krumbein, A., Schreiner, M., & Hideg, É. (2014). Singlet oxygen scavenging by leaf flavonoids contributes to sunlight acclimation in *Tilia platyphyllos*. Environmental and Experimental Botany, 100, 1-9.

Martínez-Meyer, E., Díaz-Porras, D., Peterson, A. T., & Yáñez-Arenas, C. (2013). Ecological niche structure and rangewide abundance patterns of species. Biology letters, 9(1), 20120637.

Moco, S., Bino, R. J., Vorst, O., Verhoeven, H. A., de Groot, J., van Beek, T. A., ... & De Vos, C. R. (2006). A liquid chromatography-mass spectrometry-based metabolome database for tomato. Plant physiology, 141(4), 1205-1218.

Morales, L. V., Coopman, R. E., Rojas, R., Escandón, A. B., Flexas, J., Galmés, J., ... & Corcuera, L. J. (2014). Acclimation of leaf cohorts expanded under light and water stresses: an adaptive mechanism of *Eucryphia cordifolia* to face changes in climatic conditions?. Tree Physiology, 34(12), 1305-1320.

Osorio-Olvera, L., Yañez-Arenas, C., Martínez-Meyer, E., & Peterson, A. T. (2020). Relationships between population densities and niche-centroid distances in North American birds. Ecology Letters, 23(3), 555-564.

Patel, M. K., Pandey, S., Kumar, M., Haque, M. I., Pal, S., & Yadav, N. S. (2021). Plants metabolome study: Emerging tools and techniques. Plants, 10(11), 2409.

Payne, R. J., & Egan, J. (2019). Using palaeoecological techniques to understand the impacts of past volcanic eruptions. Quaternary International, 499, 278-289.

Raza, A. (2020). Metabolomics: a systems biology approach for enhancing heat stress tolerance in plants. Plant cell reports, 1-23.

Riquelme, S., Campos, J. V., Pecio, Ł., Alzamora, R., Mardones, C., Simonet, A. M., ... & Pérez, A. J. (2022). *Sirex noctilio* infestation led to inevitable pine death despite activating pathways involved in tolerance. Phytochemistry, 203, 113350.

Rivas-Ubach, A., Pérez-Trujillo, M., Sardans, J., Gargallo-Garriga, A., Parella, T., & Penuelas, J. (2013). Ecometabolomics: optimized NMR-based method. Methods in Ecology and Evolution, 4(5), 464-473.

Rodriguez, R., Marticorena, C., Alarcón, D., Baeza, C., Cavieres, L., Finot, V. L., ... & Marticorena, A. (2018). Catálogo de las plantas vasculares de Chile. Gayana. Botánica, 75(1), 1-430.

Santini, J., Giannettini, J., Herbette, S., Pailly, O., Ollitrault, P., Luro, F., & Berti, L. (2012). Physiological and biochemical response to photooxidative stress of the fundamental citrus species. Scientia Horticulturae, 147, 126-135.
Oksanen, E., & Kontunen-Soppela, S. (2021). Plants have different strategies to defend against air pollutants.Current Opinion in Environmental Science & Health,19, 100222.

Sardans, J., & Peñuelas, J. (2014). Climate and taxonomy underlie different elemental concentrations and stoichiometries of forest species: the optimum "biogeochemical niche".Plant ecology,215, 441-455.

Sartor, T., Xavier, V. B., Falcão, M. A., Mondin, C. A., Dos Santos, M. A., Cassel, E., ... & Santarém, E. R. (2013). Seasonal changes in phenolic compounds and in the biological activities of *Baccharis dentata* (Vell.) GM Barroso.Industrial crops and products,51, 355-359.

Segovia, R. A., Pérez, M. F., & Hinojosa, L. F. (2012). Genetic evidence for glacial refugia of the temperate tree *Eucryphia cordifolia* (Cunoniaceae) in southern South America. American Journal of Botany, 99(1), 121-129.

Singh, P., Arif, Y., Bajguz, A., & Hayat, S. (2021). The role of quercetin in plants. Plant Physiology and Biochemistry, 166, 10-19.

Skrynetska, I., Ciepał, R., Kandziora-Ciupa, M., Barczyk, G., & Nadgórska-Socha, A. (2018). Ecophysiological responses to environmental pollution of

selected plant species in an industrial urban area. International Journal of Environmental Research, 12, 255-267.

Smith, R., Mathis, A. D., Ventura, D., & Prince, J. T. (2014). Proteomics, lipidomics, metabolomics: a mass spectrometry tutorial from a computer scientist's point of view. BMC bioinformatics, 15(7), 1-14.

Stark, S., Julkunen-Tiitto, R., Holappa, E., Mikkola, K., & Nikula, A. (2008). Concentrations of foliar quercetin in natural populations of white birch (*Betula pubescens*) increase with latitude. Journal of chemical ecology, 34, 1382-1391.

Sumner, L. W., Mendes, P., & Dixon, R. A. (2003). Plant metabolomics: large-scale phytochemistry in the functional genomics era. Phytochemistry, 62(6), 817-836.

Sun, B. S., Xu, M. Y., Li, Z., Wang, Y. B., & Sung, C. K. (2012). UPLC-Q-TOF-MS/MS analysis for steaming times-dependent profiling of steamed *Panax quinquefolius* and its ginsenosides transformations induced by repetitious steaming. Journal of ginseng research, 36(3), 277.

Teles, Y. C., Horta, C. C. R., Agra, M. D. F., Siheri, W., Boyd, M., Igoli, J. O., ... & Souza, M. D. F. V. D. (2015). New sulphated flavonoids from *Wissadula periplocifolia* (L.) C. Presl (Malvaceae). Molecules, 20(11), 20161-20172.

Teles, Y. C., Souza, M. S. R., & Souza, M. D. F. V. D. (2018). Sulphated flavonoids: biosynthesis, structures, and biological activities. Molecules, 23(2), 480.

Tognetti, R., Lombardi, F., Lasserre, B., Battipaglia, G., Saurer, M., Cherubini, P., & Marchetti, M. (2012). Tree-ring responses in *Araucaria araucana* to two major eruptions of Lonquimay Volcano (Chile). Trees, 26, 1805-1819.

Tugizimana, F., Piater, L., & Dubery, I. (2013). Plant metabolomics: A new frontier in phytochemical analysis. South African Journal of Science, 109(5-6), 01-11.

Valledor, L., Escandon, M., Meijon, M., Nukarinen, E., Cañal, M. J., & Weckwerth, W. (2014). A universal protocol for the combined isolation of metabolites, DNA, long RNA s, small RNA s, and proteins from plants and microorganisms. The Plant Journal, 79(1), 173-180.

Wong, C., Ling, Y. S., Wee, J. L. S., Mujahid, A., & Müller, M. (2020). A comparative UHPLC-Q/TOF–MS-based eco-metabolomics approach reveals temperature adaptation of four Nepenthes species. Scientific reports, 10(1), 21861.

Wu, J., Lv, S., Zhao, L., Gao, T., Yu, C., Hu, J., & Ma, F. (2023). Advances in the study of the function and mechanism of the action of flavonoids in plants under environmental stresses. Planta, 257(6), 108.

2.3. Application of the ecological niche centrality hypothesis to evaluate the chemical composition and biological activity in the leaves of *Eucryphia cordifolia* Cav (Cunoniaceae).

Manuscrito enviado a la revista Plant Sciencie el 28 de Julio 2023.

Application of the ecological niche centrality hypothesis to evaluate the chemical composition and biological activity in the leaves of *Eucryphia cordifolia* Cav (Cunoniaceae).

Camila Fuica-Carrasco[a*], Lía Olivares-Caro[b], Cristian Parra-Sepúlveda[c], Andy J. Pérez[b], Claudia Mardones[b], Apolinaria García-Cancino[c], Víctor Hernández[a].

[a] Departamento de Botánica, Facultad de Ciencias Naturales y Oceanográficas, Universidad de Concepción, Concepción, Chile; camilafuica@udec.cl (C.F.); vhernand@udec.cl (V. H.).

[b] Departamento de Análisis Instrumental, Facultad de Farmacia, Universidad de Concepción, Concepción, Chile; liaolivares@udec.cl (L.O.); aperezd@udec.cl (A.P.); cmardone@udec.cl (C.M.)

[c] Departamento de Microbiología, Facultad de Ciencias Biológicas, Universidad de Concepción, Chile, cparras@udec.cl (C.P.); apgarcia@udec.cl (A.G).

* Corresponding author: camilafuica@udec.cl (C.F.); Tel. +56958001427 (C.F.).

Abstract

A study of how the location of *E. cordifolia* populations in their ecological niche affects the chemical composition, antioxidant activity, and antimicrobial properties of leaves extract, was carried out with the main objective to evaluate its potential as source of bioactive compounds. The chemical composition of the leaves extracts were characterized by ultra-liquid chromatography with diode array detector coupled to mass spectrometry. The antioxidant capacity, measured by three spectrophotometric methods, was applied to extracts obtained in different seasons and locations. The antimicrobial activity was determined by disc diffusion assays, minimum inhibitory concentration, minimum bactericidal concentration, and inhibition of biofilm formation of five microorganisms.

Twenty-eight compounds were identified in the leaves extract, including flavonols, flavones, flavanols, and other bioactive compounds. In autumn and spring, the peripheral population showed higher antioxidant values according to ABTS and ORAC methods and presented higher levels of total polyphenols only in autumn. The *E. cordifolia* extracts significantly reduced the growth of *E. coli*, *S. aureus* and *P. aeruginosa* with minimum

bactericidal concentration values ranged between 1.2 - 5.3 mg/mL, being considerably lower than those reported in other investigations. The results revealed that the peripheral population showed higher inhibition of *C. glabrata* biofilm formation than the centroid and intermediate populations in both summer and autumn.

Our results represent the first comprehensive investigation of *E. cordifolia* compounds in their natural environment, and in summary suggest that their leaves are a valuable source of bioactive compounds with biotechnological potential, but this potential is dependent of their ecological niche.

Keywords: antioxidant activity, antibacterial activity, antifungal activity, environmental conditions, polyphenols, , and UHPLC-DAD-QTOF-MS/MS.

2.3.1. Introduction

Chile has an exceptional flora, with approximately 40% of the registered vascular plant species in the country being endemic, and 40% considered native (Otero et al., 2022). The richness and uniqueness of plant biodiversity in Chile make it a country with unique bioresources, thanks to its distinctive characteristics (Otero et al., 2022; Rodriguez et al., 2018). These include the geographic isolation provided by the Andes Mountains, the vast Pacific Ocean, the arid Atacama Desert, and the Patagonia region. Additionally, Chile spans across different environmental gradients, ranging from the desert in the north to the temperate rainforests in the south, covering a wide range of latitudes (18°S to 56°S) (Salehi et al., 2020). Both endemic and native plants in Chile are estimated to have the potential to be a valuable source of bioactive compounds, as they represent underexplored resources (Barrientos et al., 2020; Senhaji et al., 2020; Zargoosh et al., 2019). Due to the wide variety of climates in the country, diverse research has been conducted on numerous plant species, investigating their chemical components and biological properties, either from extracts or purified compounds (López de Dicastillo et al., 2017; Shene et al., 2009). Native

berries have been the subject of prominent study compared to leaves (Lanuza et al., 2021; Salehi et al., 2020; Simirgiotis et al., 2013).

The synthesis of specialized metabolites in plants is widely recognized as a crucial mechanism for their adaptation and survival in response to various ecological factors present in their growth environments, such as temperature, precipitation, and solar radiation, among others (Hartmann, 2007). These metabolites have been used in traditional folk medicine since ancient times to treat various diseases (López de Dicastillo et al., 2017). Among the bioactive compounds present in plants, phenolic compounds stand out for playing an important role in humans (Millán et al., 2023). These compounds have demonstrated significant pharmacological activities, such as their antioxidant function in reducing oxidative damage caused by reactive oxygen species (ROS) (Pacifico et al., 2015). This can potentially prevent the onset of chronic degenerative diseases, such as cancer, cardiovascular, and neurodegenerative disorders (Jiménez-González et al., 2018; Olivares-Caro et al., 2020). Additionally, phenolic compounds also possess antimicrobial capacity against a wide range of disease-causing microorganisms (Karahan et al., 2016).

It has been observed that the presence, quality, and yield of bioactive compounds in plants can vary significantly in response to the ecological factors they are exposed to in their natural growth habitats (Karahan et al., 2016; Lanuza et al., 2021). It has been confirmed that environmental factors defining the ecological niche of plant populations can lead to the absence of certain compounds in the same species when collected from different geographic regions (Pacifico et al., 2015). Therefore, the geographical distribution of species can be considered as a spatial manifestation of their ecological niche, where the geographic range corresponds to a mapping of the habitat suitability of species as a function of the variable abiotic and biotic environment in a geographic area (Angert, 2009). For instance, Zargoosh et al., (Zargoosh et al., 2019) demonstrated that the environmental conditions characterizing the habitat of *Scrophularia striata* affect the quantity and accumulation of specialized metabolites in this species. Therefore, it is likely that the biological activity attributed to plant species is influenced by the position of natural populations within their ecological niche (Hutchinson 1953; Maguire 1973). In other words, populations located at the periphery of the ecological niche (marginal environmental conditions) may synthesize a greater diversity of bioactive compounds compared to populations at the

center of the ecological niche (favorable environmental conditions) (Lira-Noriega & Manthey, 2014; Martínez-Meyer et al., 2013).

Eucryphia cordifolia Cav. (Cunoniaceae), commonly known as Ulmo, is a native species of the southern forests of Chile (Rodriguez et al., 2018). It is found on the slopes of both mountain ranges and can reach heights of up to forty meters. Its leaves are persistent, meaning they remain throughout all seasons of the year (Baeza et al., 2023). This species is recognized for its remarkable economic potential, primarily due to the quality of its wood, which is widely used in construction and as a source of fuel (Uteau & Donoso, 2009). Unfortunately, these characteristics have resulted in high anthropogenic pressure, leading to a vulnerable conservation status for most populations (Morales et al., 2014). Historically, *E. cordifolia* has also been valued in the beekeeping industry due to its production of floral nectar, which attracts pollinating agents (Bridi & Montenegro, 2017). This aspect has been the focus of research on the species, demonstrating that monofloral Ulmo honey extracts have beneficial effects on humans, showing activity against bacteria and fungi, as well as acting as potent antioxidants to prevent oxidative stress (Bridi & Montenegro, 2017; Sherlock et al., 2010; Velásquez et al., 2020).

While this species is primarily recognized for its ecological role in the attracts pollinating agents in the forests of southern Chile, we believe that there is still a lack of comprehensive studies detailing the complete chemical profile of *E. cordifolia* to harness the potential of its compounds. However, recent research by Viteri et al., (Viteri et al., 2021, 2022) has focused on the phytochemical study and biological activity of *E. cordifolia leaves*, specifically isolating flavonoids, and triterpenes. Therefore, the objective of this investigation is to study the complete chemical profile (UHPLC-DAD-QTOF-MS/MS), as well as the antioxidant and antimicrobial activities (antibacterial and antifungal) of leaf extracts from different populations of *E. cordifolia*, considering their location within their ecological niche (center or periphery).

2.3.2. Materials and Methods

2.3.2.1. Reagents and standars

The following commercial standards were used: procyanidin B1, catechin, and quercetin rhamnoside (<90%). Analytical grade methanol was used for the antioxidant assays, were obtained from Merck (Darmstadt, Germany). 2,2-diphenyl-1-picrylhydrazyl (DPPH), 2,2-azino-bis (3-

ethylbenzothiazoline-6-sulfonic acid) diammonium salt (ABTS), 6-hydroxy-2,5,7,8-tetramethylchromane-2-carboxylic acid (Trolox), acid gallic and Folin–Ciocalteu's phenol reagent, potassium persulfate ($K_2S_2O_8$), formic acid, acetonitrile, methanol, and water (HPLC-MS grade or hypergrade), Müeller-Hinton agar, YPD agar, McFarland and crystal violet (CV) were purchased from Merck (Darmstadt, Germany), potassium phosphate monobasic (KH_2PO_4), potassium phosphate dibasic (K_2HPO_4), azobis (2-amidinopropane) dihydrochloride (AAPH), fluorescein sodium and dimetilsulfóxido (DMSO) were purchased from Sigma-Aldrich.

2.3.2.2. *E. cordifolia* leaves

Leaf samples of *E. cordifolia* were collected following the environmental categories previously defined by Fuica-Carrasco et al., (Fuica-Carrasco et al., 2023). Coronel (36°56'45"S 73°05'10"W) centroid population, Contulmo (38°00'47"S 73°11'09"W) intermediate population 1, La Unión (Individual 1: 40°11'59"S 73°25'43"W) intermediate population 2, and Puerto Montt (Individual 1: 41°35'35"S 72°35'36"W) environmentally peripheral population. Random samples were taken from 6 trees in each environmental category during the summer, autumn, and spring seasons. In

this study, the winter season was not considered due to the restrictions imposed by the COVID-19 pandemic, which prevented the collection of samples in some populations. Fresh leaves were immediately frozen in liquid nitrogen, transported to the laboratory, and stored at -80°C until further use.

2.3.2.3. Extraction of the leaves of *E. cordifolia*

2.3.2.3.1. Chemical characterization

For metabolite extraction, frozen fresh samples were freeze-dried and ground to fine powder in a ball mill MM-400 (GmbH, Haan, Germany) at 30 Hz for 1 min (Rivas-Ubach et al., 2013). Extraction was performed following the procedure suggested by Valledor et al., (Valledor et al., 2014). Briefly, 50 mg of each sample (in triplicate, technical replicates) were extracted with 1 ml of MeOH/Cl_2CH_2/H_2O (2.5:1:0.5), shaking at 30 hz for 1 min. After centrifuging at 1300 rpm for 10 min at 4°C, 700 µL of the supernatant were transferred to new Eppendorf tubes to perform a liquid-liquid extracted adding 400 µL H_2O and 400 µL Cl_2CH_2. The tubes were shaken at 20 hz for 30 sec and subsequently centrifuged at 1300 rpm for 10 min at 4°C. 600 µL of the aqueous upper phase were recovered, transferred to new tubes, and evaporated to dryness in a vacuum centrifuge (Eppendorf, Concentrator plus)

for 5 hours at 30°C. Dried extracts were stored at -20°C until analysis. Immediately before analysis, the extracts were reconstituted in MeOH 80% in water (v/v), shaken (30 hz for 1 min) and centrifuged (1300 rpm for 10 min at 4°C).

2.3.2.3.2. Antioxidant assays

The extraction process was carried out following the method described by Olivares-Caro et al., (Olivares-Caro et al., 2020). Sixty mg of leaves (pooled from the 6 trees) were dissolved in 2 mL of MeOH and sonicated (60s at 40%A). Then, the samples were shaken for 16 hours and after this time they were centrifuged at 3000 rpm for 10 min. Subsequently, the suspending agent was recovered and transferred to a 10 mL flask. The pellet was again spiked with 2 mL of MeOH, sonicated (60s at 40%A), shaken (30 min) and centrifuged (3000 rpm for 10 min), the supernatant was recovered and returned to the 10 mL flask. This process was repeated 4 times. Finally, the extracts were filtered to avoid any impurities. For each environmental site, a stock solution of 60 mg mL^{-1} was prepared from which methanolic solutions (60-1060 µg/mL) were prepared.

2.3.2.3.3. Microbial assays

1200 mg of dried leaves were used and extracted with 70.58 ml of methanol. The extracts were then concentrated to dryness using a V-700 vacuum pump and a V-850 control system (Büchi, Flawil, Switzerland). Finally, the extracts were freeze-dried to completely remove the water content. For each environmental site, three stock solutions (32, 16 and 2 mg/mL) dissolved in DMSO were prepared.

2.3.2.4. LC-MS analysis

Analysis of the samples by LC-MS using a UHPLC-DAD system (Elute, Bruker Daltonics GmbH, Bremen, Germany) coupled to a quadrupole time-of-flight mass spectrometer equipped with an atmospheric pressure electrospray ion source (Compact ESI-QTOF, Bruker Daltonik GmbH, Bremen, Germany). Chromatographic separation of the metabolome components was performed on a Kinetex C18 UHPLC column (100 × 3.0 mm,1.7 µm, Phenomenex) using a SecurityGuard Ultra Cartridge UHPLC C18 3.0 mm pre-column. The mobile phase consisted of solvent A (water with 0.1% formic acid) and solvent B (acetonitrile with 0.1% formic acid). Gradient elution was performed as follows: 5-50% of B from 0-15 min (concave increase), 50-95% of B (linear increases) from 15-15.5 min, 95%

of B isocratic for 4 min, at a flow rate of 0.4 mL/min. The total chromatographic run time was 15 min. The oven temperature was set at 30°C and the injection volume was 2 µl.

The mass spectrometer was operated in both ESI negative and positive acquisition modes. In a mass range, of 50 to 1500 *m*/*z*, scan cycle time, 2.0 s (-ES) and 1.0 s (+ES); dry temperature, 200ºC; capillary voltage, 3.4 kV (-ES) 4.0 kV(+ES); endplate offset, 0.5 kV; desolvation gas flow, 9.0 l min^{-1} (N_2); nebulizer, 2.0 Bar. MS/MS spectra were acquired from each scan by subjecting ions (maximum 2) to collision-induced dissociation (CID) if their absolute intensities exceeded 1000 counts per 0.1s cycle, with variable collision energy in the range of 20 to 50 eV (-ES) and 5-10 eV (+ES). Active exclusion of precursor ion was applied after one spectrum, and fragmentation was reconsidered if its intensity was at least equal to the previously measured one. Internal calibration was performed with sodium formate (10 mM in iso-PrOH/H2O, 1:1, v/v), which was pumped continuously at a rate of 1 µl min-1 through a six-port-valve so that 20 µl of it was delivered to the mass spectrometer just before each analysis.

MS detection was performed using a base peak chromatogram (BPC), data processing was performed using DataAnalysis 4.4 (Bruker Daltonics GmbH) and the spectral data was filtred with an intensity threshold of 2500. Metabolite identity was determined using Metaboscape 3.0 (Bruker Daltonics GmbH), Sirius 5.0 and global databases, such as ChEBI, Chemspider, PubChem and HMDB, where MS/MS fragments, retention times and intensity of the same fragments were compared. MS data were also compared with those of other publications. In addition, pure standards were used to confirm the identity of the metabolites to achieve level A identification.

2.3.2.5. Spectrophotometry

DPPH, ABTS and Folin-Ciocalteu assays were performed in 96-well transparent microplates (BIOFOIL, TCP 001096 wells). A 96-well black polystyrene microplate (Thermo Scientific TM 437111) was used for ORAC. Two microplate readers, Epoch™ from Biotek Instruments (Winooski, VT, USA) and ELX800 from BioTek (USA) were used for antioxidant assays. The results were expressed as IC_{50} values (extract concentration providing 50% inhibition) calculated from a regression curve.

Subsequently, they were expressed in terms of µmol Trolox equivalent (TE) per mg DW (DPPH, ABTS and ORAC) and µg of gallic acid equivalents (µg GAE)/mg DW (Folin-Ciocalteu).

2.3.2.5.1. DPPH$^{\bullet}$ radical scavenging activity

Measurement of antioxidant activity by DPPH, scavenging activity was carried out by the modified method of Brand-Williamns et al., (Brand-Williams et al., 1995). 2.4 mg of the DPPH radical were diluted in 100 ml of methanol and the absorbance was adjusted to 0.7 (±0.2) at 515 nm. 30 µL of each methanolic extract of *E. cordifolia* was mixed with 270 µL of DPPH radical solution. The samples were kept in the dark for 30 min and the absorbance was recorded at 515 nm using a microplate reader. All samples were performed in triplicate. Trolox was used as a standard antioxidant to compare the antioxidant efficacy of the extracts. The percentage decrease of DPPH radical was determined by the following equation:

$$DPPH\ (\%) = [(A_{control} - A_{samples}) / A_{control} \times 100]$$

Where A*control* corresponds to the absorbance of the DPPH radical + methanol and A*samples* corresponds to the absorbance of the DPPH radical + *E. cordifolia* extracts.

2.3.2.5.2. $ABTS^{\bullet+}$ radical scavenging activity

The antioxidant capacity of *E. cordifolia* methanolic extracts was analyzed using the ABTS assay described by Re et al., (Re et al., 1999). First, the cation radical $ABTS^{\bullet+}$ was obtained by mixing ABTS (3.75 mM) with potassium persulfate (1.225) diluted in ultrapure water. Subsequently, the solution was left to incubate in the dark for 16 hours at room temperature. Then, $ABTS^{\bullet+}$ was diluted in methanol and the absorbance was adjusted 0.70 (±0.2) at 750 nm. Second, the reactions were carried out in 96-well plates, where to 180 µL of the cation radical $ABTS^{\bullet+}$ was added 20 µL of the methanolic extracts at different concentrations (60-1060 µg mL^{-1}). Finally, the absorbance of the samples was measured after 30 minutes of incubation at 734 nm. All samples were performed in triplicate. Trolox was used as a standard antioxidant to compare the antioxidant efficacy of the extracts. The percentage decrease of $ABTS^{\bullet+}$ radical was determined by the following equation:

$$ABTS\ (\%) = [(A_{control} - A_{samples}) / A_{control} \times 100]$$

Where A*control* corresponds to the absorbance of the ABTS radical + methanol and A*samples* corresponds to the absorbance of the ABTS radical + *E. cordifolia* extracts.

2.3.2.5.3. Measurement of oxygen radical absorbance capacity (ORAC)

The ORAC assay was measured with a 96-well fluorescence microplate reader as described by Ou et al., (Ou et al., 2013). To each well 150 µL fluorescein (55.6 mM) and 25 µL of *E. cordifolia* extract and Trolox (0-70 µM) were added, then the plate was incubated for 30 minutes at 37°C in the microplate reader. After the incubation time 25 µL of APPH was added to generate the oxidation process. Finally, the fluorescence kinetic reading was recorded every for a total of 2 hours. Final ORAC values were calculated using a regression equation between the trolox standard and the area under the curve (AUC).

2.3.2.5.4. Determination of total phenolic concentration

Total polyphenol content was determined by the Folin-Ciocalteu colorimetric method Mongkolsilp et al., (Mongkolsilp et al., 2004). Ten µL of each extract (150 µg/mL) were mixed with 20 µL of 1 N Folin-Ciocalteu

reagent and 200 µL of ultrapure water, then the reaction was incubated for 5 minutes. After this time, 100 µL of 15% Na_2CO_3 was added and again the reaction was incubated for 1 hour in the dark and the absorbance was read at 750 nm. All extracts were measured in triplicate and the blank was methanol (replacing the extract). Gallic acid was used as standard to perform the calibration curve (25-250 µg/mL).

2.3.2.6. Screening for antibacterial activity

The antibacterial activity of *E. cordifolia* extracts in their different positions in the ecological niche was evaluated against the following microorganisms: *Escherichia coli* ATCC 25922, *Staphylococcus aureus* ATCC 25923, *Pseudomonas aeruginosa*, *Candida albicans* ATCC 90028 and *Candida glabrata* ATCC 90030.

2.3.2.6.1. Agar well diffusion method

The methodology described by Valgas et al., (Valgas et al., 2007) was used with some modifications. Four holes (6 mm in diameter, 20-30 mm apart) were drilled in the agar. The microbial suspensions used were adjusted to approximately 1.5 x 10^8 CFU/mL (McFarland 0.5%) and spread on

Müeller-Hinton agar plates (BD Difco, Sparks, MD, USA) for Gram positive and for Gram negative microorganisms (CLSI) and for C. *albicans* YPD agar (BD Difco, Sparks, MD, USA) was used. Three serial dilutions were used, obtaining concentrations of 8, 16 and 32 mg/mL (for each extract of *E. cordifolia*), all diluted in DMSO. Consecutively 70 µL of each extract with their respective dilutions were added to each well drilled. DMSO at 50% was used as a negative control. Finally, the plates were incubated for 18-24 h at 37ºC ± 1ºC, under aerobic conditions. The inhibition halo was measured in mm and was determined by the following equation:

Inhibition of microbial growth (mm): *D-d*

Where *D* corresponds to the diameter of the halo (mm) and *d* is the diameter of the drilled wells (mm) (Nguyen et al., 2021). The results were expressed according to the criteria of Gaudana et al. (2010), where halos of 1 mm were considered as no inhibition (+/-), halos of 2 mm corresponded to a mild inhibition (+), halos between 2-5 mm, strong inhibition (++) and finally halos greater than 5 mm presented a very strong inhibition (+++).

2.3.2.6.2. Determine minimum inhibitory concentration (MIC).

The antibacterial activity of *E. cordifolia* extracts was studied using the microdilution method. Initially, a stock concentration of 32 mg/mL of *E. cordifolia* extracts was prepared and from these, serial dilutions were prepared reaching concentrations of 5.3, 2.7, 1.3 and 0.7 mg/mL, all diluted in Müeller-Hinton culture broth (*E. coli*, *S. aureus* and *P. aeruginosa*) and YPD (*C. albicans* and *C. glabrata*). Subsequently, 200 µL of each extract was aliquoted into 96-well plates and inoculated with 10 µL of each microorganism under study. Culture broth plus the microorganism was used as positive control, while only broth was used as negative control. Finally, all plates were incubated at 37°C for 18-24h. MIC values were defined as the lowest concentration of each extract that resulted in no visible growth on the broth surface (Hemeg et al., 2020).

2.3.2.6.3. Minimum bactericidal concentration (MBC).

MBC was determined by adding 10 µL of the serial dilution that showed no visible growth on MIC on blood agar plates (2.5% equine) for all *E. cordifolia* extracts. Subsequently all plates were incubated at 37ºC for 18-24h. The MBC were determined as the lowest concentrations of extract at which microbial growth did not occur (Hemeg et al., 2020).

2.3.2.6.4. Biofilm formation assay and quantification

Biofilm formation was determined as described by Bazargani & Roholoff et al., (Bazargani & Rohloff, 2016) with some modifications. The microorganisms under study were prepared in 0.5% McFarland. After preparation of the bacterial suspensions, sterile glass coverslips were placed in 24-well flat-bottom plates. A final volume of 700 µl containing each microbial suspension more the *E. cordifolia* extracts (at MBC value) was added to each well and incubated at 37°C for 24h.

Cell biomass adhering to the coverslip was determined by crystal violet (CV) staining (Negri et al. 2019). After incubation, the broth and planktonic cells were removed by aspiration and the wells were washed three times with phosphate buffered saline (PBS). Plates were dried for 10 min and then stained with 800 µL of 0.1 % w/v CV (Merck, Darmstadt, Germany) for 5 min. The CV was removed, and the wells were allowed to dry for 10 min. Subsequently, four washes with PBS were performed to remove excess free CV. The biofilm bound dye was extracted by adding 800 µl of an ethanol/acetone mixture (80:20).

Finally, 200 µl of each solution was transferred to 96-well polystyrene microplates (SPL Life Sciences) and biofilm formation levels were estimated by measuring absorbance at 590 nm using a proInfinite M200 microplate reader (Tecan Trading AG, Männedorf, Switzerland). The assay was performed at room temperature and in triplicate. As a positive control, the broth with the respective microorganism was used, and as a negative control, only McFarland 0.5% broth was used. Extracts were classified as biofilm forming when the absorbance values were twice more than the value of the positive control (Stepanović et al., 2007).

2.3.2.7. Statistical analysis

Antioxidant capacity (ABTS, DPPH and ORAC), determination of total phenol content and microbial assays were performed in triplicate. The value for each sample was calculated as the mean ± standard deviation. To determine whether population and seasonality were significant variables, a two-way ANOVA was performed with a tukey's multiple comparison analysis for antioxidant assays and a dunnet's test for microbial assays where each population was compared to a positive control.

2.3.3. Results and discussions

2.3.3.1. Identification

The base peak chromatograms (BPC) of the methanolic extracts of *E. cordifolia* leaves are shown in Figure 2.3.1 (negative ionization mode) and Figure 2.3.2 (positive ionization mode), while the metabolite name (tentative identification) corresponding to each peak number is presented in Supplementary Material (Table S3.1 and S3.2). Compounds were sorted by retention time, where peak numbers correspond to elution order, tentative assignment, metabolite class, molecular formula, theoretical and found m/z, mass error (ppm), major fragments detected in MS/MS, UV/Vis, InChI-Key, identification level and environmental population found. A detailed description of all precursor ions and their fragments was performed in negative mode, and only those ions in positive mode that were not reported in negative mode were included. The level of identification was in most cases B, based on Alseekh et al., (Alseekh et al., 2021).The main classes of compounds detected were Cyclitol carboxylic acid (n=1), tannins (n=2), flavonols (n=9), flavones (n=3), flavanones (n=3), flavanols (n=4), Cinnamic acid derivatives (n=1), Dibenzofurans (n=1), Cyclohexan sesquiterpene glycoside (n=1), and sulfated compounds (n=3). Some of these compounds

have already been identified for *E. cordifolia* in other studies, but with a targeted approach (Bate-Smith et al. 1967; Birdi et al. 2019; Viteri et al. 2021). However, this is the first study to provide a detailed description of the metabolite profile in extracts of *E. cordifolia* leaves using high-resolution MS.

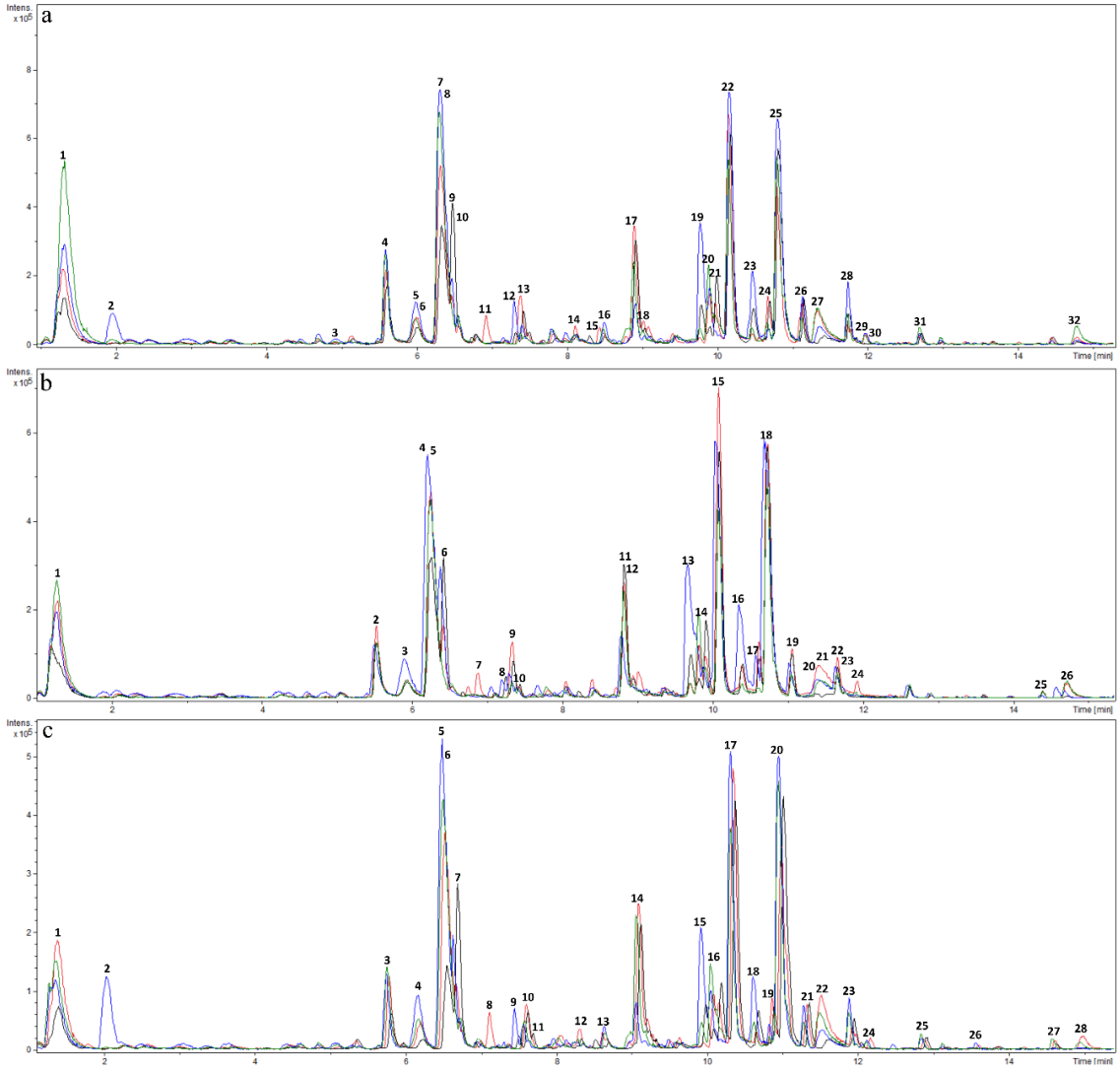

Figure 2.3.1. Base peak chromatogram (BPC) of methanolic extracts of *E. cordifolia* leaves in negative ionization mode (a) summer (b) autumn and (c) spring. In red Coronel (centroid population), in green Contulmo (intermediate population 1), in blue La Unión (intermediate population 2) and in black Puerto Montt (peripheral population).

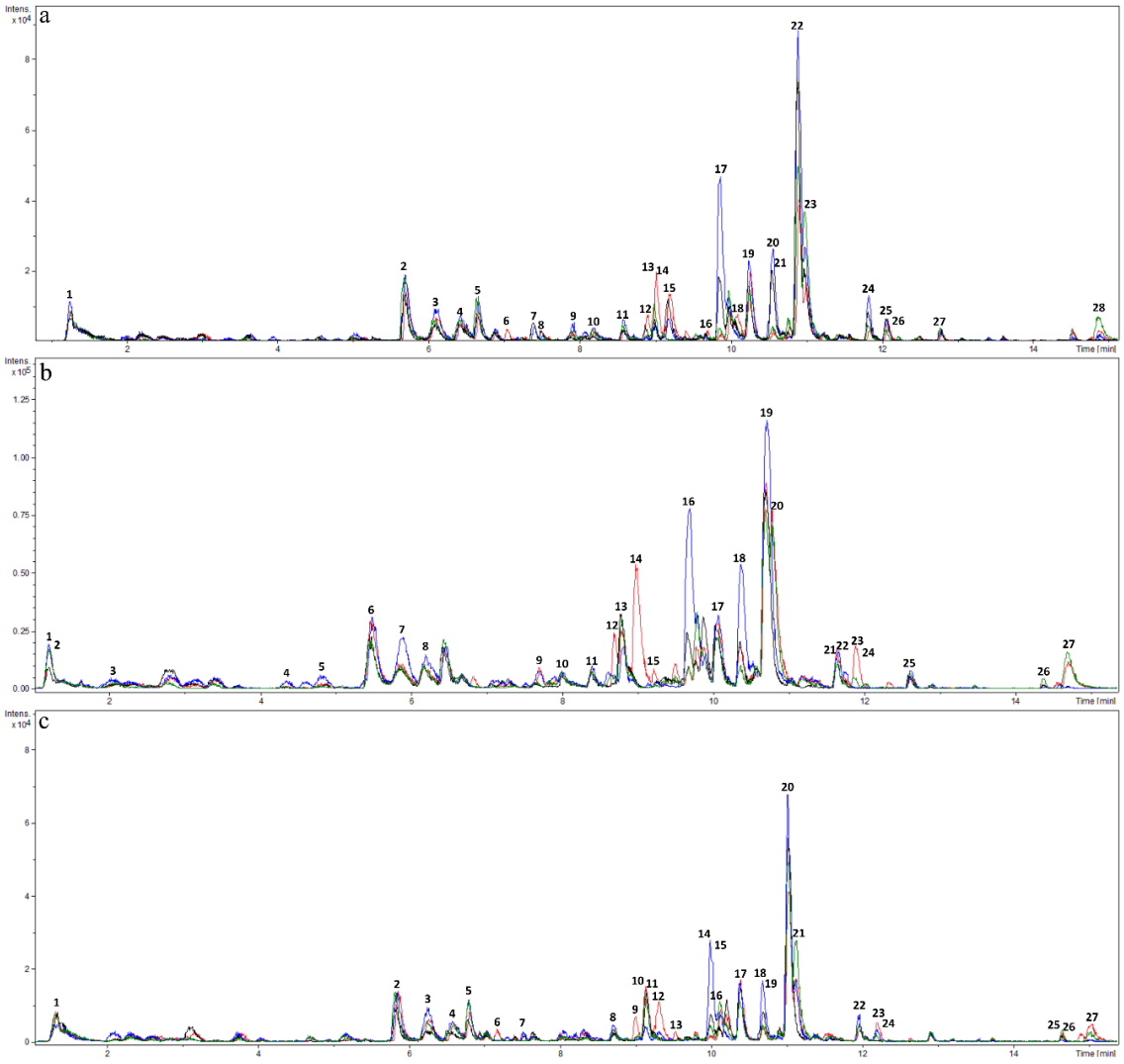

Figure 2.3.2. Base peak chromatogram (BPC) of methanolic extracts of *E. cordifolia* leaves in positive ionization mode (a) summer (b) autumn and (c) spring. In red Coronel (centroid population), in green Contulmo (intermediate population 1), in blue La Unión (intermediate population 2) and in black Puerto Montt (peripheral population).

2.3.3.1.1. Cyclitol carboxilic acid

Quinic acid: The pseudomolecular ion $[M - H]^-$ 191.0558 m/z $[C_7H_{12}O_6]$ was detected in Coronel, Contulmo, La Unión and Puerto Montt (signal 1) and in the three seasons investigated (summer, autumn and spring). The fragment 173.0458 m/z, results from dehydration of the deprotonated molecular ion and fragment ions (127.0411 and 111.0465 m/z) (Galasso et al., 2014; Galvão et al., 2023).

2.3.3.1.2. Tannins

Glucogallin: The pseudomolecular ion $[M - H]^-$ 331.0673 m/z $[C_{13}H_{16}O_{10}]$ was found in Coronel, Contulmo and La Unión in the summer season (signal 2), while in spring it was only identified in the intermediate populations of the ecological niche of *E. cordifolia* (Contulmo and La Unión) (signal 2). Its fragment ions were: 331.0674, 169.0144 (loss of glucoside) and 271.0458 m/z (Hong et al., 2021). This compound has been previously reported in extracts of *Paeonia rockii* and *Paeonia ostii* (Bai et al., 2022).

Digalloylhexose: The pseudomolecular ion $[M - H]^-$ 483.0799 m/z $[C_{20}H_{20}O_{14}]$ was found only in the intermediate population (La Union) in the

autumn season (signal 3). The fragment ions were: 131.0729, 483.0786, 211.0267 and 169.0142 (gallic acid) m/z. The pseudomolecular ion and UV spectrum coincide with those reported by Tarone et al., (Tarone et al., 2021), Osman et al., (Osman et al., 2022), and Galvão et al., (Galvão et al., 2023). Similarly, the fragment ions match the findings reported in HMDB0039179.

2.3.3.1.3. Flavonoids

Flavonols. Quercetin-hexoside isomer: The pseudomolecular ion [M - H]$^-$ 463.0905 m/z [$C_{21}H_{19}O_{12}$]$^-$ was present in all *E. cordifolia* populations and in the three seasons investigated (signal 3 and 19 in summer, signal 13 in autumn and signal 15 in spring). The fragment ions were: 463.0873, 271.0245 (aglycone moiety) and 301.0334 (quercetin aglycone) (Fraige et al., 2018; Nova-Baza et al., 2022). Bate-Smith et al., (Bate-Smith et al., 1967) demonstrated the presence of this type of flavonoids in extracts of species of the genus *Eucryphia.*

Quercetin-pentoside isomer: The pseudomolecular ion [M - H]$^-$ 433.0764 m/z [$C_{20}H_{17}O_{11}$]$^-$ was present in the four populations of *E. cordifolia* and in the three seasons investigated (signal 23 in summer, signal 16 in autumn and signal 18 in spring). For this isomer, the characteristic

quercetin-pentoside fragmentation pattern was observed: 433.0767, 271.0241 (aglycone moiety) and 301.0328 m/z (quercetin aglycone) (Lachowicz & Oszmianski, 2019).

Quercetin-rhamnoside isomer: The pseudomolecular ion $[M - H]^-$ 447.0925 m/z $[C_{21}H_{19}O_{11}]^-$ was present in the four populations of *E. cordifolia* and in the three seasons investigated (signal 25 in summer, signal 18 in autumn and signal 20 in spring). Its identity was confirmed using the quercetin-rhamnoside standard, where coincidences were found between the pseudomolecular ion and the fragment ions. The fragment ions with the highest intensity were: 447.0925, 301.0341 (quercetin aglycone) and 271.0247 m/z (aglycone moiety) . This compound has been previously isolated from leaf extracts of *E. cordifolia* (Bate-Smith et al., 1967; Viteri et al., 2022).

Kaempferol rhamnoside isomer: The pseudomolecular ion $[M - H]^-$ 431.0983 m/z $[C_{21}H_{19}O_{10}]^-$ was found in all *E. cordifolia* populations and in all seasons (signal 28 in summer, signal 22 in autumn and signal 23 in spring). The highest intensity fragment ion was 285.0385 m/z (kaempferol aglycone), 255.0304 m/z, 431.0991 m/z and 227.0358 m/z (Hofmann et al., 2016;

Maulidiani et al., 2014; Nova-Baza et al., 2022; Simirgiotis & Schmeda-Hirschmann, 2010).

Laricitrin hexoside: The pseudomolecular ion $[M - H]^-$ 493.0992 m/z $[C_{22}H_{21}O_{13}]^-$ was present in Coronel, Contulmo and La Unión in the summer season (signal 29) and in Coronel in the autumn season (signal 24). Fragmentation yielded ions 331.0466 m/z (laricitrin aglycone), 316.0232 m/z (myricetin aglycone) and 493.1006 m/z (Jiménez-Aspee et al., 2018; Mikulic-Petkovsek et al., 2017; Sanz et al., 2012; Simirgiotis et al., 2013).

Isorhamnetin-hexoside: The pseudomolecular ion $[M - H]^-$ 477.1041 m/z $[C_{22}H_{21}O_{12}]^-$ was detected in Coronel, Contulmo and La Unión for the four seasons investigated (signal 30 in summer, signal 21 in autumn and signal 24 in spring). The most intense fragment ions were 300.0286 (demethylation of aglycone), 315.0516 m/z (isorhamnetin aglycone) and 477.1074 m/z (Mikulic-Petkovsek et al., 2017; Nova-Baza et al., 2022).

Syringetin: The pseudomolecular ion $[M + H]^+$ 347.0792 m/z $[C_{17}H_{15}O_8]^+$ was found in the populations of Coronel, Contulmo and La Unión in summer (signal 15) and was only found in the Contumo population in the spring season (signal 12). The highest intensity fragment ions were:

347.0742 m/z, 331.048 m/z (demethylation) and 286.0309 m/z (demethoxylation). The UV spectrum of this compound exhibits a correspondence with the reported values for flavonols, as it presents an absorption at 356 nm (Mattivi et al., 2006; Xu et al., 2011).

Syringetin hexoside: The pseudomolecular ion $[M + H]^+$ 509.1291 m/z $[C_{23}H_{25}O_{13}]^+$ was found in the centroid population (Coronel) and in the peripheral population (Puerto Montt) in summer (signal 12). In autumn and spring, it was only present in the Coronel population (signal 9 in both cases). The fragment ions with the highest intensity were: 347.0726 m/z (syringetin aglycone), 509.1243 m/z, 286.0445 m/z (demethoxylation of aglycone) and 331.0427 m/z (demethylation of aglycone) (Ivanova et al., 2011; Pérez-Navarro et al., 2019; Y. Zhao et al., 2017).

Flavone. Luteolin: The pseudomolecular ion $[M + H]^+$ 287.0550 m/z $[C_{15}H_{11}O_6]^+$ was found in Coronel, Contulmo and Puerto Montt in summer (signal 24), in autumn and spring it was reported in all populations of *E. coridfolia* (signal 21 in both seasons). The only fragment ion detected was 287.0560 m/z, so its identity was only corroborated by its exact mass and

with the HMDB05800 database (Gao et al., 2017; Yun et al., 2006). The UV spectrum is coincident with that reported by Boué et al., (Boué et al., 2003).

Cirsiliol: The pseudomolecular ion $[M + H]^+$ 331.0787 m/z $[C_{17}H_{15}O_7]^+$ was found in Coronel, Contulmo and Puerto Montt in summer (signal 23), in autumn it was found in the populations of Coronel and Contulmo (signal 20) and in spring it was detected in Coronel, Contulmo and La Unión (signal 20). The fragment ions with the highest intensity were: 331.0783, 270.0500 and 316.0544 m/z. Their identity was only corroborated by means of their exact mass, fragmentation pattern (MSBNK-Univ_Toyama-TY000127) and UV spectra (Gevrenova et al., 2023; Grayer et al., 2001, 2010; Nikolova et al., 2006).

Tricin-O-hexoside: The pseudomolecular ion $[M + H]^+$ 493.1325 m/z $[C_{23}H_{25}O_{12}]^+$ was detected only in the centroid population (Coronel) in all seasons (signal 16 in summer, signal 15 in autumn and signal 13 in spring). The fragment ions evidenced were: 331.0755 m/z (tricin aglycone), 493.1325 m/z and 316.0596 m/z (demethylation of aglycone) pattern coincident with that reported by Galland et al., (Galland et al., 2014) and HMDB0030553.

Flavanones. Taxifolin hexoside: The pseudomolecular ion $[M - H]^-$ 465.1038 m/z $[C_{21}H_{21}O_{12}]^-$ was found only in summer in all *E. cordifolia* populations (signal 14). The fragmentation pattern considered the following major ions: 285.0409 (dihydroxylation of taxifolin), 151.0040 (taxifolin moiety) and 465.1033 m/z (Álvarez-Fernández et al., 2015).

Taxifolin pentoside: The pseudomolecular ion $[M - H]^-$ 435.0940 m/z $[C_{20}H_{19}O_{11}]^-$ was found in all populations of *E. cordifolia* and in the three seasons investigated (signal 17 in summer, signal 12 in autumn and signal 14 in spring). Its fragment ions were: 151.0331 m/z (taxifolin moiety), 285.0405 m/z (dihydroxylation of taxifolin), 435.0933 m/z and 303.0514 m/z (taxifolin aglycone) (Baloglu et al., 2019; De Rosso et al., 2020; Santos et al., 2013). The UV spectrum agrees with that reported with Ado et al., (Ado et al., 2015).

Astilbin isomer: The pseudomolecular ion $[M - H]^-$ 449.1078 m/z $[C_{21}H_{21}O_{11}]^-$ was found in all four populations of *E. cordifolia* and in the investigated seasons (signal 20 and 22 in summer, signal 14, 15 and 17 in autumn and signal 16, 17 and 19 in spring). The fragment ions with the highest intensity were: 303.0509 m/z (taxifolin aglycone), 151.0039 m/z (taxifolin moiety) and 285.0404 m/z (dihydroxylation of taxifolin) (Kedrina-

Okutan et al., 2018; Yuk et al., 2017; M. Zhao et al., 2014). The identity of the compound is coincident with that reported in extracts of *Weinmannia trichosperma* Cav. (Cunoniaceae) (Barrientos et al., 2020), a species native to Chile. In addition, this compound has been previously isolated in extracts of bark and leaves of *E. cordifolia* (Tschesche et al., 1979; Viteri et al., 2021).

Flavanols. Catechin: The pseudomolecular ion $[M - H]^-$ 289.0723 m/z $[C_{15}H_{15}O_7]^-$ was detected in all *E. cordifolia* populations and in the three seasons investigated (signal 8 in summer, signal 4 in autumn and signal 5 in spring). The fragmentation pattern is coincident with that reported by Zhao et al., (Zhao et al., 2022), where its highest intensity ions were 245.0838 (loss CO_2) and 289.0738 m/z. Furthermore, its identity was corroborated with its commercial standard, where the pseudomolecular ion and fragmentation pattern matched. On the other hand, catechin has been previously isolated in leaf extracts of *E. cordifolia* (Viteri et al., 2021).

Procyanidin B1 isomer: The pseudomolecular ion $[M - H]^-$ 577.1363 m/z $[C_{30}H_{25}O_{12}]^-$ was found in the four populations of *E. cordifolia* and in the three seasons investigated (signal 4, 5, 16 and 32 in summer, signal 2 and 26 in autumn and signal 3,4, 13 and 28 in spring). Their identity was

corroborated by using procyanidin B1 standard and furthermore their fragment ions were typical for this class of compounds which. The fragment ions of highest intensity observed were: 289.0739 m/z (catechin aglycone), 425.0878 m/z (C-ring cleavage with loss of catechol) (Ismail et al., 2019), and 577.1333 m/z, which is consistent with the patterns described by Ismail et al., (Ismail et al., 2019) and Vo et al., (Vo et al., 2022). Furthermore, the ion at 285.0739 m/z is formed through interflavonoid bond cleavage via the quinone-methyl (QM) mechanism, as described by Jerez et al., (Jerez et al., 2009).

Procyanidin C isomer: The pseudomolecular ion $[M + H]^+$ 867.2074 m/z $[C_{45}H_{39}O_{18}]^+$ was found in all *E. cordifolia* populations in summer and spring (signal 5 in both cases). It exhibited the ion 289.0693 m/z (loss catechin aglycone), 287.0443 m/z and 579.1448 m/z (loss of a flavan-3-ol unit) (Li et al., 2017).

Gambiriin: The pseudomolecular ion $[M - H]^-$ 579.1504 m/z $[C_{30}H_{27}O_{12}]^-$ was detected in all *E. cordifolia* populations only in autumn (signal 5). The fragment ions were as follows: 289.0727 (catechin aglycone), 245.0828 (generated by retro-diels-alder) and 203.0828 (cleavage of the A-

ring of flavan-3-ol) pattern coincident with that reported by Dienaite et al., (Dienaite et al., 2020).

2.3.3.1.4. Cinnamic acid derivates

Caffeoylglucoside: The pseudomolecular ion $[M - H]^-$ 341.0900 m/z $[C_{15}H_{17}O_9]^-$ was identified in the Contulmo population only in summer (signal 6). The fragment ions were as follows: 135.0460 m/z (caffeic acid moiety), 179.0364 m/z (caffeic acid) and 341.0882 m/z (Nova-Baza et al., 2022). Its fragmentation pattern is coincident with that reported in leaf extracts of *Helicrysum melaleucum* (Gouveia & Castilho, 2010) and *Prunus mume* (Zhang et al., 2015).

2.3.3.1.5. Dibenzofurans

Pseudoplacodiolic acid: The pseudomolecular ion $[M - H]^-$ 375.1081 m/z $[C_{19}H_{19}O_8]^-$ was found in Coronel, La Unión and Puerto Montt in the summer season (Signal 10). This compound is commonly characterized and identified in lichen extracts (Musharraf et al. 2015; Cornejo et al. 2016). Arche et al., (Areche et al., 2022) demonstrated the presence of this compound in *Himantormia lugubr*is, a lichen endemic to Antarctica.

However, we found no record of this type of compound in plant extracts, so we inferred that the leaves of *E. cordifolia* contained spores of some type of lichen present in the forest where the plant samples were taken.

2.3.3.1.6. Sulfated Compounds

Ethyl-5-octyl-2.2-dioxo-1.3.2-dioxathiolane-4-carboxylate: The pseudomolecular ion $[M - H]^-$ 307.1216 m/z $[C_{13}H_{23}O_6S]^-$ was detected in the four populations of *E. cordifolia* and in the three seasons investigated (signal 9 in summer, signal 6 in autumn and signal 7 in spring). The fragment ions with the highest intensity were: 307.1204 and 96.9536 m/z (sulfate).

Persicarin: The pseudomolecular ion $[M - H]^-$ 395.0095 m/z $[C_{16}H_{11}O_{10}S]^-$ was identified in all populations of *E. cordifolia* in summer (signal 18 and 27) and in spring it was present in Coronel, Contulmo and La Uníon (signal 22). The fragment ions with the highest intensity were 330.0401 m/z (dihydroxylation and demethoxylation), 287.0196 (B-ring cleavage isorhamnetin aglycone moiety), 271.0255 (isorhamnetin aglycone moiety) and 299.0199 m/z (isorhamnetin aglycone) (Teles et al., 2018).

Dimethoxy apigenin sulfonic acid: The pseudomolecular ion $[M - H]^-$ 409.0233 m/z $[C_{17}H_{13}O_{10}S]^-$ was found in Coronel, Contulmo, La Unión and Puerto Montt in summer (signal 21). The fragmentation pattern consisted of the following highest intensity ions: 329.0675 m/z (loss sulfonic acid), 271.0246 and 409.0248 m/z.

2.3.3.1.7. Cyclohexan sesquiterpene glycoside

7-Mega-stigmene-3,6,9-triol hexoside: The pseudomolecular ion $[M + HCOOH - H]^-$ 435.2236 m/z $[C_{20}H_{35}O_{10}]^-$ was found in La Unión and Puerto Montt in the summer season (signal 12). The identity of this compound could only be corroborated with the databases used in this research. The fragment ions with the highest intensity were: 435.2271 m/z (formate adduct), 389.2211 m/z $[M - H]^-$ and 161.0465 m/z (hexoside moiety).

2.3.3.1.8. Unidentified compounds

Numerous compounds that could not be identified were detected and recorded in the list under the category of "unidentified." In Tables S3.1 and S3.2, for both negative and positive ionization modes, information was

provided regarding the pseudomolecular ion, fragmentation pattern, UV/vis data, and the location of the compounds at the sampling sites.

The identification conducted allows us to infer that the chemical profile of *E. cordifolia* populations varies according to their location in the ecological niche during the evaluated season. In some cases, the absence of certain compounds in these populations has even been demonstrated. This phenomenon is primarily due to the constant environmental fluctuations to which the plants are exposed in their ecological niche (Gomes et al., 2021).

2.3.3.2. Antioxidant capacity

Given the broad diversity of chemical compounds in plants and the particularities and limitation of each antioxidant assay, it is ideally using combination of assays with different mechanisms to evaluate antioxidant potential thus allowing an exhaustive analysis (Corrêa et al., 2021; Galasso et al., 2014). Thus, *E. cordifolia* extracts were evaluated by a combination of assays: DPPH, ABTS, ORAC and total phenolic compounds and the results are shown in Figure 2.3.3.

The analysis of variance for the antioxidant assays revealed that both the position of populations in their ecological niche and seasonality were

significant variables in the study (Table S3.3). In the DPPH assay, fluctuations were observed in the antioxidant activity values, ranging from 0.056 ± 0.00 to 0.336 ± 0.01 eq. trolox μmol/mg DW across the three investigated stations. The intermediate population 2, known as La Unión, recorded the highest levels of antioxidant capacity in the three seasons (0.188 ± 0.02; 0.336 ± 0.01; and 0.217 ± 0.00 eq. trolox μmol/mg DW). On the other hand, the Contulmo population (intermediate population 1) exhibited the lowest values. No significant differences were found in the antioxidant capacity between the centroid and peripheral populations (Figure 2.3.3a). In the ABTS assay, antioxidant capacity values ranged from 0.325 ± 0.01 to 0.781 ± 0.01 eq. trolox μmol/mg DW were recorded. During the summer, the peripheral population exhibited significantly higher antioxidant activity (0.677 ± 0.03 eq. trolox μmol/mg DW) compared to the centroid population (0.403 ± 0.02 eq. trolox μmol/mg DW) and the intermediate populations (0.336 ± 0.06 and 0.567 ± 0.00 eq. trolox μmol/mg DW). However, during autumn and spring, the antioxidant capacity of the population intermediate 2 (La Unión, 0.742 ± 0.04 and 0.549 ± 0.03 eq. trolox μmol/mg DW) was significantly higher compared to the centroid population (Coronel, 0.334 ± 0.01 and 0.327 ± 0.01 eq. trolox μmol/mg DW) and the intermediate

populations (Contulmo, 0.584 ± 0.05 and 0.391 ± 0.02 eq. trolox μmol/mg DW). Our values are higher than those reported for leaf extracts of four native *Berberis* species in Chile (Nova-Baza et al., 2022). Regarding the ORAC assay, a similar trend to the ABTS assay was observed. During summer and spring, it was found that the peripheral population exhibited significantly higher antioxidant activity (34.985 ± 1.79 and 25.712 ± 1.78 eq. trolox μmol/mg DW) compared to the other populations. The levels of antioxidant capacity measured by the ORAC method in all extracts of *E. cordifolia* were significantly higher than those reported for *Ugni molinae* (8.6 ± 0.6 to 23.8 ± 1.7 μmol TE/mg DE), a native species of Chile commonly used as an infusion by indigenous communities (Peña-Cerda et al., 2017). The remarkable antioxidant capacity of *E. cordifolia* extracts is attributed to the presence of quercetin and its derivatives, compounds known for their ability to eliminate free radicals. Therefore, these compounds demonstrate their role as potent antioxidants in the context of this research (Quispe et al., 2012).

It was observed that La Unión showed higher values in total polyphenol content during the three seasons: summer (313,232 ± 10.81 eq. GA μg/mg DW), autumn (330,627 ± 5.13 eq. GA μg/mg DW), and spring (312,398 ± 17.59 eq. GA μg/mg DW). However, a significant difference in

total polyphenol content was only observed during autumn, where the peripheral population (296.736 ± 5.77 eq. GA μg/mg DW) was significantly higher than the centroid population (276.216 ± 4.47 eq. GA μg/mg DW). In contrast to the antioxidant activity, the content of phenolic compounds in *E. cordifolia* extracts was lower than that reported by Nova-Baza et al., (Nova-Baza et al., 2022). Therefore, the remarkable antioxidant capacity of *E. cordifolia* extracts may be influenced by compounds other than polyphenols.

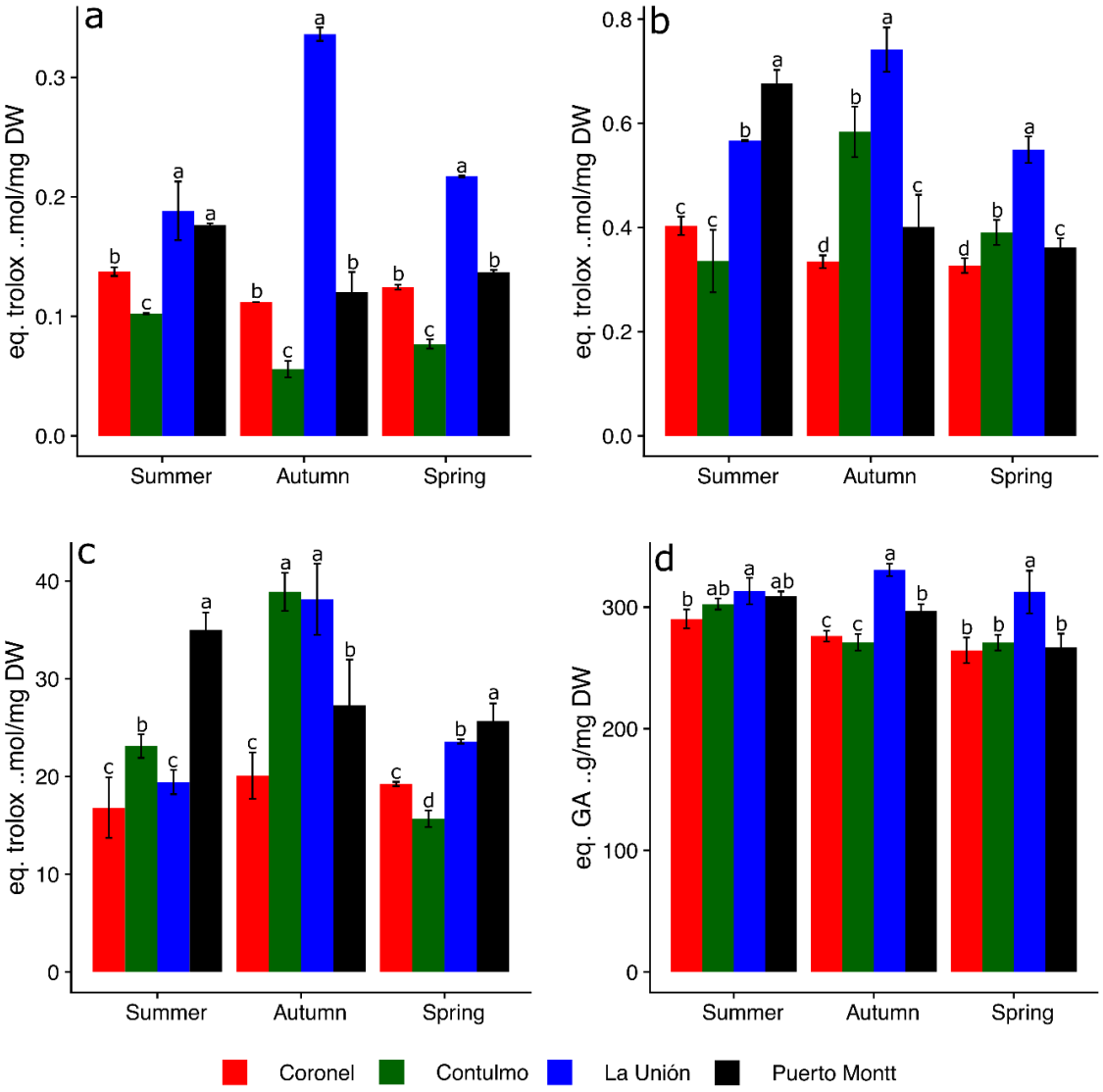

Figure 2.3.3. Antioxidant activity in extracts of *E. cordifolia* according to their position in the ecological niche a) DPPH b) ABTS c) ORAC and d) Folin-Ciocalteu.

2.3.3.3. Antimicrobial activity

The sensitivity of five microorganisms to 15 extracts of *E. cordifolia* was evaluated, considering their position in the ecological niche and seasonality. The agar well diffusion method was initially used to determine the antimicrobial potential. The diameters of the inhibition zones caused by the *E. cordifolia* extracts against the evaluated microorganisms, represented by the clear areas around the discs in Figure 2.3.4, are presented in Table S3.4.

All analyzed extracts exhibited significant antimicrobial activity against *E. coli*, *S. aureus*, and *P. aeruginosa*. However, when using low concentrations (2 and 16 mg/mL) of all tested extracts, no inhibition against *C. albicans* was detected. Furthermore, it was observed that during the summer, the peripheral population (Puerto Montt) exhibited stronger inhibition of *C. glabrata* compared to Coronel (central population), while in spring, the opposite effect was observed at the highest tested extract concentration (36 mg/mL). In autumn, a strong inhibition of *C. glabrata* was observed in both the central and peripheral populations, with weak inhibition in Contulmo. Finally, at the lowest tested extract concentration, no inhibition was demonstrated. On the other hand, Shene et al., (Shene et al., 2009)

demonstrated that extracts from murta leaves (*Ugni molinae*) exhibited good antibacterial activity, with significant inhibition values against *P. aeruginosa* and *S. aureus*, similar to our results. 178dditionally, we demonstrated an even higher inhibition on *E. coli*.

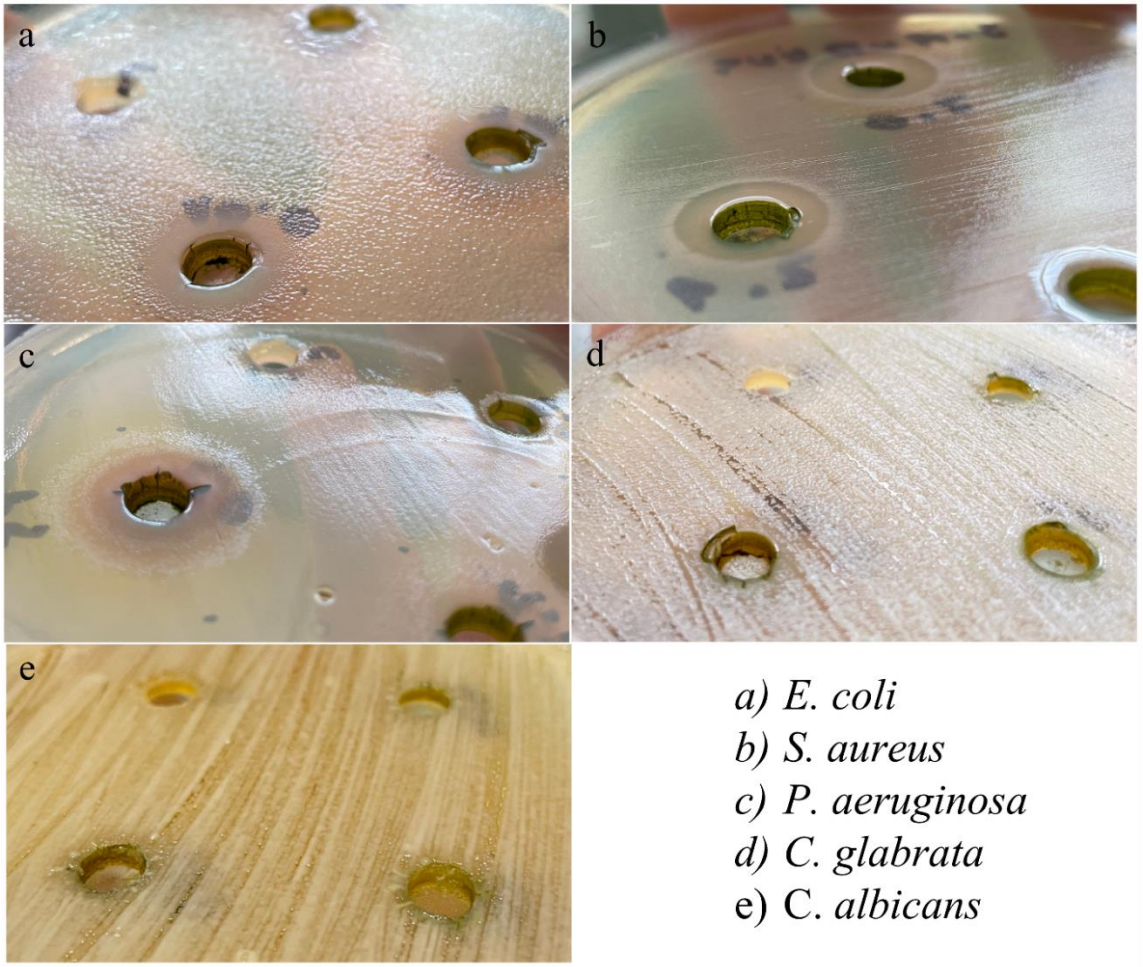

Figure 2.3.4. Diameters of the inhibition zones caused by the *E. cordifolia* extracts against the evaluated microorganisms, represented by the clear areas around the discs a) *E. coli* b) *S. aureus* c) *P. aeruginosa* d) *C. glabrata* and e) *C. albicans.*

The minimum inhibitory concentration (MiC) of the *E. cordifolia* extracts could not be determined, as they appeared very dark and concentrated (data not shown). Consequently, the MBC was evaluated using the same dilutions as those used to determine the MIC. The results of the MBC are shown in Table S3.5, where it can be observed that the extracts from the central population (Coronel), intermediate populations (Contulmo and La Unión), and the peripheral population (Puerto Montt) exhibited the lowest MBC in all three seasons evaluated, with values <0.66 mg/mL for C. albicans. The same trend was observed for *P. aeruginosa*, with a value of 1.3 mg/mL. In the case of E. *coli* and *S. aureus*, it was observed that extracts from both the central and intermediate populations, as well as the peripheral population, had the highest MBC values (>5.33 and 5.33 mg/mL). During the summer, the peripheral population (Puerto Montt) exhibited the lowest MBC value for *C. glabrata* (0.66 mg/mL), compared to the other populations which had a value of 1.3 mg/mL. In the autumn, Coronel, Contulmo, and Puerto Montt had an MBC value of 1.3 mg/mL, while La Unión had a higher value (2.66 mg/mL). Finally, in the spring, all populations had the same MBC value of 2.66 mg/ml. Regarding the MBC results, it was demonstrated that *P. aeruginosa* and *C. albicans* were the most sensitive microorganisms, as they

were inhibited by all extracts at low concentrations, without achieving a clear distinction among the different populations of *E. cordifolia* regarding their position in the ecological niche. Finally, it was observed that *E. coli* and *S. aureus* required higher concentrations of extract to be inhibited. In the study conducted by Viteri et al., (Viteri et al., 2021), the antibacterial activity of *E. cordifolia* leaf extracts were demonstrated, and in comparison, with our results, the MBC values obtained for *E. coli* (50 mg/mL), *S. aureus* (0.78 mg/mL), and *P. aeruginosa* (50 mg/mL) were significantly higher. Plant extracts exhibit antimicrobial activity as well as bacteriostatic and bactericidal effects, which are attributed to the presence of various chemical compounds. Previous studies have indicated that phenolic compounds are the most relevant group in this regard (Lemos et al., 2017; López de Dicastillo et al., 2017). In the specific case of *Ugni molinae* leaf extracts, it has been reported that flavan-3-ols and flavonol glycosides are the compounds responsible for such antimicrobial activity (Shene et al., 2009), which have also been observed in the present study. For instance, it has been demonstrated that quercetin found in plant extracts exhibits remarkable antioxidant and antibacterial activity. Furthermore, it has been demonstrated that the climate in the collection sites is the primary factor influencing the

polyphenol content and consequently, the antimicrobial activity of *Ugni molinae* leaf extracts obtained from three locations in Chile (Shene et al., 2009), which is in according the findings of this research. On the other hand, *E. cordifolia* is recognized for its significant ecological role in South American forests, due to its high rate of floral visitors, primarily bees that collect nectar for honey production. Numerous studies have shown that monofloral Ulmo honey exhibits remarkable antimicrobial activity against bacteria present in human wounds (Sherlock et al., 2010), and this activity is mainly attributed to the compounds present in the plant, which can also vary according to their geographic origin (Montenegro et al., 2021; Sherlock et al., 2010). Based on these findings, it is confirmed that the species possesses a chemical composition that imparts antibacterial properties, suggesting that leaf extract could be considered for use in biotechnological applications, either in nutraceutical formulations or food products.

The results of biofilm formation inhibition by adding subinhibitory concentrations (0.33, 0.66, 1.3, and 2.66 mg/ml) of *E. cordifolia* extracts were reported in Figure 2.3.5. Analysis of variance showed that seasonality was not a significant variable in biofilm formation among the studied

microorganisms. Instead, it was found that population had a significant effect on biofilm formation (Table S3.6).

It was observed that, in the case of *S. Aureus*, during the summer, autumn and spring, the Puerto Montt population exhibited an increase in biofilm formation compared to the centroid and intermediate populations, which was significantly different (Figure 2.3.5a). Furthermore, it was demonstrated that populations from the center to the periphery of the ecological niche of *E. cordifolia* (Coronel, Contulmo, La Unión, and Puerto Montt) were significantly different from the positive control. In the case of *P. aeruginosa*, it was found that during summer and autumn, all populations showed significant differences in biofilm formation compared to the positive control (Figure 2.3.5b). However, no significant differences in biofilm formation were observed among the populations during these periods. On the other hand, during spring, significant differences were observed between the populations and the positive control. Only the peripheral population of the ecological niche exhibited a significant inhibition in biofilm formation compared to the other populations (Figure 2.3.5b). In the case of *C. glabrata*, a general trend towards inhibition in biofilm formation was observed in all populations compared to the positive control. However, during the summer,

the population of Coronel did not show significant differences compared to the control, while during the autumn, the peripheral population of the ecological niche exhibited a higher inhibition in biofilm formation (Figure 2.3.5c). Finally, only two extracts were evaluated for *C. albicans* due to their MIC values being less than 0.66 mg/mL (Figure 2.3.5d). During autumn and spring, it was observed that these extracts exhibited significantly higher biofilm formation compared to the positive control (Figure 2.3.5d). Although favorable results were not obtained in the inhibition of biofilm formation in three of the evaluated microorganisms, it is possible that *E. cordifolia* extracts are exerting their effect during the initial bacterial adhesion stage. In this early phase, bacterial cells begin to adhere to a surface, whether biotic or abiotic. Therefore, to achieve more effective inhibition of biofilm formation in later stages such as microcolony formation or maturation (Liu et al., 2022; Zeineldin et al., 2023), it would be necessary to increase the concentration of *E. cordifolia* extracts. The structural differences in the composition of the cell wall and membranes vary according to the type of microorganism, which affects the ability of plant extracts to generate inhibition (Sánchez et al., 2016). A similar trend was observed in the case of laurel essential oil, an endemic species of Chile. At low concentrations, no favorable effect on the

inhibition of biofilms of *S. aureus* and *E. coli* was observed (Lobos et al., 2021). In the study by Cho et al., (Cho et al., 2013) it was demonstrated that the extract of *Carex pumillia* exhibits effective inhibition of biofilm formation in *P. aeruginosa* and *E. coli*, showing a concentration dependent effect.

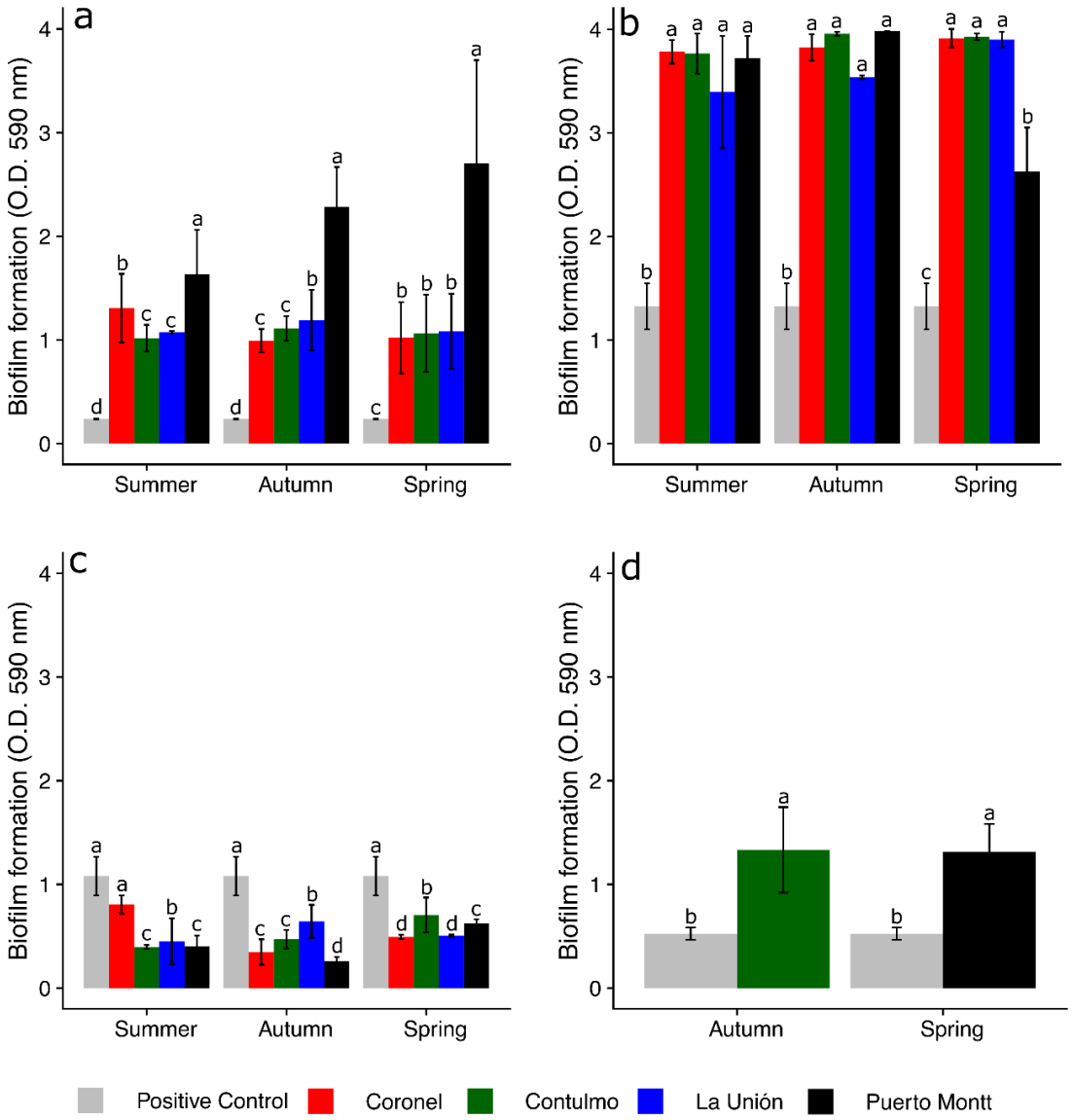

Figure 2.3.5. Biofilm reductions from *E. cordifolia* extracts according to their position in the ecological niche. A) *S. aureus* b) *P. aeruginosa* c) *C. glabrata* and d) *C. albicans.*

2.3.4. Conclusion

Our results reveal variations in the chemical profile, antioxidant activity, and antimicrobial activity of *E. cordifolia* leaf extracts, both based on the position of populations in their ecological niche and seasonal factors. This study provides novel contributions to the understanding of the chemistry of this species, which has not been previously described, and demonstrates that chemical compounds vary in relation to their position in the ecological niche. We found that in autumn and spring, the peripheral population (Puerto Montt) exhibited higher antioxidant values than the centroid population (Coronel) according to the ABTS and ORAC methods. Additionally, only in autumn, the peripheral population showed higher levels of total polyphenol content using the Folin-Ciocalteu method compared to the centroid population. Regarding antimicrobial activity, we found that the inhibition zone, MIC, and MBC depended on the concentration of the evaluated extracts in all *E. cordifolia* populations. However, a clear distinction between populations was not observed, although the concentrations used in this study were lower than those reported by other authors. Overall, *E. cordifolia* extracts were not effective in inhibiting biofilm formation in four of the evaluated microorganisms. However, the peripheral population showed

better inhibition of *C. glabrata* biofilm formation compared to the centroid and intermediate populations, both in summer and autumn.

Finally, our results suggest that the leaves of *E. cordifolia* can be considered a valuable source of bioactive compounds for biotechnological applications, such as in the nutraceutical industry. Furthermore, we emphasize the importance of ecological factors that determine the ecological niche of plants when investigating compounds with applications. It is crucial to consider that samples of the same plant collected in different climatic scenarios may exhibit variations in their compounds. Additionally, certain compounds may not be present in specific collection locations, which affects their biological activities. These considerations are relevant for the proper design of experiments and to avoid overexploitation of Chile's native and endemic resources.

Supplementary Materials: The following are available online at Table S1: Metabolic profile by UHPLC-DAD-QTOF-MS/MS of *E. cordifolia* leaves in negative ionization mode. The populations of *E. cordifolia* with respect to their ecological niche were categorized as follows: A) Coronel B) Contulmo C) La Unión D) Puerto Montt, Table 2: Metabolic profile by UHPLC-DAD-QTOF-MS/MS of *E. cordifolia* leaves in positive ionization mode. The populations of *E. cordifolia* with respect to their ecological niche were categorized as follows: A) Coronel B) Contulmo C) La Unión D) Puerto Montt, Table S3: Analysis of variance (ANOVA) to evaluate the effect of the position of *E. cordifolia* populations in their ecological niche (Coronel, Contulmo, La Unión and Puerto Montt) and seasonality (summer, autumn and spring) on antioxidant activity and polyphenol content by means of four spectrophotometric methods (DPPH, ABTS, ORAC and Folin-Ciocalteu), Table S4: Inhibition of bacterial growth from *E. cordifolia* extracts using the agar agar well diffusion method. Results expressed according to Gaudana et al., (Gaudana et al., 2010), Table S5: Antimicrobial activity of *E. cordifolia* extracts, with MBC values (mg/ml) obtained in different environmentally different populations (ecological niche) and in three different seasons of the year (summer, autumn and spring) against Gram-negative bacteria *E. coli* and *P. aeruginosa*, Gram-positive bacteria *S. aureus* and yeasts such as *C. albicans* and *C. glabrata.* Values expressed in mg/mL. Table S6: Analysis of variance (ANOVA) to evaluate the effect of the position of *E. cordifolia* populations in their ecological niche (Coronel, Contulmo, La Unión and Puerto Montt) and seasonality (Summer,

Fall and Spring) on biofilm formation in four microorganisms (*S. aureus, P. Aeruginosa*, *C. glabrata* and *C. albicans*).

Author Contributions: Conceptualization, C.F. and L.O.; methodology, C.F., L.O., C.P. and A.P.; software, C.F. and L.O.; validation, C.F.; formal analysis, C.F and L.O.; investigation, C.F. L.O., C.P. A.P. C.M., A.G., and V.H.; data curation, C.F. and L.O; writing—original draft preparation, C.F.; writing—review and editing, L.O., C.P., A.G., C.M., V.H. and A.P.; visualization, C.F.; supervision, V.H., C.M., A.G. and A.P.; project administration, C.F.; funding acquisition, C.F. and V.H. All authors have read and agreed to the published version of the manuscript.

Acknowledgments: We thank a National Forestry Corporation (CONAF) and Forestal Mininco S.A. (CMPC) or allowing us access to obtain plant material at their facilities. To the Laboratory of Natural Products Chemistry, Plant Metabolomics Laboratory and Bacterial pathogenicity laboratory of Universidad de Concepción for providing us with the facilities for sample processing and obtaining results.

Funding: This research was funded by Agencia Nacional de Investigación y Desarrollo ANID/ Beca Doctorado Nacional N°21170525, ANID/FONDECYT Regular 1181915 and ANID/FONDEQUIP EQM-170023.

References

Ado, M. A., Abas, F., Ismail, I. S., Ghazali, H. M., & Shaari, K. (2015). Chemical profile and antiacetylcholinesterase, antityrosinase, antioxidant and α-glucosidase inhibitory activity of *Cynometra cauliflora* L. leaves. *Journal of the Science of Food and Agriculture*, *95*(3), 635–642. https://doi.org/10.1002/jsfa.6832

Alseekh, S., Aharoni, A., Brotman, Y., Contrepois, K., D'Auria, J., Ewald, J., C. Ewald, J., Fraser, P. D., Giavalisco, P., Hall, R. D., Heinemann, M., Link, H., Luo, J., Neumann, S., Nielsen, J., Perez de Souza, L., Saito, K., Sauer, U., Schroeder, F. C., … Fernie, A. R. (2021). Mass spectrometry-based metabolomics: a guide for annotation, quantification and best reporting practices. In *Nature Methods* (Vol. 18, Issue 7, pp. 747–756). Nature Research. https://doi.org/10.1038/s41592-021-01197-1

Álvarez-Fernández, M. A., Cerezo, A. B., Cañete-Rodríguez, A. M., Troncoso, A. M., & García-Parrilla, M. C. (2015). Composition of nonanthocyanin polyphenols in alcoholic-fermented strawberry products using LC-MS (QTRAP), high-resolution MS (UHPLC-Orbitrap-MS), LC-DAD, and antioxidant activity. *Journal of Agricultural and Food Chemistry*, *63*(7), 2041–2051. https://doi.org/10.1021/jf506076n

Angert, A. L. (2009). The niche, limits to species' distributions, and spatio temporal variation in demography across the elevation ranges of two monkeyflowers. www.pnas.org/cgi/content/full/

Areche, C., Parra, J. R., Sepulveda, B., García-Beltrán, O., & Simirgiotis, M. J. (2022). UHPLC-MS Metabolomic Fingerprinting, Antioxidant, and Enzyme Inhibition Activities of *Himantormia lugubris* from Antarctica. *Metabolites*, *12*(6). https://doi.org/10.3390/metabo12060560

Baeza, C., Rodríguez, R., Thielemann, E., & Kottirsch, G. (2023). *Guia de Campo Arboles del Parque Botánico de Hualén* (IEB).

Bai, Z., Yu, R., Zheng, T., Sun, D., Zhou, Y., Tang, J., Zhu, H., Li, G., Niu, L., Cui, L., Du, R., Zhang, J., & Zhang, Y. (2022). A Novel Strategy for Unveiling Spatial Distribution Pattern of Gallotannins in *Paeonia rockii* and *Paeonia ostii* Based on LC–QTRAP–MS. *Metabolites*, *12*(4). https://doi.org/10.3390/metabo12040326

Baloglu, M. C., Llorent-Martínez, E. J., Aumeeruddy, M. Z., Mahomoodally, M. F., Altunoglu, Y. C., Ustaoglu, B., Ocal, M., Gürel, S., Bene, K., Sinan, K. I., & Zengin, G. (2019). Multidirectional insights on *Chrysophyllum perpulchrum* leaves and stem bark extracts: HPLC-ESI-MS n profiles, antioxidant, enzyme inhibitory, antimicrobial and cytotoxic properties. *Industrial Crops and Products*, *134*, 33–42. https://doi.org/10.1016/j.indcrop.2019.03.066

Barrientos, R., Fernández-Galleguillos, C., Pastene, E., Simirgiotis, M., Romero-Parra, J., Ahmed, S., & Echeverría, J. (2020). Metabolomic Analysis, Fast Isolation of Phenolic Compounds, and Evaluation of

Biological Activities of the Bark From *Weinmannia trichosperma* Cav. (Cunoniaceae). *Frontiers in Pharmacology*, *11*. https://doi.org/10.3389/fphar.2020.00780

Bate-Smith, E. C., Davenport, S. M., & Harborne, J. B., (1967). Comparative biochemistry of flavonoids-III. *Phytochemistry*, *6*, 1407–1413.

Bazargani, M. M., & Rohloff, J. (2016). Antibiofilm activity of essential oils and plant extracts against *Staphylococcus aureus* and *Escherichia coli biofilms*. *Food Control*, *61*, 156–164. https://doi.org/10.1016/j.foodcont.2015.09.036

Boué, S. M., Carter-Wientjes, C. H., Shih, B. Y., & Cleveland, T. E. (2003). Identification of flavone aglycones and glycosides in soybean pods by liquid chromatography-tandem mass spectrometry. *Journal of Chromatography A*, *991*(1), 61–68. https://doi.org/10.1016/S0021-9673(03)00209-7

Brand-Williams, W., Cuvelier, M. E., & Berset, C. (1995). *Use of a Free Radical Method to Evaluate Antioxidant Activity* (Vol. 28).

Bridi, R., & Montenegro, G. (2017). The Value of Chilean Honey: Floral Origin Related to their Antioxidant and Antibacterial activities. In *Honey Analysis*. InTech. https://doi.org/10.5772/67103

Cho, H. S., Lee, J. H., Ryu, S. Y., Joo, S. W., Cho, M. H., & Lee, J. (2013). Inhibition of Pseudomonas aeruginosa and *Escherichia coli* O157:H7 Biofilm formation by plant metabolite ε-viniferin. *Journal of Agricultural and Food Chemistry*, *61*(29), 7120–7126. https://doi.org/10.1021/jf4009313

Corrêa, J. G. de S., Bianchin, M., Lopes, A. P., Silva, E., Ames, F. Q., Pomini, A. M., Carpes, S. T., de Carvalho Rinaldi, J., Cabral Melo, R., Kioshima, E. S., Bersani-Amado, C. A., Pilau, E. J., de Carvalho, J. E., Ruiz, A. L. T. G., Visentainer, J. V., & Santin, S. M. de O. (2021). Chemical profile, antioxidant and anti-inflammatory properties of *Miconia albicans* (Sw.) Triana (Melastomataceae) fruits extract. *Journal of Ethnopharmacology*, *273*. https://doi.org/10.1016/j.jep.2021.113979

De Rosso, M., Panighel, A., Dalla Vedova, A., & Flamini, R. (2020). Elucidations on the structures of some putative flavonoids identified in postharvest withered grapes (Vitis vinifera L.) by quadrupole time-of-flight mass spectrometry. *Journal of Mass Spectrometry*, *55*(11). https://doi.org/10.1002/jms.4639

Dienaite, L., Pukalskiene, M., Pereira, C. V., Matias, A. A., & Venskutonis, P. R. (2020). Valorization of european cranberry bush (viburnum opulus l.) berry pomace extracts isolated with pressurized ethanol and water by assessing their phytochemical composition, antioxidant, and antiproliferative activities. *Foods*, *9*(10). https://doi.org/10.3390/foods9101413

Fraige, K., Dametto, A. C., Zeraik, M. L., de Freitas, L., Saraiva, A. C., Medeiros, A. I., Castro-Gamboa, I., Cavalheiro, A. J., Silva, D. H. S., Lopes, N. P., & Bolzani, V. S. (2018). Dereplication by HPLC-DAD-ESI-MS/MS and Screening for Biological Activities of Byrsonima Species (Malpighiaceae). *Phytochemical Analysis*, *29*(2), 196–204. https://doi.org/10.1002/pca.2734.

Fuica-Carrasco, C. A., Toro-Núñez, Ó., Lira-Noriega, A., Pérez, A. J., & Hernández, V. (2023). Metabolome expression in Eucryphia cordifolia populations: Role of seasonality and ecological niche centrality hypothesis. *Journal of Plant Research*, 1-14.

Galasso, S., Pacifico, S., Kretschmer, N., Pan, S. P., Marciano, S., Piccolella, S., Monaco, P., & Bauer, R. (2014). Influence of seasonal variation on Thymus longicaulis C. Presl chemical composition and its antioxidant and anti-inflammatory properties. *Phytochemistry*, *107*, 80–90. https://doi.org/10.1016/j.phytochem.2014.08.015

Galland, M., Boutet-Mercey, S., Lounifi, I., Godin, B., Balzergue, S., Grandjean, O., Morin, H., Perreau, F., Debeaujon, I., & Rajjou, L. (2014). Compartmentation and dynamics of flavone metabolism in dry and germinated rice seeds. *Plant and Cell Physiology*, *55*(9), 1646–1659. https://doi.org/10.1093/pcp/pcu095

Galvão, F., dos Santos, E., Gomes da Silva Dantas, F., Irlan da Silva Santos, J., da Paz Costa Sauda, T., Carvalho dos Santos, A., Carvalho Souza, R. I., da Silva Pinto, L., Ferreira Moraes, C. A., Sangalli, A., Leite Kassuya, C. A., Nogueira, C. R., & Pires de Oliveira, K. M. (2023). Chemical composition and effects of ethanolic extract and gel of *Cochlospermum regium* (Schrank) Pilg. Leaves on inflammation, pain, and wounds. *Journal of Ethnopharmacology*, *302*. https://doi.org/10.1016/j.jep.2022.115881

Gao, D., Wang, D. D., Zhang, Q., Yang, F. Q., Xia, Z. N., Zhang, Q. H., & Yuan, C. S. (2017). In Vivo Selective Capture and Rapid Identification of Luteolin and Its Metabolites in Rat Livers by Molecularly Imprinted Solid-Phase Microextraction. *Journal of Agricultural and Food Chemistry*, *65*(6), 1158–1166. https://doi.org/10.1021/acs.jafc.6b05269

Gaudana, S. B., Dhanani, A. S., & Bagchi, T. (2010). Probiotic attributes of lactobacillus strains isolated from food and of human origin. *British Journal of Nutrition*, *103*(11), 1620–1628. https://doi.org/10.1017/S0007114509993643

Gevrenova, R., Zengin, G., Sinan, K. I., Zheleva-Dimitrova, D., Balabanova, V., Kolmayer, M., Voynikov, Y., & Joubert, O. (2023). An In-Depth Study of Metabolite Profile and Biological Potential of Tanacetum balsamita L. (Costmary). *Plants*, *12*(1). https://doi.org/10.3390/plants12010022

Gomes, J. de M., Terto, M. V. C., Do Santos, S. G., da Silva, M. S., & Tavares, J. F. (2021). Seasonal variations of polyphenols content, sun protection factor and antioxidant activity of two lamiaceae species. *Pharmaceutics*, *13*(1), 1–16. https://doi.org/10.3390/pharmaceutics13010110

Gouveia, S. C., & Castilho, P. C. (2010). Characterization of phenolic compounds in Helichrysum melaleucum by high-performance liquid chromatography with on-line ultraviolet and mass spectrometry detection. *Rapid Communications in Mass Spectrometry*, *24*(13), 1851–1868. https://doi.org/10.1002/rcm.4585

Grayer, R. J., Eckert, M. R., Lever, A., Veitch, N. C., Kite, G. C., & Paton, A. J. (2010). Distribution of exudate flavonoids in the genus Plectranthus. *Biochemical Systematics and Ecology*, *38*(3), 335–341. https://doi.org/10.1016/j.bse.2010.01.014

Grayer, R. J., Veitch, N. C., Kite, rey C., Price, A. M., & Kokubun, T. (2001). Distribution of 8-oxygenated leaf-surface flavones in the genus Ocimum. www.elsevier.com/locate/phytochem

Hartmann, T. (2007). From waste products to ecochemicals: Fifty years research of plant secondary metabolism. In *Phytochemistry* (Vol. 68, Issues 22–24, pp. 2831–2846). https://doi.org/10.1016/j.phytochem.2007.09.017

Hemeg, H. A., Moussa, I. M., Ibrahim, S., Dawoud, T. M., Alhaji, J. H., Mubarak, A. S., Kabli, S. A., Alsubki, R. A., Tawfik, A. M., & Marouf, S. A. (2020). Antimicrobial effect of different herbal plant extracts against different microbial population. *Saudi Journal of Biological Sciences*, *27*(12), 3221–3227. https://doi.org/10.1016/j.sjbs.2020.08.015

Hofmann, T., Nebehaj, E., & Albert, L. (2016). Antioxidant properties and detailed polyphenol profiling of European hornbeam (Carpinus betulus L.) leaves by multiple antioxidant capacity assays and high-performance liquid chromatography/multistage electrospray mass spectrometry. *Industrial Crops and Products*, *87*, 340–349. https://doi.org/10.1016/j.indcrop.2016.04.037

Hong, Y., Liao, X., & Chen, Z. (2021). Determination of bioactive components in the fruits of Cercis chinensis Bunge by HPLC-MS/MS and quality evaluation by principal components and hierarchical cluster analyses. *Journal of Pharmaceutical Analysis*, *11*(4), 465–471. https://doi.org/10.1016/j.jpha.2020.07.010

Hvattum, E. (2002). Determination of phenolic compounds in rose hip (Rosa canina) using liquid chromatography coupled to electrospray ionisation tandem mass spectrometry and diode-array detection. *Rapid Communications in Mass Spectrometry*, *16*(7), 655–662. https://doi.org/10.1002/rcm.622

Ismail, B. B., Pu, Y., Fan, L., Dandago, M. A., Guo, M., & Liu, D. (2019). Characterizing the phenolic constituents of baobab (Adansonia digitata) fruit shell by LC-MS/QTOF and their in vitro biological activities. *Science of the Total Environment*, *694*. https://doi.org/10.1016/j.scitotenv.2019.07.193

Ivanova, V., Stefova, M., Vojnoski, B., Dörnyei, Á., Márk, L., Dimovska, V., Stafilov, T., & Kilár, F. (2011). Identification of polyphenolic compounds in red and white grape varieties grown in *R. macedonia* and changes of their content during ripening. *Food Research International*, *44*(9), 2851–2860. https://doi.org/10.1016/j.foodres.2011.06.046

Jerez, M., Sineiro, J., & Nuñez, M. J. (2009). Fractionation of pine bark extracts: Selecting procyanidins. *European Food Research and Technology*, *229*(4), 651–659. https://doi.org/10.1007/s00217-009-1096-y

Jiménez-Aspee, F., Theoduloz, C., Gómez-Alonso, S., Hermosín-Gutiérrez, I., Reyes, M., & Schmeda-Hirschmann, G. (2018). Polyphenolic profile and antioxidant activity of meristem and leaves from "chagual" (*Puya chilensis* Mol.), a salad from central Chile. *Food Research International*, *114*, 90–96. https://doi.org/10.1016/j.foodres.2018.07.051

Jiménez-González, A., Quispe, C., Bórquez, J., Sepúlveda, B., Riveros, F., Areche, C., Nagles, E., García-Beltrán, O., & Simirgiotis, M. J. (2018). UHPLC-ESI-ORBITRAP-MS analysis of the native Mapuche medicinal plant palo negro (*Leptocarpha rivularis* DC.Asteraceae) and evaluation of its

antioxidant and cholinesterase inhibitory properties. *Journal of Enzyme Inhibition and Medicinal Chemistry*, *33*(1), 936–944. https://doi.org/10.1080/14756366.2018.1466880

Karahan, F., Avsar, C., Ozyigit, I. I., & Berber, I. (2016). Antimicrobial and antioxidant activities of medicinal plant Glycyrrhiza glabra var. glandulifera from different habitats. *Biotechnology and Biotechnological Equipment*, *30*(4), 797–804. https://doi.org/10.1080/13102818.2016.1179590

Kedrina-Okutan, O., Novello, V., Hoffmann, T., Hadersdorfer, J., Occhipinti, A., Schwab, W., & Ferrandino, A. (2018). Constitutive Polyphenols in Blades and Veins of Grapevine (*Vitis vinifera* L.) Healthy Leaves. *Journal of Agricultural and Food Chemistry*, *66*(42), 10977–10990. https://doi.org/10.1021/acs.jafc.8b03418

Lachowicz, S., & Oszmianski, J. (2019). Profile of bioactive compounds in the morphological parts of wild fallopia japonica (houtt) and fallopia sachalinensis (F. Schmidt) and their antioxidative activity. *Molecules*, *24*(7). https://doi.org/10.3390/molecules24071436

Lanuza, F., Zamora-Ros, R., Petermann-Rocha, F., Martínez-Sanguinetti, M. A., Troncoso-Pantoja, C., Labraña, A. M., Leiva-Ordoñez, A. M., Nazar, G., Ramírez-Alarcón, K., Ulloa, N., Lasserre-Laso, N., Parra-Soto, S., Martorell, M., Villagrán, M., Garcia-Diaz, D. F., Andrés-Lacueva, C., & Celis-Morales, C. (2021). Advances in Polyphenol Research from Chile: A Literature

Review. In *Food Reviews International*. Taylor and Francis Ltd. https://doi.org/10.1080/87559129.2021.2009508

Lemos, M. F., Lemos, M. F., Pacheco, H. P., Guimarães, A. C., Fronza, M., Endringer, D. C., & Scherer, R. (2017). Seasonal variation affects the composition and antibacterial and antioxidant activities of Thymus vulgaris. *Industrial Crops and Products*, *95*, 543–548. https://doi.org/10.1016/j.indcrop.2016.11.008

Li, Y. F., Ouyang, S. H., Chang, Y. Q., Wang, T. M., Li, W. X., Tian, H. Y., Cao, H., Kurihara, H., & He, R. R. (2017). A comparative analysis of chemical compositions in *Camellia sinensis* var. puanensis Kurihara, a novel Chinese tea, by HPLC and UFLC-Q-TOF-MS/MS. *Food Chemistry*, *216*, 282–288. https://doi.org/10.1016/j.foodchem.2016.08.017

Lira-Noriega, A., & Manthey, J. D. (2014). Relationship of genetic diversity and niche centrality: A survey and analysis. *Evolution*, *68*(4), 1082–1093. https://doi.org/10.1111/evo.12343

Liu, S., Lu, H., Zhang, S., Shi, Y., & Chen, Q. (2022). Phages against Pathogenic Bacterial Biofilms and Biofilm-Based Infections: A Review. In *Pharmaceutics* (Vol. 14, Issue 2). MDPI. https://doi.org/10.3390/pharmaceutics14020427

Lobos, O., Padilla, C., Barrera, A., Lopez-Cabana, Z., Mora, C., Abaca, P., & Carrasco-Sánchez, V. (2021). Antibiofilm and antifungal activities of *Laurelia sempervirens* (chilean laurel) essential oil. *Jundishapur Journal of Natural Pharmaceutical Products*, *16*(4). https://doi.org/10.5812/jjnpp.113611

López de Dicastillo, C., Bustos, F., Valenzuela, X., López-Carballo, G., Vilariño, J. M., & Galotto, M. J. (2017). Chilean berry *Ugni molinae* Turcz. fruit and leaves extracts with interesting antioxidant, antimicrobial and tyrosinase inhibitory properties. *Food Research International*, *102*, 119–128. https://doi.org/10.1016/j.foodres.2017.09.073

Lorena, C., Ressaissi, A., & Serralheiro, M. L. (2022). Bioactives from *Psidium guajava* leaf decoction: LC-HRMS-MS-Qtof identification, bioactivities and bioavailability evaluation. *Food Chemistry Advances*, *1*. https://doi.org/10.1016/j.focha.2021.100003

Martínez-Meyer, E., Díaz-Porras, D., Peterson, A. T., & Yáñez-Arenas, C. (2013). Ecological niche structure and rangewide abundance patterns of species. *Biology Letters*, *9*(1), 1–5. https://doi.org/10.1098/RSBL.2012.0637

Mattivi, F., Guzzon, R., Vrhovsek, U., Stefanini, M., & Velasco, R. (2006). Metabolite profiling of grape: Flavonols and anthocyanins. *Journal of Agricultural and Food Chemistry*, *54*(20), 7692–7702. https://doi.org/10.1021/jf061538c

Maulidiani, Abas, F., Khatib, A., Shaari, K., & Lajis, N. H. (2014). Chemical characterization and antioxidant activity of three medicinal *Apiaceae* species. *Industrial Crops and Products*, *55*, 238–247. https://doi.org/10.1016/j.indcrop.2014.02.013

Mikulic-Petkovsek, M., Krska, B., Kiprovski, B., & Veberic, R. (2017). Bioactive Components and Antioxidant Capacity of Fruits from Nine Sorbus Genotypes. *Journal of Food Science*, *82*(3), 647–658. https://doi.org/10.1111/1750-3841.13643

Millán, D., Malebran, C., & Ormazábal-Toledo, R. (2023). Towards a rational design of natural deep eutectic solvents for the extraction of polyphenols from *Luma apiculata*. *Journal of Molecular Liquids*, *372*. https://doi.org/10.1016/j.molliq.2022.121155

Mongkolsilp, S., Pongbupakit, I., Sae-Lee, N., & Sitthithaworn, W. (2004). Radical Scavenging Activity and Total Phenolic Content of Medicinal Plants Used in Primary Health Care. In *SWU J Pharm Sci* (Vol. 9, Issue 1).

Montenegro, G., Velásquez, P., Viteri, R., & Giordano, A. (2021). Changes in the antibacterial capacity of Ulmo honey in relation to the contribution of Eucryphia cordifolia pollen. *Journal of Food and Nutrition Research*, *60*(3), 279283.

Morales, L. V., Coopman, R. E., Rojas, R., Escandón, A. B., Flexas, J., Galmés, J., García-Plazaola, J. I., Gago, J., Cabrera, H. M., & Corcuera, L. J. (2014). Acclimation of leaf cohorts expanded under light and water stresses: An adaptive mechanism of *Eucryphia cordifolia* to face changes in climatic conditions? *Tree Physiology*, *34*(12), 1305–1320. https://doi.org/10.1093/treephys/tpu085

Nguyen, N. H., Nhi, T. T. Y., Van Nhi, N. T., Cuc, T. T. T., Tuan, P. M., & Nguyen, D. H. (2021). Comparative Study of the Silver Nanoparticle Synthesis Ability and Antibacterial Activity of the Piper Betle L. And Piper Sarmentosum Roxb. Extracts. *Journal of Nanomaterials*, *2021*. https://doi.org/10.1155/2021/5518389

Nikolova, M. T., Grayer, R. J., Genova, E., & Porter, E. A. (2006). Exudate flavonoids from *Bulgarian* species of Salvia. *Biochemical Systematics and Ecology*, *34*(4), 360–364. https://doi.org/10.1016/j.bse.2005.11.006

Nova-Baza, D., Olivares-Caro, L., Bustamante, L., Pérez, A. J., Vergara, C., Fuentealba, J., & Mardones, C. (2022). Metabolic profile and antioxidant capacity of five *Berberis* leaves species: A comprehensive study to determine their potential as natural food or ingredient. *Food Research International*, *160*. https://doi.org/10.1016/j.foodres.2022.111642

Olivares-Caro, L., Radojkovic, C., Chau, S. Y., Nova, D., Bustamante, L., Neira, J. Y., Perez, A. J., & Mardones, C. (2020). *Berberis microphylla* G.

Forst (calafate) berry extract reduces oxidative stress and lipid peroxidation of human LDL. *Antioxidants*, *9*(12), 1–20. https://doi.org/10.3390/antiox9121171

Osman, E. E. A., Mohamed, A. S., Elkhateeb, A., Gobouri, A., Abdel-Aziz, M. M., & Abdel-Hameed, E. S. S. (2022). Phytochemical investigations, antioxidant, cytotoxic, antidiabetic and antibiofilm activities of *Kalanchoe laxiflora* flowers. *European Journal of Integrative Medicine*, *49*. https://doi.org/10.1016/j.eujim.2021.102085

Otero, M. C., Fuentes, J. A., Atala, C., Cuadros-Orellana, S., Fuentes, C., & Gordillo-Fuenzalida, F. (2022). Antimicrobial Properties of Chilean Native Plants: Future Aspects in Their Application in the Food Industry. In *Foods* (Vol. 11, Issue 12). MDPI. https://doi.org/10.3390/foods11121763

Ou, B., Chang, T., Huang, D., & Prior, R. L. (2013). Determination of total antioxidant capacity by oxygen radical absorbance capacity (ORAC) using fluorescein as the fluorescence probe: First action 2012.23. *Journal of AOAC International*, *96*(6), 1372–1376. https://doi.org/10.5740/jaoacint.13-175

Pacifico, S., Galasso, S., Piccolella, S., Kretschmer, N., Pan, S. P., Marciano, S., Bauer, R., & Monaco, P. (2015). Seasonal variation in phenolic composition and antioxidant and anti-inflammatory activities of *Calamintha nepeta* (L.) Savi. *Food Research International*, *69*(1), 121–132. https://doi.org/10.1016/j.foodres.2014.12.019

Peña-Cerda, M., Arancibia-Radich, J., Valenzuela-Bustamante, P., Pérez-Arancibia, R., Barriga, A., Seguel, I., García, L., & Delporte, C. (2017). Phenolic composition and antioxidant capacity of *Ugni molinae* Turcz. leaves of different genotypes. *Food Chemistry*, *215*, 219–227. https://doi.org/10.1016/j.foodchem.2016.07.159

Pérez-Navarro, J., Izquierdo-Cañas, P. M., Mena-Morales, A., Martínez-Gascueña, J., Chacón-Vozmediano, J. L., García-Romero, E., Hermosín-Gutiérrez, I., & Gómez-Alonso, S. (2019). Phenolic compounds profile of different berry parts from novel *Vitis vinifera* L. red grape genotypes and Tempranillo using HPLC-DAD-ESI-MS/MS: A varietal differentiation tool. *Food Chemistry*, *295*, 350–360. https://doi.org/10.1016/j.foodchem.2019.05.137

Quispe, C., Viveros-Valdez, E., & Schmeda-Hirschmann, G. (2012). Phenolic Constituents of the Chilean Herbal Tea *Fabiana imbricata* R. et P. *Plant Foods for Human Nutrition*, *67*(3), 242–246. https://doi.org/10.1007/s11130-012-0302-4

Re, R., Pellegrini, N., Proteggente, A., Pannala, A., Yang, M., & Rice-Evans, C. (1999). Antioxidant activity applying an improved abts radical cation decolorization assay.

Rivas-Ubach, A., Pérez-Trujillo, M., Sardans, J., Gargallo-Garriga, A., Parella, T., & Peñuelas, J. (2013). Ecometabolomics: optimized NMR-based

method. *Methods in Ecology and Evolution*, *4*(5), 464–473. https://doi.org/10.1111/2041-210X.12028

Rodriguez, R., Marticorena, C., Alarcón, D., Baeza, C., Cavieres, L., Finot, V. L., Fuentes, N., Kiessling, A., Mihoc, M., Pauchard, A., Ruiz, E., Sanchez, P., Marticorena, A., & Bot, G. (2018). Catálogo de las plantas vasculares de Chile Catalogue of the vascular plants of Chile. *Artículo original*. *75*(1), 1–430.

Salehi, B., Sharifi-Rad, J., Herrera-Bravo, J., Salazar, L. A., Delporte, C., Barra, G. V., Cazar Ramirez, M.-E., López, M. D., Ramírez-Alarcón, K., Cruz-Martins, N., & Martorell, M. (2020). Ethnopharmacology, Phytochemistry and Biological Activities of Native Chilean Plants. *Current Pharmaceutical Design*, *27*(7), 953–970. https://doi.org/10.2174/1381612826666201124105623

Sánchez, E., Rivas Morales, C., Castillo, S., Leos-Rivas, C., García-Becerra, L., & Ortiz Martínez, D. M. (2016). Antibacterial and Antibiofilm Activity of Methanolic Plant Extracts against Nosocomial Microorganisms. *Evidence-Based Complementary and Alternative Medicine*, *2016*. https://doi.org/10.1155/2016/1572697

Santos, A., Barros, L., Calhelha, R. C., Dueñas, M., Carvalho, A. M., Santos-Buelga, C., & Ferreira, I. C. F. R. (2013). Leaves and decoction of Juglans regia L.: Different performances regarding bioactive compounds and in vitro

antioxidant and antitumor effects. *Industrial Crops and Products*, *51*, 430–436. https://doi.org/10.1016/j.indcrop.2013.10.003

Sanz, M., Fernández de Simón, B., Esteruelas, E., Muñoz, Á. M., Cadahía, E., Hernández, M. T., Estrella, I., & Martinez, J. (2012). Polyphenols in red wine aged in acacia (*Robinia pseudoacacia*) and oak (*Quercus petraea*) wood barrels. *Analytica Chimica Acta*, *732*, 83–90. https://doi.org/10.1016/j.aca.2012.01.061

Senhaji, S., Lamchouri, F., & Toufik, H. (2020). Phytochemical Content, Antibacterial and Antioxidant Potential of Endemic Plant *Anabasis aretioïdes* Coss. & Moq. (Chenopodiaceae). *BioMed Research International*, *2020*. https://doi.org/10.1155/2020/6152932

Shene, C., Reyes, A. K., Villarroel, M., Sineiro, J., Pinelo, M., & Rubilar, M. (2009). Plant location and extraction procedure strongly alter the antimicrobial activity of murta extracts. *European Food Research and Technology*, *228*(3), 467–475. https://doi.org/10.1007/s00217-008-0954-3

Sherlock, O., Dolan, A., Athman, R., Power, A., Gethin, G., Cowman, S., & Humphreys, H. (2010). Comparison of the antimicrobial activity of Ulmo honey from Chile and Manuka honey against methicillin-resistant *Staphylococcus aureus*, *Escherichia coli* and *Pseudomonas aeruginosa*. *BMC Complementary and Alternative Medicine*, *10*. https://doi.org/10.1186/1472-6882-10-47

Simirgiotis, M. J., Bórquez, J., & Schmeda-Hirschmann, G. (2013). Antioxidant capacity, polyphenolic content and tandem HPLC-DAD-ESI/MS profiling of phenolic compounds from the South American berries *Luma apiculata* and *L. chequén*. *Food Chemistry*, *139*(1–4), 289–299. https://doi.org/10.1016/j.foodchem.2013.01.089

Simirgiotis, M. J., & Schmeda-Hirschmann, G. (2010). Direct identification of phenolic constituents in Boldo Folium (*Peumus boldus* Mol.) infusions by high-performance liquid chromatography with diode array detection and electrospray ionization tandem mass spectrometry. *Journal of Chromatography A*, *1217*(4), 443–449. https://doi.org/10.1016/j.chroma.2009.11.014

Stepanović, S., Vuković, D., Hola, V., Di Bonaventura, G., Djukić, S., Ćirković, I., & Ruzicka, F. (2007). Quantification of biofilm in microtiter plates: Overview of testing conditions and practical recommendations for assessment of biofilm production by staphylococci. *APMIS*, *115*(8), 891–899. https://doi.org/10.1111/j.1600-0463.2007.apm_630.x

Tarone, A. G., Goupy, P., Ginies, C., Marostica, M. R., & Dufour, C. (2021). Advanced characterization of polyphenols from *Myrciaria jaboticaba* peel and lipid protection in in vitro gastrointestinal digestion. *Food Chemistry*, *359*. https://doi.org/10.1016/j.foodchem.2021.129959

Teles, Y. C. F., Souza, M. S. R., & De Souza, M. de F. V. (2018). Sulphated flavonoids: Biosynthesis, structures, and biological activities. In *Molecules* (Vol. 23, Issue 2). MDPI AG. https://doi.org/10.3390/molecules23020480

Tschesche, R., Delhvi, S., Sepulveda, S., & Breitmaier, E.,. (1979). Eucryphin, a new chromone rhamnoside from the bark of Eucryphia cordifolia. *Phytochemistry*, *18*, 867–869.

Uteau, D., & Donoso, P. J. (2009). Early individual growth of Eucryphia cordifolia and *Laurelia sempervirens* planted under different competition conditions in south-central Chile. In *Cien. Inv. Agr* (Vol. 36, Issue 1). www.rcia.puc.cl

Valgas, C., Machado De Souza, Simone Elza, Smânia, F. A., & Smânia, A. (2007). Screening methods to determine antibacterial activity of natural products. *Brazilian Journal of Microbiology*, *38*, 369–380.

Valledor, L., Escandón, M., Meijón, M., Nukarinen, E., Cañal, M. J., & Weckwerth, W. (2014). A universal protocol for the combined isolation of metabolites, DNA, long RNAs, small RNAs, and proteins from plants and microorganisms. *Plant J.*, *79*(1), 173–180. https://doi.org/10.1111/TPJ.12546

Velásquez, P., Montenegro, G., Leyton, F., Ascar, L., Ramirez, O., & Giordano, A. (2020). Bioactive compounds and antibacterial properties of

monofloral Ulmo honey. *CYTA - Journal of Food*, *18*(1), 11–19. https://doi.org/10.1080/19476337.2019.1701559

Verardo, V., Arráez-Román, D., Segura-Carretero, A., Marconi, E., Fernández-Gutiérrez, A., & Caboni, M. F. (2010). Identification of buckwheat phenolic compounds by reverse phase high performance liquid chromatography-electrospray ionization-time of flight-mass spectrometry (RP-HPLC-ESI-TOF-MS). *Journal of Cereal Science*, *52*(2), 170–176. https://doi.org/10.1016/j.jcs.2010.04.009

Viteri, R., Giordano, A., Montenegro, G., & Zacconi, F. (2021). *Eucryphia cordifolia* extracts: Phytochemical screening, antibacterial and antioxidant activities. *Natural Product Research*, *36*(16), 4177–4181. https://doi.org/10.1080/14786419.2021.1960525

Viteri, R., Giordano, A., Montenegro, G., & Zacconi, F. C. (2022). Flavonoids and triterpenes isolated from *Eucryphia cordifolia* (Cunoniaceae). *Biochemical Systematics and Ecology*, *104*. https://doi.org/10.1016/j.bse.2022.104476

Vo, G. T., Liu, Z., Chou, O., Zhong, B., Barrow, C. J., Dunshea, F. R., & Suleria, H. A. R. (2022). Screening of phenolic compounds in australian grown grapes and their potential antioxidant activities. *Food Bioscience*, *47*. https://doi.org/10.1016/j.fbio.2022.101644

Xu, Y., Simon, J. E., Welch, C., Wightman, J. D., Ferruzzi, M. G., Ho, L., Passinetti, G. M., & Wu, Q. (2011). Survey of polyphenol constituents in grapes and grape-derived products. In *Journal of Agricultural and Food Chemistry* (Vol. 59, Issue 19, pp. 10586–10593). American Chemical Society. https://doi.org/10.1021/jf202438d

Yuk, H. J., Oh, K. Y., Kim, D.-Y., Song, H.-H., Kim, J. Y., Oh, S.-R., & Ryu, H. W. (2017). Metabolomic Profiling, Antioxidant and Anti-inflammatory Activities of Hypericum Species Growing in South Korea. In *NPC Natural Product Communications* (Vol. 12, Issue 7).

Yun, J. H., Tomas-Barberan, F. A., Kader, A. A., & Mitchell, A. E. (2006). The flavonoid glycosides and procyanidin composition of Deglet Noor dates (*Phoenix dactylifera*). *Journal of Agricultural and Food Chemistry*, *54*(6), 2405–2411. https://doi.org/10.1021/jf0581776

Zargoosh, Z., Ghavam, M., Bacchetta, G., & Tavili, A. (2019). Effects of ecological factors on the antioxidant potential and total phenol content of *Scrophularia striata* Boiss. *Scientific Reports*, *9*(1). https://doi.org/10.1038/s41598-019-52605-8

Zeineldin, M., Esmael, A., Al-Hindi, R. R., Alharbi, M. G., Ashenafi Bekele, D., & Teklemariam, A. D. (2023). Beyond the Risk of Biofilms: An Up-and-Coming Battleground of Bacterial Life and Potential Antibiofilm Agents. In *Life* (Vol. 13, Issue 2). MDPI. https://doi.org/10.3390/life13020503

Zhang, X., Lin, Z., Fang, J., Liu, M., Niu, Y., Chen, S., & Wang, H. (2015). An on-line high-performance liquid chromatography-diode-array detector-electrospray ionization-ion-trap-time-of-flight-mass spectrometry-total antioxidant capacity detection system applying two antioxidant methods for activity evaluation of the edible flowers from *Prunus mume*. *Journal of Chromatography A*, *1414*, 88–102. https://doi.org/10.1016/j.chroma.2015.08.033

Zhao, M., Xu, J., Qian, D., Guo, J., Jiang, S., Shang, E. xin, & Duan, J. ao. (2014). Identification of astilbin metabolites produced by human intestinal bacteria using UPLC-Q-TOF/MS. *Biomedical Chromatography*, *28*(7), 1024–1029. https://doi.org/10.1002/bmc.3111

Zhao, Y., Cao, J., Zhao, J., Wei, P., Wu, R., Zhang, J., & Wan, L. (2022). Chemical analysis of *Chrysosplenium* from different species by UPLC-Q exactive orbitrap HRMS and HPLC-DAD. *Journal of Pharmaceutical and Biomedical Analysis*, *218*. https://doi.org/10.1016/j.jpba.2022.114861

Zhao, Y., Wu, X., Yu, L., & Chen, P. (2017). Retention of polyphenols in blueberries (*Vaccinium corymbosum*) after different cooking methods, using UHPLC–DAD–MS based metabolomics. *Journal of Food Composition and Analysis*, *56*, 55–66. https://doi.org/10.1016/j.jfca.2016.12.003

CAPITULO 3: DISCUSION GENERAL

Evaluar los cambios del metaboloma resulta fundamental para comprender su función en la adaptación y el éxito reproductivo de las poblaciones naturales. En este contexto, sostenemos que la hipótesis de la centralidad en el nicho ecológico establece una herramienta base para analizar cómo varía el metabolismo en entornos locales y a lo largo de gradientes ambientales en organismos que no son modelos tradicionales de estudio. De esta forma, nuestra investigación representa un enfoque multidisciplinario pionero al fusionar dos campos de estudio: la ecología y la metabolómica.

Dentro de este contexto, nuestros resultados sugirieron que: 1) las poblaciones centrales y periféricas no siguen necesariamente un gradiente ambiental latitudinal obvio para *E. cordifolia* en Chile, (2) la similitud metabólica entre poblaciones se explica mejor por la estacionalidad que por la posición del nicho, (3) la diversidad metabolómica es mayor a medida que nos alejamos del centro del nicho ecológico, (4) existen cambios entre el metaboloma de la población centroide y periférica, donde al menos un metabolitos genera dicha distinción, (5) los extractos de hojas de *E. cordifolia* presentan una capacidad antioxidante alta, cuya variabilidad depende del

método espectrofotométrico empleado, la estacionalidad y su posición en el nicho. En general, se observa una mayor capacidad antioxidante en las poblaciones periféricas y 6) finalmente, los extractos de *E. corifolia* no muestran eficacia en la inhibición de la formación de biopelículas en tres de los microorganismos investigados. No obstante, se destaca que la población periférica logra una mejor inhibición sobre *C. glabrata* durante las estaciones de verano y otoño.

3.1. Poblaciones centrales y periféricas y gradiente ambiental de *E. cordifolia* en Chile

La distribución de las especies a menudo se ha descrito como una manifestación espacial de su nicho ecológico (sensu Hutchinson, 1957), bajo el supuesto de que los procesos que definen y gobiernan la presencia dentro del espacio del nicho también determinan el desempeño de las especies dentro de él (de Medeiros et al. 2018; Baer & Maron 2020). En esta investigación determinamos que el metaboloma al igual que la distribución, abundancia (Martínez-Meyer et al. 2013) y diversidad genética (Lira-Noriega & Manthey et al. 2014) de las poblaciones, se encuentra determinado por la posición que tienen estas dentro de su nicho ecológico (Martínez-Meyer et al. 2013) (centroide o periférica) (Capítulo 2.1). Desde una perspectiva

molecular, se presume que cada especie exhibe un metaboloma singular y altamente adaptable, lo que le permite realizar ajustes necesarios para asegurar funciones bioquímicas y fisiológicas, manteniendo su estado homeostático de acuerdo con los recursos disponibles en el ecosistema (Gargallo-Garriga et al., 2020).

En esta investigación se utilizó el modelamiento del nicho para estimar poblaciones centrales y periféricas para poner a punto la hipótesis de la centralidad del nicho ecológico y su relación con el metaboloma de *E. cordifolia*. Los modelos de nicho hacen predicciones basadas en correlaciones entre registros de la presencia (o presencia y ausencia) de una especie y las condiciones ambientales en la ubicación del registro (Peterson et al. 2011). Básicamente estos modelos predicen los valores de idoneidad del hábitat con base en las respuestas modeladas de la especie a su entorno (Morente-López et al. 2020). En esta investigación, el modelamiento resultó sumamente útil para caracterizar el nicho ambiental de las diversas poblaciones estudiadas de *E. cordifolia*, permitiendo definir tanto los límites climáticos de las especies (población periférica) como su el óptimo ecológico (población centroide) (Capitulo 2.1).

El gradiente latitudinal de Chile desempeña un papel fundamental en la variabilidad de sus climas, lo que resulta en una geografía única que engloba diversas regiones climáticas, cada una con características distintivas (Luebert & Pliscoff 2017) y en el cual se distribuye la especie en estudio. Siguiendo la dualidad de Hutchinson, que establece una correspondencia entre los espacios ambientales y geográficos (Colwell y Rangel, 2009), se observó que las áreas correspondientes al centroide (Coronel) o a la periferia (Puerto Montt) del nicho no siguen un patrón norte-sur en la geografía. Esto podría ser resultado de la topografía abrupta lo que genera diversidad de microclimas (Luebert y Pliscoff, 2006).

3.2. Variaciones metabólicas en poblaciones de *E. cordifolia* según su posición en el nicho ecológico y la estacionalidad

Se demostró que la similitud de los perfiles metabólicos de las poblaciones de *E. cordifolia* fueron mayormente explicados por la estacionalidad que por la posición que ocupan las especies dentro de su nicho ecológico. Sin embargo, como tendencia generalizada se vio que las poblaciones presentaron un perfil similar a la población cercana al óptimo ecológico (centroide). Este patrón podría explicarse por la influencia de las

condiciones ambientales locales dispuestas a lo largo del gradiente de idoneidad y lo estables que son las condiciones a lo largo del año, forzando la producción de metabolitos que pueden dar lugar a una mayor diversidad de arreglos en la periferia del nicho. Además, este resultado podría estar influenciado por las condiciones microclimáticas del ambiente, que no son capturadas dentro del modelamiento de nicho ecológico, ya que generalmente los modelos de nicho utilizan datos macroclimáticos (Csergö et al. 2017).

Por otra parte, la diversidad metabolómica a lo largo de las estaciones demostró que las poblaciones periféricas presentar mayor diversidad de metabolitos secundarios que la población centroide (Capitulo 2.1; Figura 2.1.5). Este resultado fue confirmado con el estudio metabolómico, donde el uso de análisis multivariado permitió generar una diferenciación metabólica precisa entre las poblaciones (Capitulo 2.2; Figuras 2.2.1, 2.2.2, 2.2.3). Como tendencia general, los metabolitos regulados al alza en la población de Puerto Montt fueron derivados de quercetina, Kaempherol-3-O-ramnoside, luteolina, procianidina B1 y compuestos sulfónicos; todos estos ausentes en la población centroide. La respuesta metabolómica indica que la estacionalidad podría tener un efecto directo en los patrones de asignación de recursos, lo que reflejaría diversas demandas fisiológicas asociadas con el

crecimiento, la defensa y la reproducción (Gomes et al., 2019). Por su parte, la población ambientalmente periférica podría inducir el desarrollo de estrategias específicas de adaptación a condiciones ambientales cambiantes (Gouvea et al., 2012; Ma et al., 2011; Zhou et al., 2019) sintetizando compuestos diferenciadores respecto al centroide.

Si bien uno de los inconvenientes que presentó esta investigación y que se evidencian en los datos ya mostrados, es que la población de Contulmo presenta un comportamiento distinto en relación con las otras poblaciones y estimamos que esto se debe a la presencia de herbívora que había en esa población. Lamentablemente un parámetro que no pudo ser controlado y tampoco considerado en el modelamiento del nicho ecológico, ya que este solo se basa en variables ambientales abióticas (Soberón et al. 2017).

Actualmente existe un vacío en el desarrollo de bases de datos que reporten interacciones bióticas. En la población de Coronel, se observó una alta actividad antropogénica, ya que esta población se encuentra ubicada en una matriz altamente fragmentada con la influencia de plantaciones forestales de árboles exóticos (Braun et al., 2017; Echeverria et al., 2006). Esto podría resultar en una presión de competencia generalizada por los recursos, lo que potencialmente afectaría el *fitness* de las poblaciones locales debido a

desviaciones en la producción de metabolitos secundarios (Lieurance et al., 2015; Ramawat y Goyal, 2020).

3.3. Uso de la hipótesis de la centralidad en el nicho ecológico para la exploración de compuestos bioactivos de *E. cordifolia* con fines biotecnológicos

En esta investigación, además de analizar las variaciones en el metaboloma de *E. cordifolia* relacionadas con la hipótesis de la centralidad del nicho ecológico, también nos interesó explorar la aplicabilidad de esta propuesta para la identificación de compuestos bioactivos y sus posibles beneficios. Un estudio reciente realizado por Díaz-Foriester et al. (2019) demostró que especies pertenecientes a la familia *Cunoniaceae* tienen propiedades medicinales en Chile. Por ejemplo, se ha observado que la presencia de compuestos como taninos en estas especies puede tener diversos efectos farmacológicos, como propiedades antibacterianas, antivirales, inmunomoduladoras y antiinflamatorias.

Hasta el momento, esta investigación representa el primer estudio que ofrece una descripción detallada del perfil químico completo de las hojas de individuos de *E. cordifolia* en cuatro poblaciones distintas. Durante el desarrollo de este estudio, se logró identificar una variedad de compuestos,

incluyendo taninos, flavonoles, flavonas, flavanonas y compuestos sulfatados, entre otros (Capítulo 2.3). Estos mostraron variaciones significativas tanto entre las diferentes poblaciones analizadas como en función de la estacionalidad.

Otro estudio relevante sobre la identificación de compuestos en *E. cordifolia* fue llevado a cabo por Viteri et al. (2020). En su investigación, identificaron seis compuestos en total, incluyendo flavonoides y triterpenos, pero solamente en extractos de hojas de una localidad en el sur de Chile (Puerto Varas). Algunos de estos compuestos coinciden con los hallazgos reportados en nuestra investigación. Además, nuestros resultados son consistentes con los informes presentados por Bate-Smith et al. (1967), quienes utilizaron compuestos polifenólicos como flavonoides para diferenciar entre especies del género *Eucryphia* a nivel geográfico.

Se observaron variaciones en la actividad antioxidante de la especie, dependiendo del método espectrofotométrico utilizado (Capitulo 2.3). Los resultados más significativos se obtuvieron mediante los métodos ABTS y ORAC, especialmente en la población centroide y periférica (Figura 2.3.3). La última población presentó los valores más altos de actividad antioxidante durante los períodos de verano y otoño, lo cual sugiere la existencia de un

mecanismo de adaptación para ajustar la asignación de recursos en respuesta a las condiciones locales de crecimiento de *E. cordifolia*. Este ajuste podría estar relacionado con la síntesis de metabolitos secundarios especializados, como se plantea en un estudio reciente realizado por Otero et al. (2023).

Por otra parte, nuestros valores de capacidad antioxidante superaron los reportados para otras especies nativas de Chile, como *Berberis*, *Ugni molinae*, *Drimys winteri*, entre otras (Peña-Cerda et al. 2017; Bridi et al. 2019; Nova-Baza et al. 2022). Como se mencionó en el Capitulo 2.2.3, los compuestos que mostraron una diferencia significativa entre las poblaciones centroide y periférica fueron la quercetina y sus derivados. Este compuesto ha sido ampliamente reconocido como un potente antioxidante natural, capaz de prevenir la formación de especies reactivas de oxígeno, principales responsables del desarrollo de múltiples enfermedades en humanos (Muñoz et al. 2011; David et al. 2016; Gastaldi et al. 2018).

Además, se registró un aumento en la presencia de persicarina en la población ambientalmente periférica. En un estudio previo, Ku et al. (2013) aislaron persicarina e isorhamnetina de *Oenanthe javanica* y evaluaron sus actividades anticoagulantes. Los resultados demostraron que el grupo fosfato

de persicarina incrementa las actividades anticoagulantes y profibrinolíticas en comparación con la isorhamnetina.

Los extractos de *E. cordifolia* exhibieron una actividad antimicrobiana clara y eficaz frente a los patógenos *E. coli*, *S. aureus* y *P. aeruginosa* en ensayos *in vitro* iniciales, incluso a concentraciones bajas (8, 16 y 32 mg/mL). Estos resultados fueron significativamente más prometedores que los hallazgos de Viteri et al. (2021), quienes ensayaron el extracto de *E. cordifolia* a una concentración de 100 mg/mL contra *S. aureus* y *P. aeruginosa*. Por otra parte, los ensayos de inhibición de la formación de biopelículas no fueron los esperados, ya que sólo registramos resultados positivos sobre uno (*C. glabrata*) de los cuatro microorganismos estudiados. Solo durante los períodos de verano y otoño, la población ambientalmente periférica mostró una notable inhibición en la formación de biopelículas de *C. glabrata* (Capitulo 2.3.3.3; Figura 2.3.5). Este microrganismo es ampliamente conocido por causar infecciones en el tracto urinario y el torrente sanguíneo en humanos, y su tratamiento farmacológico suele ser complicado debido a su alta resistencia a fármacos del tipo azólicos (Tapia et al. 2008). Esta resistencia aumenta su patogenicidad, lo que representa un desafío mayor en su manejo clínico.

En la actualidad, la investigación sobre el potencial de las plantas para combatir la formación de biopelículas de microrganismos patógenos ha experimentado un notable aumento. Esto se debe, en gran parte, a la amplia variedad de metabolitos secundarios que presentan y a su perfil de seguridad (Shene et al. 2008). Por ejemplo, se ha demostrado que los extractos de hierbas contienen la enzima glucósido hidrolasa que contribuye a la degradación de las cadenas de polisacáridos, dividiéndolas en subunidades más pequeñas o monómeros que ayudan a reducir la biopelícula (Lahiri et al. 2019). Incluso se ha reportado que los compuestos fenólicos tienen la capacidad de inhibir la formación de biopelículas (Blando et al. 2019).

Considerando estos antecedentes, los compuestos presentes en los extractos de *E. cordifolia* (específicamente, los de la periferia del nicho) podrían ser candidatos prometedores como compuestos bioactivos para el tratamiento de este tipo de infecciones en humanos. Dada la naturaleza de los metabolitos que se han identificado en nuestra investigación, existe una posibilidad de que estos extractos puedan ofrecer una estrategia efectiva contra las biopelículas de los microrganismos patógenos, brindando así una opción terapéutica potencialmente más segura y eficaz.

Nuestro estudio se destaca por ser pionero al abordar la relación entre la hipótesis de la centralidad del nicho ecológico y el metaboloma de la especie nativa *E. cordifolia*. Mediante el uso de la metabolómica, que combina la separación cromatográfica con la espectrometría de masas, junto con análisis multivariados, obtuvimos información detallada sobre los metabolitos presentes en esta especie. Estos enfoques nos permitieron distinguir entre las poblaciones centrales y periféricas, lo que a su vez nos ayudó a comprender mejor cómo la variación del ambiente influye en la composición química de *E. cordifolia*. Además, demostramos que los compuestos presentes en los extractos de esta planta exhiben actividades biológicas destacadas en comparación con otras especies de interés medicinal en Chile. Por tanto, nuestros datos respaldan la idea de que la hipótesis de la centralidad del nicho ecológico puede ser una herramienta valiosa para la búsqueda de compuestos beneficiosos en plantas.

Una limitación recurrente en la investigación de los metabolitos secundarios en plantas con aplicaciones prácticas reside en el hecho de que, con frecuencia, el muestreo de las especies se lleva a cabo en áreas cercanas a las locaciones de estudio. Esta práctica tiende a subestimar la influencia de los factores ecológicos presentes en los hábitats de crecimiento sobre la

regulación del metabolismo. Como hemos mencionado previamente, la diversidad, abundancia y especificidad de estos metabolitos están moldeados por las variaciones ambientales en su entorno. En consecuencia, la aplicación de modelos de nichos ecológicos para definir poblaciones centrales y periféricas respecto de las variables ambientales emerge como una herramienta valiosa, ya que contribuye a anticipar la variabilidad metabolómica en las plantas. En otras palabras, esta aproximación proporciona una orientación más precisa para guiar el muestreo en condiciones de campo. Es decir, si nuestro objetivo es descubrir nuevos metabolitos con potencial como compuestos bioactivos en aplicaciones prácticas, sería recomendable enfocar el muestreo hacia la periferia del nicho ecológico. Aquí, las condiciones ambientales son más estresantes que en el centroide, lo que aumenta la probabilidad de encontrar una mayor diversidad de metabolitos únicos. Finalmente, con este estudio multidisciplinario es posible realizar diseños experimentales adecuados y prevenir la sobreexplotación de los recursos nativos y endémicos de Chile, ya que abarca un ecosistema diverso de especies utilizadas con fines medicinales. Estas herramientas nos permitirán utilizar de manera más sustentable y responsable los recursos naturales de nuestro país.

CAPITULO 4: CONCLUSION GENERAL

Este es el primer estudio multidisciplinario que estable una relación entre la hipótesis de la centralidad del nicho ecológico en relación con el metabolismo en la especie nativa *E. cordifolia*. Nuestro estudio muestra que conectar estos campos es prometedor para comprender las respuestas adaptativas de las plantas ante el ambiente.

Nuestros resultados revelan diferencias metabólicas entre las dos poblaciones de *E. cordifolia* (centro y periferia), con un número limitado de metabolitos que contribuyen a esta disparidad, tales como derivados de quercetina, compuestos sulfurados entre otros.

Aunque no medimos las condiciones climáticas *in situ*, se observaron diferencias bioclimáticas significativas entre Coronel y Puerto Montt. Estas diferencias climáticas se centran en las temperaturas estacionales y la cantidad de precipitaciones que tiene cada sitio; Puerto Montt presenta un clima templado, con temperaturas más bajas y recibe una mayor cantidad de precipitaciones que Coronel. Mientras que esta última, presenta un clima de transición mediterráneo-templado con una marcada influencia oceánica.

Los extractos de *E. cordifolia* presentaron una gran capacidad antioxidante, respaldada por diversos métodos espectrofotométricos en

ensayos *in vitro*. La población periférica exhibió los valores más altos durante los periodos de otoño y primavera para ABTS y ORAC. Además, demostró eficacia en la inhibición de diversos microorganismos de interés clínico (*E. coli*, *S. aureus*, *P. aeruginosa*, *C. glabrata* y *C. albicans*), pero solo en las etapas iniciales de crecimiento. Sin embargo, bajo modelos *in vitro* más avanzados, como la determinación de la inhibición de la biopelícula, solo se observó un efecto positivo sobre *C. glabrata*.

Los datos sugieren que, al combinar la hipótesis de la centralidad del nicho ecológico con un estudio metabólico, se pueden identificar metabolitos diferenciados según las variables ambientales de cada sitio. Asimismo, se resalta el valor de las hojas debido a la presencia de compuestos bioactivos con un prometedor potencial biotecnológico.

Finalmente, respondiendo a la hipótesis de esta tesis doctoral, es posible destacar que:

- La combinación de herramientas de modelamiento del nicho ecológico junto con la herramienta analítica metabolómica basada en UHPL-DAD-QTOF-MS/MS, posibilitó la evaluación de la diversidad metabólica y la identificación de metabolitos distintivos entre la población centroide y periférica.

- La realización de estudios *in vitro*, como la evaluación de la actividad antioxidante y antimicrobiana, reveló que la población periférica mostró una notable capacidad antioxidante y antimicrobiana en comparación con las otras poblaciones investigadas en este estudio.

Referencias Generales

Acevedo, F., Torres, P., Oomah, B. D., de Alencar, S. M., Massarioli, A. P., Martín-Venegas, R., ... & Rubilar, M. (2017). Volatile and non-volatile/semi-volatile compounds and in vitro bioactive properties of Chilean Ulmo (*Eucryphia cordifolia* Cav.) honey. Food Research International, 94, 20-28.

Allwood, J. W., De Vos, R. C., Moing, A., Deborde, C., Erban, A., Kopka, J., ... & Hall, R. D. (2011). Plant metabolomics and its potential for systems biology research: Background concepts, technology, and methodology. Methods in enzymology, 500, 299-336.

Anzano, A., Bonanomi, G., Mazzoleni, S., & Lanzotti, V. (2021). Plant metabolomics in biotic and abiotic stress: a critical overview. Phytochemistry Reviews, 1-22.

Arbona, V., Manzi, M., de Ollas, C., & Gómez-Cadenas, A. (2013). Metabolomics as a tool to investigate abiotic stress tolerance in plants. International journal of molecular sciences, 14(3), 4885-4911.

Arroyo, M. T. K., Marquet, P., Marticorena, C., Simonetti, J., Cavieres, L., Squeo, F., ... & Massardo, F. (2008). El hotspot chileno, prioridad mundial para la conservación. Biodiversidad de Chile, Patrimonio y Desafíos, 90-93.

Barve, N., Barve, V., Jiménez-Valverde, A., Lira-Noriega, A., Maher, S. P., Peterson, A. T., ... & Villalobos, F. (2011). The crucial role of the accessible

area in ecological niche modeling and species distribution modeling. Ecological modelling, 222(11), 1810-1819.

Bate-Smith, E. C., Davenport, S. M., & Harborne, J. B. (1967). Comparative biochemistry of flavonoids-III.: A correlation between chemistry and plant geography in the genus *Eucryphia*. Phytochemistry, 6(10), 1407-1413.

Blando, F., Russo, R., Negro, C., De Bellis, L., & Frassinetti, S. (2019). Antimicrobial and antibiofilm activity against *Staphylococcus aureus* of Opuntia ficus-indica (L.) Mill. cladode polyphenolic extracts. Antioxidants, 8(5), 117.

Bridi, R., & Montenegro, G. (2017). The value of chilean honey: Floral origin related to their antioxidant and antibacterial activities. Honey Analysis; Arnaut, V., Ed.; Intechopen: Rijeka, Croatia, 63-78.

Bull-Hereñu, K., Ronse de Craene, L., & Pérez, F. (2018). Correlación del tamaño del meristema floral y el número de órganos en *Eucryphia* (Cunoniaceae). Revista de investigación de plantas, 131, 429-441.

Canuto, G. A., Costa, J. L. D., da Cruz, P. L., Souza, A. R. L. D., Faccio, A. T., Klassen, A., ... & Tavares, M. F. (2018). Metabolômica: definições, estado-da-arte e aplicações representativas. Química Nova, 41, 75-91.

Csergő, A. M., Salguero-Gómez, R., Broennimann, O., Coutts, S. R., Guisan, A., Angert, A. L., ... & Buckley, Y. M. (2017). Less favourable climates constrain demographic strategies in plants. *Ecology letters*, *20*(8), 969-980.

David, A. V. A., Arulmoli, R., & Parasuraman, S. (2016). Overviews of biological importance of quercetin: A bioactive flavonoid. *Pharmacognosy reviews*, 10(20), 84.

da Silva, G. S., Canuto, K. M., Ribeiro, P. R. V., de Brito, E. S., Nascimento, M. M., Zocolo, G. J., ... & de Jesus, R. M. (2017). Chemical profiling of guarana seeds (*Paullinia cupana*) from different geographical origins using UPLC-QTOF-MS combined with chemometrics. Food Research International, 102, 700-709.

de Medeiros, C. M., Hernández-Lambraño, R. E., Ribeiro, K. A. F., & Sánchez Agudo, J. Á. (2018). Living on the edge: do central and marginal populations of plants differ in habitat suitability?. Plant Ecology, 219(9), 1029-1043.

de Oliveira, A. M. F., Pinheiro, L. S., Pereira, C. K. S., Matias, W. N., Gomes, R. A., Chaves, O. S., ... & de Assis, T. S. (2012). Total phenolic content and antioxidant activity of some *Malvaceae* family species. Antioxidants, 1(1), 33-43.

De Vos, R. C., Moco, S., Lommen, A., Keurentjes, J. J., Bino, R. J., & Hall, R. D. (2007). Untargeted large-scale plant metabolomics using liquid

chromatography coupled to mass spectrometry. Nature protocols, 2(4), 778-791.

Díaz-Forestier, J., Gómez, M., Celis-Diez, J. L., & Montenegro, G. (2016). Nectary structure in four melliferous plant species native to Chile. Flora 221, 100-106.

Díaz, I. A., Correa, C., Peña-Foxon, M. E., Méndez, M. A., & Charrier, A. (2010). First record on an amphibian in the canopy of temperate rainforests of southern South America: *Eupsophus calcaratus* (Cycloramphidae). Bosque, 31(2).

Dunn, W. B. (2008). Current trends and future requirements for the mass spectrometric investigation of microbial, mammalian and plant metabolomes. Physical biology, 5(1), 011001.

Escobar, B., Donoso, C., Zúñiga A. (2006). *Eucryphia cordifolia*. En: Donoso C (ed) Especies arbóreas de los bosques templados de Chile y Argentina. Autoecología. Marisa Cúneo Ediciones, Valdivia, Chile, pp 246–255.

Fiehn, O. (2002). Metabolomics—the link between genotypes and phenotypes. Functional genomics, 155-171.

Figueroa, J. A., Cabrera, H. M., Queirolo, C., & Hinojosa, L. F. (2010). Variability of water relations and photosynthesis in *Eucryphia cordifolia* Cav. (Cunoniaceae) over the range of its latitudinal and altitudinal distribution in Chile. Tree physiology, 30(5), 574-585.

Gastaldi, B., Marino, G., Assef, Y., Silva Sofrás, F. M., Catalan, C. A. N., & González, S. B. (2018). Nutraceutical properties of herbal infusions from six native plants of Argentine Patagonia. Plant foods for human nutrition, 73, 180-188.

Gorrochategui, E., Jaumot, J., Lacorte, S., & Tauler, R. (2016). Data analysis strategies for targeted and untargeted LC-MS metabolomic studies: Overview and workflow. TrAC Trends in Analytical Chemistry, 82, 425-442.

Hutchinson, G. (1957). Concluding remarks cold spring harbor symposia on quantitative biology, 22: 415–427.

Jha, A. K., & Sit, N. (2022). Extraction of bioactive compounds from plant materials using combination of various novel methods: A review. Trends in Food Science & Technology, 119, 579-591.

Jiménez-González, A., Quispe, C., Bórquez, J., Sepúlveda, B., Riveros, F., Areche, C., ... & Simirgiotis, M. J. (2018). UHPLC-ESI-ORBITRAP-MS analysis of the native Mapuche medicinal plant palo negro (*Leptocarpha rivularis* DC. Asteraceae) and evaluation of its antioxidant and cholinesterase

inhibitory properties. Journal of Enzyme Inhibition and Medicinal Chemistry, 33(1), 936-944.

Kanehisa, M., Sato, Y., Kawashima, M., Furumichi, M., & Tanabe, M. (2016). KEGG as a reference resource for gene and protein annotation. Nucleic acids research, 44(D1), D457-D462.

Kim, H. K., & Verpoorte, R. (2010). Sample preparation for plant metabolomics. Phytochemical Analysis: An International Journal of Plant Chemical and Biochemical Techniques, 21(1), 4-13.

Kim, S., Chen, J., Cheng, T., Gindulyte, A., He, J., He, S., ... & Bolton, E. E. (2019). PubChem 2019 update: improved access to chemical data. Nucleic acids research, 47(D1), D1102-D1109.

Krastanov, A. (2010). Metabolomics—The state of art. Biotechnology & Biotechnological Equipment, 24(1), 1537-1543.

Kumar, N., & Goel, N. (2019). Phenolic acids: Natural versatile molecules with promising therapeutic applications. Biotechnology Reports, 24,1-10.

Lahiri, D., Dash, S., Dutta, R., & Nag, M. (2019). Elucidating the effect of anti-biofilm activity of bioactive compounds extracted from plants. Journal of biosciences, 44(2), 52.

Leibold, M. A., & Geddes, P. (2005). El concepto de nicho en las metacomunidades. Ecología austral, 15(2), 117-129.

Li, Y., Kong, D., Fu, Y., Sussman, M. R., & Wu, H. (2020). The effect of developmental and environmental factors on secondary metabolites in medicinal plants. Plant Physiology and Biochemistry, 148, 80-89.

Lira-Noriega, A., Soberón, J., & Miller, C. P. (2013). Process-based and correlative modeling of desert mistletoe distribution: a multiscalar approach. Ecosphere, 4(8), 1-23.

Lira-Noriega, A., & Manthey, J. D. (2014). Relationship of genetic diversity and niche centrality: a survey and analysis. Evolution, 68(4), 1082-1093.

Maguire Jr, B. (1973). Niche response structure and the analytical potentials of its relationship to the habitat. The American Naturalist, 107(954), 213-246.

Mahieu, N. G., Genenbacher, J. L., & Patti, G. J. (2016). A roadmap for the XCMS family of software solutions in metabolomics. Current opinion in chemical biology, 30, 87-93.

Martínez-Meyer, E., Díaz-Porras, D., Peterson, A. T., & Yáñez-Arenas, C. (2013). Ecological niche structure and rangewide abundance patterns of species. Biology letters, 9(1), 20120637.

Martínez-Gutiérrez, P. G., Martínez-Meyer, E., Palomares, F., & Fernández, N. (2018). Niche centrality and human influence predict rangewide variation in population abundance of a widespread mammal: The collared peccary (*Pecari tajacu*). Diversity and Distributions, 24(1), 103-115.

Millán, D., Malebran, C., & Ormazábal-Toledo, R. (2023). Towards a rational design of natural deep eutectic solvents for the extraction of polyphenols from *Luma apiculata*. Journal of Molecular Liquids, 372, 121155.

Morales, J. (2013). Información tecnológica de productos forestales no madereros del bosque nativo en chile: Antecedentes Silvícolas y Tecnológicos *Eucryphia cordifolia* (Ulmo). 1-27.

Morales, L. V., Coopman, R. E., Rojas, R., Escandón, A. B., Flexas, J., Galmés, J., ... & Corcuera, L. J. (2014). Acclimation of leaf cohorts expanded under light and water stresses: an adaptive mechanism of *Eucryphia cordifolia* to face changes in climatic conditions?. Tree Physiology, 34(12), 1305-1320.

Morente-López, J., Kass, J. M., Lara-Romero, C., Serra-Diaz, J. M., Soto-Correa, J. C., Anderson, R. P., & Iriondo, J. M. (2020). Ecological niche models as hypothesis generators of functional genetic differentiation and potential local adaptation in a Mediterranean alpine ecosystem. BioRxiv, 2020-02.

Muñoz, O., Christen, P., Cretton, S., Backhouse, N., Torres, V., Correa, O., ... & Delporte, C. (2011). Chemical study and anti-inflammatory, analgesic and antioxidant activities of the leaves of Aristotelia chilensis (Mol.) Stuntz, Elaeocarpaceae. Journal of Pharmacy and Pharmacology, 63(6), 849-859.

Obata, T., & Fernie, A. R. (2012). The use of metabolomics to dissect plant responses to abiotic stresses. Cellular and Molecular Life Sciences, 69, 3225-3243.

Ochoa-Zavala, M., Osorio-Olvera, L., Cerón-Souza, I., Rivera-Ocasio, E., Jiménez-Lobato, V., & Núñez-Farfán, J. (2022). Reduction of Genetic Variation When Far From the Niche Centroid: Prediction for Mangrove Species. Frontiers in Conservation Science, 129.

Olivares-Caro, L., Radojkovic, C., Chau, S. Y., Nova, D., Bustamante, L., Neira, J. Y., ... & Mardones, C. (2020). Berberis microphylla G. Forst (Calafate) Berry Extract Reduces Oxidative Stress and Lipid Peroxidation of Human LDL. Antioxidants, 9(12), 1171.

Osorio-Olvera, L., Lira-Noriega, A., Soberón, J., Peterson, A. T., Falconi, M., Contreras-Díaz, R. G., ... & Barve, N. (2020). ntbox: An r package with graphical user interface for modelling and evaluating multidimensional ecological niches. Methods in Ecology and Evolution, 11(10), 1199-1206.

Osorio-Olvera, L., Soberón, J., & Falconi, M. (2019). On population abundance and niche structure. Ecography, 42(8), 1415-1425.

Otero, M. C., Fuentes, J. A., Atala, C., Cuadros-Orellana, S., Fuentes, C., & Gordillo-Fuenzalida, F. (2022). Antimicrobial Properties of Chilean Native Plants: Future Aspects in Their Application in the Food Industry. Foods, 11(12), 1763.

Otero, C., Klagges, C., Morales, B., Sotomayor, P., Escobar, J., Fuentes, J. A., ... & Rodríguez-Díaz, M. (2023). Anti-inflammatory chilean endemic plants. Pharmaceutics, 15(3), 897.

Pacifico, S., Galasso, S., Piccolella, S., Kretschmer, N., Pan, S. P., Marciano, S., ... & Monaco, P. (2015). Seasonal variation in phenolic composition and antioxidant and anti-inflammatory activities of *Calamintha nepeta* (L.) Savi. Food Research International, 69, 121-132.

Peterson, A. T., & Soberón, J. (2012). Species distribution modeling and ecological niche modeling: getting the concepts right. Natureza & Conservação, 10(2), 102-107.

Peterson, A. T., Soberón, J., Pearson, R. G., Anderson, R. P., Martínez-Meyer, E., Nakamura, M., & Araújo, M. B. (2011). Ecological niches and geographic distributions (MPB-49). In Ecological Niches and Geographic Distributions (MPB-49). Princeton University Press.

Pownitha, K. V., Hulegaru Nagaraja, P. B., Charles, B., Vasudeva, R., Aravind, N. A., & Ravikanth, G. (2022). Ecological niche modelling to identify suitable sites for cultivation of two important medicinal lianas of the Western Ghats, India. *Tropical Ecology*, *63*(3), 423-432.

Raza, A. (2020). Metabolomics: a systems biology approach for enhancing heat stress tolerance in plants. Plant Cell Reports, 1-23.

Ren, S., Hinzman, A. A., Kang, E. L., Szczesniak, R. D., & Lu, L. J. (2015). Computational and statistical analysis of metabolomics data. Metabolomics, 11, 1492-1513.

Rodriguez, R., Marticorena, C., Alarcón, D., Baeza, C., Cavieres, L., Finot, V. L., ... & Marticorena, A. (2018). Catálogo de las plantas vasculares de Chile. Gayana. Botánica, 75(1), 1-430.

Sagarin, R. D., Gaines, S. D., & Gaylord, B. (2006). Moving beyond assumptions to understand abundance distributions across the ranges of species. Trends in ecology & evolution, 21(9), 524-530.

Salehi, B., Sharifi-Rad, J., Herrera-Bravo, J., Salazar, L. A., Delporte, C., Barra, G. V., ... & Martorell, M. (2021). Ethnopharmacology, phytochemistry and biological activities of native chilean plants. Current Pharmaceutical Design, 27(7), 953-970.

Sampaio, B. L., & Costa, F. B. D. (2018). Influence of abiotic environmental factors on the main constituents of the volatile oils of *Tithonia diversifolia*. Revista Brasileira de Farmacognosia, 28, 135-144.

Schencke, C., Vásquez, B., Sandoval, C., & del Sol, M. (2016). El rol de la miel en los procesos morfofisiológicos de reparación de heridas. International Journal of Morphology, 34(1), 385-395.

Schrimpe-Rutledge, A. C., Codreanu, S. G., Sherrod, S. D., & McLean, J. A. (2016). Untargeted metabolomics strategies—challenges and emerging directions. Journal of the American Society for Mass Spectrometry, 27(12), 1897-1905.

Segovia, R. A., Pérez, M. F., & Hinojosa, L. F. (2012). Genetic evidence for glacial refugia of the temperate tree *Eucryphia cordifolia* (Cunoniaceae) in southern South America. American Journal of Botany, 99(1), 121-129.

Smith-Ramírez, C., Ramos-Jiliberto, R., Valdovinos, F. S., Martínez, P., Castillo, J. A., & Armesto, J. J. (2014). Decadal trends in the pollinator assemblage of *Eucryphia cordifolia* in Chilean rainforests. Oecologia, 176, 157-169.

Smith, C. A., O'Maille, G., Want, E. J., Qin, C., Trauger, S. A., Brandon, T. R., ... & Siuzdak, G. (2005). METLIN: a metabolite mass spectral database. Therapeutic drug monitoring, 27(6), 747-751.

Soberon, J., & Peterson, A. T. (2005). Interpretation of models of fundamental ecological niches and species' distributional areas. Biodiversity informatics, 2, 1-10.

Soberón, J. (2007). Grinnellian and Eltonian niches and geographic distributions of species. Ecology letters, 10(12), 1115-1123.

Soberón, J., & Nakamura, M. (2009). Niches and distributional areas: concepts, methods, and assumptions. Proceedings of the National Academy of Sciences, 106(2), 19644-19650.

Soberón, J., & Townsend Peterson, A. (2011). Ecological niche shifts and environmental space anisotropy: a cautionary note. Revista mexicana de biodiversidad, 82(4), 1348-1355.

Soberón, J., Osorio-Olvera, L., & Peterson, T. (2017). Diferencias conceptuales entre modelación de nichos y modelación de áreas de distribución. Revista mexicana de biodiversidad, 88(2), 437-441.

Stanimirova, I., Daszykowski, M., & Walczak, B. (2007). Dealing with missing values and outliers in principal component analysis. Talanta, 72(1), 172-178.

Tapia, C. (2008). *Candida glabrata*. *Revista chilena de infectología*, *25*(4), 293-293.

Traquete, F., Luz, J., Cordeiro, C., Sousa Silva, M., & Ferreira, A. E. (2021). Binary Simplification as an Effective Tool in Metabolomics Data Analysis. Metabolites, 11(11), 788.

Tsugawa, H., Cajka, T., Kind, T., Ma, Y., Higgins, B., Ikeda, K., ... & Arita, M. (2015). MS-DIAL: data-independent MS/MS deconvolution for comprehensive metabolome analysis. Nature methods, 12(6), 523-526.

Uteau, D., & Donoso, P. J. (2009). Early individual growth of *Eucryphia cordifolia* and *Laurelia sempervirens* planted under different competition conditions in south-central Chile. Ciencia e investigación agraria, 36(1), 85-96.

Viteri, R., Giordano, A., Montenegro, G., & Zacconi, F. C. (2022). Flavonoids and triterpenes isolated from *Eucryphia cordifolia* (Cunoniaceae). Biochemical Systematics and Ecology, 104, 104476.

Walker, T. W., Alexander, J. M., Allard, P. M., Baines, O., Baldy, V., Bardgett, R. D., ... & Salguero-Gómez, R. (2022). Functional Traits 2.0: The power of the metabolome for ecology. Journal of Ecology, 110(1), 4-20.

Wollenweber, E., Dörr, M., Rozefelds, A. C., Minchin, P., & Forster, P. I. (2000). Variation in flavonoid exudates in *Eucryphia* species from Australia and South America. Biochemical Systematics and Ecology, 28(2), 111-118.

Worley, B., & Powers, R. (2016). PCA as a practical indicator of OPLS-DA model reliability. Current Metabolomics, 4(2), 97-103.
Xia, J., & Wishart, D. S. (2011). Web-based inference of biological patterns, functions and pathways from metabolomic data using MetaboAnalyst. Nature protocols, 6(6), 743-760.

Yang, L., Wen, K. S., Ruan, X., Zhao, Y. X., Wei, F., & Wang, Q. (2018). Response of plant secondary metabolites to environmental factors. Molecules, 23(4), 762.

Yang, M., Li, Z., Liu, L., Bo, A., Zhang, C., & Li, M. (2020). Ecological niche modeling of Astragalus membranaceus var. mongholicus medicinal plants in Inner Mongolia, China. *Scientific Reports*, *10*(1), 12482.

Yañez-Arenas, C., Martínez-Meyer, E., Mandujano, S., & Rojas-Soto, O. (2012). Modelling geographic patterns of population density of the white-tailed deer in central Mexico by implementing ecological niche theory. Oikos, 121(12), 2081-2089.

Yañez, C., Martín, G., Osorio-Olvera, L., Escobar-Luján, J., Castaño-Quintero, S., Chiappa-Carrara, X., & Martínez-Meyer, E. (2020). The abundant niche-centroid hypothesis: key points about unfilled niches and the potential use of supraspecfic modeling units. Biodiversity Informatics, 15(3), 92-102.

Zanatta, A. C., Vilegas, W., & Edrada-Ebel, R. (2021). UHPLC-(ESI)-HRMS and NMR-based metabolomics approach to access the seasonality of *Byrsonima intermedia* and *Serjania marginata* From Brazilian Cerrado Flora diversity. Frontiers in chemistry, 9, 710025 1-17.

ANEXOS

2.1. Supplementary data 1: Metabolome expression in *Eucryphia cordifolia Cav*. populations: Role of seasonality and ecological niche centrality hypothesis.

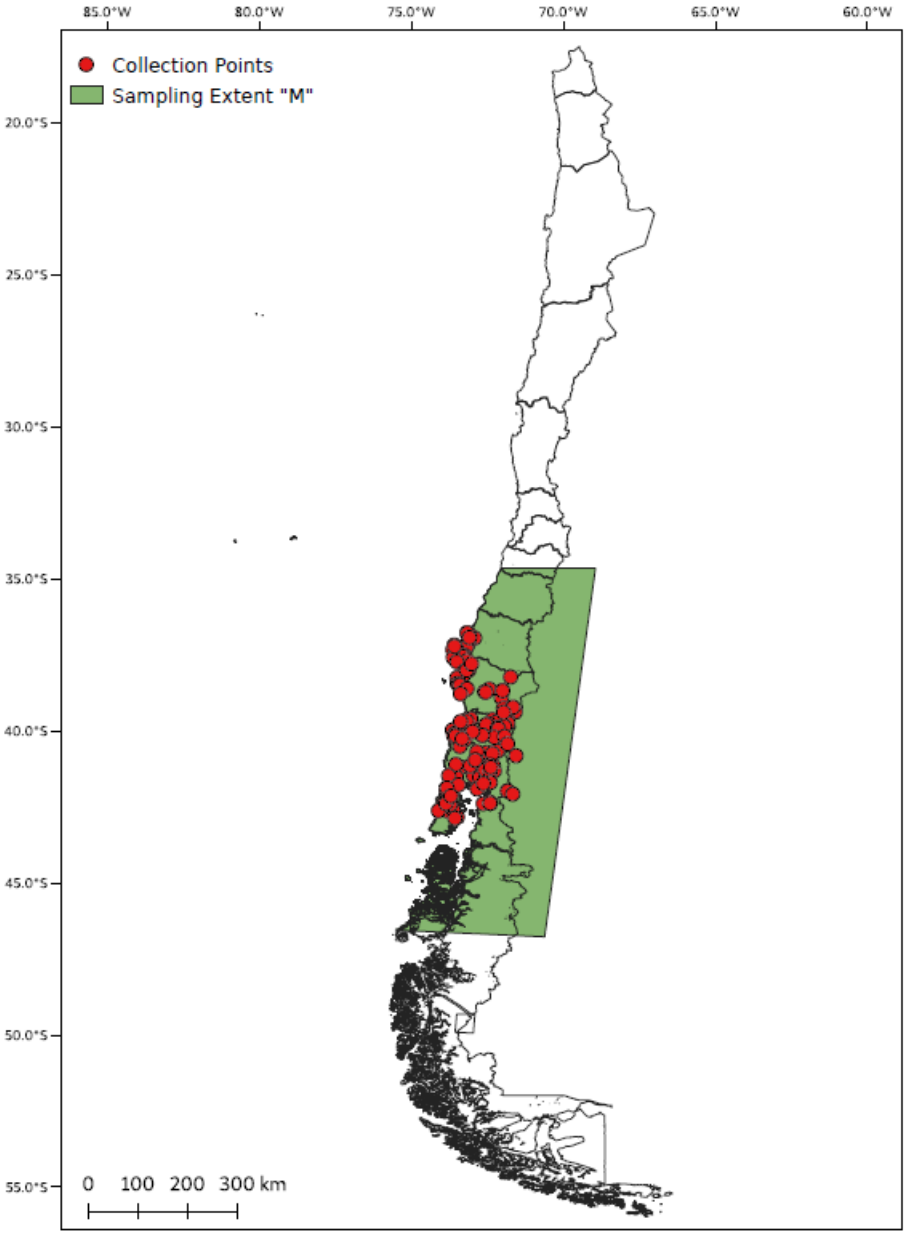

Fig. S1.1. Hypothetical dispersal and survival area of *E. cordifolia* ("M"). The red circles on the map correspond to observations from GBIF, CONC and Segovia et al. (2012).

1) Validation of the model pROC-AUC

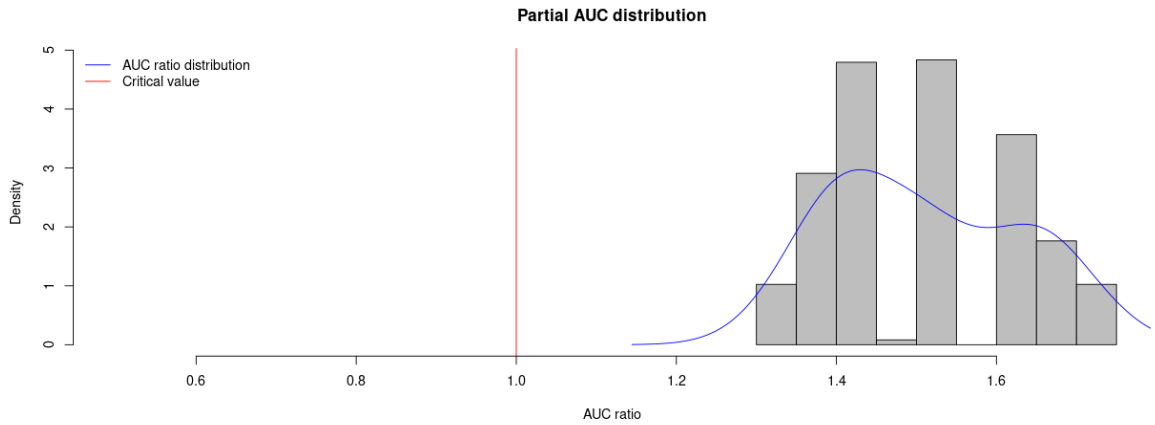

Fig. S1.2. Partial distribution of the area under the curve (AUC) ratio of *E. cordifolia* generated after 500 simulations. The shaded bars with bell-shaped curve shows the frequency distribution of the ratios between AUC from model prediction and AUC random.

Statistics for Partial ROC after 500 simulations:

- The mean value for AUC ratio at, 0.95 is: 1.51112
- The mean value for partial AUC at, 0.95 is: 0.6588327
- The mean value for partial AUC at random is: 0.4337786
- The mean value of AUC after 500 iterations is: 0.9001241

Statistics for the difference between AUC random and AUC from model prediction

Ho: The difference between AUC from model prediction and AUC at random is <=0

Ha: The difference between AUC from model prediction and AUC at random is >0

n	ean	d	edian	ad	in	ax	ange	kew	urtosis
88	.51	.11	1 .51	.16	.32	.74	.42	.28	- 1.22

The *p*-value for the difference between means (AUC random and AUC partial) is: 0 *** (Ho Rejected)

2) Binomial Test.

	N pixels in predicted map	N pixels in binary map	Proportion of total area in binary map	N of success	N of fails	p-value
Count	628263	68905	0.11	65	30	0 (***)

Statistics for the difference in the predictability between binary map and random model

Ho: The difference between binary map from model prediction and random prediction is <=0

Ha: The difference between AUC from model prediction and AUC at random is>0

The *p*-value for the difference between binary and random model prediction is: 0 *** (Ho Rejected).

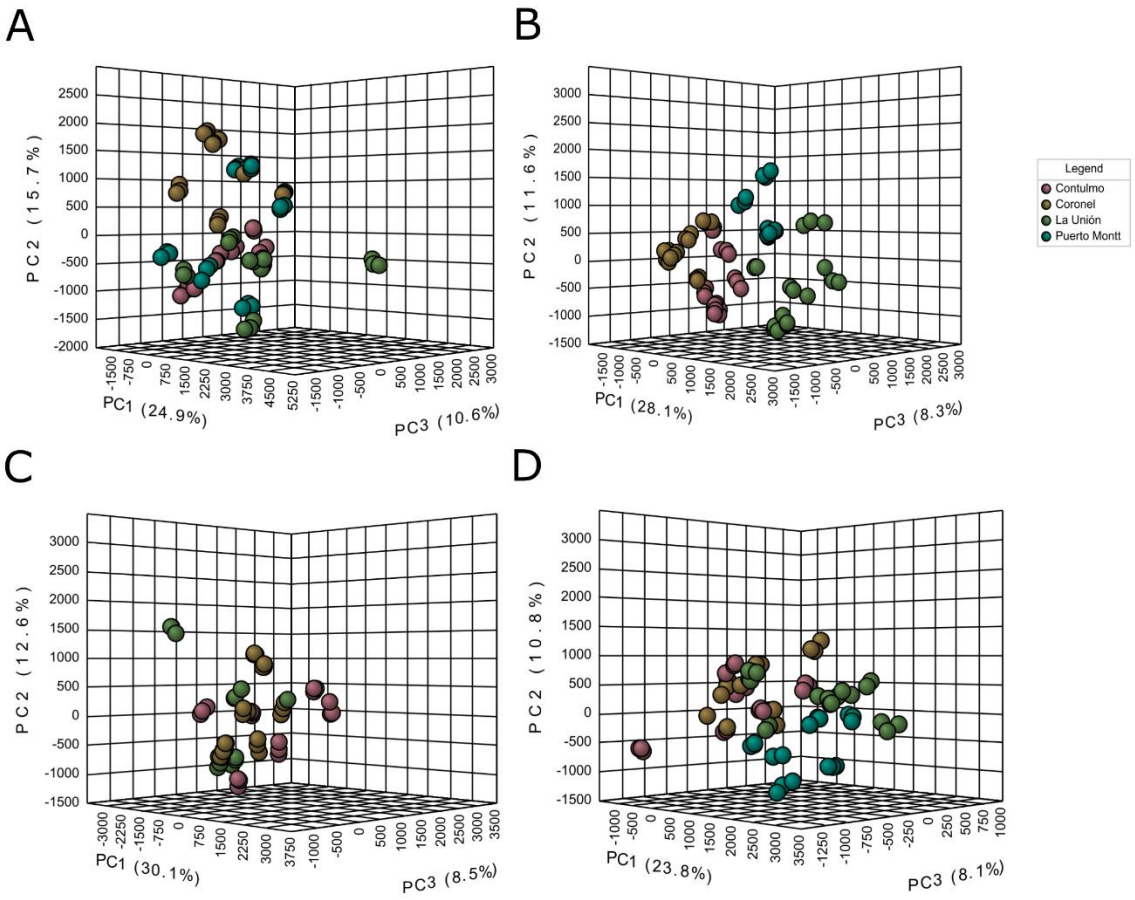

Fig. S1.3. 3D principal component analysis (PCA) based on metabolic data in negative ion mode according to the position of *E. cordifolia* populations in their ecological niche (A) Summer (B) Autumn (C) Winter and (D) Spring.

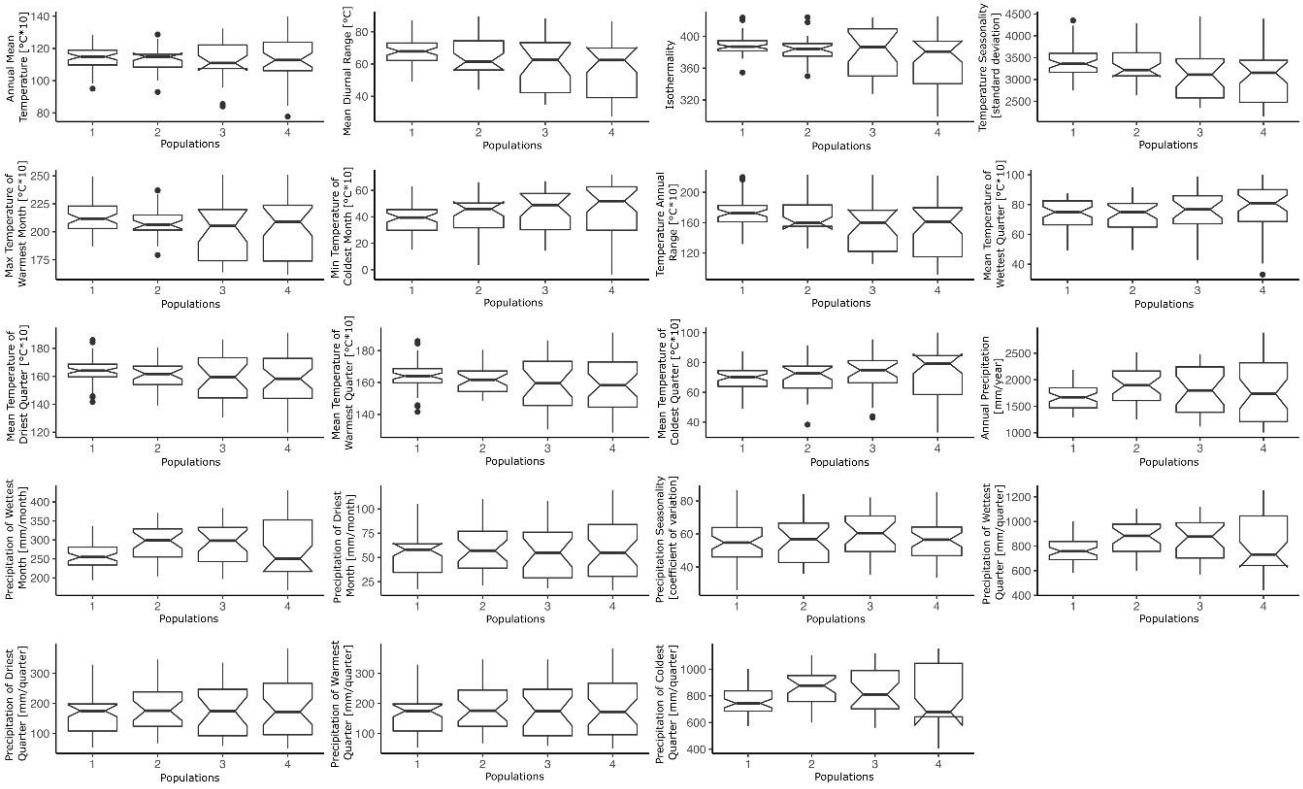

Fig. S1.4. Contribution of climatic variables (CHELSA) for the different strata of *E. cordifolia* (1) Coronel (2) Contulmo (3) La Unión (4) Puerto Montt**.**

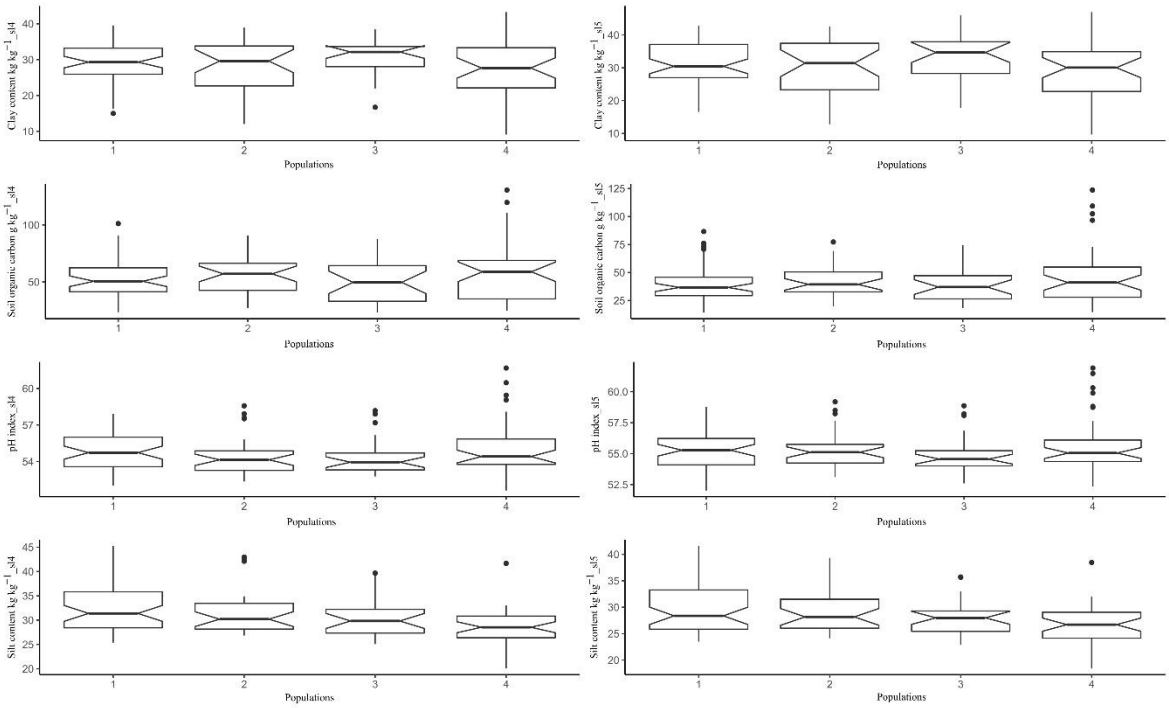

Fig. S1.5. Main soil properties considered for *E. cordifolia* populations (1) Coronel (2) Contulmo (3) La Unión (4) Puerto Montt. Used at a spatial resolution of 250 m. Sl4 and sl5 correspond to the standard depth used (30 and 60 cm).

Fig. S1.6. Photographs of *E. cordifolia* showing herbivore damage for the four populations investigated (A) Coronel (B) Contulmo (C) La Unión (D) Contulmo.

Table S1.1. Geographical location, date of sampling of *E. cordifolia* in the four seasons (summer, autumn, winter and spring), temperature and average precipitation at sampling location.

Locality	Geographical Reference	Season	Data	Temperature (°C)	Precipitation (mm)
Alto Escuadrón Coronel, Bio Bio Region	Individual 1: 36°56'45''S 73°05'10'' W				
	Individual 2: 36°56'43''S 73°05'13'' W	Spring	22-11-2019	20.1	0
	Individual 3: 36°56'40''S 73°05'14'' W	Summer	12-02-2020	22.5	0.1
	Individual 4: 36°56'37''S 73°05'15'' W	Autumn	03-06-2020	13.2	11.4
	Individual 5: 36°56'34''S 73°05'15'' W	Winter	31-08-2020	14.1	2.64
	Individual 6: 36°56'36''S 73°05'12'' W				
Contulmo National Monument Contulmo, Bio Bio Region	Individual 1: 38°00'47'' S 73°11'09''W				
	Individual 2: 38°00'46'' S 73°11'12''W	Spring	22-11-2019	19.4	1.32
	Individual 3: 38°00'45'' S 73°11'16''W	Summer	12-02-2020	25.4	1.16
	Individual 4: 38°00'42'' S 73°11'19''W	Autumn	03-06-2020	11.7	7.51
	Individual 5: 38°00'39'' S 73°11'21''W	Winter	31-08-2020	12.5	3.18
	Individual 6: 38°00'42'' S 73°11'14''W				
Alerce Costero National Park La Unión, Los Lagos Region	Individual 1: 40°11'59'' S 73°25'43''W				
	Individual 2: 40°12'02'' S 73°25'42''W	Spring	10-12-2019	22.4	0.59
	Individual 3: 40°12'04'' S 73°25'39''W	Summer	18-02-2020	24.5	0.08
	Individual 4: 40°12'07'' S 73°25'36''W	Autumn	09-06-2020	11.3	13.49
	Individual 5: 40°12'09'' S 73°25'33''W	Winter	14-09-2020	15	2.05
	Individual 6: 40°12'09'' S 73°25'28''W				
Alerce Andino National Park Puerto Montt, Los Lagos Region	Individual 1: 41°35'35'' S 72°35'36''W				
	Individual 2: 41°35'31'' S 72°35'36''W	Spring	11-12-2019	18.7	1.96
	Individual 3: 41°35'28'' S 72°35'38''W	Summer	19-02-2020	20.1	1.76
	Individual 4: 41°35'25'' S 72°35'40''W	Autumn	10-06-2020	10.7	6.58
	Individual 5: 41°35'23'' S 72°35'43''W	Winter	*	*	*
	Individual 6: 41°35'21'' S 72°35'46''W				

* population not screened due to limited access due to COVID-19 pandemic restrictions.

2.2. Supplementary data 2: Enfoque metabolómico no dirigido para evaluar la variación intraespecífica de metabolitos secundarios en poblaciones de *Eucryphia cordifolia* Cav. (Cunoniaceae) en función de su nicho ecológico.

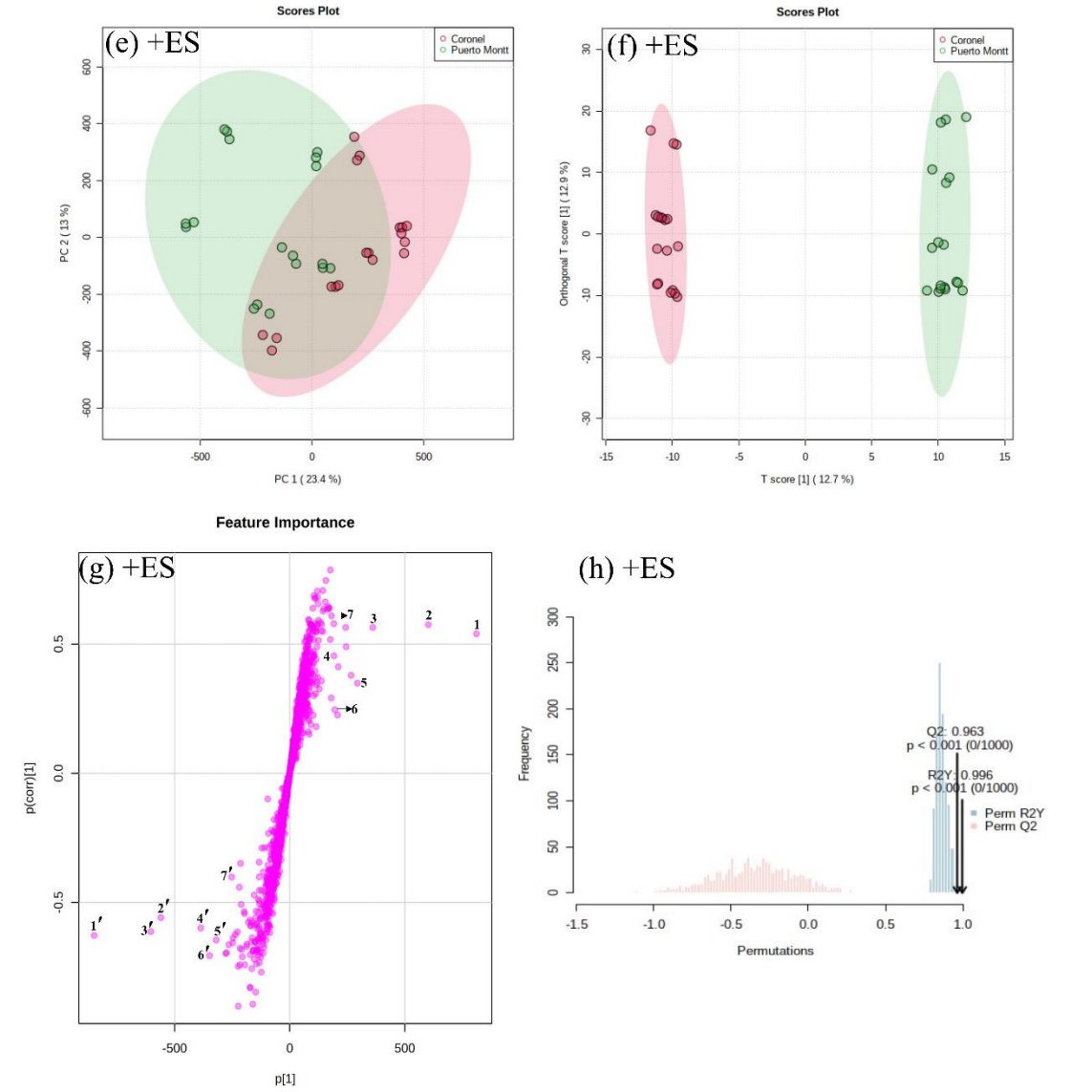

Fig S2.1. (a) análisis de Componentes Principales (PCA) basado en el conjunto de datos LC-MS adquiridos en modo de ionización negativo (+ESI) para las poblaciones centroide y periférica de *E. cordifolia* en la estación de Verano (b) gráfico de *score* del modelo supervisado OPLS-DA (c) diagrama *S*-plot, que ilustra la covarianza p[1] frente a la correlación p(cor)[1] de las variables del componente discriminante del modelo OPLS-DA (d) validación cruzada y prueba de permutación para el modelo OPLS-DA.

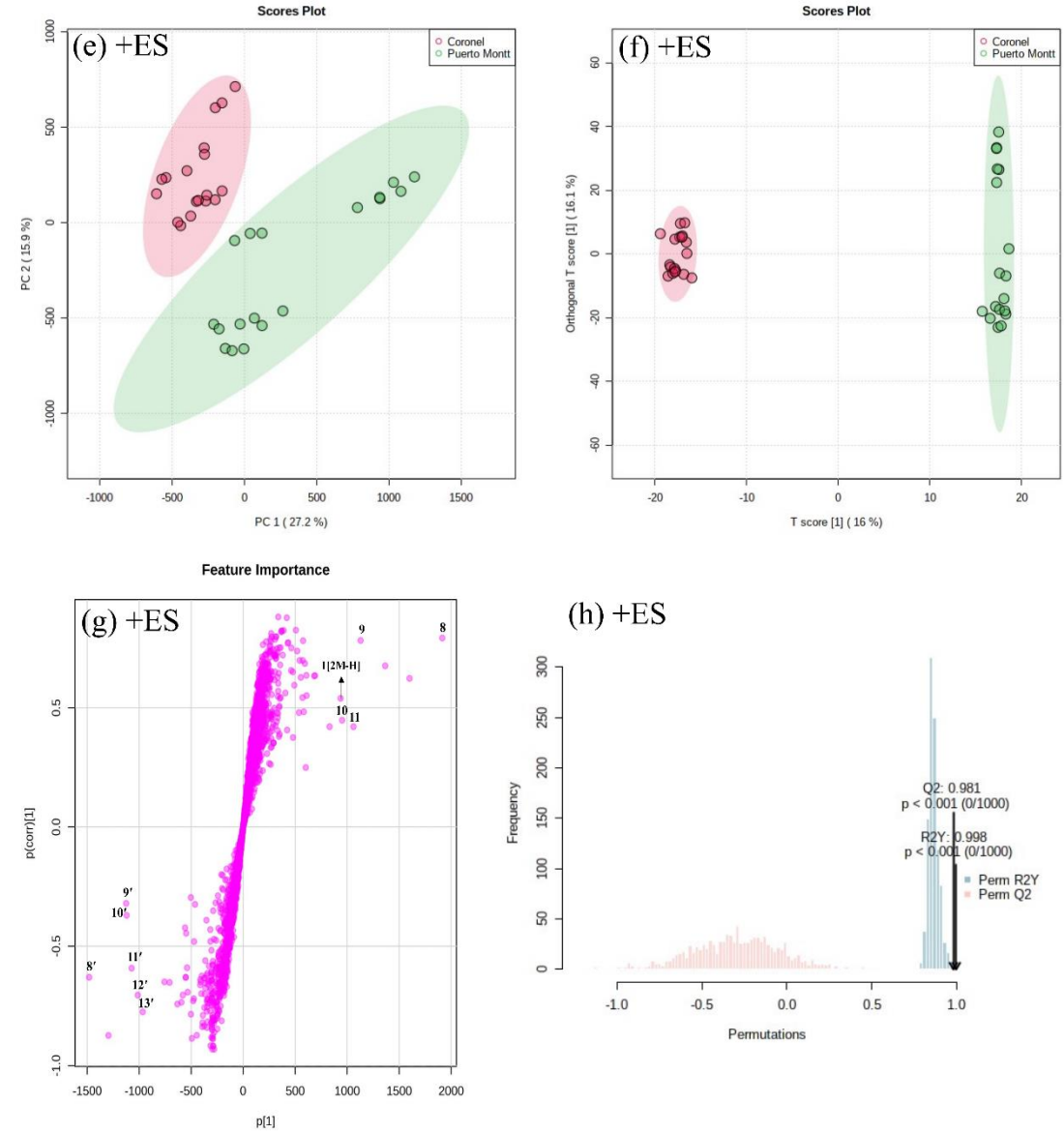

Fig S2.2. (a) análisis de Componentes Principales (PCA) basado en el conjunto de datos LC-MS adquiridos en modo de ionización negativo (+ESI) para las poblaciones centroide y periférica de *E. cordifolia* en la estación de Otoño (b) gráfico de *score* del modelo supervisado OPLS-DA (c) diagrama *S*-plot, que ilustra la covarianza p[1] frente a la correlación p(cor)[1] de las variables del componente discriminante del modelo OPLS-DA (d) validación cruzada y prueba de permutación para el modelo OPLS-DA.

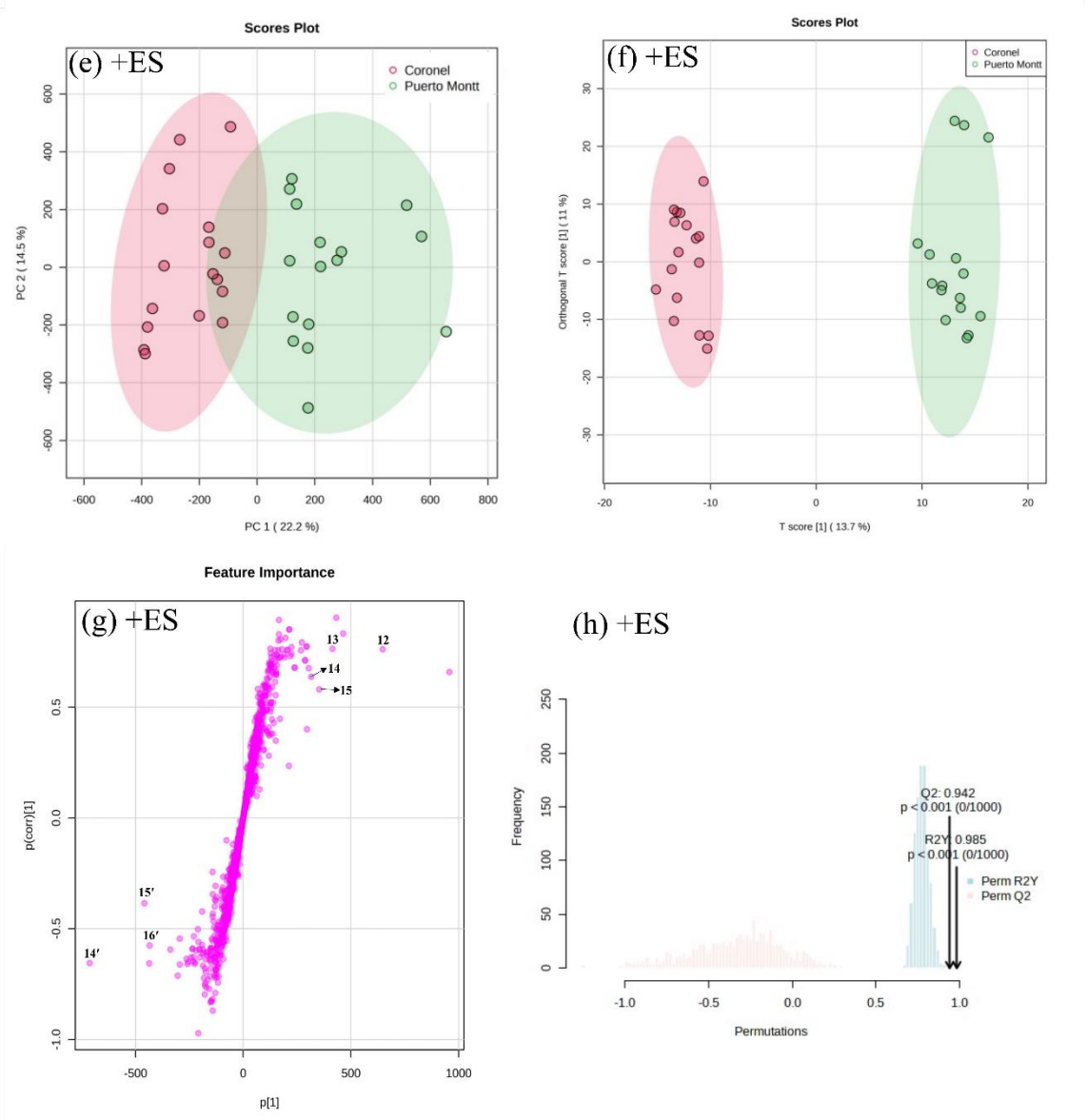

Fig S2.3. (a) análisis de Componentes Principales (PCA) basado en el conjunto de datos LC-MS adquiridos en modo de ionización negativo (+ESI) para las poblaciones centroide y periférica de *E. cordifolia* en la estación de Primavera (b) gráfico de *score* del modelo supervisado OPLS-DA (c) diagrama *S*-plot, que ilustra la covarianza p[1] frente a la correlación p(cor)[1] de las variables del componente discriminante del modelo OPLS-DA (d) validación cruzada y prueba de permutación para el modelo OPLS-DA.

Tabla S2.1. Se presentan los datos químicos de metabolitos relevantes para distinguir entre la población centroide y periférica de *E. cordifolia*, clasificados por estación y analizados en modo de ionización positivo (+ES) por UHPLC-DAD-QTOF-MS/MS.

No	Rt (min)	Putative metabolite name	Metabolite class	Mol . formula	ESI (-) Theor m/z	ESI (-) Meas m/z	ESI (+) Theor m/z	ESI (+) Meas m/z	m/z error (ppm) [a]	MS/MS ESI (-) fragments (int. %)	MS/MS ESI (+) fragments (int. %)	UV/Vis (nm)	InChI-Key	Ident. level (A-D)
VERANO														
Metabolitos regulados al alza en hojas de *E. cordifolia* localizadas en Puerto Montt al compararlas con las de Coronel														
1	10.88	Quercetin I	Flavonol	$C_{15}H_{10}O_7$	n.d.	n.d.	303.0499	303.0513 $[M+H]^+$	4.51, n.d.	n.d.	303.0 (100)	216	REFJWTPEDVJJIY-UHFFFAOYSA-N	B
2	9.85	Quercetin II	Flavonol	$C_{15}H_{10}O_7$	n.d.	n.d.	303.0499	303.0569 [M+H]+	2.95, n.d	n.d.	303.0 (100)	216	REFJWTPEDVJJIY-UHFFFAOYSA-N	B
3	9.85	Quercetin-3-O-hexoside	Flavonol glycoside	$C_{21}H_{20}O_{12}$	463.0881	463.0879 $[M-H]^-$	465.1028	465.1037 $[M+H]^+$	2.10, 0.12	463.0 (100), 271.0 (58), 255.0 (25), 227.0 (3), 178.9 (1), 151.0 (5)	303.0 (100), 257.0 (2), 229.0 (2)	215	OVSQVDMCBVZWGM-QSOFNFLRSA-N	B
4	10.88	Quercetin-3-O-deoxyhexoside	Flavonols glycoside	$C_{21}H_{20}O_{11}$	447.0933	447.0921 $[M-H]^-$	449.1078	449.1091 $[M+H]^+$	2.89, 2.55	447.0 (100), 300.0 (58), 271.0 (50), 255.0 (24), 277.0 (3), 178.9 (2)	303.0 (100), 257.0 (2), 229.0 (2), 129.0 (5)	211	OXGUCUVFOIWWQJ-HQBVPOQASA-N	B
5	10.06	Taxifolin	Flavanone	$C_{15}H_{12}O_7$	303.0506	303.051 $[M-H]^-$	305.0665	305.0661 [M+H]+	2.04, 1.27	125.0 (100), 150.0 (17), 178.9 (28), 285.0 (57)	123.0 (100)	201, 290	CXQWRCVTCMQVQX-LSDHHAIUSA-N	B

6	5.69	Procyanidin B1	Flavanols	$C_{30}H_{26}O_{12}$	577.1351	577.1348 $[M-H]^-$	579.1497	579.1497 $[M+H]^+$	0.3, 0.58	577.1 (51), 425.0 (66), 289.0 (100), 254.0 (24), 125.0 (75)	570.0 (16), 427.0 (42), 409.0 (48), 280.0 (49), 127.0 (100),	203,280	XFZJEEAOWLFHDH-NFJBMHMQSA-N	B
7	11.81	Luteolin	Flavone	$C_{15}H_{10}O_6$	n.d.	n.d.	287.055	287.0557 $[M+H]^+$	3.19, n.d	n.d.	287.056 (100)	216, 265, 356	IYRMWMYZSQPJKC-UHFFFAOYSA-N	B
Metabolitos regulados a la baja en hojas de *E. cordifolia* localizadas en Puerto Montt al compararlas con las de Coronel														
1′	10.98	Cirsiliol	Flavone	$C_{17}H_{14}O_7$	329.0667	329.0665 $[M-H]^-$	331.0812	331.0820 $[M+H]^+$	2.22, 0.66	314.0 (100), 299.0 (5), 286.0 (8), 271.0 (59), 257.0 (1), 242.0 (8)	331.0 (100), 315.0 (14), 298.0 (10), 285.0 (7), 270.0 (17), 257.0 (3), 241.0 (5)	207, 349	IMEYGBIXGJLUIS-UHFFFAOYSA-N	B
2′	8.99	Taxifolin	Flavanone	$C_{15}H_{12}O_7$	n.d.	n.d.	305.0667	305.0656 $[M+H]^+$	3.61, n.d.	n.d.	287.0 (18), 259.0 (76), 231.0 (73), 213.0 (14), 195.0 (12), 161.0 (8)	212, 286	CXQWRCVTCMQVQX-UHFFFAOYSA-N	B
3′	9.17	Syringetin	Flavonol	$C_{17}H_{14}O_8$	345.0616	345.0616 $[M-H]^-$	347.0668	347.0767 $[M+H]^+$	1.68, n.d.	303.0 (100),	347.0 (100), 332.0 (13), 314.0 (9), 286.0 (13), 269.0 (2), 257.0 (3), 241.0 (3), 229.0 (4), 201.0 (4), 147.0 (3), 128.0 (1)	212	KIGVXRGRNLQNNI-UHFFFAOYSA-N	B
4′	8.78	Syringetin-hexoside	Flavonol	$C_{23}H_{24}O_{13}$	507.1144	507.1140 $[M-H]^-$	509.129	509.1289 $[M+H]^+$	0.26, 0.91	507.1 (11), 345.0 (100), 330.0 (17), 287.0 (43), 259.0 (59), 243.0 (3)	509.1 (41), 347.0 (100), 331.0 (21), 314.0 (18), 286.0 (29)	212	JMFWYRWPJVEZPV-AVGVHVDKSA-N	B
5′	8.87	Isorhamnetin -hexoside	Flavonol	$C_{22}H_{22}O_{12}$	477.1038	477.1111 $[M-H]^-$	479.1184	479.1165 $[M+H]^+$	0.59		302.0403, 317.0646, 274.0463	216, 280	CQLRUIIRRZYHHS-LFXZADKFSA-N	B

6′	9.39	Tricin hexoside	Flavone	$C_{23}H_{24}O_{12}$	490.1337	491.1193 $[M-H]^-$	492.1341	493.1339 $[M+H]^+$	0.35, 0.86	491.0 (89), 329.0 (92), 314.0 (92), 271.0 (100), 242.0 (11), 214.0 (3)	493.0 (78), 331.0 (100), 316.0 (18), 298.0 (32), 270.0 (32)	215	FLSOTPIEF VBPBU-LDBVRRDL SA-N	B
7′	12.04	Laricitrin hexoside	Flavonol	$C_{22}H_{22}O_{13}$	n.d.	n.d.	495.1133	495.1141 $[M+H]^+$	1.3, n.d.	n.d.	333.0567, 495.1048, 318.0345, 319.0378	217, 350	ODXINVOIN FDDDD-CLXWZIMC SA-N	B
OTOÑO														
Metabolitos regulados al alza en hojas de *E. cordifolia* localizadas en Puerto Montt al compararlas con las de Coronel														
8	9.68	Quercetin III	Flavonol	$C_{15}H_{12}O_7$	301.0353	301.0352 $[M-H]^-$	303.0499	303.0523 $[M+H]^+$	7.54, 0.43	303.0 (100)	259.0 (100), 241.0 (23), 231.0 (64), 149.0 (48).	203-286	REFJWTPED VJJIY-UHFFFAOY SA-N	B
9	9.68	Quercetin-3-O-hexoside	Flavonol glycoside	$C_{21}H_{20}O_{12}$	463.0881	463.0878 $[M-H]^-$	465.1027	465.1265 $[M+H]^+$	7.44, 0.82	463.0 (100), 300.0 (65), 271.0 (55), 255.0 (24), 243.0 (12), 151.0 (4)	303.0 (100), 257.0 (8), 229.0 (2)	255, 355	OVSQVDMC BVZWGM-QSOFNFLRS A-N	B
10	5.49	Procyanidin B1	Flavanols	$C_{30}H_{26}O_{12}$	577.1424	577.1348 $[M+H]^-$	579.1427	579.1518 $[M+H]^+$	3.97, 0.78	577.1 (74), 425.0 (100), 407.0 (71), 289.0 (93), 273.0 (7), 245.0 (23), 203.0 (12)	579.1 (12), 439.0 (2), 409.0 (41), 289.0 (41), 247.0 (21), 163.0 (19), 127.0 (100)	203	XFZJEEAO WLFHDH-NFJBMHMQ SA-N	B
11	9.89	Taxifolin	Flavanone	$C_{15}H_{12}O_7$	303.0583	303.0507 $[M-H]^-$	305.0655	305.0681 $[M+H]^+$	8.49, 0.92	255.2 (100), 216.1 (95)	259.0 (100), 241.0 (23), 231.0 (64), 149.0 (48).	203, 286	CXQWRCVT CMQVQX-UHFFFAOY SA-N	B
Metabolitos regulados a la baja en hojas de *E. cordifolia* localizadas en Puerto Montt al compararlas con las de Coronel														
8′	8.8	Taxifolin	Flavanone	$C_{15}H_{12}O_7$	303.0583	303.0506 $[M-H]^-$	305.0655	305.0677 $[M+H]^+$	7.27, 1.97	255.2 (27), 216.1 (100), 130.0 (18)	287.0 (25), 259.0 (69), 241.0 (3), 231.0 (100), 213.0 (18), 123.0 (75)	203, 290	CXQWRCVT CMQVQX-UHFFFAOY SA-N	B
9′	10.79	Cirsiliol	Flavone	$C_{17}H_{14}O_7$	n.d.	n.d.	331.0787	331.0869 $[M+H]^+$	2.84, n.d	n.d.	331.0844, 270.0546, 316.0604	203, 346	IMEYGBIXG JLUIS-	B

													UHFFFAOYSA-N	
10′	8.99	Syringetin	Flavonol	$C_{17}H_{14}O_8$	345.0688	345.0613 $[M-H]^-$	347.0761	347.0779 $[M+H]^+$	5.96, 0.89	345.0 (43), 315.0 (16), 287.0 (72), 271.0 (17), 259.0 (8), 243.0 (9), 231.0 (19)	347.0 (100), 332.0 (12), 314.0 (9), 301.0 (1), 286.0 (13), 269.0 (1), 257.0 (4)	203, 296	KIGVXRGRNLQNNI-UHFFFAOYSA-N	B
11′	8.78	Syringetin-hexoside	Flavanone	$C_{23}H_{24}O_{13}$	507.1144	507.1138 $[M-H]^-$	509.1289	509.1307 $[M+H]^+$	5.26, 1.13	507.1 (11), 345.0 (100), 330.0 (17), 315.0 (8), 287.0 (43)	509.1 (41), 347.0 (100), 331.0 (21), 314.0 (18), 286.0 (29)	220	JMFWYRWPJVEZPV-AVGVHVDKSA-N	B
12′	14.7	Procyanidin B. isomer	Flavanols	$C_{30}H_{26}O_{12}$	577.1345	577.1351 $[M-H]^-$	579.1497	579.1580 $[M+H]^+$	3.84, 1.20	577.1 (93), 431.0 (10), 269.0 (100), 145.0 (64)	579.1 (2)271.0 (100), 147.0 (3)	219-317	XFZJEEAOWLFHDH-NFJBMHMQSA-N	B
13′	9.5	Tricin hexoside	Flavone glycoside	$C_{23}H_{24}O_{12}$	491.1267	491.1190 $[M-H]^-$	493.1393	493.1364 $[M+H]^+$	5.93, 0.69	491.1 (57), 329.0 (98), 314.0 (42), 271.0 (100)	493.1 (74), 331.0 (100), 315.0 (24), 298.0 (22), 270.0 (43)	203	FLSOTPIEFVBPBU-LDBVRRDLSA-N	B
PRIMAVERA														
Metabolitos regulados al alza en hojas de *E. cordifolia* localizadas en Puerto Montt al compararlas con las de Coronel														
12	10	Quercetin	Flavonol	$C_{15}H_{10}O_7$	n.d.	n.d.	303.0499	303.0509 $[M+H]^+$	3.31, n.d.	n.d.	303.0 (100)	251	REFJWTPEDVJJIY-UHFFFAOYSA-N	B
13	10	Quercetin-3-O-hexoside	Flavonol glycoside	$C_{21}H_{20}O_{12}$	463.0881	463.0879 $[M-H]^-$	465.1027	465.1035 $[M+H]^+$	3.19, 0.12	463.0 (100), 271.0 (58), 255.0 (25), 227.0 (3), 178.9 (1), 151.0 (5)	303.0 (100), 257.0 (2), 229.0 (2)	215	OVSQVDMCBVZWGM-QSOFNFLRSA-N	B
14	11.96	Luteolin	Flavone	$C_{15}H_{10}O_6$	285.0405	285.0392 $[M-H]^-$	287.0561	287.0551 $[M+H]^+$	3.81, 4.50	282.2 (100), 211.0 (77)	287.0 (100)	258	IYRMWMYZSQPJKC-UHFFFAOYSA-N	B

15	11.03	Quercetin-rhamnoside	Flavonol glycoside	$C_{21}H_{20}O_{11}$	447.0919	447.0932 $[M-H]^-$	449.1078	449.1096 $[M+H]^+$	4.09	301.0 (100)	303.0 (100), 257.0 (2), 229.0 (2), 129.0 (4)	279, 349	OXGUCUVFOIWWQJ-HQBVPOQASA-N	B
Metabolitos regulados a la baja en hojas de *E. cordifolia* localizadas en Puerto Montt al compararlas con las de Coronel														
14′	9.14	Taxifolin	Flavonols	$C_{15}H_{12}O_7$	303.051	303.0506 $[M-H]^-$	305.0655	305.0665 $[M+H]^+$	3.32, 1.26	216.1 (100)	259.0 (74), 231.0 (80), 153.0 (100), 123.0 (83), 123.0 (83), 287.0 (9)	254, 289	CXQWRCVTCMQVQX-UHFFFAOYSA-N	B
15′	11.14	Cirsiliol	Flavone	$C_{17}H_{14}O_7$	n.d.	n.d.	331.0812	331.0824 $[M+H]^+$	3.53, n.d	331.0 (100), 270.0 (16), 213.0 (9), 316.0 (14)	331.0 ()	203, 346	IMEYGBIXGJLUIS-UHFFFAOYSA-N	B
16′	9.32	Syringetin	Flavonol	$C_{17}H_{14}O_8$	345.0645	345.0615 $[M-H]^-$	347.0761	347.0768 $[M+H]^+$	2.01, 0.32	300.0 (100), 315.0 (27), 287.0 (88), 271.0 (29), 259.0 (4), 243.0 (11), 213.0 (11), 176.0 (23), 148.0 (10), 109.0 (10)	347.0 (100), 332.0 (12), 314.0 (9), 286.0 (14), 257.0 (2), 229.0 (5), 213.0 (2)	259-286	KIGVXRGRNLQNNI-UHFFFAOYSA-N	B

[a]: "Error medio de masa exacta para los modos de adquisición ESI negativo y positivo."; [b]: fragmentación en fuente; UV/Vis: Absorbancia máxima; InChI-Key: Identificador internacional de la IUPAC para sustancias químicas según PubChem; Nivel de identificación (A-D): A–*standard*, B–MS/MS, C–MS^E, D–MS; I, II: compuestos isobáricos con espectro MS/MS similar; n.d.: no detectado.

2.3. Supplementary data 3: Application of the ecological niche centrality hypothesis to evaluate the chemical composition and biological activity in the leaves of *Eucryphia cordifolia* Cav (Cunoniaceae).

Table S3.1: Metabolic profile by UHPLC-DAD-QTOF-MS/MS of *E. cordifolia* leaves in negative ionization mode (-ES). The populations of *E. cordifolia* with respect to their ecological niche were categorized as follows: A) Coronel B) Contulmo C) La Unión D) Puerto Montt

Nº	Rt (min)	Putative metabolite name	Metabolite class	Mol formula	ESI (-) Theor m/z	ESI (-) Found m/z	m/z error (ppm)[a]	MS/MS ESI (-) fragments (int. %)	UV/Vis (nm)	InChI-Key	Ident. level (A-D)	Populations *E. cordifolia*
Summer												
1	1.33	Quinic acid	Cyclitol carboxylic acid	$C_7H_{12}O_6$	191.0561	191.0558 $[M-H]^-$	1.41	191.0567, 127.0411, 173.0458, 111.0465	203	AAWZDTNXLSGCEK-ZHQZDSKASA-N	B	A, B, C and D
2	1.97	Glucogallin	Tanins	$C_{13}H_{16}O_{10}$	331.0671	331.0672 $[M-H]^-$	0.37	331.0674, 169.0144, 271.0458	205	GDVRUDXLQBVIKP-HQHREHCSSA-N	B	A, B and C
3	4.94	Quercetin hexoside	Flavonols	$C_{21}H_{20}O_{12}$	463.0881	463.0905 $[M-H]^-$	0.37	463.0871, 271.0259, 301.0349	205-328	GDVRUDXLQBVIKP-HQHREHCSSA-N	B	A, B, C and D
4	5.6	Procyanidin B1 isomer	Flavanols	$C_{30}H_{26}O_{12}$	577.1351	577.1348 $[M-H]^-$	0.58	289.0739, 425.0902, 577.1379	204	XFZJEEAOWLFHDH-NFJBMHMQSA-N	A	A, B, C and D
5	6	Procyanidin B1 isomer	Flavanols	$C_{30}H_{26}O_{12}$	577.1351	577.1363 $[M-H]^-$	0.52	425.0897, 289.0734, 577.1381	204-275	XFZJEEAOWLFHDH-NFJBMHMQSA-N	A	A, B, C and D

6	6	Caffeoylglucoside isomer	Cinnamic acid derivates	$C_{15}H_{18}O_9$	341.0878	341.0900 $[M-H]^-$	1.15	135.0460, 179.0364, 341.0882	205-274	WQSDYZZEIBAPIN-VBQORRLJSA-N	B	B and C
7	6.3	Gambiriin	Flavanols	$C_{30}H_{30}O_{13}$	579.1507	579.1535 [M-H-H2O]-	0.53	289.0741, 245.0840, 203.0726	202-204-230	UNSZUCUHDNOPMN-FJPKCJJDSA-N	B	A, B, C and D
8	6.3	Catechin	Flavanols	$C_{15}H_{16}O_7$	289.0717	289.0723 $[M-H]^-$	1.99	245.0838, 289.0738	204-279	OFUMQWOJBVNKLR-NQQJLSKUSA-N	A	A, B, C and D
9	6.47	Ethyl-5-octyl-2.2-dioxo-1.3.2-dioxathiolane-4-carboxylate	Sulfonate	$C_{13}H_{24}O_6S$	307.1221	307.1217 $[M-H]^-$	1.41	307.1204, 96.9536	250	HWYWSWKEJSIOBK-UHFFFAOYSA-N	B	A, B, C and D
10	6.5	Pseudoplacodiolic acid	Dibenzofurans	$C_{19}H_{20}O_8$	375.1085	375.1081 $[M-H]^-$	1.29	307.1207, 96.9590, 167.0370, 308.1203	207	HCSONWDCGXFSJK-UHFFFAOYSA-N	D	A, C and D
11	6.9	Unidentified	Unidentified	n.d	n.d	439.1814 $[M-H]^-$	n.d	393.1794, 163.0625, 205.0745, 265.0927	209	n.d	n.d	A
12	7.3	7-Megaestigmene-3,6,9-triol hexoside	Cyclohexan sesquiterpene glycoside	$C_{19}H_{34}O_8$	435.2236	435.2236 [M + HCOOH - H]-	0.1	435.2271, 389.2211, 161.0465	278	MRPDHXXPDCVBPQ-AATRIKPKSA-N	B	C and D
13	7.4	Unidentified	n.d	n.d	n.d	431.1939 $[M-H]^-$	n.d	179.0577, 431.1924, 225.0642, 432.1952	209-270	n.d	n.d	A, B, C and D
14	8.12	Taxifolin hexoside	Flavanones	$C_{21}H_{22}O_{12}$	465.1038	465.1031 $[M-H]^-$	0.12	285.0409, 151.0040, 465.1033	205-284	BBFYUPYFXSSMNV-HMGRVEAOSA-N	B	A, B, C and D

15	8.44	Unidentified	n.d	n.d	n.d	453.1789 $[M-H]^-$	n.d	453.1827, 454.1848, 96.9602, 273.1181	209-280	n.d	n.d.	A
16	8.49	Procyanidin B1	Flavanols	$C_{30}H_{26}O_{12}$	577.1351	577.133 $[M-H]^-$	0.6	289.0693, 125.0241, 577.1337	210-280	XFZJEEAOWLFHDH-NFJBMHMQSA-N	A	A, B, C and D
17	8.89	Taxifolin pentoside	Flavanones	$C_{20}H_{20}O_{11}$	435.0933	435.0927 $[M-H]^-$	1.28	151.0034, 285.0404, 435.0933, 303.0510	290	UKSPRKDZNYSFRL-ARLBNVOWSA-N	B	A, B, C and D
18	8.95	Persicarin	Sulfated	$C_{16}H_{12}O_{10}S$	395.0078	395.0095 $[M-H]^-$	0.08	330.0401, 287.0196, 271.0255, 299.0199	206-280	UZMAPBJVXOGOFT-UHFFFAOYSA-N	B	A, B, C and D
19	9.85	Quercetin-hexoside	Flavonol	$C_{21}H_{20}O_{12}$	463.0881	463.0879 $[M-H]^-$	0.69	463.0873, 271.025, 301.0350	205-354	OVSQVDMCBVZWGM-QSOFNFLRSA-N	B	B, C and D
20	9.97	Astilbin isomer	Flavanone	$C_{21}H_{22}O_{11}$	449.1089	449.1087 $[M-H]^-$	0.63	303.0527, 151.0044, 285.0421, 449.1122	291	ZROGCCBNZBKLEL-MPRHSVQHSA-N	B	A, B, C and D
21	10.01	Dimethoxy apigenin sulfonic acid	Flavone Sulfonate	$C_{17}H_{14}O_{10}S$	409.0235	409.0233 $[M-H]^-$	0.44	329.0675, 271.0246, 409.0248	202-289	WHUWTHLRYAPDIX-UHFFFAOYSA-N	B	A, B, C and D
22	10.15	Astilbin isomer	Flavanone	$C_{21}H_{22}O_{11}$	449.1089	449.1063 $[M-H]^-$	2.55	151.0045, 285.0416, 303.0515, 449.1108	202-289	ZROGCCBNZBKLEL-MPRHSVQHSA-N	B	A, B, C and D
23	10.45	Quercetin pentoside	Flavonols	$C_{20}H_{18}O_{11}$	433.0776	433.0773 $[M-H]^-$	0.66	433.0787, 271.0258, 301.0345	205-354	PZZRDJXEMZMZFD-UHFFFAOYSA-N	B	A, B, C and D

24	10.75	Unidentified	n.d.	n.d	n.d	449.1092 $[M-H]^-$	n.d	151.0036, 285.0398, 303.0501, 449.1072	205-289	n.d	n.d	A, B, C and D
25	10.8	Quercetin-rhamnoside	Flavonols	$C_{21}H_{20}O_{11}$	447.0932	447.0937 $[M-H]^-$	2.55	447.0942, 301.0358, 271.0253	205-255-348	OXGUCUVFOIWWQJ-HQBVPOQASA-N	A	A, B, C and D
26	11.1	Unidentified	n.d	n.d	n.d	433.115 $[M-H]^-$	n.d	433.1145, 152.0116, 269.0461, 179.0005ç	217-285	n.d	B	A, B, C and D
27	11.35	Persicarin	Sulfated	$C_{16}H_{12}O_{10}S$	395.0078	395.0078 $[M-H]^-$	0.16	271.0259	217-250	CZFNXFXZXWDYMZ-UHFFFAOYSA-N	B	A, B and C
28	11.73	Kaempferol rhamnoside	Flavonols	$C_{21}H_{20}O_{10}$	431.0984	431.0983 $[M-H]^-$	0.1	285.0415, 255.0304, 431.0991, 227.0358	264	SOSLMHZOJATCCP-AEIZVZFYSA-M	B	A, B, C and D
29	11.9	Laricitrin hexoside	Flavonols	$C_{22}H_{22}O_{13}$	493.0987	493.1003 $[M-H]^-$	0.03	331.0466, 316.0232, 493.1006	217-340	ODXINVOINFDDDD-CLXWZIMCSA-N	B	A, B and C
30	11.96	Isorhamnetin - hexoside	Flavonols	$C_{22}H_{22}O_{12}$	477.1038	477.1059 $[M-H]^-$	0.62	300.0287, 315.0536, 477.1074	217-360	CQLRUIIRRZYHHS-LFXZADKFSA-N	B	A, B and C
31	12.68	Unidentified	n.d	n.d	n.d	585.2341 $[M-H]^-$	n.d	345.1340, 330.1102, 585.2354, 586.2390	217-280	n.d	n.d	A, B, C and D
32	14.77	Procyanidin B isomer	Flavanols	$C_{30}H_{26}O_{12}$	577.1351	577.1345 $[M-H]^-$	1.15	269.0461, 577.1361, 145.0296	220	XFZJEEAOWLFHDH-UKWJTHFESA-N	B	A, B, C and D

Autumn

1	1.29	Quinic acid	Cyclitol carboxylic acid	$C_7H_{12}O_6$	192.0633	191.0559 [M-H]-	0.86	191.0562, 127.0396, 173.0453	202, 204, 208, 212, 240	AAWZDTNXLSGCEK-WYWMIBKRSA-N	B	A, B, C and D
2	5.52	Procyanidin B1 isomer	Flavanols	$C_{30}H_{26}O_{12}$	578.1424	577.1347 [M-H]-	0.48	289.0715, 425.0878, 577.1333	202-270	XFZJEEAOWLFHDH-UKWJTHFESA-N	A	A, B, C and D
3	5.9	Digalloylhexose	Tannins	$C_{20}H_{20}O_{14}$	483.078	483.0799 [M-H]-	0.28	131.0729, 483.0786, 211.0267	204-270	YCSGOZQKYXSHOY-UHFFFAOYSA-N	B	C
4	6.2	Catechin	Flavanols	$C_{15}H_{16}O_7$	289.0717	289.0723 [M-H]-	1.18	289.0744, 245.0825	203-278	OFUMQWOJBVNKLR-NQQJLSKUSA-N	A	A, B, C and D
5	6.24	Gambiriin	Flavanols	$C_{30}H_{28}O_{12}$	579.1579	579.1504 [M-H]-	0.17	289.0727, 245.0828, 203.0828	203-278	OFUMQWOJBVNKLR-NQQJLSKUSA-N	B	A, B, C and D
6	6.4	Ethyl-5-octyl-2.2-dioxo-1.3.2-dioxathiolane-4-carboxylate	Sulfated	$C_{13}H_{24}O_6S$	307.122	307.1216 [M-H]-	1.57	307.1230, 96.9613	205-270	HWYWSWKEJSIOBK-UHFFFAOYSA-N	B	A, B, C and D
7	6.9	Unidentified	n.d	n.d.	n.d.	439.1086 [M-H]-	n.d.	393.1761, 163.0616, 205.0706, 265.0900	213-280	n.d.	n.d.	A
8	7.08	Unidentified	n.d	n.d.	n.d.	435.2258 [M-H]-	n.d.	161.0469, 188.0636, 389.2177, 121.0414	212-277	n.d.	n.d.	C and D
9	7.33	Unidentified	n.d	n.d.	n.d.	431.1914 [M-H]-	n.d.	179.0573, 431.1938, 119.0350, 432.1934	213-278	n.d.	n.d.	A, B, C and D

10	7.41	Unidentified	n.d	n.d.	n.d.	461.1669	[M-H]-	n.d.	415.1613, 269.1034, 416.1635, 161.0457	216-280	n.d.	n.d.	A, B, C and D
11	8.81	Unidentified	n.d	n.d.	n.d.	303.0504	[M-H]-	n.d.	216.1234, 217.1244, 130.0875, 178.9954	202-290	n.d.	n.d.	A, B and D
12	8.81	Taxifolin pentoside	Flavanones	$C_{20}H_{20}O_{11}$	435.0933	435.0940	[M-H]-	1.14	151.0331, 285.0405, 435.0933, 303.0514	202-297	UKSPRKDZNYSFRL-ARLBNVOWSA-N	B	A, B, C and D
13	9.69	Quercetin hexoside	Flavonols	$C_{21}H_{20}O_{12}$	463.0881	463.0881	[M-H]-	0.82	463.0873, 271.0245, 301.0334	204-255-354	OVSQVDMCBVZWGM-QSOFNFLRSA-N	B	A, B, C and D
14	9.8	Astilbin isomer	Flavanones	$C_{21}H_{22}O_{11}$	449.1089	449.1078	[M-H]-	1.09	303.0509, 151.0039, 285.0404, 449.1087	203-291	UKSPRKDZNYSFRL-ARLBNVOWSA-N	B	A, B, C and D
15	10.1	Astilbin isomer	Flavanones	$C_{21}H_{22}O_{12}$	450.1089	449.1078	[M-H]-	210	151.0036, 285.0403, 303.0513, 449.1090	201-290	UKSPRKDZNYSFRL-ARLBNVOWSA-N	B	A, B, C and D
16	10.38	Quercetin pentoside	Flavonols	$C_{20}H_{18}O_{11}$	433.0777	433.0764	[M-H]-	1.76	300.0270, 433.0767, 271.0241, 301.0328, 255.0297, 243.0301	212-350	PZZRDJXEMZMZFD-BWYUNELBSA-N	B	A, B, C and D
17	10.6	Astilbin isomer	Flavanones	$C_{21}H_{22}O_{11}$	449.1089	449.1081	[M-H]-	0.47	151.0035, 285.0397, 303.0506, 449.1095	216-290	UKSPRKDZNYSFRL-ARLBNVOWSA-N	B	A, C and D
18	10.72	Quercetin-rhamnoside	Flavonols	$C_{21}H_{20}O_{11}$	447.0932	447.0925	[M-H]-	2.54	447.0921, 301.0341, 271.0236	205-255-349	OXGUCUVFOIWWQJ-HQBVPOQASA-N	A	A, B, C and D

19	11	Unidentified	n.d	n.d.	n.d.	433.1139	[M-H]-	n.d.	433.1136, 152.0116, 269.0456, 178.9989	219-287	n.d.	n.d.	A, B, C and D
20	11.4	Unidentified	n.d	n.d.	n.d.	435.1301	[M-H]-	n.d.	273.0762, 437.0992, 269.0402, 386.9846	218-350	n.d.	n.d.	A, B and C
21	11.41	Isorhamnetin - hexoside	Flavonols	$C_{22}H_{22}O_{12}$	447.1038	477.1048	[M-H]-	1.66	315.0510, 300.0255	218-350	CQLRUIIRRZYHHS-LFXZADKFSA-N	B	A, B and C
22	11.65	Kaempferol rhamnoside	Flavonols	$C_{21}H_{20}O_{10}$	431.1056	431.0983	[M-H]-	0.7	285.0385, 227.0340, 255.0282, 431.0974	218-350	SOSLMHZOJATCCP-AEIZVZFYSA-N	B	A, B, C and D
23	11.65	Unidentified	n.d	n.d.	n.d.	499.0858	[M-H]-	n.d.	431.0984, 285.0401, 284.0323, 432.0953	219-346	n.d.	n.d.	A, B, C and D
24	11.9	Laricitrin hexoside	Flavonols	$C_{22}H_{22}O_{13}$	493.0987	493.0992	[M-H]-	1.9	331.0457, 316.0237, 493.0984	218-360	ODXINVOINFDDDD-CLXWZIMCSA-N	B	A
25	14.38	Unidentified	n.d	n.d.	n.d.	673.3424	[M-H]-	n.d.	209.1170, 227.1278, 210.1220, 445.2059	221	n.d.	n.d.	A, B, C and D
26	14.7	Procyanidin B isomer	Flavanols	$C_{30}H_{26}O_{12}$	578.1351	577.1336	[M-H]-	1.2	269.0447, 145.0292, 577.1334	220-340	XFZJEEAOWLFHDH-UKWJTHFESA-N	B	A, B, C and D
						Spring							
1	1.4	Quinic acid	Cyclitol carboxylic acid	$C_7H_{12}O_6$	191.0561	191.0560	[M-H]-	0.66	191.0560, 127.0400, 173.0458	205	AAWZDTNXLSGCEK-ZHQZDSKASA-N	B	A, B, C and D

2	2.07	Glucogallin	Tanins	$C_{13}H_{16}O_{10}$	331.067	331.0663 [M-H]-	0.76	331.0668, 169.0136, 271.0459	212-279	GDVRUDXLQBVIKP-HQHREHCSSA-N	B	B and C
3	5.78	Procyanidin B1 isomer	Flavanols	$C_{30}H_{26}O_{12}$	577.1351	577.1351 [M-H]-	0.54	289.0725, 425.0883, 577.1342	202-279	XFZJEEAOWLFHDH-NFJBMHMQSA-N	A	A, B, C and D
4	6.19	Procyanidin B1 isomer	Flavanols	$C_{30}H_{26}O_{12}$	577.1351	577.1346 [M-H]-	0.44	425.0873, 289.0713, 577.1353	204-270	XFZJEEAOWLFHDH-NFJBMHMQSA-N	A	A, B, C and D
5	6.52	Catechin	Flavanols	$C_{15}H_{14}O_6$	289.0717	289.0711 [M-H]-	1.3	289.0715, 245.0811	203-279	OFUMQWOJBVNKLR-NQQJLSKUSA-N	A	A, B, C and D
6	6.52	Gambiriin	Flavanols	$C_{30}H_{30}O_{13}$	579.1507	579.1499 $[M-H-H2O]^-$	0.2	289.0717, 245.0820, 203.0711	203-279	UNSZUCUHDNOPMN-FJPKCJJDSA-N	B	A, B, C and D
7	6.67	Ethyl-5-octyl-2.2-dioxo-1.3.2-dioxathiolane-4-carboxylate	Sulfated	$C_{13}H_{24}O_6S$	307.122	307.1222 [M-H]-	0.94	307.112, 96.9609	207-280	HWYWSWKEJSIOBK-UHFFFAOYSA-N	B	A, B, C and D
8	7.11	Unidentified	n.d	n.d	n.d	439.1823 [M-H]-	n.d	394.1818, 163.0568, 393.1752	207	n.d	n.d	A and D
9	7.33	Unidentified	n.d	n.d	n.d	435.2223 [M-H]-	n.d	435.2222, 389.2174, 161.0450, 390.2149	205-280	n.d	n.d	C and D
10	7.6	Unidentified	n.d	n.d	n.d	431.1913 [M-H]-	n.d	179.0572, 431.1958, 225.0636, 119.0361	207-270	n.d	n.d	A, B, C and D
11	7.66	Unidentified	n.d	n.d	n.d	461.1669 [M-H]-	n.d	415.1641, 269.1073, 416.1474, 461.1630	207-280	n.d	n.d	A, B, C and D

12	8.3	Taxifolin hexoside	Flavanones	$C_{21}H_{22}O_{12}$	465.1038	465.1039	[M-H]-	0.25	151.0039, 285.0408, 465.1028	205-280	BBFYUPYFXSSMNV-HMGRVEAOSA-N	B	A, B, C and D
13	8.66	Procyanidin B1 isomer	Flavanols	$C_{30}H_{26}O_{12}$	577.1351	577.1344	[M-H]-	0.23	289.0687, 425.0818	204-280	XFZJEEAOWLFHDH-NFJBMHMQSA-N	A	A, B, C and D
14	9.08	Taxifolin pentoside	Flavanones	$C_{20}H_{20}O_{11}$	435.0933	435.0927	[M-H]-	0.47	151.0038, 285.0409, 435.0934, 303.0502	202-289	UKSPRKDZNYSFRL-ARLBNVOWSA-N	B	A, B, C and D
15	9.94	Quercetin-hexoside	Flavonols	$C_{21}H_{20}O_{12}$	463.0881	463.0876	[M-H]-	0.09	463.0877, 271.0245, 301.0335	204-354	OVSQVDMCBVZWGM-QSOFNFLRSA-N	A	A, B, C and D
16	10.15	Astilbin isomer	Flavanones	$C_{21}H_{22}O_{11}$	449.1089	449.1096	[M-H]-	1.49	151.0039, 285.0421, 449.1099, 303.0545	210-280	ZROGCCBNZBKLEL-MPRHSVQHSA-N	B	A, B, C and D
17	10.34	Astilbin isomer	Flavanones	$C_{21}H_{22}O_{11}$	450.1089	449.1087	[M-H]-	1.27	151.0039, 285.0408, 303.0514, 449.1092	202-289	ZROGCCBNZBKLEL-MPRHSVQHSA-N	B	A, B, C and D
18	10.64	Quercetin pentoside	Flavonols	$C_{20}H_{18}O_{11}$	433.077	433.0772	[M-H]-	0.75	433.0777, 271.0245, 301.0339	207-354	PZZRDJXEMZMZFD-UHFFFAOYSA-N	B	A, B, C and D
19	10.92	Astilbin isomer	Flavanones	$C_{21}H_{22}O_{11}$	449.1089	449.1091	[M-H]-	3.26	151.0038, 285.0399, 303.0515, 449.1093	205-288	ZROGCCBNZBKLEL-MPRHSVQHSA-N	B	A, C and D
20	10.97	Quercetin-rhamnoside	Flavonols	$C_{21}H_{20}O_{11}$	447.0932	447.0925	[M-H]-	2.37	447.0925, 301.0341, 271.0247	204-255-349	OXGUCUVFOIWWQJ-HQBVPOQASA-N	A	A, B, C and D

21	11.3	Unidentified	n.d	n.d	n.d	433.1140	[M-H]-	n.d	433.1135, 152.0115,269.0458, 178.9990	216-280	n.d	n.d	A, B, C and D
22	11.54	Persicarin	Sulfonate	$C_{16}H_{12}O_{10}S$	395.0078	395.0080	[M-H]-	0.62	271.0256	215	CZFNXFXZXWDYMZ-UHFFFAOYSA-N	B	A, B and C
23	11.9	Kaempferol rhamnoside	Flavonols	$C_{21}H_{20}O_{10}$	431.0984	431.0983	[M-H]-	0.57	285.0402, 431.0978, 255.0307, 227.0346	216-250	SOSLMHZOJATCCP-AEIZVZFYSA-M	B	A, B, C and D
24	12.13	Isorhamnetin - hexoside	Flavonols	$C_{22}H_{22}O_{12}$	477.1037	477.1041	[M-H]-	0.32	300.0286, 315.0516, 477.1084	216-350	CQLRUIIRRZYHHS-LFXZADKFSA-N	B	A, B and C
25	12.86	Unidentified	n.d	n.d	n.d	585.2329	[M-H]-	n.d	n.d	n.d	n.d	n.d	A, B, C and D
26	13.82	Unidentified	n.d	n.d	n.d	603.3223	[M-H]-	n.d	603.3202, 604.3242, 605.3189,	218	n.d	n.d	A and D
27	14.59	Unidentified	n.d	n.d	n.d	673.3428	[M-H]-	n.d	209.1183, 209.1537, 210.1255, 227.1279	220-280	n.d	n.d	A, C and D
28	15	Procyanidin B isomer	Flavanols	$C_{30}H_{26}O_{12}$	577.1351	577.1314	[M-H]-	1.46	577.1357, 269.0444, 145.0312	219-330	XFZJEEAOWLFHDH-NFJBMHMQSA-N	B	A, B, C and D

Table S3.2: Metabolic profile by UHPLC-DAD-QTOF-MS/MS of *E. cordifolia* leaves in positive ionization mode (+ES). The populations of *E. cordifolia* with respect to their ecological niche were categorized as follows: A) Coronel B) Contulmo C) La Unión D) Puerto Montt.

N°	Rt (min)	Putative metabolite name	Metabolite class	Mol formula	ESI (+) Theor m/z	ESI (+) Found m/z	m/z error (ppm)[a]	MS/MS ESI (-) fragments (int. %)	UV/Vis (nm)	InChI-Key	Ident. level (A-D)	Populations *E. cordifolia*
Summer												
1	1.27	Unidentified	n.d	n.d	n.d	381.0779 $[M+H]^+$	n.d	381.0834	203, 207	n.d	n.d	A, B, C and D
2	5.7	Procyanidin B1 isomer	Flavanols	$C_{30}H_{26}O_{12}$	579.1499	579.1463 $[M+H]^+$	0.3	127.038, 289.068, 409.0866, 2710625	278	XFZJEEAOWLFHDH-NFJBMHMQSA-N	A	A, B, C and D
3	6.1	Procyanidin B1 isomer	Flavanols	$C_{30}H_{26}O_{12}$	579.1497	579.1475 $[M+H]^+$	0.29	127.0368, 139.0402, 191.0319, 201.0528	206	XFZJEEAOWLFHDH-NFJBMHMQSA-N	A	A, B, C and D
4	6.42	Catechin	Flavanols	$C_{15}H_{14}O_6$	291.0863	291.0853 $[M+H]^+$	1.68	139.0363, 123.0418, 147.0421, 119.0491	203, 279	PFTAWBLQPZVEMU-UKRRQHHQSA-N	A	A, B, C and D
5	6.65	Procyanidin C isomer.	Flavanols	$C_{45}H_{38}O_{18}$	867.213	867.2074 $[M+H]^+$	1.45	289.0657, 579.1448		MOJZMWJRUKIQGL-XILRTYJMSA-N	B	A, B, C and D
6	7.02	Unidentified	n.d	n.d	n.d	417.1715 $[M+H]^+$	n.d	417.1715	208	n.d	n.d	A
7	7.39	Unidentified	n.d	n.d	n.d	413.2109 $[M+H]^+$	n.d	413.2109	209	n.d	n.d	C and D
8	7.5	Unidentified	n.d	n.d	n.d	409.1781 $[M+H]^+$	n.d	409.1781	209	n.d	n.d	D

9	7.89	Unidentified	n.d	n.d	n.d	147.0416 [M+H]+	n.d	147.0417	207, 283, 310	n.d	n.d	B and C
10	8.18	Procyanidin C isomer.	Flavanols	$C_{45}H_{38}O_{18}$	867.213	867.2099 [M+H]+	1.21	289.0693, 287.0443, 579.1429	204, 279	MOJZMWJRUKIQGL-XILRTYJMSA-N/MOJZMWJRUKIQGL-XILRTYJMSA-N	B	A, B and C
11	8.57	Procyanidin B1 isomer	Flavanols	$C_{30}H_{26}O_{12}$	579.1497	579.1428 $[M+H]^+$	0.31	127.0378, 291.0822, 287.0511, 409.095	205, 280	XFZJEEAOWLFHDH-VUGKQVTMSA-N	B	A, B, C and D
12	8.87	Syringetin hexoside	Flavonol	$C_{23}H_{24}O_{13}$	509.129	509.1291 $[M+H]^+$	0.26	347.0726, 509.1243, 286.0445, 331.0427	209, 278	JMFWYRWPJVEZPV-AVGVHVDKSA-N	B	A and D
13	8.99	Unidentified	n.d	n.d	n.d	305.0664 $[M+H]^+$	n.d.	123.0542, 231.0612, 259.0539, 153.017	201, 290	n.d	n.d	A, B, C and D
14	8.99	Unidentified	n.d	n.d	n.d	459.0888 [M+H]+	n.d.	459.0848, 578.0848, 460.1677, 327.0445	203, 287	n.d	n.d	A and B
15	9.17	Syringetin	Flavonol	$C_{17}H_{14}O_8$	347.0761	347.0767 $[M+H]^+$	0.08	347.0742, 331.048, 286.0309	210, 276, 356	KIGVXRGRNLQNNI-UHFFFAOYSA-N	B	A, C and D
16	9.66	Tricin-*O*-hexoside	Flavone	$C_{23}H_{24}O_{12}$	493.134	493.1325 $[M+H]^+$	0.35	331.0775, 493.1325	213, 340	FLSOTPIEFVBPBU-LDBVRRDLSA-N	B	A
17	9.9	Quercetin hexoside	Flavonol	$C_{21}H_{20}O_{12}$	465.1028	465.1037 $[M+H]^+$	0.69	303.0477, 304.0530, 257.0475, 121.0266	205	OVSQVDMCBVZWGM-QSOFNFLRSA-N	B	C and D

18	10.24	Unidentified	n.d	n.d	n.d	305.0668 $[M+H]^+$	1.27	123.0399, 128.0674, 129.0715, 149.0226	205	n.d.	n.d.	A, B, and D
19	10.24	Astilbin isomer	Flavanone	$C_{21}H_{22}O_{11}$	451.1234	451.1223 [M+H]+	3.1	305.0649, 129.0535, 231.0637, 259.058	203, 288	ZROGCCBNZBKLEL-MPRHSVQHSA-N	B	A, C and D
20	10.54	Quercetin	Flavonol	$C_{15}H_{10}O_7$	303.058	303.058 $[M+H]^+$	1.06	303. 0435, 115.525, 303.1148	206, 354	REFJWTPEDVJJIY-UHFFFAOYSA-N	B	D
21	10.55	Quercetin pentoside	Flavonol	$C_{20}H_{18}O_{11}$	435.0921	435.0896 [M+H]+	2.1	303.0476, 304.0493, 257.0429, 137.0178	207, 354	PZZRDJXEMZMZFD-UHFFFAOYSA-N	B	C and D
22	10.88	Quercetin-rhamnoside	Flavonol	$C_{21}H_{20}O_{11}$	449.1078	449.1091 $[M+H]^+$	2.89	303.0481, 304.0511, 129.0531, 257.0423	204, 255, 349	OXGUCUVFOIWWQJ-HQBVPOQASA-N	A	A, B, C and D
23	10.98	Cirsiliol	Flavone	$C_{17}H_{14}O_7$	331.0812	331.0787 $[M+H]^+$	2.22	331.0783, 270.05, 316.0544	210, 348	IMEYGBIXGJLUIS-UHFFFAOYSA-N	B	A, B and D
24	11.81	Luteolin	Flavone	$C_{15}H_{10}O_6$	287.055	287.055 $[M+H]^+$	3.19	287.056	216, 265, 356	IYRMWMYZSQPJKC-UHFFFAOYSA-N	B	A,B and D
25	12.1	Isorhamnetin - hexoside	Flavonol	$C_{22}H_{22}O_{12}$	479.1184	479.1165 $[M+H]^+$	0.59	302.0403, 317.0646, 274.0463	216, 280	CQLRUIIRRZYHHS-LFXZADKFSA-N	B	A,B,C and D
26	12.1	Laricitrin hexoside	Flavonol	$C_{22}H_{22}O_{13}$	495.1133	495.1103 $[M+H]^+$	1.3	333.0567, 495.1048, 318.0345, 319.0378	217, 350	ODXINVOINFDDDD-CLXWZIMCSA-N	B	A, C and D
27	12.8	Unidentified	n.d	n.d	n.d	609.2247 $[M+H]^+$	n.d	609.2293, 610.2295	n.d	n.d	n.d	A, B, C and D

28	14.9	Procyanidin B. isomer	Flavanols	$C_{30}H_{26}O_{12}$	579.1497	579.1475 $[M+H]^+$	1.23	271.0584, 272.062, 579.1320, 273.0940	220, 330	XFZJEEAOWLFHDH-UKWJTHFESA-N	B	A and B
Autumn												
1	1.21	Unidentified	n.d	n.d.	n.d.	381.0936 $[M+H]^+$	n.d.	381.0998, 201.0554, 1024.0644	215	n.d.	n.d.	A, B, C and D
2	1.21	Unidentified	n.d	n.d.	n.d.	543.1507 $[M+H]^+$	n.d.	543.1516, 544.1527, 354,6118, 245.0653	215	n.d.	n.d.	A, B, C and D
3	2.83	Unidentified	n.d	n.d.	n.d.	311.0782 $[M+H]^+$	n.d.	311.0738, 312.0778	205, 260	n.d.	n.d.	A, B, C and D
4	4.4	Unidentified	n.d	n.d.	n.d.	447.1076 $[M+H]^+$	n.d.	123.0458, 401.0932, 429.0961, 430.0993	201-280	n.d.	n.d.	C
5	4.82	Quercetin hexoside	Flavonol	$C_{21}H_{20}O_{12}$	465.1027	465.1172 $[M+H]^+$	1.09	123.0466, 313.0645, 465.119, 419.1047	203-278	OVSQVDMCBVZWGM-QSOFNFLRSA-N	B	C
6	5.49	Procyanidin B1 isomer	Flavanols	$C_{30}H_{26}O_{12}$	579.152	579.1593 $[M+H]^+$	3.97	127.0398, 289.0747, 427.1083, 287.0578, 409.1012, 139.0394, 291.0886	201-203-278	XFZJEEAOWLFHDH-NFJBMHMQSA-N	A	A, B, C and D
7	5.89	Procyanidin B1 isomer	Flavanols	$C_{30}H_{26}O_{12}$	579.152	579.1714 $[M+H]^+$	4.15	127.0423, 287.0627, 289.0785, 257.0535, 275.0645	203-280	XFZJEEAOWLFHDH-NFJBMHMQSA-N	A	A, B, C and D

8	6.2	Catechin	Flavanols	C15H14O6	291.0863	291.0853 $[M+H]^+$	5.8	139.0436, 123.0482, 147.0512, 119.0528	203-206-279	PFTAWBLQPZVEMU-UKRRQHHQSA-N	A	A, B, C and D
9	7.72	Syringetin hexoside	Flavonol	$C_{23}H_{24}O_{13}$	509.1289	509.1373 $[M+H]^+$	3.66	347.0809, 314.0431, 286.0513, 348.0789, 331.0504	303-277	JMFWYRWPJVEZPV-AVGVHVDKSA-N	B	A
10	8.02	Unidentified	n.d	n.d.	n.d.	305.0793 $[M+H]^+$	n.d.	123.0595, 259.0657	203-281	n.d.	n.d.	A, B, C and D
11	8.4	Procyanidin B1 isomer	Flavanols	$C_{30}H_{26}O_{12}$	579.1497	579.1716 $[M+H]^+$	4.25	409.1059, 289.0811, 123.0470, 271.0657	203-278	XFZJEEAOWLFHDH-NFJBMHMQSA-N	A	A, B, C and D
12	8.7	Syringetin hexoside	Flavonol	$C_{23}H_{24}O_{13}$	509.1293	509.1362 $[M+H]^+$	5.26	347.0795, 509.1360, 286.0505, 348.0834, 332.0561	203-345	JMFWYRWPJVEZPV-AVGVHVDKSA-N	B	A
13	8.8	Unidentified	n.d	n.d.	n.d.	459.0927 $[M+H]^+$	n.d.	259.0633, 231.0695, 123.0453, 153.0797	203-288	n.d.	n.d	A, B, C and D
14	8.99	Unidentified	n.d.	n.d.	n.d.	347.0817 $[M+H]^+$	n.d.	n.d.	n.d.	.nd	n.d.	A
15	9.22	Tricin-*O*-hexoside	Flavone	$C_{23}H_{24}O_{12}$	493.134	493.1406 $[M+H]^+$	3.19	331.0837, 493.1396, 316.0596	203-277	FLSOTPIEFVBPBU-LDBVRRDLSA-N	B	A
16	9.68	Quercetin hexoside	Flavonol	$C_{21}H_{20}O_{12}$	465.1027	465.1265 $[M+H]^+$	7.44	303.0634, 304.0678, 229.0608	206-255-355	OVSQVDMCBVZWGM-QSOFNFLRSA-N	B	A, B, C and D

17	10.06	Astilbin isomer	Flavonol	$C_{21}H_{22}O_{11}$	451.1234	451.1323 $[M+H]^+$	7.41	305.0715, 129.0753, 231.0697, 259.0653, 287.0612, 287.0612, 147.0690, 149.0263	206-220-289	ZROGCCBNZBKLEL-MPRHSVQHSA-N	B	A, B, C and D
18	10.37	Quercetin pentoside	Flavonol	$C_{20}H_{18}O_{11}$	435.0921	435.115 $[M+H]^+$	7.7	303.0655, 304.0718, 257.0560, 285.0491, 305.0681	203-351	PZZRDJXEMZMZFD-BWYUNELBSA-N	B	A, B, C and D
19	10.7	Quercetin-rhamnoside	Flavonol	$C_{21}H_{20}O_{11}$	449.1078	449.1091 $[M+H]^+$	6.76	303.0646, 304.0685, 129.0614, 229.0614, 257.0560	207-255-350	OXGUCUVFOIWWQJ-HQBVPOQASA-N	A	A, B, C and D
20	10.79	Cirsiliol	Flavone	$C_{17}H_{14}O_7$	331.0787	331.0869 $[M+H]^+$	7.83	331.0844, 270.0546, 316.0604	203-346	IMEYGBIXGJLUIS-UHFFFAOYSA-N	B	A and B
21	11.64	Luteolin	Flavone	$C_{15}H_{10}O_6$	287.055	287.0596 $[M+H]^+$	8.07	287.0557	207-350	IYRMWMYZSQPJKC-UHFFFAOYSA-N	B	A, B, C and D
22	11.64	Unidentified	n.d.	n.d.	n.d.	433.1203 $[M+H]^+$	n.d.	n.d.	n.d.	n.d.	n.d.	A, B, C and D
23	11.88	Isorhamnetin - hexoside	Flavonol	$C_{22}H_{22}O_{12}$	479.1184	479.1264 $[M+H]^+$	5.76	317.0675, 302.0441, 479.1201, 318.0699	206-350	CQLRUIIRRZYHHS-LFXZADKFSA-N	B	A and B
24	11.89	Laricitrin hexoside	Flavonol	$C_{22}H_{22}O_{13}$	495.1133	495.1200 $[M+H]^+$	6.71	333.0670, 318.0436, 495.1224, 334.0700	206, 350	ODXINVOINFDDDD-CLXWZIMCSA-N	B	A

25	12.61	Unidentified	n.d	n.d	n.d	557.2549 $[M+H]^+$	n.d.	167.0731, 211.1014, 347.1563	206, 278	n.d.	n.d.	A, B, C and D
26	14.37	Unidentified	n.d	n.d	n.d	639.3459 $[M+H]^+$	n.d.	477.2930, 211.1376, 207.1221, 411.2098	219, 280	n.d.	n.d.	B
27	14.7	Procyanidin B. isomer	Flavanols	$C_{30}H_{26}O_{12}$	579.1497	579.1580 $[M+H]^+$	3.84	271.0642, 272.0671, 273.0673, 147.0498, 272.2670	219-317	XFZJEEAOWLFHDH-NFJBMHMQSA-N	B	A and B
Spring												
1	1.33	Unidentified	n.d.	n.d.	n.d.	381.0812 $[M+H]^+$	n.d.	381.081	206	n.d.	n.d.	A, B and C
2	5.84	Procyanidin B1	Flavanols	$C_{30}H_{26}O_{12}$	579.1499	579.1519 $[M+H]^+$	0.3	409.0913, 427.0986, 289.0809, 291.0876	203, 279	XFZJEEAOWLFHDH-UKWJTHFESA-N	A	A, B, C and D
3	6.25	Procyanidin B1	Flavanols	$C_{30}H_{26}O_{13}$	579.1498	579.1519 $[M+H]^+$	0.12	427.1039, 289.0751, 127.0421, 409.0952	204	XFZJEEAOWLFHDH-UKWJTHFESA-N	A	A, B and C
4	6.61	Catechin	Flavanols	$C_{15}H_{14}O_6$	291.0863	291.0889 $[M+H]^+$	0.99	139.0406, 123.0435, 147.0488, 119.0478	203, 279	OFUMQWOJBVNKLR-NQQJLSKUSA-N	A	A, B, C and D
5	6.8	Procyanidin C isomer.	Flavanols	$C_{45}H_{38}O_{18}$	867.213	867.2134 $[M+H]^+$	1.87	289.0665, 579.1790, 287.0685	203, 279	MOJZMWJRUKIQGL-XILRTYJMSA-N	B	A, B, C and D
6	7.16	Unidentified	n.d	n.d	n.d	417.1760 $[M+H]^+$	n.d.	417.1695, 418.1751	207, 280	n.d.	n.d.	A
7	7.53	Unidentified	n.d	n.d	n.d	413.2109 $[M+H]^+$	n.d	413.2131	206, 280	n.d	n.d.	C

8	8.72	Procyanidin B1	Flavanols	$C_{30}H_{26}O_{12}$	579.1497	579.1522 $[M+H]^+$	0.33	409.0906, 287.0579, 123.0421, 257.0419	206, 279	XFZJEEAOWLFHDH-UKWJTHFESA-N	A	A, B, C and D
9	9.01	Syringetin hexoside	Flavonol	$C_{23}H_{24}O_{13}$	509.1293	509.1291 $[M+H]^+$	0.62	347.0765, 509.1284, 286.0498	207, 350	JMFWYRWPJVEZPV-AVGVHVDKSA-N	B	A
10	9.14	Unidentified	n.d	n.d	n.d	459.0927 $[M+H]^+$	n.d	459.0934	200, 289	n.d.	n.d.	A, B and D
11	9.14	Unidentified	n.d	n.d	n.d	305.0674 $[M+H]^+$	n.d	123.0449, 153.0207, 259.0887, 259.0603, 167.0344	202, 288	n.d.	n.d.	A, B, C and D
12	9.32	Syringetin	Flavonol	$C_{17}H_{14}O_8$	347.0761	347.0792 $[M+H]^+$	2.01	347.0780, 286.0460, 331.0427	207, 350	KIGVXRGRNLQNNI-UHFFFAOYSA-N	B	A
13	9.53	Tricin-*O*-hexoside	Flavone	$C_{23}H_{24}O_{12}$	493.134	493.137 $[M+H]^+$	1.28	331.0845, 316.0554, 493.1403	208, 280	FLSOTPIEFVBPBU-LDBVRRDLSA-N	B	A
14	10	Quercetin-hexoside	Flavonol	$C_{21}H_{20}O_{12}$	465.1028	465.1037 $[M+H]^+$	3.19	303.0503, 304.0524, 257.0404, 229.0460	205, 255, 353	OVSQVDMCBVZWGM-QSOFNFLRSA-N	B	C and D
15	10	Quercetin	Flavonol	$C_{15}H_{10}O_7$	303.0499	303.0518 [M+H]+	3.31	303.0467	205, 255, 354	REFJWTPEDVJJIY-UHFFFAOYSA-N	A	B, C and D
16	10.13	Unidentified	n.d	n.d	n.d	305.0674 $[M+H]^+$	n.d.	123.0428	206, 350	n.d.	n.d.	A, C and C
17	10.39	Unidentified	n.d	n.d	n.d	305.0689 $[M+H]^+$	n.d.	642.6144, 123.0488, 139.0526, 153.0252	200, 289	n.d.	n.d.	A, B, C and D

18	10.69	Quercetin pentoside	Flavonol	$C_{20}H_{18}O_{11}$	435.0921	435.115 [M+H]+	2.76	303.0509, 304.0546, 257.0437, 274.0446	207, 353	PZZRDJXEMZMZFD-BWYUNELBSA-N	B	C and D
19	10.69	Quercetin	Flavonol	$C_{15}H_{10}O_7$	303.0499	303.0527 $[M+H]^+$	5.18	303.0492	206, 353	REFJWTPEDVJJIY-UHFFFAOYSA-N	B	A, B, C and D
20	11.03	Quercetin-rhamnoside	Flavonol	$C_{21}H_{20}O_{11}$	449.1078	449.1098 $[M+H]^+$	4.09	3030513, 304.0555, 129.0575, 257.0443	206, 255, 349	OXGUCUVFOIWWQJ-HQBVPOQASA-N	B	A, B, C and D
21	11.14	Cirsiliol	Flavone	$C_{17}H_{14}O_7$	331.0812	331.0829 $[M+H]^+$	1.38	331.0813, 270.0517, 316.0570	208, 345	IMEYGBIXGJLUIS-UHFFFAOYSA-N	B	A, B and C
22	11.96	Luteolin	Flavone	$C_{15}H_{10}O_6$	287.055	287.0568 $[M+H]^+$	3.81	287.0596	216, 350	IYRMWMYZSQPJKC-UHFFFAOYSA-N	B	A, B, C and D
23	12.18	Isorhamnetin hexoside	Flavonol	$C_{22}H_{22}O_{12}$	479.1184	479.1188 $[M+H]^+$	1.43	317.0655, 302.0408, 302.0852, 479.1183	216, 370	CQLRUIIRRZYHHS-LFXZADKFSA-N	B	C
24	12.2	Laricitrin hexoside	Flavonol	$C_{22}H_{22}O_{13}$	495.1133	495.1162 [M+H]+	2	333.0606, 318.0356, 495.1151, 334.0628	216, 350	ODXINVOINFDDDD-CLXWZIMCSA-N	B	A and C
25	14.64	Unidentified	n.d	n.d	n.d	697.3441 [M+H]+	n.d	697.3462, 469.2030, 689.3419, 251.1344	219, 280	n.d	n.d.	B
26	14.64	Unidentified	n.d	n.d	n.d	639.338 [M+H]+	n.d	105.0861, 478.3205, 193.1241, 211.1288	219, 280	n.d	n.d.	B

27	14.99	Procyanidin B isomer	Flavanols	$C_{30}H_{26}O_{13}$	579.1497	579.1513 $[M+H]^+$	1.37	271.0607, 272.0661, 273.0661, 147.0429	218,350	XFZJEEAOWLFHDH-UKWJTHFESA-N	B	A and B

Table S3.3: Analysis of variance (ANOVA) to evaluate the effect of the position of *E. cordifolia* populations in their ecological niche (Coronel, Contulmo, La Unión and Puerto Montt) and seasonality (summer, autumn and spring) on antioxidant activity and polyphenol content by means of four spectrophotometric methods (DPPH, ABTS, ORAC and Folin-Ciocalteu).

Antioxidant methods	Variable	*gl*	*F*	*p*
DPPH	Population	3	60.54	< 0.001
	Season	2	149.96	< 0.001
	Population : Season	6	135.01	< 0.001
ABTS	Population	3	80.12	< 0.001
	Season	2	10.64	< 0.001
	Population : Season	6	16.02	< 0.001
ORAC	Population	3	42.10	< 0.001
	Season	2	35.20	< 0.001
	Population : Season	6	17.73	< 0.001
Folin-Ciocalteu	Population	3	30.33	< 0.001
	Season	2	9.16	< 0.01
	Population : Season	6	2.59	< 0.1

Table S3.4: Inhibition of bacterial growth from *E. cordifolia* extracts using the agar agar well diffusion method. Results expressed according to Gaudana et al. (2010).

Season		**Summer**			**Autumn**			**Spring**		
		Concentrations mg/mL								
Microorganism	Population	36	16	8	36	16	8	36	16	8
E. coli 25922	Coronel	+++	+++	++	+++	+++	+++	+++	+++	+++
	Contulmo	+++	+++	+++	+++	+++	+++	+++	+++	+++
	La Unión	+++	+++	+++	+++	+++	+++	+++	+++	+++
	Puerto Montt	+++	+++	+++	+++	+++	+++	+++	+++	+++
S. aureus 6538-p	Coronel	+++	+++	+++	+++	+++	+++	+++	+++	+++
	Contulmo	+++	+++	+++	+++	+++	++	+++	+++	+++
	La Unión	+++	+++	+++	+++	+++	+++	+++	+++	+++
	Puerto Montt	+++	+++	+++	+++	+++	+++	+++	+++	+++
P. aeruginosa 27853	Coronel	+++	+++	+++	+++	+++	+++	+++	+++	+++
	Contulmo	+++	+++	+++	+++	+++	+++	+++	+++	+++
	La Unión	+++	+++	+++	+++	+++	+++	+++	+++	+++
	Puerto Montt	+++	+++	+++	+++	+++	+++	+++	+++	+++
C. albicans 90028	Coronel	++	(+/-)	(+/-)	++	(+/-)	(+/-)	(+/-)	(+/-)	(+/-)
	Contulmo	++	(+/-)	(+/-)	++	(+/-)	(+/-)	++	(+/-)	(+/-)
	La Unión	++	(+/-)	(+/-)	(+/-)	(+/-)	(+/-)	(+/-)	(+/-)	(+/-)
	Puerto Montt	+	(+/-)	(+/-)	++	(+/-)	(+/-)	(+/-)	(+/-)	(+/-)
C. glabrata 90030	Coronel	++	(+/-)	(+/-)	+++	++	(+/-)	+++	++	(+/-)
	Contulmo	+++	++	(+/-)	++	(+/-)	(+/-)	+++	(+/-)	(+/-)
	La Unión	+++	++	(+/-)	+++	++	(+/-)	+++	(+/-)	(+/-)
	Puerto Montt	+++	(+/-)	(+/-)	+++	++	(+/-)	++	++	(+/-)

Table S3.5: Antimicrobial activity of *E. cordifolia* extracts, with MBC values (mg/ml) obtained in different environmentally different populations (ecological niche) and in three different seasons of the year (summer, autumn and spring) against Gram-negative bacteria *E. coli* and *P. aeruginosa*, Gram-positive bacteria *S. aureus* and yeasts such as *C. albicans* and *C. glabrata*. Values expressed in mg/mL.

Season	**Population**	***E. coli***	***S. aureus***	***P. aeruginosa***	***C. albicans***	***C. glabrata***
Summer	Coronel	>5.33	5.33	1.3	<0.66	1.3
Summer	Contulmo	>5.33	5.33	1.3	<0.66	1.3
Summer	La Unión	>5.33	5.33	1.3	<0.66	1.3
Summer	Puerto Montt	>5.33	5.33	1.3	<0.66	0.66
Autumn	Coronel	>5.33	5.33	1.3	<0.66	1.3
Autumn	Contulmo	>5.33	5.33	1.3	<0.66	1.3
Autumn	La Unión	>5.33	5.33	1.3	<0.66	2.66
Autumn	Puerto Montt	>5.33	5.33	1.3	0.66	1.3
Spring	Coronel	>5.33	5.33	1.3	<0.66	2.66
Spring	Contulmo	>5.33	5.33	1.3	0.66	2.66
Spring	La Unión	>5.33	5.33	1.3	<0.66	2.66
Spring	Puerto Montt	>5.33	5.33	1.3	<0.66	2.66

Table S3.6: Analysis of variance (ANOVA) to evaluate the effect of the position of *E. cordifolia* populations in their ecological niche (Coronel, Contulmo, La Unión and Puerto Montt) and seasonality (Summer, Fall and Spring) on biofilm formation in four microorganisms (*S. aureus, P. Aeruginosa*, *C. glabrata* and *C. albicans*).

Microorganism	Variable	*gl*	*F*	*p*
S. aureus	Population	4	29.591	< 0.001
	Season	2	0.734	> 0.001
P. aeruginosa	Population	4	82.02	< 0.001
	Season	2	1.07	> 0.001
C. glabrata	Population	4	15.490	< 0.001
	Season	2	1.243	> 0.001
C. albicans	Population	2	15.4	< 0.001
	Season	1	0.0	> 0.001